

©2008

Sezgin Kiren

ALL RIGHTS RESERVED

I. SPIRODIEPOXIDE APPLICATION: PSYMBERIN

II. DIRECT CARBINOLAMIDE SYNTHESIS

By

SEZGIN KIREN

A dissertation submitted to the

Graduate School-New Brunswick

Rutgers, The State University of New Jersey

In partial fulfillment of the requirements

For the degree of

Doctor of Philosophy

Graduate Program in Chemistry

Written under the direction of

Dr. Lawrence J. Williams Ph.D.

And approved by

New Brunswick, New Jersey

October, 2008

ABSTRACT OF THE DISSERTATION

III. SPIRODIEPOXIDE APPLICATION: PSYMBERIN

II. DIRECT CARBINOLAMIDE SYNTHESIS

by SEZGIN KIREN

Dissertation Director:

Professor Lawrence J. Williams

The complete structure of Psymberin was determined with the application of the Universal NMR database approach. A formal synthesis of psymberin was completed with the application of spirodiepoxides. An assembly of a dihydroisocoumarin ring was accomplished from a complex aldehyde and an anion derived from a pentasubstituted arene. A new condition to couple an aldehyde and an amide was achieved to reach a carbinolamide moiety. This condition was applied for the synthesis of analogs and hybrid structures. In a separate study, a metal and a ligand were investigated to promote the coupling between thioacids and azides.

ACKNOWLEDGEMENT

I would like to thank to Professor Lawrence J. Williams for his sage advice, guidance and support throughout my career.

I would also like to thank Professor Spencer Knapp, Professor Daniel Seidel and Professor Edmond J. LaVoie for being on my thesis defense committee. I would like to thank Professor Spencer Knapp and Professor Daniel Seidel for their help and stimulating discussions.

I also thank Dr. Tom Emge for obtaining all the crystallographic data.

I would like to thank Dr. Ning Shangguan for his valuable help and Dr. Partha Ghosh for insightful discussions. I would thank all the past and present members of the Williams group for generous support.

Finally, I would like to thank to all my friends and Dr. Ahmet Tarik Baykal for their deepest friendship.

DEDICATION

This thesis is dedicated to my family.

Table of Contents

Abstract of Dissertation	ii
Acknowledgment	iii
Dedication	iv
Chapter I Structure Elucidation of Psymberin	
1.1 Introduction: Pederin Family	1
1.2 A new member of the Pederin Family	3
1.3 Biological Activity	3
1.4 Structural Determination of Irciniastatin A and Psymberin	6
1.4.1 Pettit Group: Irciniastatin A	6
1.4.2 Crew Group: Psymberin	7
1.5 Universal NMR Database Approach	8
1.6 Synthesis of the Anti and Syn Models	9
1.7 Results and Discussions	12
1.8 Coupling Constant Analysis	14
1.9 Degradation Studies	16
1.10 References	18
Chapter II Synthetic Strategies for Pederin Family Members	
2.1 Introduction	22
2.2 Synthesis of Tetrahydropyran ring	26
2.2.1 The Matsumoto Strategy	26

2.2.2 The Hoffmann Strategy	27
2.2.3 The Nakata Strategy	27
2.2.4 The Rawal Strategy	28
2.3 Synthesis of the Trioxadecalin ring	29
2.4 Synthesis of the Psymberic acid	30
2.5 Synthesis of the Right Segment of Psymberin	31
2.5.1 The De Brabander Strategy	31
2.5.2 The Floerancig Strategy	32
2.6 References	35

Chapter III Spirodiepoxide Application: Psymberin

3.1 Background Information for Spirodiepoxides	37
3.2 Spirodiepoxides in Psymberin Synthesis: 1 st generation	42
3.3 Synthesis of the Rawal Intermediate	55
3.4 Completion of the Formal Synthesis of Psymberin	56
3.5 Spirodiepoxides in Psymberin Synthesis: 2 nd generation	61
3.6 References	67

Chapter IV Direct Carbinolamide Synthesis

4.1 Introduction	70
4.2 Direct Aldehyde-Amide Coupling	74
4.3 Results for Boron Imidates with Aldehydes	76
4.4. Complex Amide and Aldehyde Coupling: Analogs	78

4.5. Stability of Carbinolamides	81
4.6 Scope of the boron imidates	83
4.7 References	85
 Chapter V Metal Promoted Thioacid-Azide Coupling	
5.1 Introduction	86
5.2 Discussions for the mechanism of the Thioacid-azide coupling	95
5.3 References	103
 Experimental Data	
General	104
Chapter I	105
Chapter III	128
Chapter IV	148
Chapter V	159
 Selected ^1H and ^{13}C NMR Spectra	 173
Curriculum Vitae	258

List of Tables

Table 1 LC ₅₀ Values for Psymberin	5
Table 2 Optimization of Cupling Reaction	77
Table 3 Screening of Metal Promoter	90
Table 4 Results from Iron (III) Chloride and Thionoester Coupling	91
Table 5 Results from Iron (III) Chloride and Thioacid Coupling	92
Table 6 Results from Using Different Bases	92
Table 7 Results from Thioacid-Azide Coupling	94

List of Figures

Figure 1 Representative Members of the Pederin Family	2
Figure 2 Structural Similarities within the Pederin Family	2
Figure 3 Psymberin	3
Figure 4 Reported Structure of Irciniastatin A by Pettit	6
Figure 5 Reported Structure of Psymberin by Crews	7
Figure 6 Anti and Syn Models	9
Figure 7 Crystal Structure of Anti Model	12
Figure 8 Differences in ^1H and ^{13}C NMR between Models and Psymberin	13
Figure 9 Coupling Constants Analysis for Psymberin	15
Figure 10 Total Synthesis of Pederin Family Members by Different Groups	23
Figure 11 Disconnections for the Synthesis of Pederin and Mycalamide A	24
Figure 12 Disconnections for Psymberin	25

List of Schemes

Scheme 1 Anti and Syn Products from Grignard and Keck Reaction	10
Scheme 2 Synthesis of Anti (S2.5) and Syn (S2.8) Models	11
Scheme 3 Degradation Studies	17
Scheme 4 The Matsumoto Strategy	26
Scheme 5 The Hoffmann Strategy	27
Scheme 6 The Nakata Strategy	28
Scheme 7 The Rawal Strategy	29
Scheme 8 The Rawal Strategy	30
Scheme 9 The De Brabander Strategy	30
Scheme 10 The De Brabander Strategy	31
Scheme 11 The De Brabander Strategy	32
Scheme 22 The Floerancig Strategy	33
Scheme 22 The Floerancig Strategy	34
Scheme 24 SDE Formation and Opening	37
Scheme 25 SDEs by the Crandall Group	38
Scheme 26 Cyclization of Allenic alcohols	39
Scheme 27 Crystal Structure of SDE	40
Scheme 28 Transition Models for SDE opening	41
Scheme 29 Synthetic Plan: 1 st Generation	43
Scheme 30 Stereoselectivity in Allene Oxidation	44
Scheme 31 Simple Allene Cyclizations	45

Scheme 32 Preliminary Results for Model Allenes	46
Scheme 33 Myers Allene Synthesis	47
Scheme 34 Synthetic Strategy for Allene S29.6	48
Scheme 35 Preparation of Alkyne and Weinreb Amide	49
Scheme 36 Noyori Reduction	50
Scheme 37 Formation of the Key Allene	51
Scheme 38 Cyclization of Allene	52
Scheme 39 SDE formation from Allene	53
Scheme 40 Oxidation of Epimeric Allenes	53
Scheme 41 Stable SDEs	54
Scheme 42 Synthesis of the Rawal Intermediate	55
Scheme 43 Completion of the Pyran Ring	57
Scheme 44 Aromatization of Dimedone	58
Scheme 45 Mechanism of Aromatization	58
Scheme 46 Formation of Arene S44.2	59
Scheme 47 Anion Formation from Arene S42.2	59
Scheme 48 Completion of Formal Synthesis	60
Scheme 49 Synthetic Strategy for 2 nd Generation	62
Scheme 50 DMDO Oxidation of Allene in FR Synthesis	62
Scheme 51 Stability of Arenes	63
Scheme 52 Revised 2 nd Generation Strategy	63
Scheme 53 Synthesis of Ketone S53.3	64
Scheme 54 Paterson Aldol Reaction	64

Scheme 55 Asymmetric Reduction of Hydroxyl Ketone	65
Scheme 56 DMDO Oxidation of Allenes	66
Scheme 57 The Matsumoto Strategy	71
Scheme 58 De Brabander Synthesis of Psymberin	72
Scheme 59 The Roush Strategy	72
Scheme 60 Huang's Strategy	73
Scheme 61 Direct Aldehyde-Amide Coupling	74
Scheme 62 Zampanolide Synthesis	75
Scheme 63 Direct Coupling of Amide S63.1 and S63.3	75
Scheme 64 Simple Aldehyde and Amide Coupling	76
Scheme 65 Examples of Aldehyde-Amide Coupling	78
Scheme 66 Preparation of Complex Amides	79
Scheme 67 Complex Aldehydes Preparation	80
Scheme 68 Examples of Complex Amide and Aldehyde Coupling	81
Scheme 69 Elimination Products	81
Scheme 70 Stable Carbinolamides	82
Scheme 71 Methylation of the Carbinolamide S64.3	83
Scheme 72 Examples of Electron Rich and Poor Azides	86
Scheme 73 Mechanism for Electron Withdrawing Azides	87
Scheme 74 Mechanism for Electron Rich Azides	87
Scheme 75 Coupling of Thioacid and Thionoester with Azide	88
Scheme 76 Results for Different Iron Halides	93
Scheme 77 The Azides Failed to Couple	95

Scheme 78 Control Reactions for Azide and Thioacid	95
Scheme 79 Side and by-Products from Amidation	96
Scheme 80 Dimer and Benzyl Azide	96
Scheme 81 Stable and Unstable Hydrosulfamines	98
Scheme 82 The Mechanism for Decomposition S-Aroylhydrosulfamines	98
Scheme 83 Control Reactions on Side Product S79.1	99
Scheme 84 The Proposed Mechanism of the Amide Formation from S79.1	100
Scheme 85 The Mechanism for the Formation of S79.1	101
Scheme 86 The Formation the Intermediate S86.3	102

List of Abbreviations

°C	degrees Celsius
2,6-lut.	2,6-lutidine
Ac	acetate
acac	acetylacetonate
Bn	benzyl
Boc	<i>t</i> -butyloxycarbonyl
Bu	butyl
δ	chemical shift (parts per million)
d	doublet
DCM	dichloromethane
DIAD	diisopropyl azodicarboxylate
DIBAL-H	diisobutylaluminum hydride
DMAP	4-(<i>N,N</i> -dimethylamino)pyridine
DMDO	dimethyldioxirane
DMF	dimethylformamide
ee	enantiomeric excess
FCC	flash column chromatography
h	hour(s)
Hz	hertz
<i>i</i>	iso
imid.	imidazole
LC ₅₀	concentration that will eliminate 50% of a given population when administered as a single dose
m	multiplet
M	molar (moles/liter)

<i>m/z</i>	mass to charge ratio
m-CBA	meta-chlorobenzoic acid
m-CPBA	meta-chloroperoxybenzoic acid
Me	methyl
min	minutes
ml	milliliters
mol	moles
MOM	methoxymethyl
MS	molecular sieves
Ms	methanesulfonyl
MTP	methoxytrifluoromethylphenyl
n-BuLi	n-butyllithium
NMR	nuclear magnetic resonance
Nu	nucleophile
[O]	oxidant
OTf	trifluoromethanesulfonyl
P	protecting group (generic)
<i>p</i>	para
Pd/C	palladium on carbon
Ph	phenyl
PMB	(4-methoxy)benzyl
PMP	4-methoxyphenyl
ppm	parts per million

Chapter I

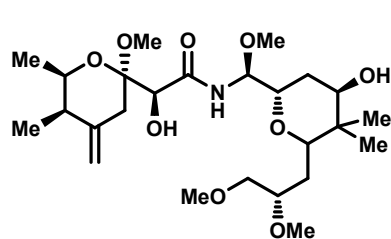
Structure Elucidation of Psymberin

I. Introduction: Pederin Family

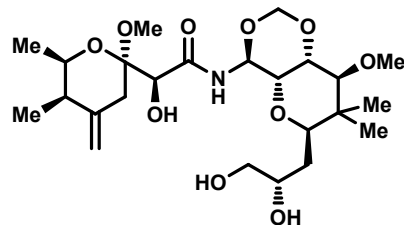
A potent insect toxin was isolated in 1949 from *Paederus fuscipes*, a Japanese beetle known for its severely irritating bite. This natural product was named pederin and its structure was determined by X-ray crystallography in 1968.¹ Over the years, a large family of natural products, named after pederin due to structural resemblance, has been discovered. The pederin family is now composed of more than 30 members, including myclamides A-B,² onnamides A-F³ and theopederins A-L,⁴ icadamides A-B,⁵ pseudopederin and pederone⁶, which were all isolated from marine sponges unlike the first member pederin (See Figure 1).

The members of the pederin family contain different tetrahydropyran rings on each side of an amide. The left segment (**F2.1**) is identical within the family, whereas there are slight structural differences in the right segment (**F2.3**) from member to member. The other striking similarity is that both segments are bridged by *O*-methyl carbinolamide (**F2.2**), which is a rare functional group in organic chemistry.

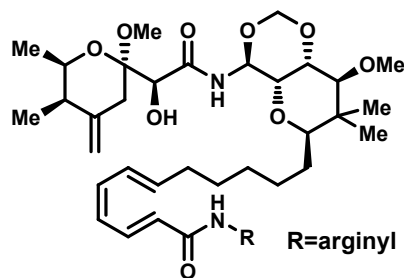
Figure 1 Representative Members of the Pederin Family



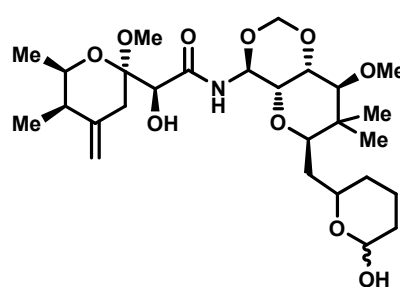
Pederin (F1.1)



Mycalamide A (F1.2)

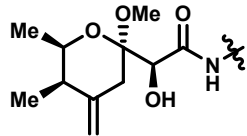


Onnamide A (F1.3)

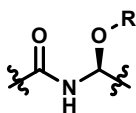


Theopederin A (F1.4)

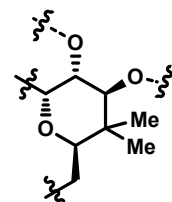
Figure 2 Structural Similarities within the Pederin Family



Left Segment (F2.1)



**O-methyl
carbinolamide (F2.2)**

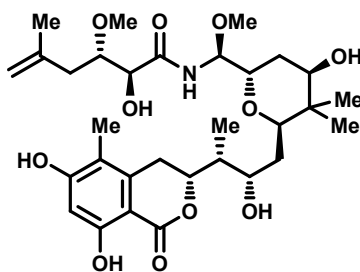


Right Segment (F2.3)

II. A new Member of the Pederin Family: Psymberin

The Pettit and Crews groups independently isolated a new member of the pederin family in 2004. It was isolated from the marine sponge *Ircinia ramose* and named irciniastatin A by the Pettit group.⁷ Shortly thereafter, the Crews group reported the isolation of this natural product from the marine sponge *Psammocinia*, located in the waters of Papua New Guinea, and named it psymberin.⁶ This natural product was considered a new member for the pederin family as it has a highly substituted tetrahydropyran ring “the right segment” like the pederin molecules and the *O*-methyl carbinolamide functional group. The dihydroisocoumarin ring moiety and lack of an exocyclic olefin containing tetrahydropyran ring constitute the structural differences of psymberin from the other pederin members.

Figure 3 Psymberin



Psymberin (F3)

III. Biological Activity

Many members of the pederin family possess potent antiviral and antitumor properties apparently due to their ability to arrest protein synthesis. Pederin was shown to efficiently inhibit mitosis of HeLa cells and block protein and DNA synthesis.⁸

Mycalamides displayed inhibition toward marine leukemia P388, human promyelocytic (HL-60), human lung (A549) and colon (HT-29) carcinoma cells at nanomolar levels. Mycalamide A also exhibited remarkable immunosuppressant activity at the picomolar level, making it more potent than the clinical agents FK506 and cyclosporine.⁹

The biological activity of psymberin was interestingly different from the other members in the pederin family. Unlike all the other family members, which showed near equipotent cytotoxicity against different tumor cell lines, psymberin exhibited remarkably selective cytotoxicity. The Crews group reported that the difference in activity can be as much as 10,000-fold. As shown in the Table 1, LC₅₀ values were found to be around 2.5 nM against several melanoma, colon and breast cancer cell lines whereas it was found to be around 2.5 μ M against all leukemia cell lines investigated.⁶

Due to the biological activity and structural differences between psymberin and members of the pederin family, a structure-activity relationship study is expected to reveal significant information regarding the biological action of these natural products. It is believed that the *O*-alkyl carbinolamide (**F2.2**, pg. 2) is necessary for cytotoxicity within all of the pederins. The right segment (**F2.3**, pg. 3) may not be crucial for the selective cytotoxicity since psymberin doesn't possess the typical tetrahydropyran ring. The dihydroisocoumarin moiety and vinylic methyl termini could also be reasons for the unprecedented selective cytotoxicity of psymberin.

Table 1 Differential Cell Line Sensitivities (LC₅₀) to Psymberin as Identified in the NCI Developmental Therapeutics in Vitro Screening Program

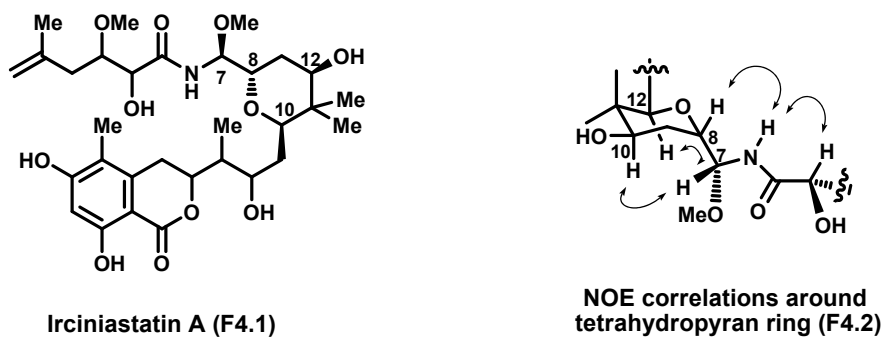
Cell line	LC₅₀ (M)	Cell line	LC₅₀ (M)
leukemia		melanoma	
CCRF-CEM	$>2.5 \times 10^{-5}$	LOX IMVI	$>2.5 \times 10^{-5}$
HL-60(TB)	$>2.5 \times 10^{-5}$	MALME-3M	$<2.5 \times 10^{-9}$
K-563	$>2.5 \times 10^{-5}$	SK-MEL-2	$>2.5 \times 10^{-5}$
MOLT-4	$>2.5 \times 10^{-5}$	SK-MEL-5	$<2.5 \times 10^{-9}$
RPMI-8226	$>2.5 \times 10^{-5}$	SK-MEL-28	1.41×10^{-5}
SR	$>2.5 \times 10^{-5}$	UACC-257	$>2.5 \times 10^{-5}$
		UACC-62	$<2.5 \times 10^{-9}$
breast cancer		colon cancer	
MCF7	$>2.5 \times 10^{-5}$	HCC-2998	3.76×10^{-7}
HS 578T	$>2.5 \times 10^{-5}$	HCT-116	$<2.5 \times 10^{-9}$
MDA-MB-435	$<2.5 \times 10^{-9}$	HT29	$>2.5 \times 10^{-5}$
NCI-ADR-RES	1.9×10^{-5}	SW-620	$>2.5 \times 10^{-5}$
T-47D	1.36×10^{-5}		

IV. Structural Determination of Irciniastatin A and Psymberin

A. Pettit Group: Irciniastatin A

As shown in Figure 4, the Pettit group was able to assign the structure of irciniastatin A (F4.1) by the use of high resolution mass spectroscopy and 2D-NMR spectroscopy.⁷ Even though they were not able to fully define the assignment of relative and absolute configuration of the molecule, they deciphered the simple connectivity by 2D NMR techniques (principally APT, HMQC, HMBC, and ROESY). HMBC experiments were used to identify the amide linkage and to correlate the amide proton to the C₆ carbonyl carbon. Furthermore, interpretation of NOE enhancements provided the assignment of the relative stereochemistry of the carbinolamide and the tetrahydropyran ring. 2D-NOESY and ROESY experiments along with NOE correlations were particularly useful in the deduction of the relative configuration of the four stereogenic centers. They assigned those stereocenters as 7*R*, 8*S*, 10*R* and 12*R*. In addition to this, they defined the molecular formula as C₃₁H₄₈NO₁₁ from the molecular ion peak at m/z 610.3228 [M + H]⁺ with the high-resolution FAB mass spectrometry.

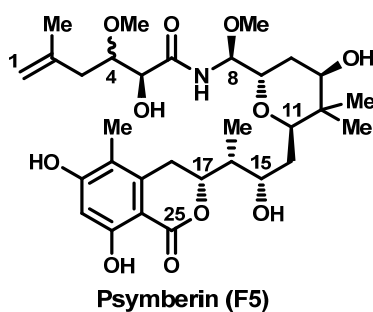
Figure 4 Reported Structure of Irciniastatin A by Pettit group



B. Crews Group: Psymberin

The Crews group employed similar NMR techniques and analyses to determine the structure of psymberin.⁷ Unlike the Pettit group, they were able to assign the relative configuration of most of the stereocenters in the natural product by analyzing NOESY and COSY data as well as ¹H NMR coupling constants. Moreover, they used the spectral data obtained from the pederin family members as a reference to assign the absolute stereochemistry based on the following considerations; (a) a probable shared biogenetic origin, (b) analogous NMR data, (c) comparable cytotoxicity, and (d) similar $[\alpha]$ values.¹⁰ They assigned 7 chiral centers as 5*S*, 8*S*, 9*S*, 11*R*, 13*R*, 15*S*, 16*R* and also determined the C17 chiral center to be *R* due to a positive Cotton effect generated by the chiral dihydroisocoumarin moiety. Nevertheless, the Crews group was unable to define the configuration at the C4 stereocenter.

Figure 5 Reported Structure of Psymberin by the Crews group



Both proposed structures shared similarities in the carbon skeleton and relative configuration of the core tetrahydropyran ring. The only difference was the Crews group assigned the chiral center at C8 in psymberin as *S* while the Pettit group assigned it as *R*.¹¹ Based on the similarities it was tempting to speculate that psymberin and irciniastatin

A were the same compounds. Matching NMRs of the two molecules was inconclusive since NMR spectrums were taken in different solvents (CDCl_3 by the Pettit group and CD_3OD by the Crews group).

V. Structural Elucidation of Psymberin: Universal NMR Database Approach

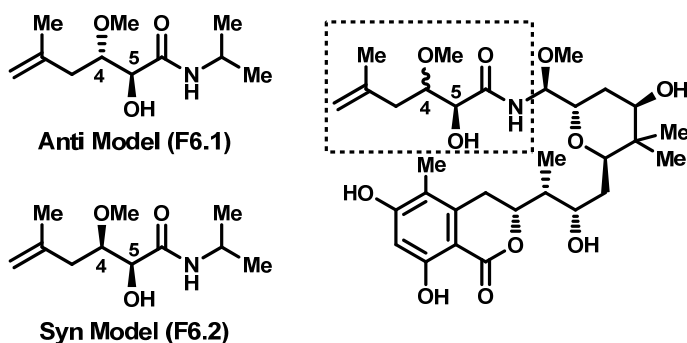
Structure elucidation of complex natural products represents a real challenge. Even modern NMR techniques may not generate adequate data for this task. For this reason Kishi and coworkers devised a novel approach to assign the relative and absolute configuration.¹² The concept and logic of this approach is to: (a) conceptually divide the molecules into small pieces (stereoclusters), (b) compare the NMR profile of a stereocluster to the NMR profile of a synthetic analog of each possible diastereomer, (c) predict the natural product based on the similarity of the NMR profile.

The hypotheses which were developed and later proved experimentally for the approach was (a) the spectroscopic signatures of these stereoclusters are inherent to the specific stereochemical arrangement of the substituents on the carbon chain, (b) the spectroscopic properties of these stereoclusters are independent of the rest of the molecule. On the basis of these observations, the logic and guidelines were advanced to determine a stereocluster in a molecule. Kishi's group proved the efficiency, reliability and applicability of the approach on the complete structural assignment of several complex natural products.¹³

The complete structure of psymberin could not be determined because there was an ambiguity at one stereocenter of the amide side chain. The configuration of the C5 stereocenter was assigned based on analogy to the members of the pederin family but the

configuration of the C4 chiral center could not be assigned by multidimensional NMR spectroscopy. Our first task was to assign the relative stereochemistry of the amide side chain, since we were drawn to synthesize psymberin as well as its analogs. Therefore we applied the universal NMR database approach developed by Kishi and coworkers.¹⁴ We easily identified the stereocluster based on this approach and built an anti (**F6.1**) and a syn (**F6.2**) model which were related to the corresponding stereocluster.

Figure 6 Anti and Syn Models

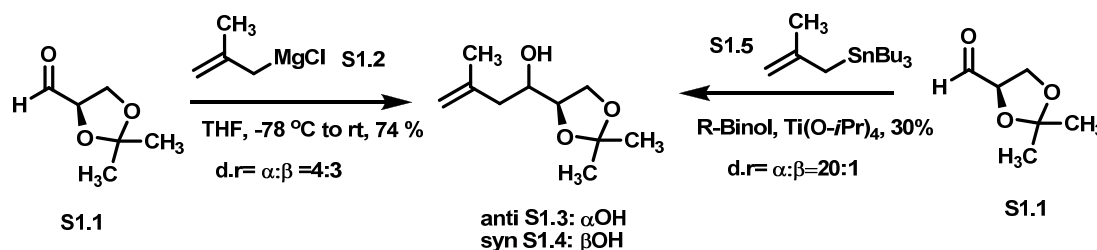


VI. Synthesis of the Anti and Syn Models

The synthesis of the anti (**F6.1**) and syn (**F6.2**) models commenced with the coupling of methallyl magnesium chloride¹⁵ (**S1.2**) with acetonide-protected glyceraldehyde¹⁶ (**S1.1**) derived from D-Mannitol (Scheme 1). This reaction afforded the product in 74% yield as an inseparable mixture of alcohols **S1.3** and **S1.4** (dr: 4:3). In order to obtain a single diastereomer of both **S1.3** and **S1.4** with high yield and diastereoselectivity, we tried the Keck reaction¹⁷ conditions and treated the same aldehyde with methallyl stannate **S1.5** and chiral ligand R-BINOL. Although this reaction resulted in the formation of a single isomer **S1.3** with high selectivity, the yield was low

(~30%). As a result, we decided to pursue the Grignard addition reaction because it yielded both of the alcohols in high yield.

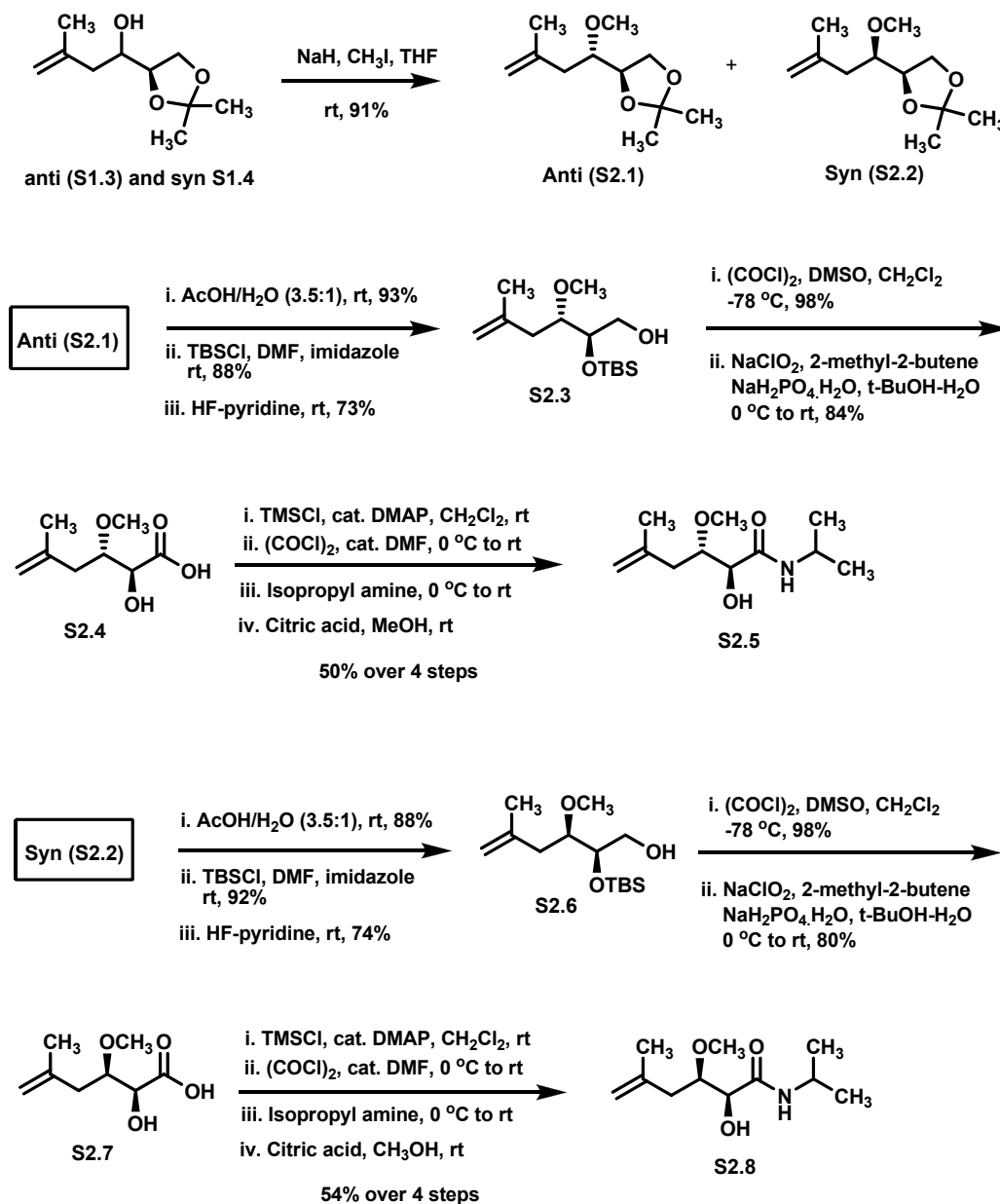
Scheme 1 Anti(S1.3) and Syn(S1.4) Products from Grignard and Keck reaction



We treated the alcohol mixture with MeI under basic conditions and conveniently separated the anti (S2.1) and syn (S2.2) products by silica gel chromatography. We also obtained the anti product from methylation of the Keck reaction intermediate, which served as a reference for the structural assignment of the anti product.

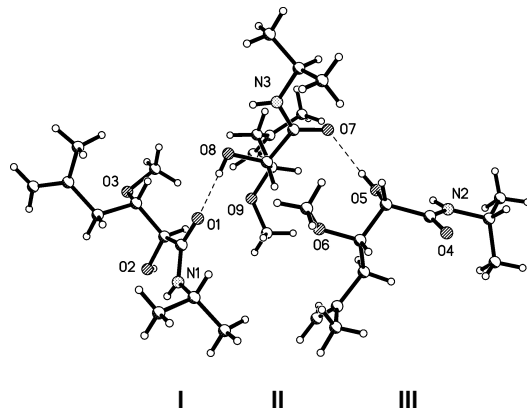
From this point on both the anti and syn compounds were treated under the same conditions to synthesize the models (Scheme 2). Acetonide deprotection under acidic conditions afforded anti and syn diols.¹⁸ Silylation of both hydroxyl groups followed by selective deprotection of the primary TBS group yielded the anti (S2.3) and syn (S2.7) alcohols. Oxidation of the alcohols, first to aldehyde under Swern oxidation conditions followed by oxidation of the resultant aldehydes, gave anti (S2.4) and syn (S2.7) hydroxyl carboxylic acids.¹⁹ The cleavage of the secondary TBS group was affected under the Pinnick oxidation condition. The synthesis of the corresponding anti and syn amide models from hydroxyl carboxylic acid was accomplished in one pot by protection of the hydroxyl group with TMS followed by acyl chloride formation and subsequent amidation and finally deprotection of the TMS group.²⁰ The anti (S2.5) and syn (S2.8) models were obtained in 50% and 54% yields, respectively.

Scheme 2 Synthesis of Anti (S2.5) and Syn (S2.8) Models



Surprisingly, the anti model was a white solid while the syn model was an oily compound. The structural proof of the anti model was unambiguously established by single-crystal X-ray crystallography, which revealed three closely related conformers (Figure 7).

Figure 7 Crystal structure: three conformers of the Anti model compound (F6.1).



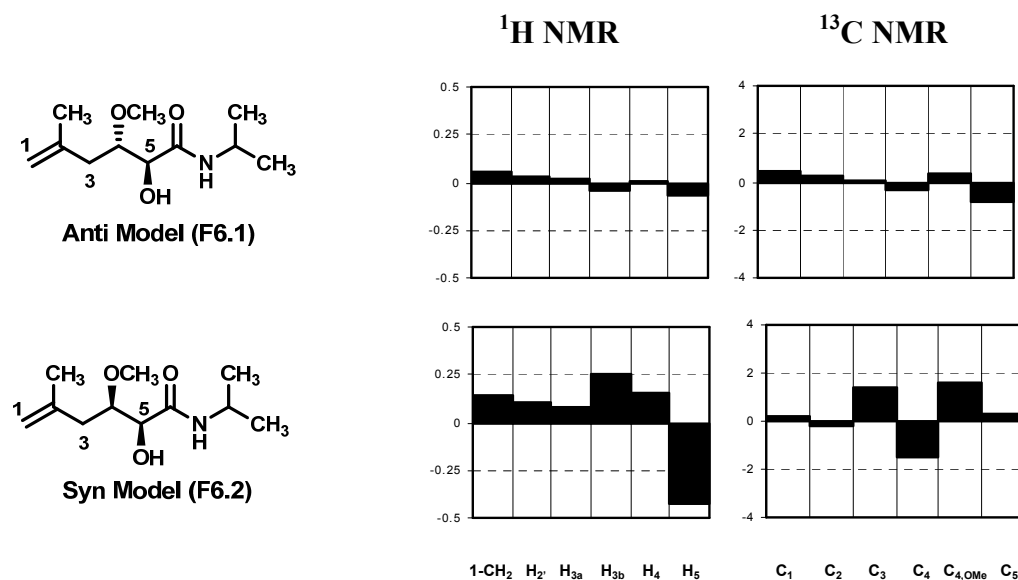
VII. Results and Discussions

The ^1H and ^{13}C NMR chemical shifts were determined for the model anti (**F6.1**) and syn (**F6.2**) compounds and compared to reported chemical shifts of psymberin. The data is represented in the histogram below where the difference ($\Delta\delta$) in chemical shifts for some key proton and carbon signals are calculated. As it is seen in Figure 8, the ^1H and ^{13}C NMR chemical shifts of the anti isomer and natural product show little differences, whereas corresponding chemical shifts for the syn isomer differ more with the chemical shifts of the natural product. This trend is especially apparent in the key signals of H3a, H3b, H4, H5, C3, C4, C4-OMe.

The Universal NMR Databases approach, where structural elucidation is achieved by spectral data comparison of complex structures to that of constructed simpler stereoclusters, has been successfully applied to natural products like tetrafibricin, desertomycin, oasomycin.^{16,17} This idea is based on that the chemical shift of a proton or carbon of a stereocluster is dependent on the relative stereochemistry resulting in different NMR signatures for the diastereoisomers. Provided the ^1H and ^{13}C chemical shifts of a short

model polyol differ from the mean chemical shifts of a set of polyols by ~ 0.10 ppm and ~ 1.0 ppm respectively, the difference is regarded as a significant.²¹ The difference is assumed insignificant if the differential is smaller than 0.05 ppm and 0.50 ppm for ^1H and ^{13}C respectively. Thus, there are two criteria that have to be met for NMR database approach to be valid: a) the difference in chemical shifts between the mismatched diastereomer and the unassigned complex structure must be significant and b) the difference between matched diastereomer and the unassigned complex structure must be insignificant.

Figure 8 Differences in ^1H and ^{13}C chemical shifts between Models and Psymberin²²

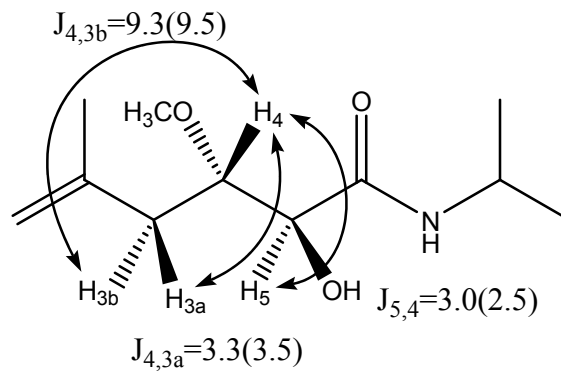


In the above study we showed that both criteria for NMR database approach are met, which led to the conclusion that the configuration of the amide side chain of psymberin is *anti*. This approach for structural assignment can not be applied for all stereoclusters. For instance, the ^1H and ^{13}C chemical shift differences of unfunctionalized 1,2-diols are very small such that one can not differentiate between diastereomers. For

such stereoclusters the $\Delta\delta$ of the ^1H signals are <0.04 ppm and $\Delta\delta$ is <0.4 ppm for ^{13}C signals so the application of this method for the structural assignment of complex natural products might be problematic.^{5e,21} However, in such cases like that of amide side chain in psymberin, the 1,2-diol stereocluster is more functionalized and thus the diastereomers exhibit different NMR profiles.²³ The anti model (**F6.1**) and the natural product (**F5**) have a good correlation with a $\Delta\delta$ of <0.05 ppm for ^1H and <0.5 ppm for ^{13}C , whereas the syn model displays >0.15 ppm and >1.0 ppm differences for ^1H and ^{13}C , respectively.

VIII. Coupling Constant Analysis

For the structural proof of the natural product we also examined the homology of the coupling constants between the models and psymberin (Figure 9). The particular protons that were used for the analysis were vicinal protons H5-H4, H4-H3a and H4-H3b. For the anti model (**F6.1**) the coupling constant for the H5-H4 was 3.0 Hz whereas it was 1.8 Hz for the syn model (**F6.2**). The anti isomer also showed similar coupling constant values for the other two vicinal protons H4-H3a and H4-H3b, while it was inconclusive for the syn model because couplings appear as multiplets. Furthermore we calculated the estimated coupling constants from the crystal structure of three conformers for the anti model based on the average dihedral angles. The coupling constants that were obtained from the Karplus equation for the anti model (**F6.1**) were in good agreement with the natural product, as shown in figure 9. Even though the coupling constants for the natural product were taken in solution, they approximately matched what would be expected for the three conformers in the crystal.²⁴ The results support the *anti* assignment of the side chain of the natural product.

Figure 9 Coupling Constants Analysis for Psymberin²⁵

		H-H Coupling Constants		
		Estimated Average ^a	Anti Model (F6.1)	Psymberin
$\psi(H_5, H_4)$	-65.8	1-3	3.0	2.5
$\Phi(H_4, H_{3a})$	-66.1	1-3	3.0	3.5
$\theta(H_4, H_{3b})$	176.7	9-10	9.3	9.5

^a Conformers in crystal structure

IX. Stereochemical Assignment of Amide Side Chain by Degradation Studies

Floreancig and coworkers used a different approach to assign the stereochemistry of the amide side chain.²⁶ They compared the products that were obtained from acid-mediated degradation of both models and psymberin. The models used for the studies were anti (**S3.3**), *ent*-anti (**S3.7**), syn (**S3.4**), *ent*-syn (**S3.8**) (Scheme 3). These molecules were readily accessed from methyl glycerate (**S3.1** and **S3.5**), which can be prepared in enantiomerically form from D-serine and L-serine. The esters (**S3.1** and **S3.5**) were reduced to the corresponding aldehydes (**S3.2** and **S3.6**) in 3 steps. Methallylation of the aldehydes (**S3.2** and **S3.6**) afforded the separable anti and syn products which were then carried on the corresponding carboxylic acids (anti; **S3.3** and **S3.7**, syn; **S3.4** and **S3.8**) in 3 steps. The last step transformation of the carboxylic acids into the *O*-methyl protected carbinolamides (anti; **S3.9** and **3.11**, syn; **3.13** and **3.15**) by the application of the Matsumoto protocol.²⁷ Exposure of these models to H₂SO₄ in MeOH at 60 °C for 12 h afforded the corresponding cyclized products (anti **S3.10** and **S3.12**, syn **S3.14** and **S3.16**). These tetrahydrofurans were separable by GC and characterized by NOESY experiment to establish the spatial relation between the methoxy and carbomethoxy groups. Interestingly no epimerization was observed at the alpha position of the ester under the reaction conditions.

Similarly, they treated psymberin with H₂SO₄ in MeOH at 60 °C for 12 h and obtained the cyclized tetrahydrofuran, which matched with the product produced from model **S3.11**, as determined by GC-MS. They concluded that the relative and absolute stereochemistry of the amide side chain should be anti 4*S*, 5*S* as in model **S3.11**, which is consistent with the NMR database approach applied by our group.¹⁸

REFERENCE

- 1) (a) Furusaki, A.; Watanabe, T.; Matsumoto, T.; Yanagiya, M. *Tetrahedron Lett.* **1968**, *60*, 6301. (b) Bonamartini, C. A.; Mangia, A.; Nardelli, M.; Pelizzi, G. *Gazz. Chim. Ital.* **1971**, *101*, 591.
- 2) (a) Perry, N. B.; Blunt, J. W.; Munro, M. H. G.; Pannell, L. K. *J. Am. Chem. Soc.* **1988**, *110*, 4850. (b) Perry, N. B.; Blunt, J. W.; Munro, M. H. G.; Thompson, A. M. *J. Org. Chem.* **1990**, *55*, 223.
- 3) (a) Sakemi, S.; Ichiba, T.; Kohmaoto, S.; Saucy, G.; Higa, T. *J. Am. Chem. Soc.* **1988**, *110*, 4851. (b) Matsunaga, S.; Fusetani, N.; Nakao, Y. *Tetrahedron* **1992**, *48*, 8369. (c) Kobayashi, J.; Itagaki, F.; Shigemori, H.; Sasaki, T. *J. Nat. Prod.* **1993**, *56*, 976. (d) Vuong, D.; Capon, R. J.; Lacey, E.; Gill, J. H.; Heiland, K.; Friedel, T. *J. Nat. Prod.* **2001**, *64*, 640.
- 4) (a) Fusetani, N.; Sugawara, T.; Matsunaga, S. *J. Org. Chem.* **1992**, *57*, 3828. (b) Tsukamoto, S.; Matsunaga, S.; Fusetani, N.; Toh-E, A. *Tetrahedron* **1999**, *55*, 13697. (c) Paul, G. K.; Gunasekera, S. P.; Longley, R. E.; Shirley, A. *J. Nat. Prod.* **2002**, *65*, 59.
- 5) Clardy, J.; He, H. *U. S. Patent* **1995**, 5,476,953
- 6) Cichewicz, R. H.; Valeriote, F. A.; Crews, P. *Org. Lett.* **2004**, *6*, 1951. All the members of this class of natural product are listed in the supporting information.
- 7) Pettit, G. R.; Xu, J. P.; Chapuis, J. C.; Pettit, R. K.; Tackett, L. P.; Doubek, D. L.; Hooper, J. N. A.; Schmidt, J. M. *J. Med. Chem.* **2004**, *47*, 1149. Also reported the isolation of irciniastatin B from the same sponge. The hydroxyl group in tetrahydropyran ring is in the oxo form in this natural product.
- 8) (a) Soldati, M.; Fioretti, A.; Ghone, M. *Experienta* **1996**, *22*, 176. (b) Brega, A.; Falaschi, A.; Decarli, L.; Pavan, M. *J. Cell. Biol.* **1968**, *36*, 485. (c) Levine, M. R.; Dancis, J.; Pavan, M.; Cox, R. P. *Pediat. Res.* **1974**, *8*, 606.
- 9) (a) Burres, N. S.; Clement, J. J. *Cancer Res.* **1989**, *49*, 2935. (b) Ogawara, H.; Higashi, K.; Uchino, K.; Perry, N. B. *Chem. Pharm. Bull.* **1991**, *39*, 2152. (c) Galvine, F.; Freeman, G. J.; Razi-Wolf, Z.; Benacerraf, B.; Nadler, L.; Reiser, H. *Eur. J. Immunol.* **1993**, *23*, 283. (d) Thompson, A. M.; Blunt, J. W.; Munro, M. H. G.; Clark, B. M. *J. Chem. Soc., Perkin Trans. I* **1994**, 1025. (e) Thompson, A. M.; Blunt, J. W.; Munro, M. H. G.; Perry, N. B. *J. Chem. Soc., Perkin Trans. I* **1995**, 1233.
- 10) Piel, J.; Hui, D.; Wen, G.; Butzke, D.; Platzner, M.; Fusetani, N.; Matsunaga, S. *Proc. Natl. Acad. Sci. U.S.A.* **2004**, *101*, 16222-16227 and Piel, J.; Butzke, D.; Fusetani, N.; Hui, D.; Platzner, M.; Wen, G.; Matsunaga, S. *J. Nat. Prod.* **2005**, *68*, 472-479.
- 11) Both groups used slightly different numbering. C7 in ircinastatin is the same

stereocenter as C8 in psymberin.

12) (a) Kobayashi, Y.; Tan, C.-H.; Kishi, Y. *Angew. Chem., Int. Ed.* **2000**, *39*, 4279-4281. (b) Tan, C.-H.; Kobayashi, Y. Kishi, Y. *Angew. Chem., Int. Ed.* **2000**, *39*, 4282-4284. (c) Kobayashi, Y.; Tan, C.-H.; Kishi, Y. *J. Am. Chem. Soc.* **2001**, *123*, 2076-2078. (d) Higashibayashi, S.; Czechtizky, W.; Kobayashi, Y.; Kishi, Y. *J. Am. Chem. Soc.* **2003**, *125*, 14379-14393. (e) Higashibayashi, S.; Kishi, Y. *Tetrahedron* **2004**, *60*, 11977-11982.

13) (a) Lee, J.; Kobayashi, Y.; Tezuka, K.; Kishi, Y. *Org. Lett.* **1999**, *1*, 2177-2180. (b) Kobayashi, Y.; Lee, J.; Tezuka, K.; Kishi, Y. *Org. Lett.* **1999**, *1*, 2181-2184. (c) Kobayashi, Y.; Tan, C.-H.; Kishi, Y. *Helv. Chim. Acta* **2000**, *83*, 2562-2571. (d) Fidanze, S.; Song, F.; Szlosek-Pinaud, M.; Small, P. L.; Kishi, Y. *J. Am. Chem. Soc.* **2001**, *123*, 10117-10118. (e) Benowitz, A. B.; Fidanze, S.; Small, P. L.; Kishi, Y. *J. Am. Chem. Soc.* **2001**, *123*, 5128-5129. (f) Kobayashi, Y.; Hayashi, N.; Tan, C.-H.; Kishi, Y. *Org. Lett.* **2001**, *3*, 2245-2248. (g) Hayashi, N.; Kobayashi, Y.; Kishi, Y. *Org. Lett.* **2001**, *3*, 2249-2252. (h) Kobayashi, Y.; Hayashi, N.; Kishi, Y. *Org. Lett.* **2001**, *3*, 2253-2255. (i) Kobayashi, Y.; Hayashi, N.; Kishi, Y. *Org. Lett.* **2002**, *4*, 411-414. (j) Kobayashi, Y.; Czechtizky, W.; Kishi, Y. *Org. Lett.* **2003**, *5*, 93-96. (k) Kobayashi, Y.; Hayashi, N.; Kishi, Y. *Tetrahedron Lett.* **2003**, *44*, 7489-7491. (l) Boyle, C. D.; Harmange, J.-C.; Kishi, Y. *J. Am. Chem. Soc.* **1994**, *116*, 4995-4996. See also ref. 16.

14) Kiren, S.; Williams, L. J. *Org. Lett.* **2005**, *7*, 2905.

15) Masilamani, D.; Manahan, E. H.; Vitrone, J.; Rogic, M. M. *J. Org. Chem.* **1983**, *48*, 4918-4931.

16) Schmid, C. R.; Bryant, J. D.; Dowalatzedah, M.; Phillips, J. L.; Prather, D. E.; Schantz, R. D.; Sear, N. L.; Vianco, C. S. *J. Org. Chem.* **1991**, *56*, 4056-4058.

17) Keck, G. E.; Tarbet, H. K.; Geraci, S. L. *J. Am. Chem. Soc.* **1993**, *115*, 8467-8468. Keck, G. E.; Krishnamurthy, D.; Grier, M. C. *J. Org. Chem.* **1993**, *58*, 6543-6544.

18) Taber, D. F.; Xu, M.; Hartnett, J. C. *J. Am. Chem. Soc.* **2002**, *124*, 13121-13126.

19) To see the synthesis of similar aldehydes check; (a) Nazare, M.; Waldmann, H. *Chem. Eur. J.* **2001**, *7*, 3363-3376. (b) Enders, D.; Lenzen, A.; Muller, M. *Synthesis* **2004**, *9*, 1486-1496. For a related aldehyde-to-carboxylic acid oxidation see: (a) Fujiwara, K.; Awakura, D.; Tsunashima, M.; Nakamura, A.; Honma, T.; Murai, A. *J. Org. Chem.* **1999**, *64*, 2616-2617. (b) Arefolov, A.; Panek, J. S. *Org. Lett.* **2002**, *4*, 2397-2400

20) Kelly, S. E.; Lacour, T. G. *Synth. Comm.* **1992**, *22*, 859-869.

21) The Ref 12 discusses the limitations and difficulties of the Universal NMR database approach. Vicinal diols are mentioned in Ref. 12e. See also (a) Matsumori, N.; Kaneno, D.; Murata, M.; Nakamura, H.; Tachibana, K. *J. Org. Chem.* **1999**, *64*, 866-876. (b) Bifulco, G.; Bassarello, C.; Riccio, R.; Gomez-Paloma, L. *Org. Lett.* **2004**, *6*, 1025-1028. (c) Dambruoso, P.; Bassarello, C.; Bifulco, G.; Appendino, G. Battaglia, A.; Fontana, G.; Gomez-Paloma, L. *Org. Lett.* **2005**, *7*, 983-986. (d) Dambruoso, P.; Bassarello, C.; Bifulco, G.; Appendino, G. Battaglia, A.; Guerrini, A.; Fontana, G.; Gomez-Paloma, L. *Tetrahedron Lett.* **2005**, *46*, 3411-3415.

22) (A) Difference between ^1H - δ of psymberin (**F5**) and the anti and syn (**F6.2**) model. (B) Difference between ^{13}C - δ of **F5** and the anti (**F6.1**) and syn (**F6.2**) model. The x-axis identifies the signal (^1H or ^{13}C) and the y-axis corresponds to $\Delta\delta = \delta(\text{F5}) - \delta(\text{anti or syn})$. Data collected at 300MHz for ^1H and 75MHz for ^{13}C in CD_3OD . The chemical shift data for **F5** was taken from reference 6.

23) Ref 21c focuses on the fact that a densely functionalized mixed secondary/tertiary system was not applicable to the NMR database approach. It was not necessary to apply correlation factors as in 21c.

24) Duin, M. V.; Baas, J. M. A.; Graaf, B. v. d. *J. Org. Chem.* **1986**, *51*, 1298-1302.

25) The crystal structure of anti model provided the average the dihedral angles. Karplus relation provided the estimated coupling constants. Spectral data for anti and psymberin (ref 6) collected in CD_3OD .

26) Green, M. E.; Rech, J. C.; Floreancig, P. E. *Org. Lett.* **2005**, *7*, 4117-4120.

27) See chapter 4 for References.

Chapter II

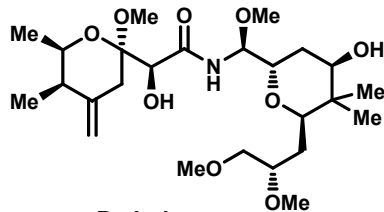
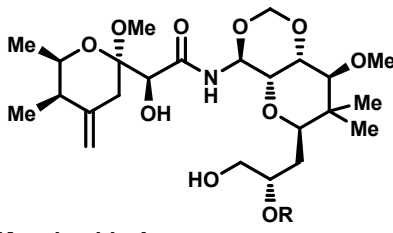
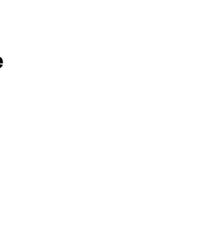
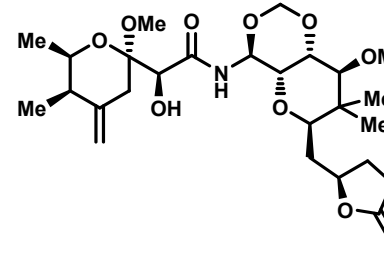
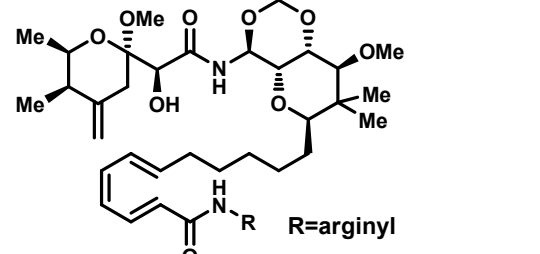
Synthetic Strategies for Pederin Family members

I. Introduction

Due to its high structural complexity and selective cytotoxicity we were drawn to develop a synthesis of the new member of the pederin family, psymberin. We sought to develop synthetic strategies to reach this molecule as well as analogous and hybrid structures, which may help in understanding the exceptional biological activity of the natural product. In order to achieve this difficult task we sought to take advantage of the tactics which were developed for the synthesis of the other members of the pederin family. In this chapter we deal with some examples of strategies developed by different groups in the past three decades. In light of these strategies we will focus on our two novel approaches to psymberin in the next two chapters.

As shown in Figure 10 many groups have spent a great deal of synthetic effort to finish total syntheses of the members of the pederin family,¹⁻⁵ as well as the partial and formal syntheses of these compounds.⁶ Obviously, the challenges posed by these molecules stimulated many groups to execute creative synthetic tactics. Among these there is one common strategy that every group, without exception, applied: convergent construction of the molecules. This reasonable tactic has been very effective and applicable to all the members of the family.

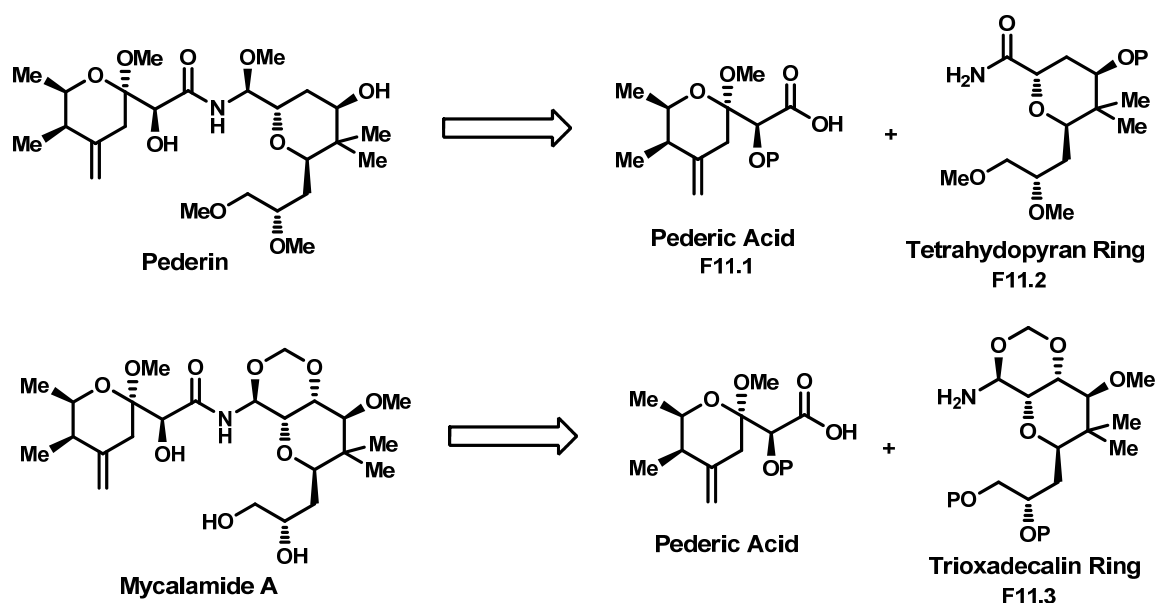
Figure 10 Total Syntheses of Pederin Family Members by Different Groups

					
Pederin		R=H, Mycalamide A		R=Me, Mycalamide B	
LLS		LLS		LLS	
Matsumoto (1988)	30 steps	Kishi (1990)	34 steps	Kishi (1990)	35 steps
Nakata (2002)	24 steps	Roush (2000)	31 steps	Kocienski (2000)	32 steps
Kocienski (2000)	25 steps	Trost (2003)	22 steps		
Rawal (2007)	12 steps	(Formal Synthesis)			
		Rawal (2005)	21 Steps		
		Toyota (2006)	34 steps		
LLS=Longest Linear Sequence					
					
Theopederin D		Onnamide A			
LLS		LLS			
Kocienski (2000)	34 steps	Kishi (1991)	25 steps		

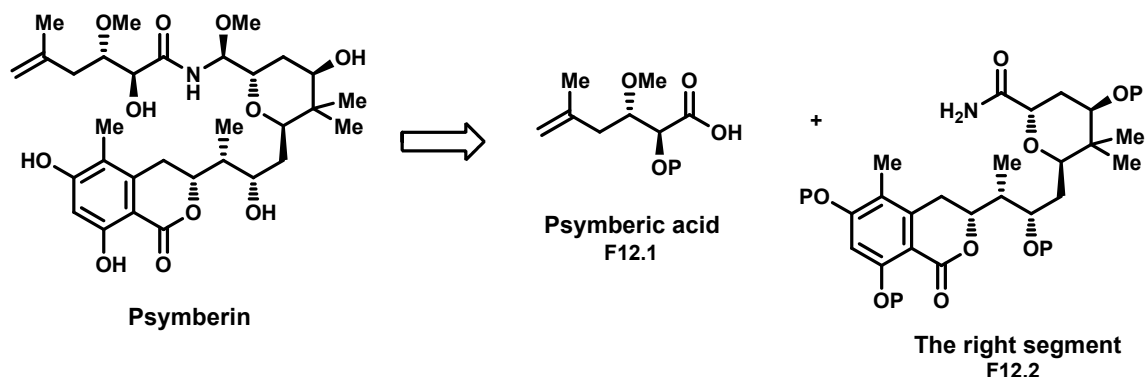
We mentioned the similar structural units within the family members in Figure 2 (pg 2). In the case of the application of convergent synthesis, the left (F2.1) and right (F2.3) segments of the members constitute two simpler units to reach the target molecules (Figure 11). One unit is the pederic acid (F11.1). However, the other unit is either the core tetrahydropyran ring (F11.2) as seen in pederin or the trioxadecalin ring (F11.3) as seen in mycalamides, theopederins and onnamides. Even though highly efficient syntheses of these units have been published, the real challenge comes from

joining the units. Formation of the *O*-methyl carbinolamide (**F2.2**) from two units is a difficult task, since it is a very sensitive functional group. Nevertheless, there are several methods that can be applied to join these two units through the formation of *O*-methyl carbinolamide, which will be discussed in detail in chapter 4.

Figure 11 Disconnections for the Synthesis of Pederin and Mycalamide A



Similarly, the convergent synthesis of the psymberin can be done by joining two halves at the carbinolamide bond (Figure 12). The left segment, called psymberic acid (**F12.1**), is analogous to pederic acid (**F11.1**) in other members. The right segment, containing the core tetrahydropyran ring (**F11.2**) as in pederin, is additionally flanked by a dihydroisocumarin ring. The trioxadecalin ring (**F11.3**) looks similar since it bears a closely related core tetrahydropyran ring with an affixed six- membered ring.

Figure 12 Disconnection for Psymberin

In 2005, the De Brabander group reported the first total synthesis of psymberin via the disconnection shown in Figure 12.⁷ Later, the Floreancig group published a partial synthesis with the same strategy (**F12.2**).⁸ Lastly, the Huang group came up with an interesting strategy by employing a linear synthetic strategy to finish the total synthesis.⁹

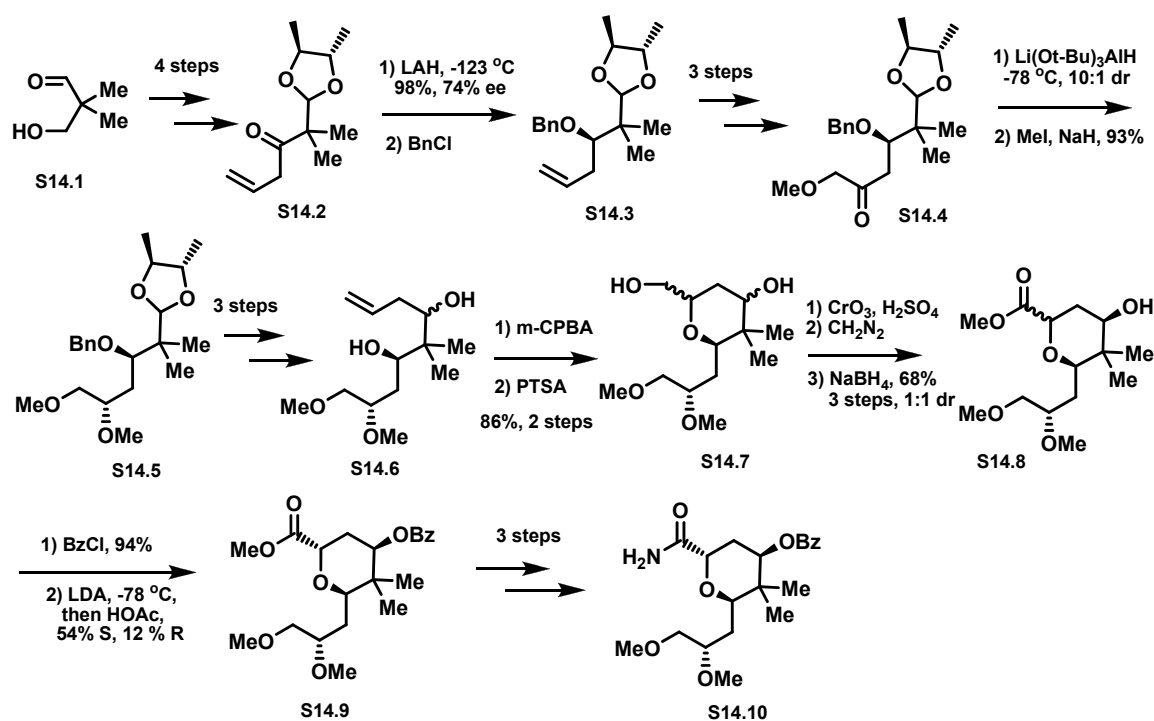
Our synthetic strategy also depended on the disconnection shown in Figure 12.¹⁰ We accomplished the synthesis of the psymberic acid segment (**F12.1**), which was mentioned in Chapter 1 (Scheme 2). The construction of the right segment (**F12.2**) with a novel strategy and the formation of the O-methyl carbinolamide (**F2.2**) will be the focus of chapter 3 and 4, respectively. In this chapter, we will cover some elegant synthetic strategies for the synthesis of the tetrahydropyran ring and trioxadecalin ring systems from the literature. In addition to this, the syntheses of psymberic acid and the right segment of psymberin by the De Brabander and Floreancig groups are summarized. However, Huang's total synthesis of psymberin as well as completion of the total synthesis of pederin and the myclamides are addressed in Chapter 4.

II. Synthesis of the Tetrahydropyran Ring

A. The Matsumoto Strategy

The early synthetic efforts to construct the tetrahydropyran ring were reported by Matsumoto in 1982.^{1a-e} The key step in their synthesis was the substrate directed asymmetric reduction of the ketone of **S14.2** and, later, the ketone of **S14.4**. The core ring formation was obtained from the epoxide under acidic conditions (**S14.6**→**S14.7**). Regardless, the selectivity for the formation of the epoxide was low. The stereochemistry of the ester group in **S14.8** was set by enolization and then kinetic protonation of **S14.9**, which provided the desired product **S14.10** in low yield and selectivity. This route was too lengthy, consisting of 23 steps.

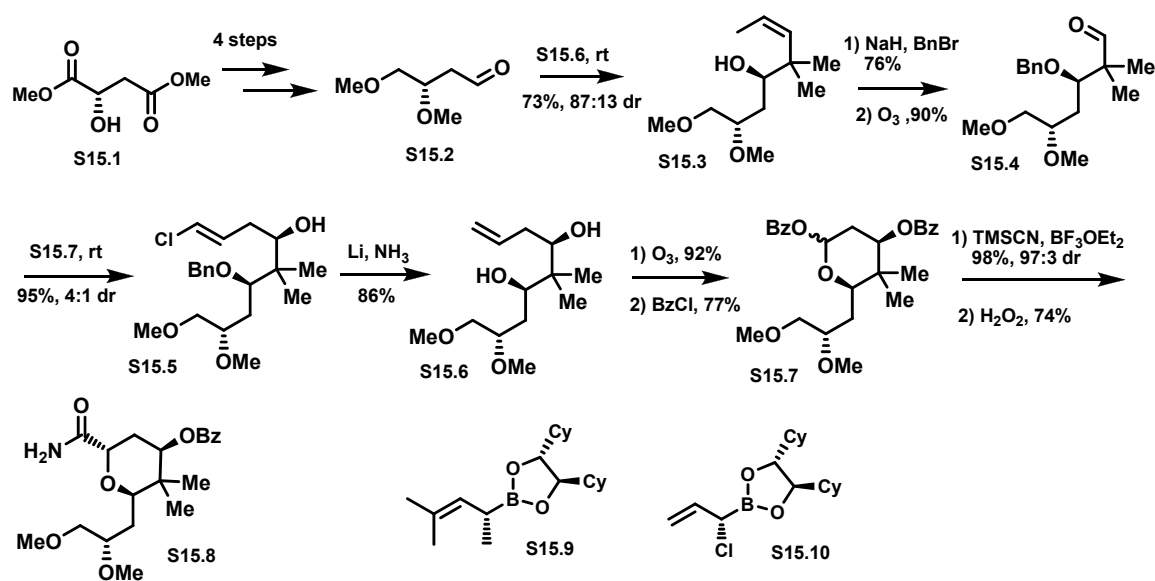
Scheme 14 The Matsumoto Strategy



B. The Hoffmann Strategy;

A concise and highly efficient synthesis was accomplished by the Hoffman group.^{6a-c} The first key step was asymmetric allylation of aldehyde **S15.2** with chiral borane reagent (**S15.9**), which gave good yield and moderate selectivity. The second key step was again asymmetric allylation of aldehyde **S15.4**, but this time with the different chiral borane reagent **S15.10**. Likewise, a fairly good yield and moderate selectivity was obtained from this reaction. Ozonolysis of the double bond in **S15.6** afforded the cyclic core structure in its hemiacetal form, which was subsequently protected with a benzoyl group (**S15.7**). They completed the synthesis of the ring by introducing a cyano group to **S15.7** followed by oxidation to the amide **S15.8**.

Scheme 15 The Hoffmann Strategy

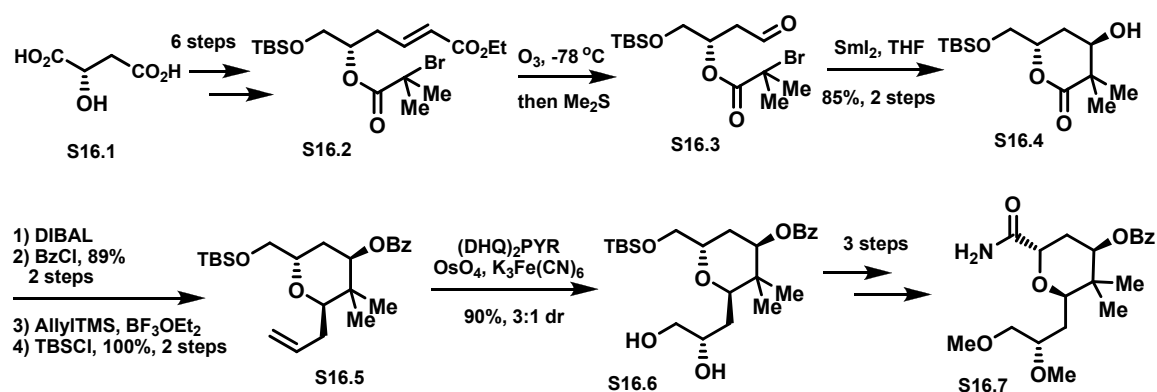


C. The Nakata Strategy

Another elegant synthesis of the tetrahydropyran was accomplished by the Nakata group.^{1h} They applied a SmI₂-mediated intramolecular Reformatsky reaction to utilize the

core ring (**S16.1**→**S16.2**). This reaction took place smoothly, which afforded one single product in 85% yield. After introduction of an allyl group to **S16.3** with complete axial selectivity, the Sharpless asymmetric dihydroxylation of the double bond in **S16.3** furnished diol **S16.4** in good yield, albeit with low selectivity (3:1). The synthesis of **S16.5** was completed in 16 steps with a 35% overall yield.

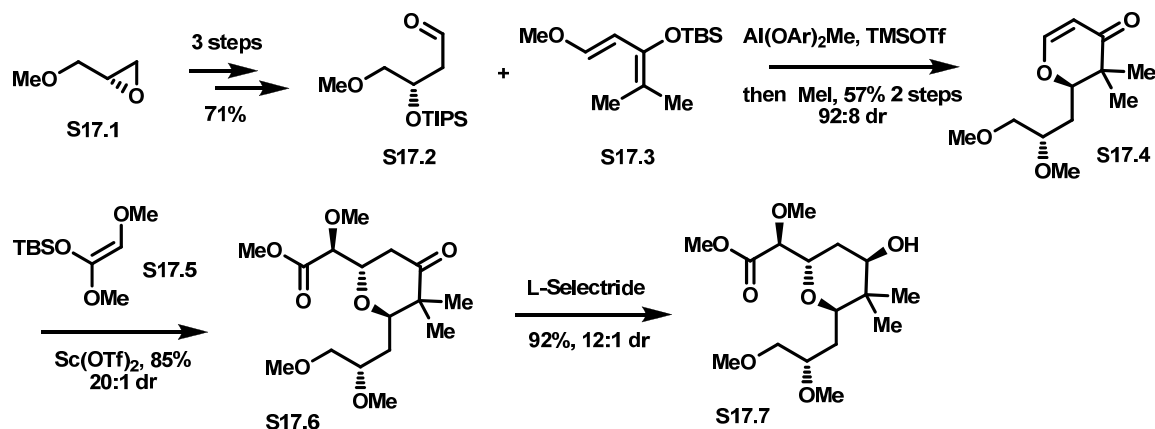
Scheme 16 The Nakata Strategy



D. The Rawal Strategy

Recently, the Rawal group came up with an outstanding strategy for the synthesis of the core ring of pederin (Scheme 17).^{1m} Assembly of the ring was convergently furnished by a three-step reaction sequence from aldehyde **S17.2**. Firstly, they applied a hetero-Diels-Alder reaction (or Mukaiyama Aldol cyclization) between aldehyde **S17.2** and diene **S17.3**, which took place with excellent diastereoselectivity. Secondly, they took advantage of a Mukaiyama-Michael reaction to combine pyranone **S17.4** and silyl ketene **S17.5**, which also proceeded with excellent diastereoselectivity. Finally, the reduction of pyranone **S17.6** with L-Selectride predominantly afforded the desired product (**S17.7**) in 7 steps overall.

Scheme 17 The Rawal Strategy

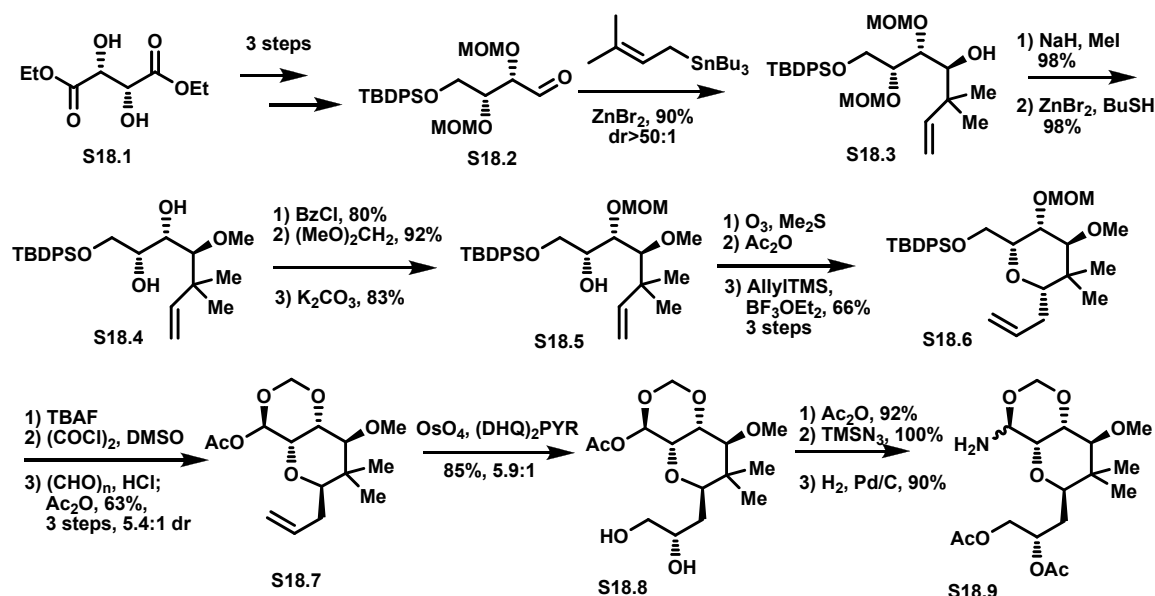


III. Synthesis of the Trioxadecalin Ring

The Rawal Strategy

The Rawal group has also recently published the total synthesis of mycalamide A.^{1h} They applied effective and stereoselective methods for the preparation of the trioxadecalin ring (**F11.2**) and pederic acid (**F11.1**). Their synthesis started with methyl tartarate (**S18.1**), which was transformed into the aldehyde (**S18.2**) in 4 steps (Scheme 18). A chelation-controlled methallylation furnished alcohol **S18.3** as a single diastereomer. After protecting group manipulations, **S18.5** was treated with ozone and then acetic anhydride. The resulting lactol acetate was treated with allyltrimethylsilane and $\text{BF}_3 \cdot \text{OEt}_2$ to provide **S18.6** as a single diastereomer. Transformation of **S18.6** to **S18.7** was accomplished in three steps, which afforded the product in a ratio of 5.4:1. Asymmetric dihydroxylation resulted in the formation of the desired diol (**S18.8**), which was then protected as the corresponding acetate. The anomeric acetate was transformed to an azide with TMSN_3 , which was reduced to a mixture of amina diastereomers (**S18.9**). They completed the synthesis in 21 steps and 10.5% overall yield.

Scheme 18 The Rawal strategy

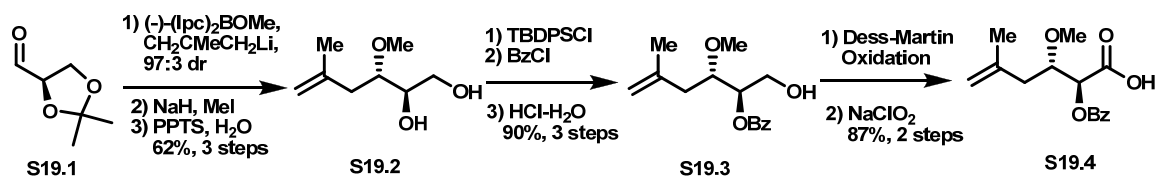


IV. Synthesis of the Psymberic Acid

The De Brabander Strategy

The De Brabander group started the synthesis of the target with the protected glyceraldehyde **S19.1** and treated it with a chiral borane reagent ((-)-Ipc₂BOMe) to afford an anti product which was methylated and deprotected to give the diol (**S19.2**).⁷ The antipodal borane reagent ((+)-Ipc₂BOMe) was used to obtain the corresponding syn compound. Both anti and syn products were elaborated to their respective final carboxylic acids after a series of protecting group manipulation and oxidation reactions shown in Scheme 19.

Scheme 19 The De Brabander Strategy



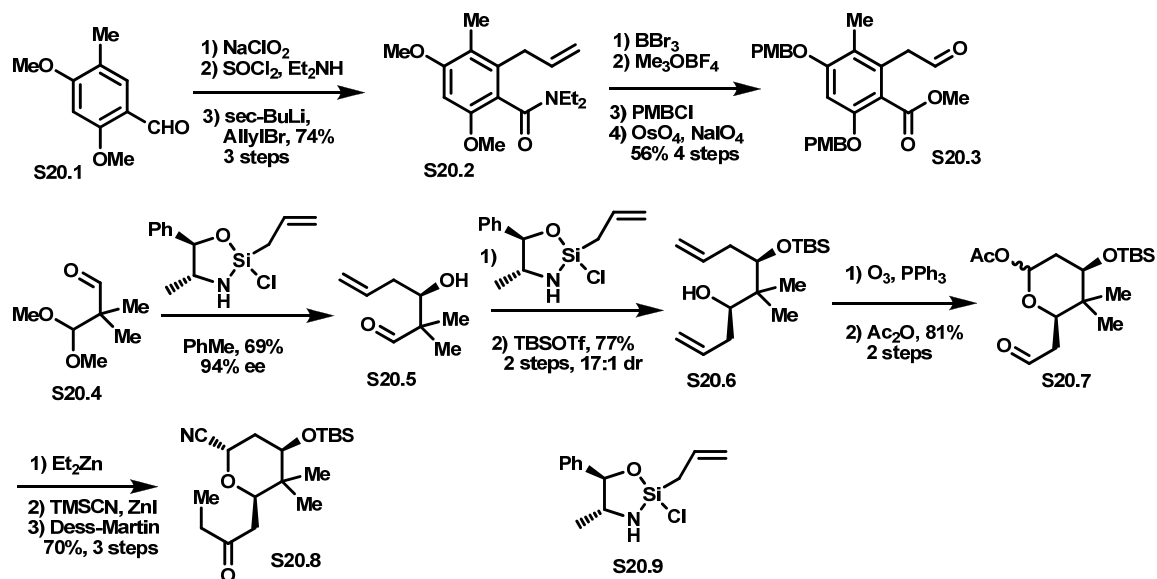
V. Synthesis of the Right Segment of Psymberin

A. The De Brabander Strategy

The synthesis of this segment stemmed from the coupling of two simpler units. The aryl fragment **S20.3** (Scheme 20) was finished in 7 steps from aryl aldehyde **S20.1** by employing such reaction conditions as: a) oxidation/amidation, (b) *ortho*-methylation/allylation, (c) methyl ether deprotection with BBr₃, (d) methyl ester formation, (e) protection with PMB group, (f) oxidative double bond cleavage.

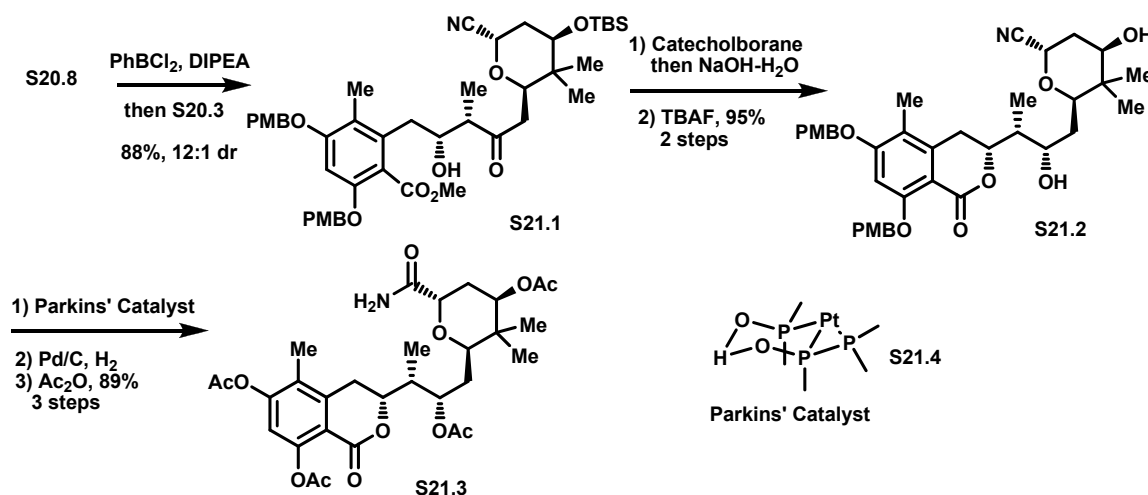
The core pyran ring formation commenced with the application of asymmetric allylation of aldehydes **S20.4** and **S20.5** with Leighton's silane reagent (**S20.9**) to furnish a C₂-symmetrical diol, which was monosilylated to give **S20.6**. Ozonolysis followed by acetylation gave **S20.7**. The synthesis was completed by addition of an ethyl group to **S20.7**, displacement of acetate with TMSCN and then oxidation of a secondary alcohol to ketone **S20.8**.

Scheme 20 The De Brabander Strategy



The coupling of the two units (**S20.2** and **S20.8**) was accomplished via an aldol reaction to afford the major syn product **S21.1**. 1,3 syn reduction of **S21.1** with catecholborane and then basic work-up gave a lactone, which was desilylated with TBAF to yield **S21.2**. The final steps to get the right segment **S21.3** were a hydrolysis of the nitrile group with the Parkins catalyst (**S21.4**), deprotection of the PMB group by hydrogenation and, lastly, acetylation of the hydroxyl groups with acetic anhydride.

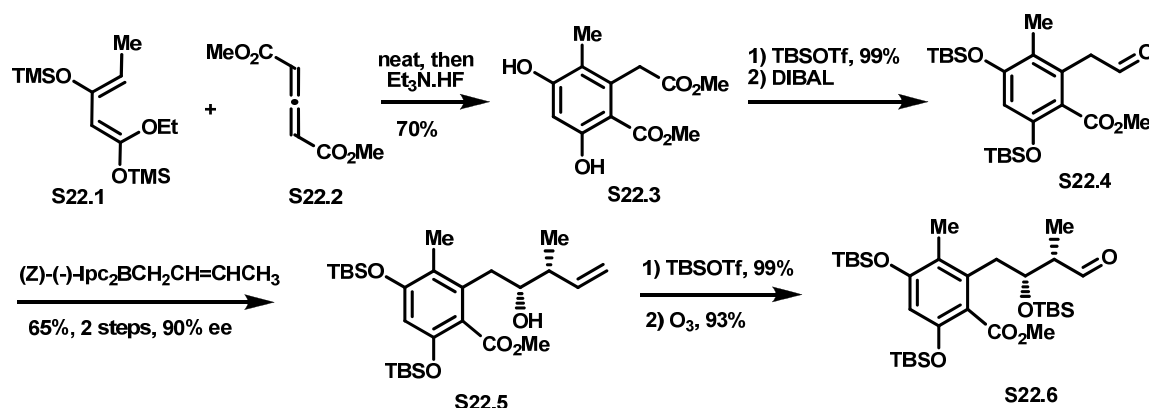
Scheme 21 The De Brabander Strategy



B. The Floreancig Strategy

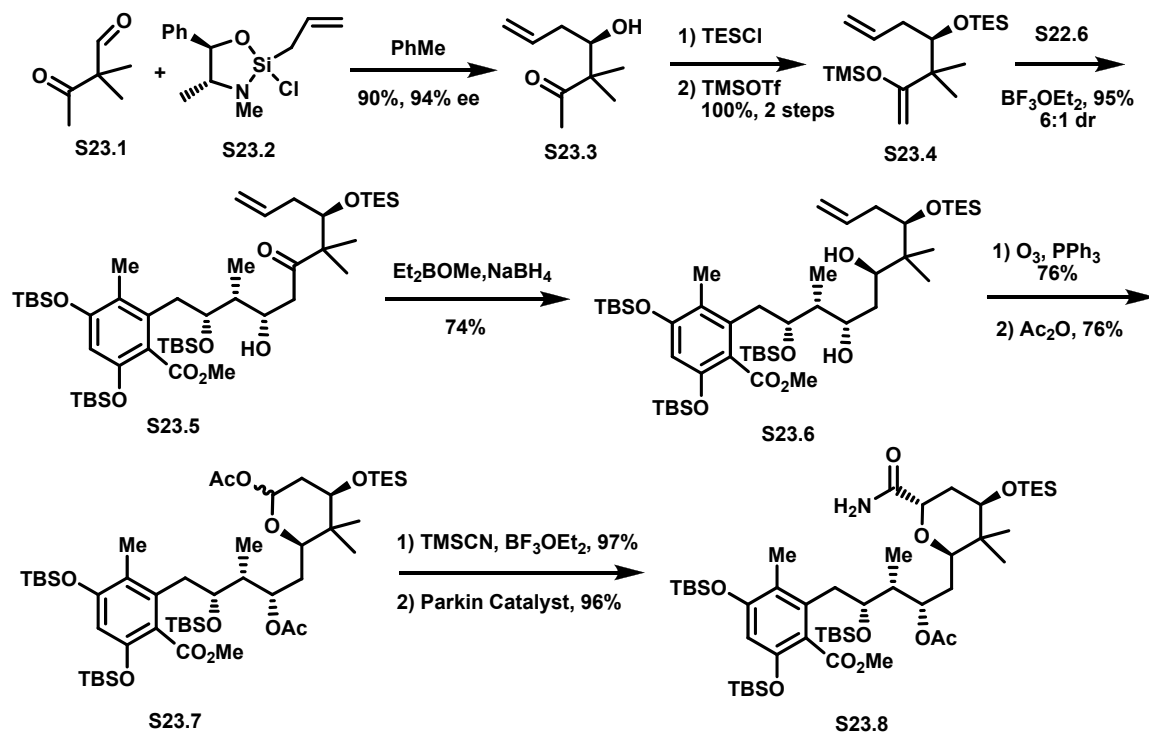
This group accomplished the synthesis of the right segment from the coupling of **S22.6** and **S23.6**.⁸ They used the Diels-Alder cycloaddition reaction between diene **S22.1** and allene **S22.2** as a key step in the preparation of the arene partner **S22.6**, which efficiently yielded 70% of the product. Protection of **S22.3** with TBS followed by reduction with DIBAL furnished aldehyde **S22.4**, which was exposed to the Brown crotylation conditions to produce **S22.5** as a single diastereomer. Protection with TBS followed by ozonolysis completed the synthesis of **S22.6**.

Scheme 22 The Floerancig Strategy



The preparation of the second coupling partner **S23.4** started from the reaction of aldehyde **S23.1** with Leighton's silane reagent **S23.2**, which gave the alcohol (**S23.3**) in high yield and selectivity. Protection with TES followed by TMS enol ether formation furnished **S23.4** quantitatively. **S22.6** and **S23.4** were coupled through a Mukaiyama aldol reaction in the presence of $\text{BF}_3 \cdot \text{OEt}_2$, which gave the desired product (**S23.5**) selectively in high yield. Substrate directed asymmetric reduction of **S23.5** afforded a single product (**S23.6**) in 74% yield. Ozonolysis followed by acetylation resulted in formation of tetrahydropyran **S23.7**. Exposure of **S23.7** to TMSCN replaced the anomeric acetyl group with a nitrile, which was then oxidized to amide **S23.8** with the Parkins catalyst (**S21.4**). They finished the synthesis of this segment in 12 steps from known materials in 15% overall yield. It should be noted, however, that this is a partial synthesis.

Scheme 23 The Floerancig Strategy



REFERENCES

1) For total and partial syntheses of pederin: (a) Tsuzuki, K.; Watanabe, T.; Yanagiya, M.; Matsumoto, T. *Tett. Lett.* **1976**, 4745. (b) Yanagiya, M.; Matsuda, F.; Hasegawa, K.; Matsumoto, T. *Tett. Lett.*, **1982**, 23, 4039. (c) Matsuda, F.; Yanagiya, M.; Matsumoto, T. *Tett. Lett.*, **1982**, 23, 4043. (d) Matsumoto, T.; Matsuda, F.; Hasegawa, K.; Yanagiya, M. *Tetrahedron*, **1984**, 40, 2337. (e) Matsuda, F.; Tomiyoshi, N.; Yanagiya, M.; Matsumoto, T. *Tetrahedron*, **1988**, 44, 7063. (f) Nakata, T.; Nagao, S.; Mori, N.; Oishi, T. *Tett. Lett.* **1985**, 26, 6461. (g) Nakata, T.; Nagao, S.; Oishi, T. *Tett. Lett.* **1985**, 26, 6465. (h) Takemura, T.; Nishii, Y.; Takahashi, S.; Kobayashi, J.; Nakata, T. *Tetrahedron*, **2002**, 58, 6359. (i) Willson, T. M.; Kocienski, P.; Jarowicki, K.; Issac, K.; Faller, A.; Campbell, S. F.; Bordner, J. *Tetrahedron* **1990**, 46, 1757. (j) Willson, T. M.; Kocienski, P.; Jarowicki, K.; Issac, K.; Hitchcock, P. M.; Faller, A.; Campbell, S. F.; *Tetrahedron* **1990**, 46, 1767. (k) Kocienski, P.; Jarowicki, K.; Marczak, S. *Synthesis* **1991**, 1191. (l) Kocienski, P.; Narquizian, R.; Raubo, P.; Smith, C.; Farrugia, L. J.; Muir, K.; Boyle, F. T. *J. Chem. Soc. Perkin Trans I* **2000**, 2357-2384. (m) Jewett, J. C.; Rawal, V. H. *Angew. Chem.* **2007**, 6622-6624.

2) For total and partial syntheses of mycalamides A: (a) Hong, C. Y.; Kishi, Y. *J. Org. Chem.* **1990**, 55, 4242. (b) Nakata, T.; Matsukura, H.; Jian, D. L.; Nagashima, H.; *Tett. Lett.* **1994**, 35, 8229. (c) Nakata, T.; Fukui, H.; Nakagawa, T.; Matsukura, H.; *Heterocycles* **1996**, 42, 159. (d) Analogs of mycalamides, Fujita, K.; Nakagawa, T.; Koshino, H.; Nakata, T. *Bioorg. Med. Chem. Lett.* **1997**, 7, 2081. (e) Trotter, N. S.; Takahashi, S.; Nakata, T. *Org. Lett.* **1999**, 1, 957-959. (f) Roush, W. R.; Marron, T. G. *Tetrahedron Lett.* **1993**, 34, 5421. (g) Pfeifer, L. A.; Roush, W. R. *Org. Lett.* **2000**, 2, 859. (h) Sohn, J.-H.; Waizumi, N.; Rawal, V. H. *J. Am. Chem. Soc.* **2005**, 127, 7290-7291. (i) Trost, B. M.; Yang, H.; Probst, G. D. *J. Am. Chem. Soc.* **2004**, 126, 48. (j) Toyota, M.; Hirota, M.; Hirano, H.; Ihara, M. *Org. Lett.* **2000**, 2, 2031-2034. (k) Kagawa, N.; Ihara, M.; Toyota, M. *Org. Lett.* **2006**, 8, 875-878.

3) Total synthesis of mycalamide B: (a) see ref. 2a. (b) Synthesis of 18-O-methyl Mycalamide B. Kocienski, P.; Raubo, P.; Davis, J. K.; Boyle, F. T.; Davies, D. E.; Richter, A. *J. Chem. Soc. Perkin Trans I* **1996**, 1797. (c) Kocienski, P. J.; Narquizian, R.; Raubo, P.; Smith, C.; Boyle, F. T. *Synlett* **1998**, 869.

4) Total syntheses of theopederin D: Kocienski, P. J.; Narquizian, R.; Raubo, P.; Smith, C.; Boyle, F. T. *Synlett* **1998**, 1432.

5) Total syntheses of onnamide A: Hong, C. Y.; Kishi, Y. *J. Am. Chem. Soc.* **1991**, 113, 9693.

6) Other synthetic studies for pederin family: (a) Hoffmann, R. W.; Schlapbach, A. *Tetrahedron* **1992**, 34, 7903. (b) Hoffmann, R. W.; Schlapbach, A. *Tett. Lett.* **1993**, 34, 7903. (c) Hoffmann, R. W.; Breitfelder, S.; Schlapbach, A. *Helv. Chim. Acta*, **1996**, 79, 346. (d) Meinwald, J.; *Pure and Appl. Chem.* **1977**, 49, 1275-1290. (e) Adams, M. A.; Duggan, J.; Smolanoff, J.; Meinwald, A. *J. Am. Chem. Soc.* **1979**, 101, 5364.

-
- 7) Jiang, X.; Garcia-Fortanet, J.; De Brabander, J. K. *J. Am. Chem. Soc.* **2005**, *127*, 11254.
- 8) Rech, J. C.; Floreancig, P. E. *Org. Lett.* **2005**, *7*, 5175.
- 9) Huang, X.; Shao, N.; Palani, A.; Aslanian, R.; Buevich, A. *Org. Lett.* **2007**, *9*, 2597.
- 10) Shangguan, N.; Kiren, S.; Williams, L. J. *Org. Lett.* **2007**, *9*, 1093.

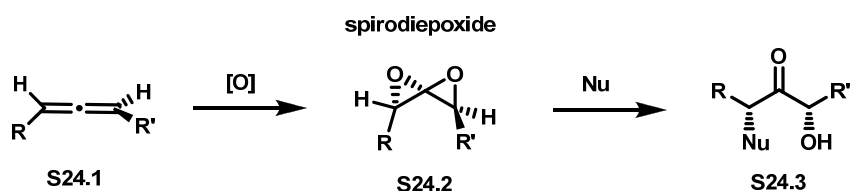
Chapter III

Spirodiepoxide Application: Psymberin

I. Background Information for Spirodiepoxides

Spirodiepoxides (SDE) result from the double oxidation of an allene (Scheme 24, S24.1→S24.2). These molecules have an unusual structure bearing two affixed epoxides and represent a rare functional group. They are electrophilic compounds which would be expected to readily react with nucleophiles. Opening of SDEs with nucleophiles leads to a motif that has a ketone, alcohol and substituent corresponding to the nucleophile (S24.3). It also generates two stereocenters at the alpha positions of the ketone. The major product is syn. As with other cascade reactions, allene oxidation to SDEs offers a new way to access densely functionalized structures.

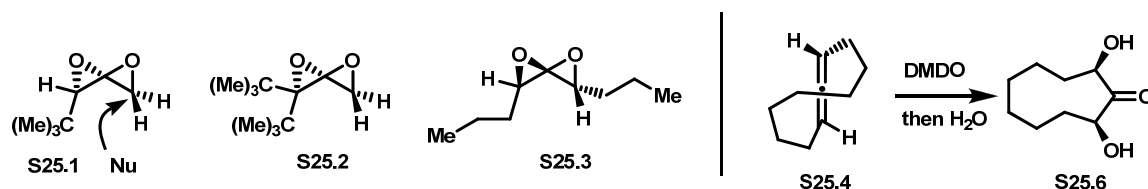
Scheme 24 SDE Formation and Opening



The oxidation of allenes can be accomplished by either a peracid oxidant or a neutral non-nucleophilic oxidant such as dimethyl dioxirane (DMDO). Decomposition of SDEs to various products can occur due to the acid by-product of oxidation by a peracid. However, DMDO affects a clean oxidation leading to isolable SDEs. The Crandall group performed initial studies of the formation and reactivity of SDEs after the discovery of

DMDO.¹ The SDEs studied were derived from unfunctionalized, achiral, symmetric allenes (Scheme 25, **S25.1**→**S25.3**). The addition of different types of nucleophiles to these SDEs, both intermolecularly and intramolecularly, was studied, which afforded modest product formation. The heteroatom nucleophiles for intermolecular opening of SDEs were water, alcohols, acetic acid, amines imidazole, thiophenol, fluoride and chloride.¹ⁱ The addition of these nucleophiles was observed to attack at the less sterically hindered carbon atom of the SDE functionality in S_N2 fashion. Also, the addition of water to the cyclic SDE **S25.4** showed that both hydroxyl groups were oriented in the same direction (**S25.6**), which was the only example demonstrating that the syn product is the major product obtained from addition of a nucleophile to a SDE.¹ⁱ

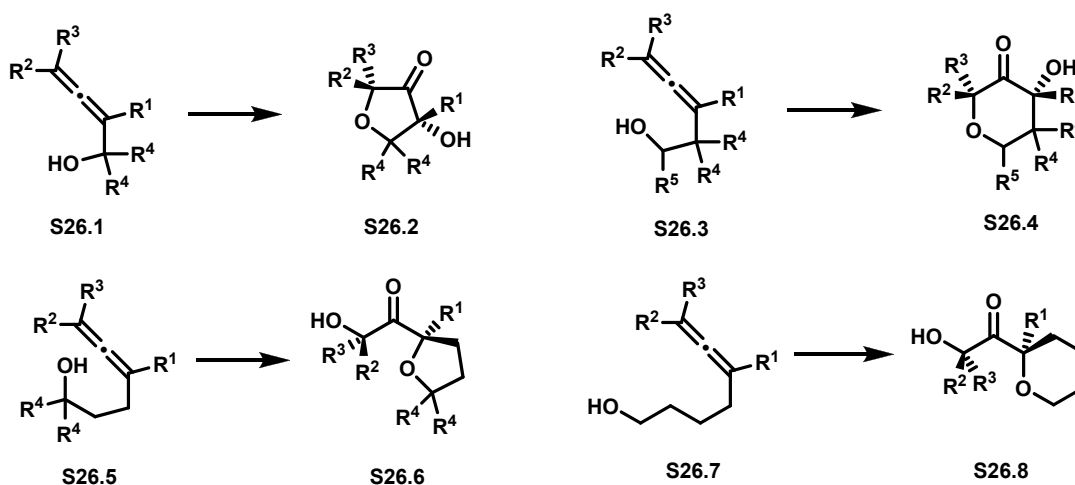
Scheme 25 SDEs by the Crandall Group



In the case of intramolecular nucleophilic addition to a SDE they reported formation of functionalized oxygen heterocycles from allenes tethered with three types of functional groups; (a) alcohols, (b) carboxylic acids, (c) aldehydes. The opening of α,δ -allenyl alcohols formed the furan products (**S26.1**→**S26.2** and **S26.5**→**S26.6**), while β,γ -allenyl alcohols gave the pyran products (**S26.3**→**S26.4** and **S26.7**→**S26.8**).^{1g,1j} Relatively simple allenes, where R¹, R², R³, R⁴ were either H or CH₃ groups, were used for the investigation. The primary and tertiary alcohols were observed to efficiently open SDE intramolecularly, while no secondary alcohol openings were reported. The

regiochemistry of ring closure was dictated by the number of carbons in the tethered chain in order to give favorable five or six-membered heterocycles by either exo or endo-cyclization.²

Scheme 26 Cyclization of Allenic Alcohols



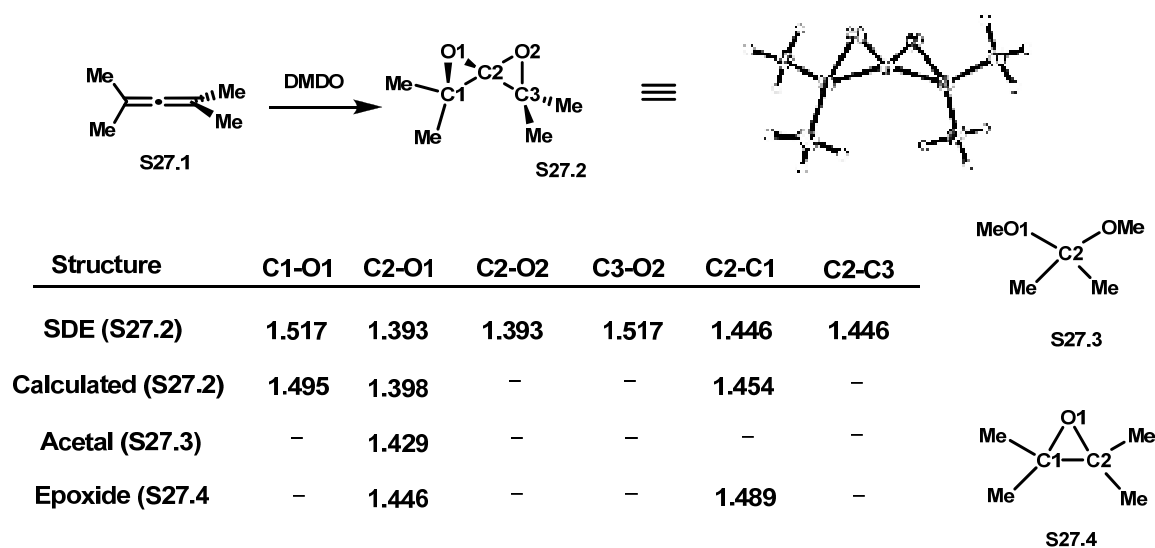
They also showed cyclization of several simple allenyl carboxylic acids to provide five or six membered functionalized lactones.^{1h,1j} Moreover, oxidation of allenyl aldehydes and ketones led to the formation of corresponding cyclized products, which were either hemiacetals or ketals depending on the solvent used.^{1k} Interestingly, no oxidation of aldehydes was observed since it is slower than that of an allene.

The Williams group has focused on developing new reactions and applying them to the synthesis of biologically and chemically important molecules.³ The first use of SDE in total synthesis was elegantly demonstrated in the synthetic studies for the natural product, epoximicin.^{3f} In the course of these studies, it was also shown that SDEs can be opened by different nucleophiles such as azides, the anion from of benzenesulfonamide, lithium benzimidate and others. Additionally, the opening of SDEs with organocuprates

was developed and the efficiency of this methodology was demonstrated in the synthesis of a stereotetrad found in 9*S*-dihydroerythronolide A.^{3e}

Our group also obtained the first crystal structure of the SDE derived from oxidation of tetramethyl allene (Scheme 27).^{3c} Surprisingly, treatment of the allene (**S27.1**) with DMDO afforded the solid SDE (**S27.2**) which has a low melting point and thus purified by sublimation. The crystal structure data revealed significant information regarding key bond lengths, which were highlighted by the comparison to the data of a simple acetal (**S27.3**) and epoxide (**S27.4**). Significant structural features of SDE include; (a) shorter C2-O1/O2 bond lengths than simple acetals, (b) shorter C2-C1/C3 and C2-O1/O2 bonds than epoxides, (c) longer C1-O1 and C3-O2 bonds than epoxides. These data were also compared and matched to the data obtained computationally.

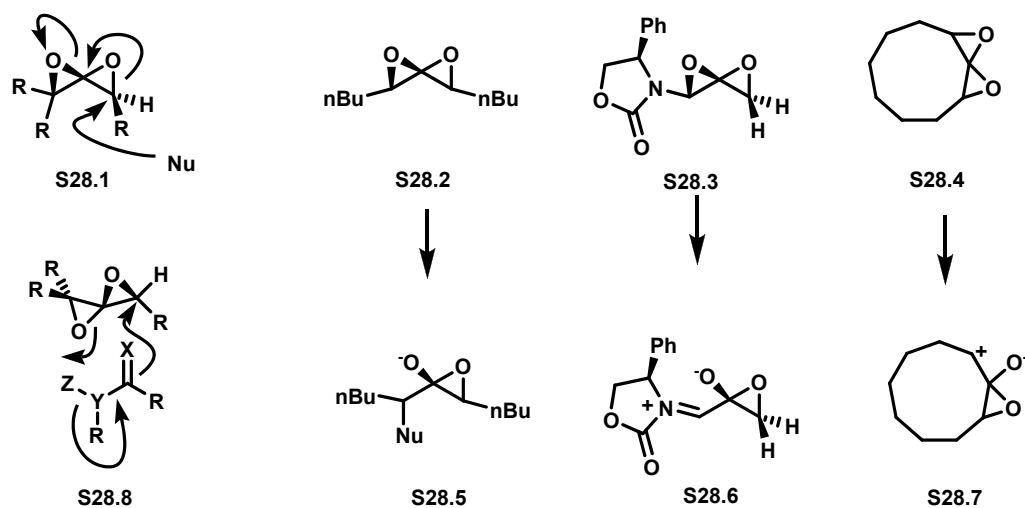
Scheme 27 Crystal Structure of SDE



The mechanism of SDE opening is probably a one step process, even though there are some reported mechanistic models which involve charged intermediates (**S28.1** versus **S28.2**, **S28.3**, and **S28.4**). It is known that anionic nucleophiles open SDEs readily.

However, SDEs must be activated for neutral nucleophiles. These hydrogen-bonding activators are mostly hydroxylic reagents like water or methanol. A new type of nucleophiles which both activate and open SDEs was discovered by our group. We demonstrated an elegant way to form heterocycles from neutral nucleophiles such as benzamide, thiobenzamide and benzamidine.^{3c} The transition model (**S28.8**) proposed for these transformation features similarly concerted opening of the activated SDE. This was also supported by computed transition models. It revealed that the C1-O1 bond lengthens, the O1-C2 bond shortens, and the C2-O2 bond lengthens when nucleophiles attack the SDE (Scheme 28).

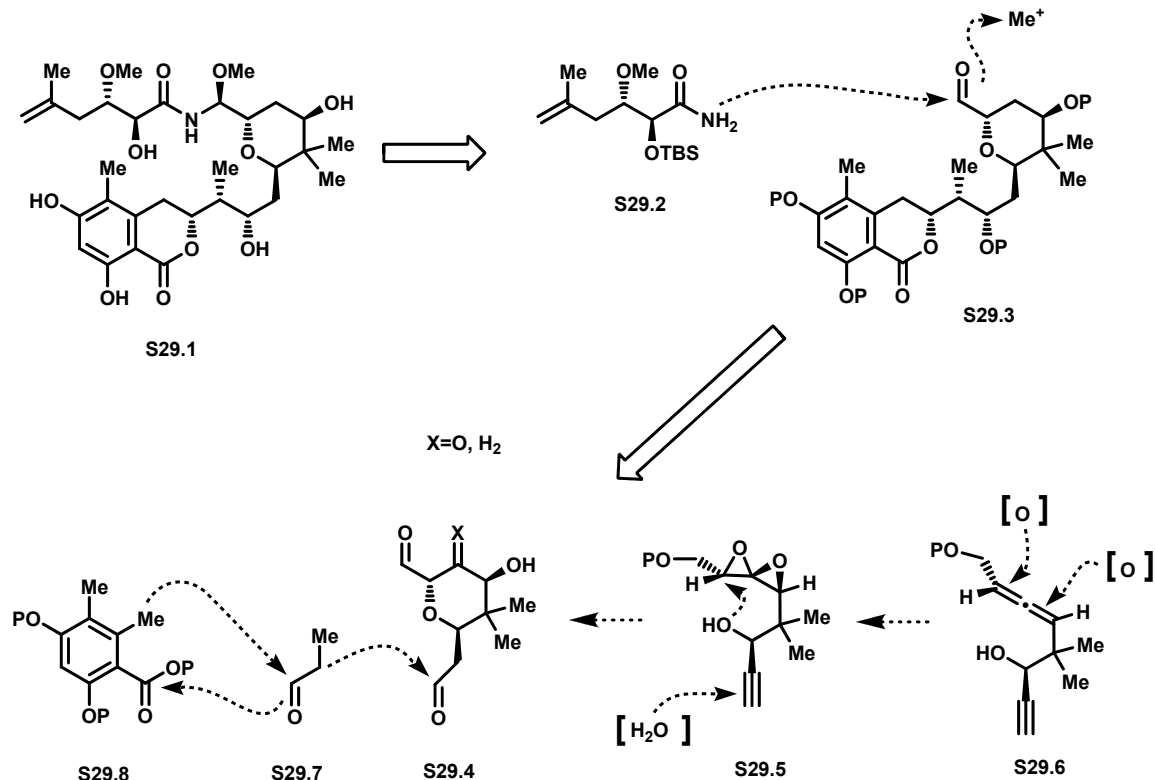
Scheme 28 Transition Models for SDE Opening



II. Spirodiepoxides in Psymberin Synthesis: 1st generation

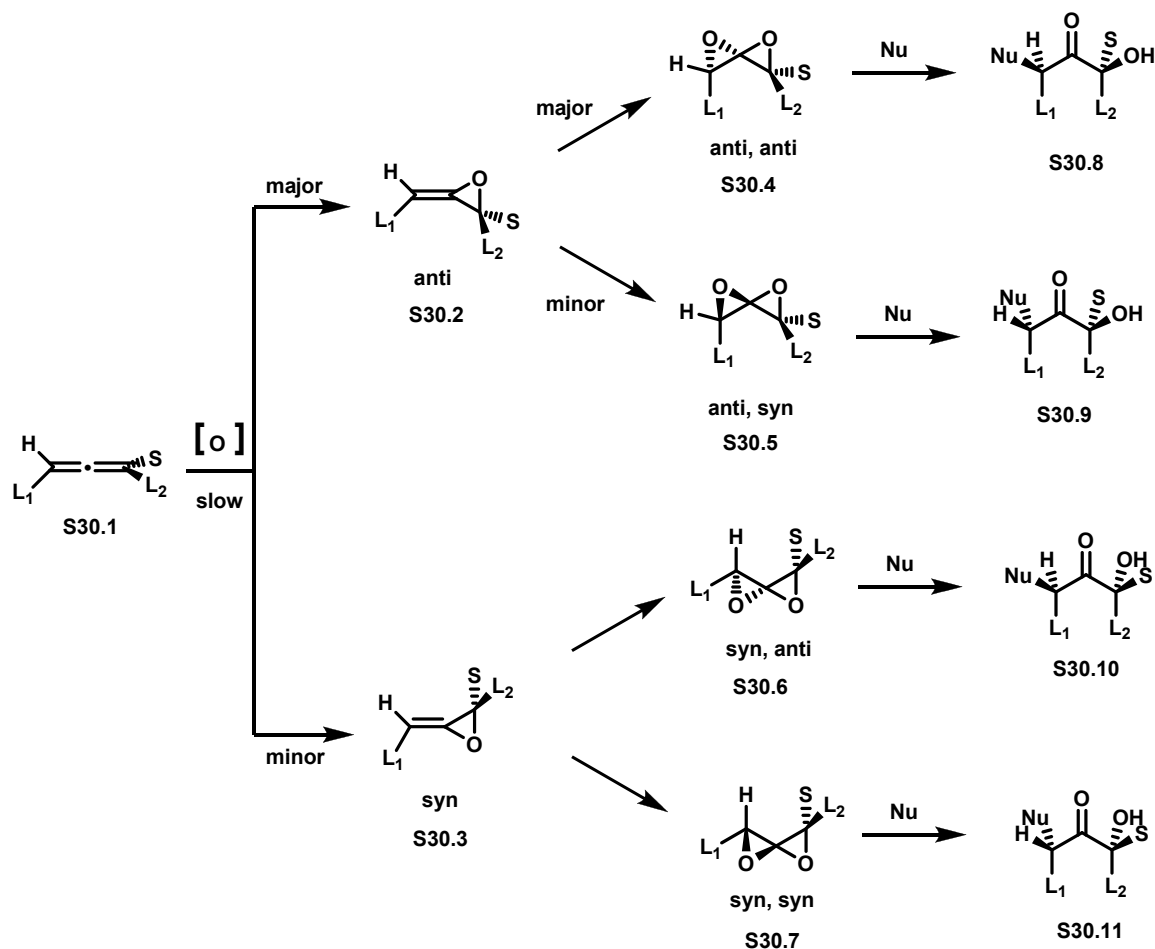
As mentioned earlier, we wanted to synthesize psymberin and its analogs as well as hybrid structures. Therefore, we needed a novel and feasible strategy to reach this goal. As expected, the natural product **S29.1** was bisected into two segments; psymberic amide **S29.2** and the right segment **S29.3**. Preparation of **S29.3** of psymberin was a challenge as it contains a highly substituted core tetrahydropyran ring and an appended dihydroisocoumarin ring. We envisioned the core tetrahydropyran ring **S29.4** could be accessed from SDE **S29.5**, which would be derived from oxidation of allene **S29.6**. This key step would give us both a highly oxygenated (X=O) and subsequently a simpler ring (X=H), which would enable us to prepare a range of psymberin analogs and hybrid structures. Addition of a propionate unit **S29.7** followed by dihydroisocoumarin ring formation using **S29.8** would complete the synthesis of the right segment. Direct coupling of these two units will be discussed in chapter 4.

Scheme 29 Synthetic Plan: 1st generation



Unlike alkenes, oxidation of allenes includes a problem of regioselectivity. In general, the more substituted double bond will be more easily oxidized because it is more electron rich. In the case of mono- and tri-substituted allene the more substituted double bond will be oxidized first, but in case of di- and tetrasubstituted allenes regioselectivity may be governed by steric and electronic effects. The oxidation of trisubstituted and disubstituted allenes was demonstrated in Scheme 30. Another problem is stereoselectivity. The oxidation should take place on the face of the double bond which is most accessible.

Scheme 30 Stereoselectivity in Allene Oxidation

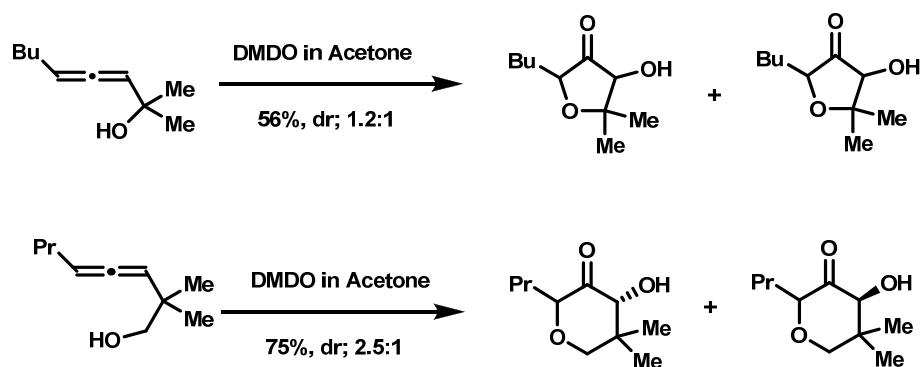


The first oxidation is comparatively slow and leads to the formation of major-anti (S30.2) and minor-syn (S30.3) allene oxides. The allene oxides which are very reactive because of their electron rich nature should oxidize rapidly and result in formation of SDEs.⁴ The other problem is opening of a SDE regioselectively. The nucleophilic attack takes place on the carbon with less substituents for S_N2-like reactions and could give up to four different products (S30.8, S30.9, S30.10, S30.11). S30.8 and S30.11 as well as S30.9 and S30.10 are enantiomers. The major product should be S30.8 resulting from the anti-anti SDE (S30.4), whereas the minor will be S30.9, formed from S30.5. The formation of the antipodal products (S30.10 and S30.11) may not be observable if the

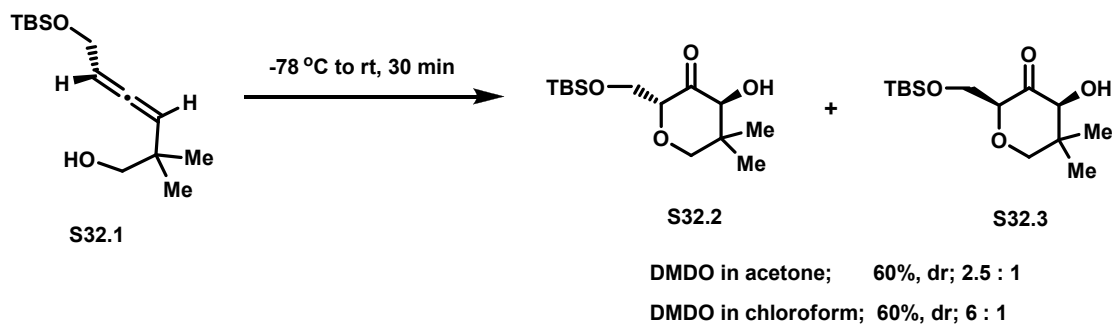
formation of the syn allene oxide (**S30.3**) is low. The ratio of the second oxidation will reflect the ratio of the major and minor products. For example, if the selectivity of the first oxidation is high ($>20:1$) and the second oxidation is low ($2:1$), the ratio of products will appear to be $2:1$. Therefore, an enantiomerically pure product could be obtained from optically pure allene.

The initial work done by Crandall's group showed the formation of cyclic ethers from the oxidation of simple, unfunctionalized and achiral allenes (Scheme 26).^{1g,1j} The major problem was that the selectivity of oxidation was not synthetically useful, for example, see Scheme 31. However, our group aimed to increase the stereoselectivity of allene oxidation and to demonstrate the application in complex molecule synthesis. Dr. Shangguan, a former graduate student in our group, did some preliminary studies on the oxidation of allenes structurally similar to **S29.6**. Allene **S32.1** was prepared and treated with DMDO in acetone (Scheme 32). The corresponding SDE was cyclized immediately and afforded the isolable trans (**30.2**) and cis (**S30.3**) products in modest yield (60%) and in a ratio of 2.5 to 1, respectively.^{3d}

Scheme 31 Simple Allene Cyclizations



Scheme 32 Preliminary Results for Model Allenes



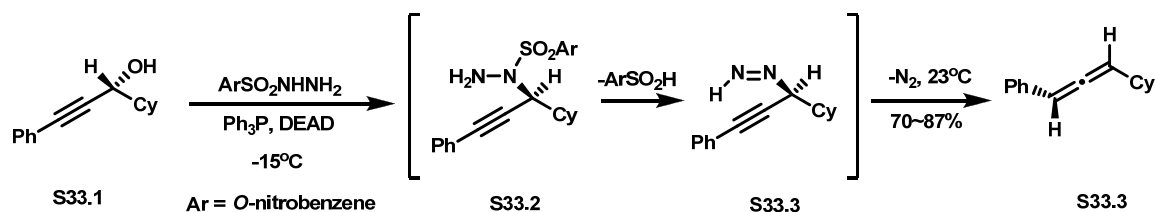
The Murray group developed a procedure to prepare DMDO in acetone.⁵ Acetone is easily oxidized to DMDO upon treatment with potassium monopersulfate (Oxone[®]) at room temperature. The low-boiling solution of DMDO in acetone is then distilled and condensed with a cold trap. The resulting solution is a low concentration of DMDO (0.05-0.1M). However, Messeguer's group reported a modified procedure to increase the concentration of DMDO in different solvents such as chloroform, dichloromethane, ethyl acetate and toluene. The concentration of DMDO can approach 0.3 M after extraction with chloroform. This group also checked the reactivity of a DMDO solution in chloroform by epoxidation of cis-stilbene and found out that epoxidation takes place much faster than with DMDO in acetone solution.

When allene **S32.1** was treated with DMDO in chloroform, the trans **S32.2** and cis **S32.3** products were formed in a 6:1 ratio (Scheme 32). The improved stereoselectivity of the DMDO oxidation in chloroform could be a consequence hydrogen bonding formation between DMDO and chloroform, which would make it bulkier and more active than DMDO in acetone. This could result in an increase in the selectivity of the second oxidation of an allene. Our group demonstrated the improvement of stereoselectivity in SDE formation on simple and complex allenes by using DMDO in chloroform. In

addition to this, different solvent systems have also been studied to increase stereoselectivity on the oxidation of allenes.⁶

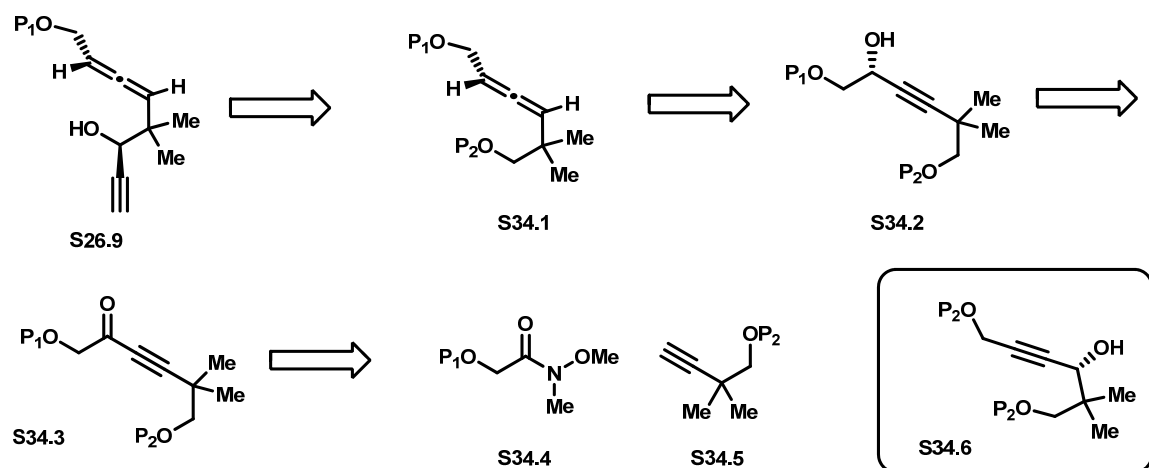
We aimed to synthesize the target allene (**S29.6**) asymmetrically. For this purpose, we pursued the Myers method to reach **S29.6** as it provides enantiomerically pure 1,3-disubstituted allenes in a single pot from propargyl alcohols.⁷ In this procedure, optically pure propargyl alcohols (**S33.1**) are treated with *O*-nitrobenzenesulfonyl hydrazide under Mitsunobu conditions to afford the optically pure adduct **S33.2** with inversion at the stereocenter. Elimination followed by ene rearrangement in situ give rise to the formation of enantiopure allenes (Scheme 33).

Scheme 33 Myers Allene Synthesis



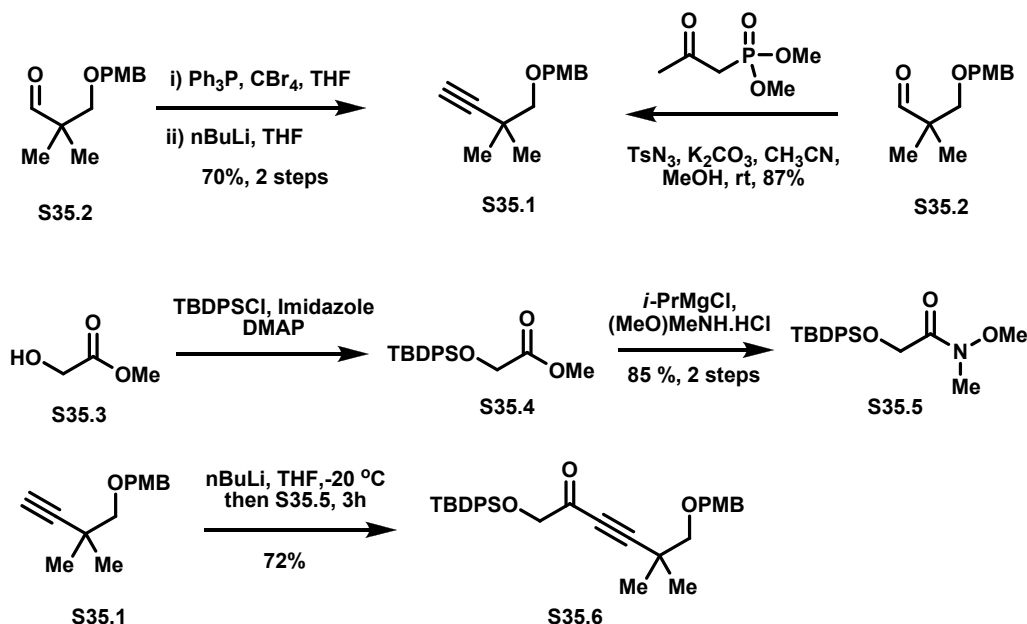
The strategy for the key allene **S29.6** leading to the core pyran ring is shown in Scheme 34. We reasoned that a simple allene (**S34.1**) could be accessed from propargyl alcohols **S34.2** and **S34.6** under the Myers conditions. Using alcohol **S34.2** would be a better choice since the first step, a Mitsunobu inversion reaction, would suffer from the presence of a neopentyl center in alcohol **S34.6**. The preparation of alkynone **S34.3** would be accomplished from the coupling of Weinreb amide (**S34.4**) and alkyne (**S34.5**).

Scheme 34 Synthetic Strategy for Allene S29.6



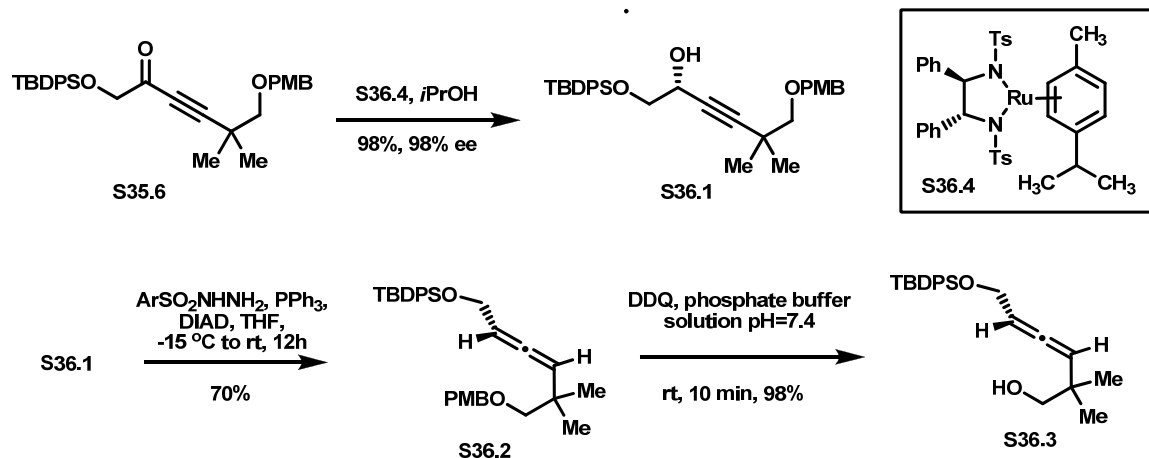
The synthesis is presented in Scheme 35. The alkyne (**S35.1**) was prepared using two different conditions from the same starting material. Under the Corey-Fuchs condition, aldehyde **S35.2** was reacted first with triphenylphosphine and tetrabromomethane to yield a dibromoalkene compound, which on treatment with *n*-BuLi afforded the alkyne in 70% yield after two steps.⁸ This reaction, when used in large scale, produced amounts of insoluble triphenylphosphine oxide solid as a by-product that were not easy to separate from the desired product. The Seyferth-Gilbert condition converted **S35.2** to **S35.1** in a higher yield 87% and provided an easier work-up to remove all the solids with a water wash.⁹ For the Weinreb amide synthesis (**S35.5**), the methyl glycolate (**S35.3**) was first protected with TBDPS and was then added to a solution of *i*-PrMgCl and Me(OMe)NH.HCl to give **S35.5**.¹⁰ To couple these two units, **S35.1** was first deprotonated with *n*-BuLi reagent and then treated with **S35.4** to give alkynone **S35.6** in 72% yield.

Scheme 35 Preparation of Alkyne and Weinreb amide



The asymmetric reduction of alkynone (**S35.6**) was achieved by using the Noyori condition (Scheme 36).¹¹ To a solution of Ru catalyst with chiral ligand (**S36.4**) in isopropanol was added a solution of (**S35.6**) in isopropanol at room temperature, which produced the product readily in 98% yield. The optical purity of the propargyl alcohol (**S36.1**) was measured by Mosher esters analysis and found to be 98% ee. It is known that a terminal alkyne can poison the Noyori catalyst. Therefore, using pure starting material is crucial for the reaction. The next step was the application of Myers' method to furnish the optically pure allene (**S36.2**) from **S36.1**, which gave the desired product in 70% yield. The side product of this reaction was found to be a product resulting from migration of the TBDPS group from primary alcohol to secondary alcohol. Also, the yield of the reaction was sensitive to the purity of the *O*-nitrobenzensulfonyl hydrazide, as reported by Myers.⁶

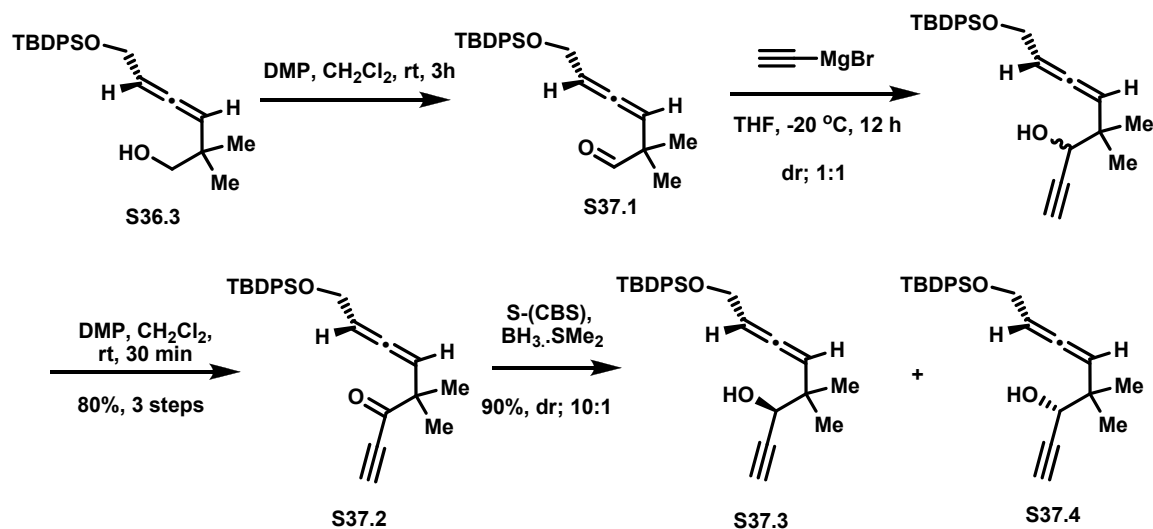
Scheme 36 Noyori Reduction



Treatment of **S36.2** with DDQ resulted in cleavage of the PMB group. The by-product anisaldehyde interestingly had the same R_f value with the original product and was hard to remove by FCC. However, reduction of it with NaBH_4 provided a clean separation of the allenyl alcohol (**S36.3**).

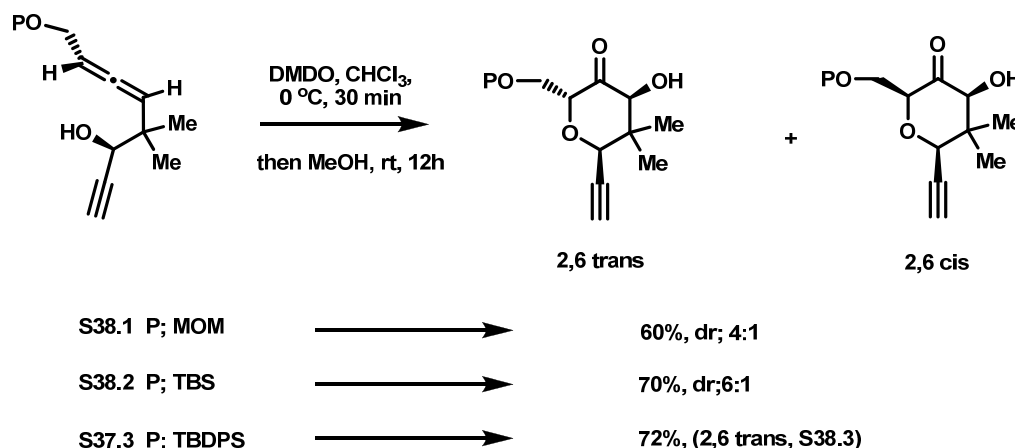
Oxidation of **S36.2** with Dess-Martin afforded the aldehyde (**S37.1**, Scheme 37), which was then treated with ethynylmagnesium bromide at low temperature to give rise to a mixture of **S37.3** and **S37.4** (dr; 1:1, determined by ^1H NMR). The diastereomeric mixture of alcohol products was exposed to the Dess-Martin reagent to afford the ketone **S37.2** in 80% yield over 3 steps. The asymmetric reduction of **S37.2** was accomplished by use of Corey-Bakshi-Shibata (*S*-isomer) reagent to give inseparable alcohols (**S37.3** and **S37.4**) in 90% yield.¹² The ratio of the reaction was 10:1, determined by ^1H NMR.

Scheme 37 Formation of the Key Allene



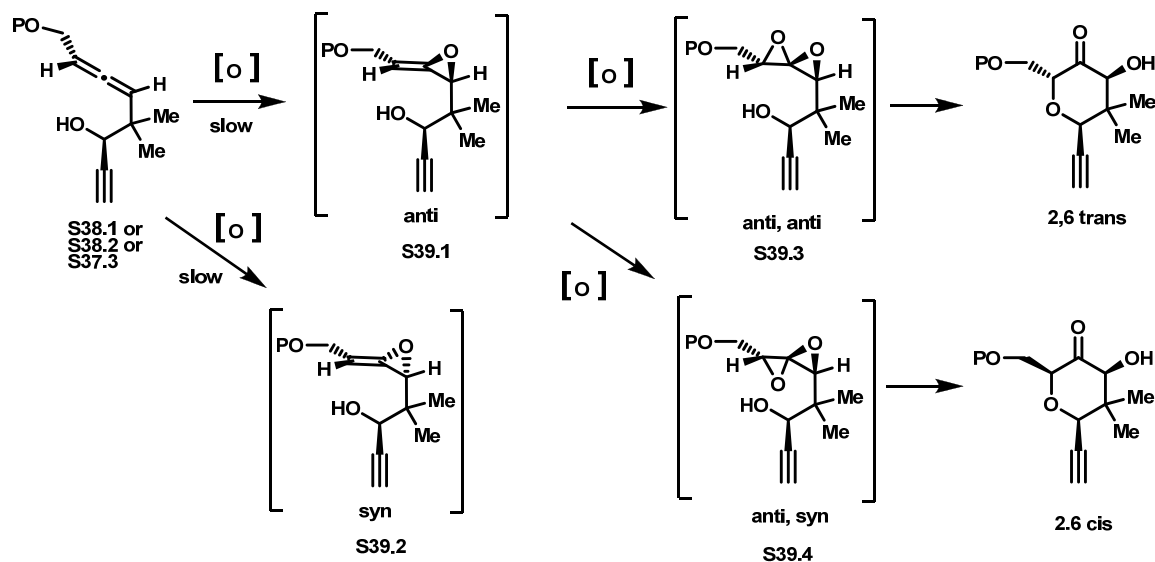
Dr. Shangguan prepared allenes **S38.1** and **S38.2** (Scheme 38). The general procedure applied for allene oxidation was: a solution of an allene in chloroform at low temperature was treated with a freshly prepared solution of DMDO. After 30 min, MeOH was added to the reaction mixture and stirred for 12h. Gratifyingly, cyclization of SDEs from all three allenes afforded 2,6 substituted trans and cis pyranones. In all cases, the 2,6 trans product was the major one. It was observed that the selectivity of the SDE formation changed with the size of the protecting groups. The bulkier they are the more selective product formation is. The smallest MOM protecting group gave a 4:1 ratio, TBS gave a 6:1 ratio. The bulkiest TBDPS group yielded 72% of the 2,6 trans disubstituted pyranone **S36.3**. With this reaction, the chemo-, regio- and stereo- selective oxidation of 1,3 disubstituted allenes was accomplished as planned. Consequently, the TBDPS group was found to be optimal for the synthesis of the target. Also, the terminal alkyne stayed intact since it is known that its oxidation with DMDO is slower than that of an allene.¹³

Scheme 38 Cyclization of Allenes



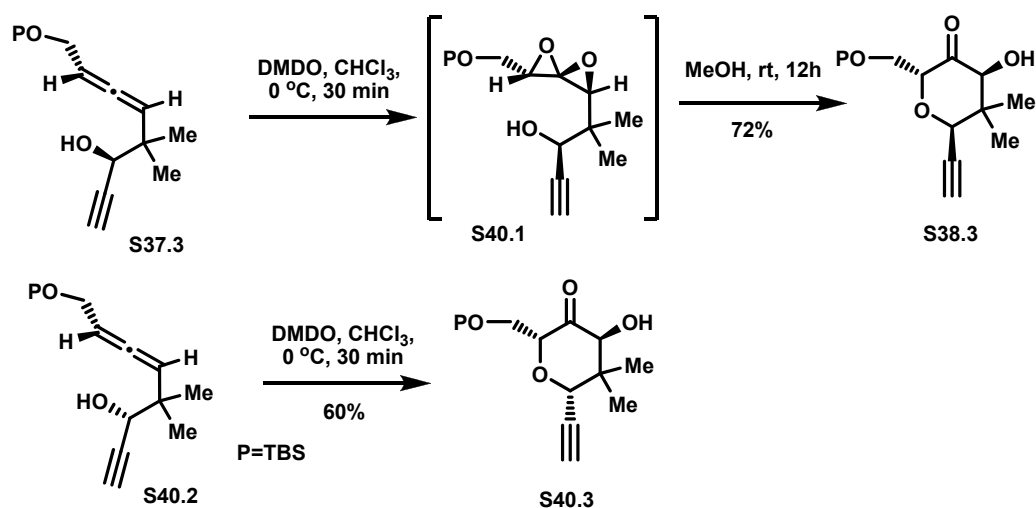
The DMDO oxidation of allenenes in Scheme 38 gave only two isomers out of a possible four (check Scheme 30) and that the selectivity of oxidation changes with the size of protecting group were interesting observations. These results can be reasoned from stepwise oxidation of allene explained as followed. The first oxidation takes place regioselectively on the double bond distal to the oxygen substituent which deactivates the proximal double bond. Moreover, this oxidation occurs slowly and highly stereoselectively, giving the anti allene oxide (**S39.1**) as the major intermediate and the syn allene oxide as minor intermediate (**S39.2**). Also, the size of the protecting groups appears to play a role in the selective formation of **S39.1** and **S39.2**. The second oxidation of **S39.1** should take place very fast and less stereoselectively, giving **S39.3** as the major SDE, since the sterically demanding *tert*-butyl group induces the delivery of oxygen from the opposite face. The minor SDE would be **S39.2**. **S39.3** and **S39.4** lead to the formation of the observed trans and cis products, respectively. The second of oxidation of the minor syn intermediate (**S39.2** could furnish the antipodal trans and cis products, but they could not be observed.

Scheme 39 SDE Formation from Allene



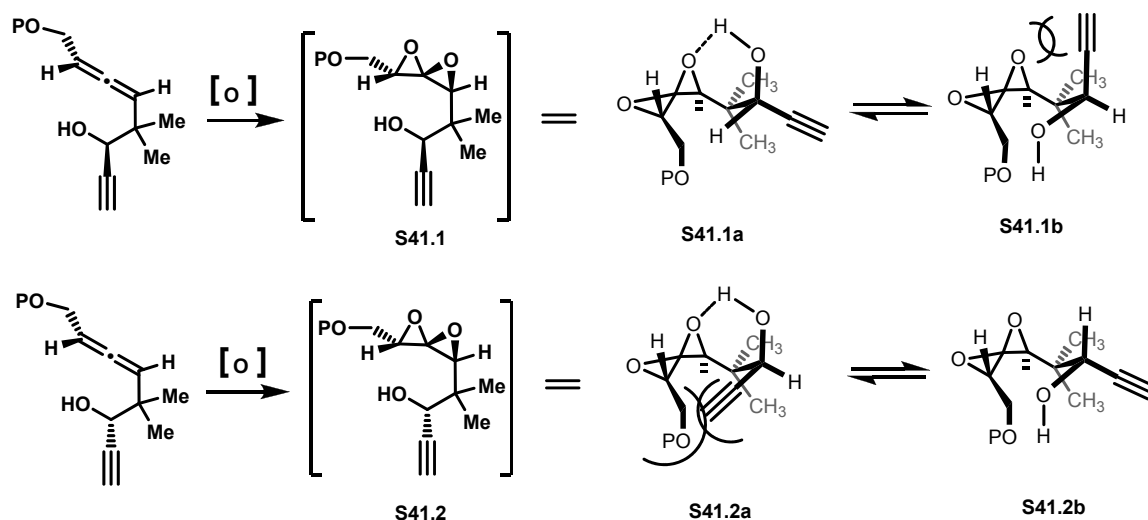
During the oxidation of allene **S37.3**, we needed to use MeOH whereas it was not necessary for the epimeric allene **S40.2** (also, P=MOM gave the same result) which cyclizes spontaneously to give the pyran ring (**S40.3**) without observing SDE (Scheme 38). These results led us to conclude that there is, surprisingly, a stable SDE (**S40.1**) formation upon oxidation of these types of allenes.

Scheme 40 Oxidation of Epimeric Allenes



The different behavior of these allenes upon oxidation and the unusual stability of the resultant SDEs could be rationalized from the conformational preferences of the SDEs shown in Scheme 41. The resistance of SDE toward cyclization could be due to both stabilization of conformer **S41.1a** via favorable intramolecular hydrogen bonding and possible destabilization of reactive conformer **S41.1b** by steric interactions between alkyne and SDE. In the case of the epimeric allene (**S40.2**) oxidation, the reactive conformer **S41.2b**, which led directly to pyranone (**S.41.2**), would be favorable because the other conformer (**S41.2a**) suffers from severe steric interactions. Therefore, the cyclization of **S41.2b** would take place faster than **S41.1a**. MeOH may act to disrupt hydrogen bonding in **S41.1a** and promote cyclization. Additionally, the side products resulting from opening of **S41.1** with MeOH was observed in low yield (<10%).

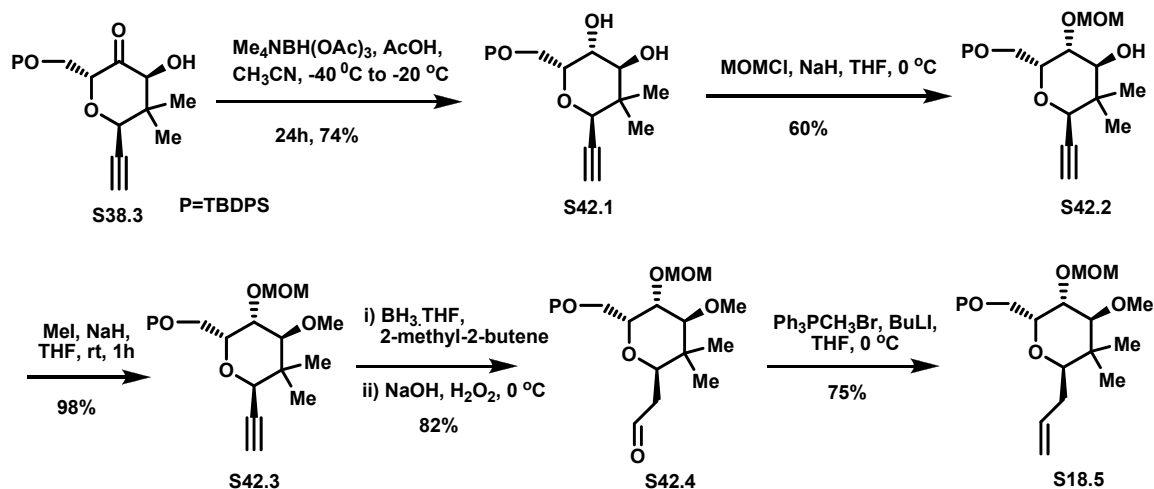
Scheme 41 Stable SDEs



III. Synthesis of the Rawal Intermediate

We targeted compound **S18.5** (Scheme 18) in the Rawal mycalamide synthesis in order to show a novel approach to access the trioxadecalin ring systems in the pederins, which would also enable us to clarify the relative configuration of the product (**S38.3**) obtained from DMDO oxidation of the key allene (**S37.3**). The **S38.3** was selectively reduced with sodium triacetoxyborohydride to give the trans diol (**S42.1**) as the major product in 74%.¹⁴ The hydroxyl group distal to the neopentyl center was selectively protected with a MOM group to give **S42.2** in 60% yield. The second protection furnished almost quantitatively **S42.3**. Hydroboration and then oxidation of **S42.3** gave rise to aldehyde **S42.4**, which was exposed to a Wittig ylide to give the alkene (**S18.5**). Based on ¹H NMR matching, the relative stereochemistry of the pyranone **S38.3** and the diol **S42.1** was proven to be correct.

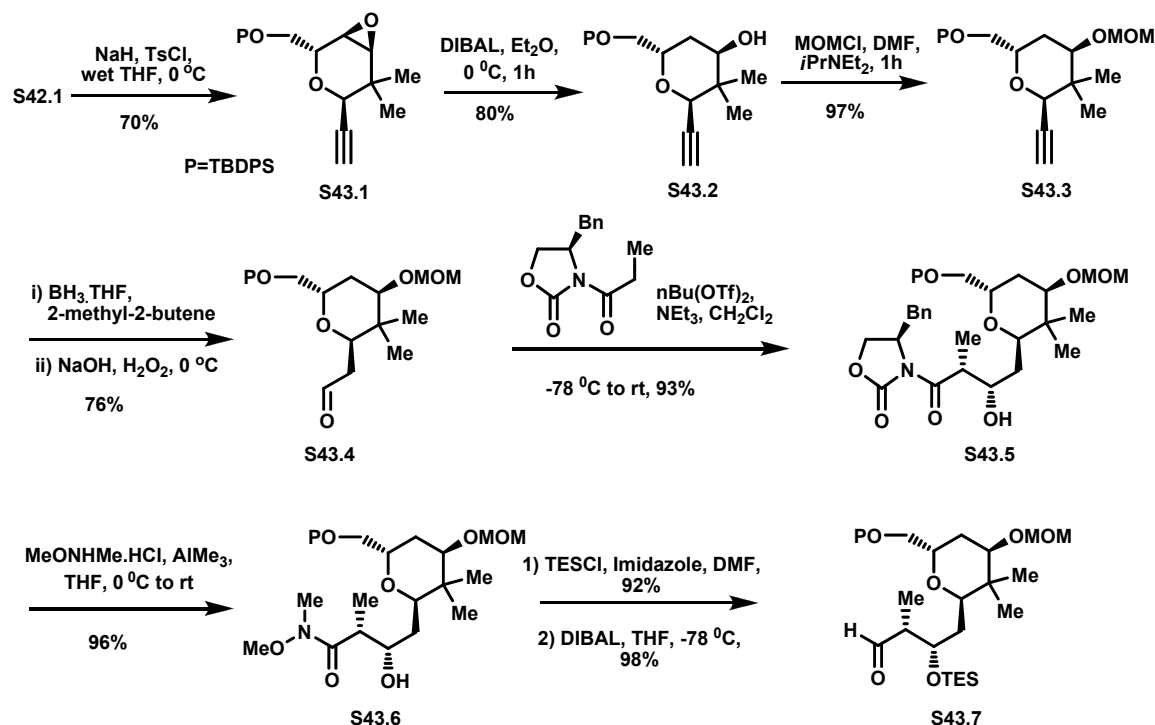
Scheme 42 Synthesis of the Rawal Intermediate



IV. Completion of the Formal Synthesis of Psymberin

In order to convert the carbonyl group in **S38.3** to a methylene, the known procedures such as hydrazine and dithiane formation were applied. But these conditions failed to give desired product formation. Nonetheless, removal of the ketone was accomplished from the pyranone (**S38.3**) in three steps. First, **S38.3** was selectively reduced to diol **S42.1** as shown in Scheme 42. Second, **S42.1** was converted to epoxide **S43.1** by treatment with tosyl chloride and NaH in wet THF (Scheme 43). For the direct epoxide formation, it is required to use wet THF, otherwise, the monotosylation of the alpha hydroxyl group in **S42.1** was observed, which could subsequently be converted to the epoxide upon treatment with NaH in wet THF. The different reactivity of both the hydroxyl groups in tosylation reaction may result from sterics. The S_N2 type displacement of tosylate with the β-hydroxyl anion is geometrically suitable to form epoxide **S43.1**. Finally, reductive opening of **S43.1** by DIBAL provided the alcohol (**S43.2**).¹⁵ The yield of the DIBAL reaction depends on the reaction time (80%, in 1h). Longer reaction times could cause cleavage of the TBDPS group and reduction of the alkyne to an alkene at the same time. **S43.1** was protected with MOM to give **S43.3** in high yield. Hydroboration/oxidation of **S43.3** gave rise to aldehyde **S43.4**, which was exposed to aldol reaction conditions to afford the major syn product (**S43.5**) in 93% yield.¹⁶ The formal synthesis of the psymberin was completed by Dr Shangguan. Briefly, conversion of **S43.5** to Weinreb amide **S43.6**, protection with a TES group and then reduction of the amide set the aldehyde (**S43.7**) for another crucial step, which was coupling with an arene partner to form the dihydroisocoumarin ring.¹⁷

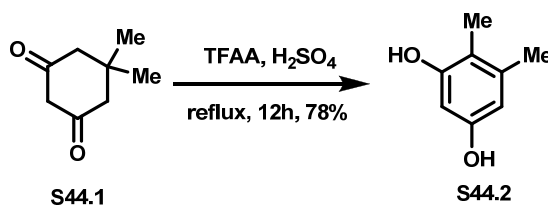
Scheme 43 Completion of Pyran Unit



To construct the dihydroisocoumarin ring, we envisioned a combination of the pentasubstituted arene (**S29.8**, Scheme 29) with an aldehyde in a single step. To do this, the ortho-toluate carbanion generated from **S29.8** with base reacts with an aldehyde to give rise to the lactone.¹⁸ Generation of similar types of carbanions and reaction with different electrophiles such as Weinreb amides and esters are reported in the literature.¹⁹ In particular, the Staunton group demonstrated formation of a lactone ring along with the side products from coupling of an aldehyde with a simple *O*-toluate carbanion.^{17e}

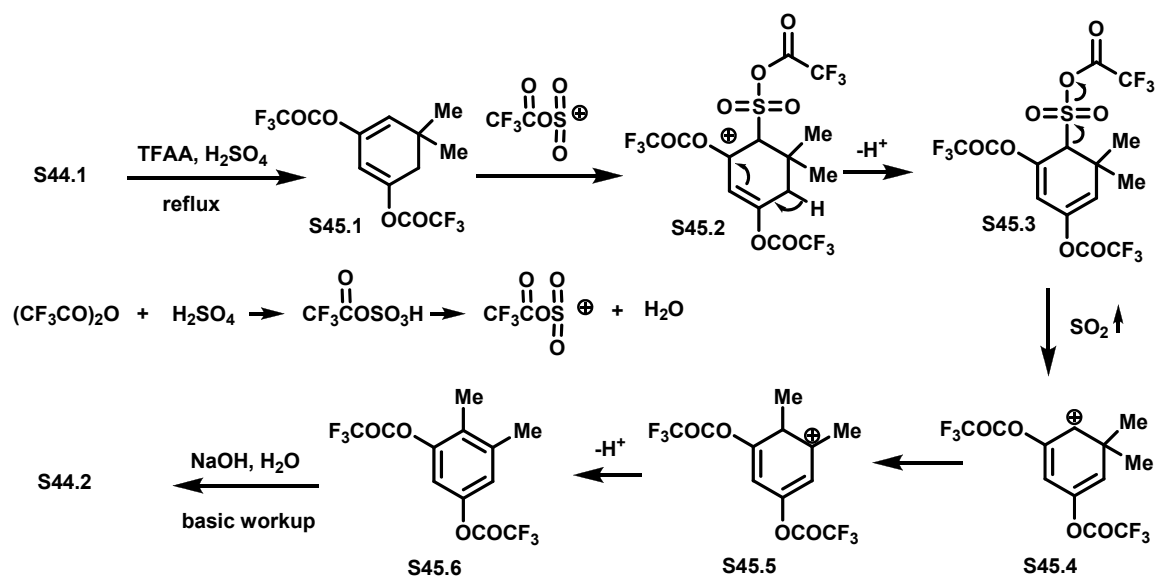
The synthesis of the arene commenced with the transformation of dimedone (**S44.1**) to the aromatic product (**S44.2**, Scheme 44). Von Doering first reported the reaction by using acetic acid anhydride and sulfuric acid.²⁰ However, Nelson's group optimized it by using trifluoroacetic anhydride.²¹

Scheme 44 Aromatization of Dimedone



A reasonable mechanism of the interesting aromatization is given in Scheme 45. The key features of the mechanism are the addition of a sulfonium cation generated from sulfuric acid and trifluoroacetic anhydride to **S45.1** to generate cationic intermediate **S45.2**. After deprotonation, evolution of SO_2 from **S45.3** takes place to generate **S45.4**. 1,2 methyl migration followed by aromatization afforded **S45.6**, which gave the desired product after basic hydrolysis.

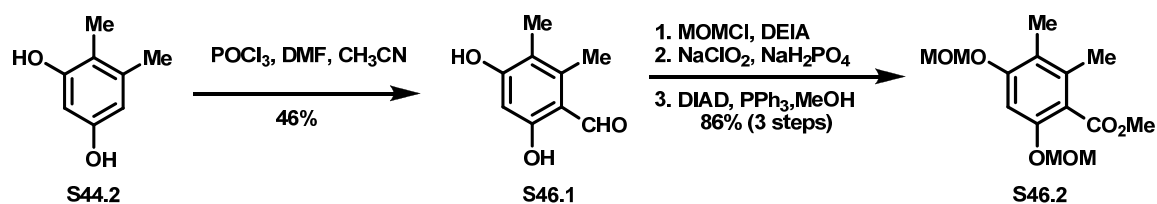
Scheme 45 Mechanism of Aromatization



The next step was the formylation of **S44.2** by applying the Vilsmeier-Haack reaction.²² The arene (**S44.2**) was exposed to phosphorous oxychloride and DMF in acetonitrile. Even though the yield of the reaction is 46%, this condition was safer than

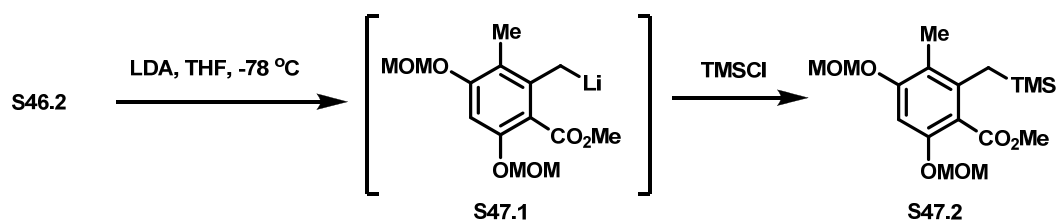
the Gatterman reaction, in which hazardous reagents like zinc cyanide and hydrochloric acid are used.²³ The resulting hydroxyl aldehyde (**S46.1**) was masked as a MOM ether, oxidized to the carboxylic acid, and converted to the methyl ester (**S46.2**). The yield of the reaction sequence was 86% after three steps.

Scheme 46 Formation of Arene S44.2



In order to see the formation of *O*-toluate carbanion formation, **S46.2** was treated with LDA at low temperature (Scheme 45). The deep red color indicated enolate formation (**S47.1**). Addition of TMSCl gave **S47.2**. In addition, the studies showed the MOM protection group was stable, while the silyl and Bn protecting groups did not survive under the reaction conditions.

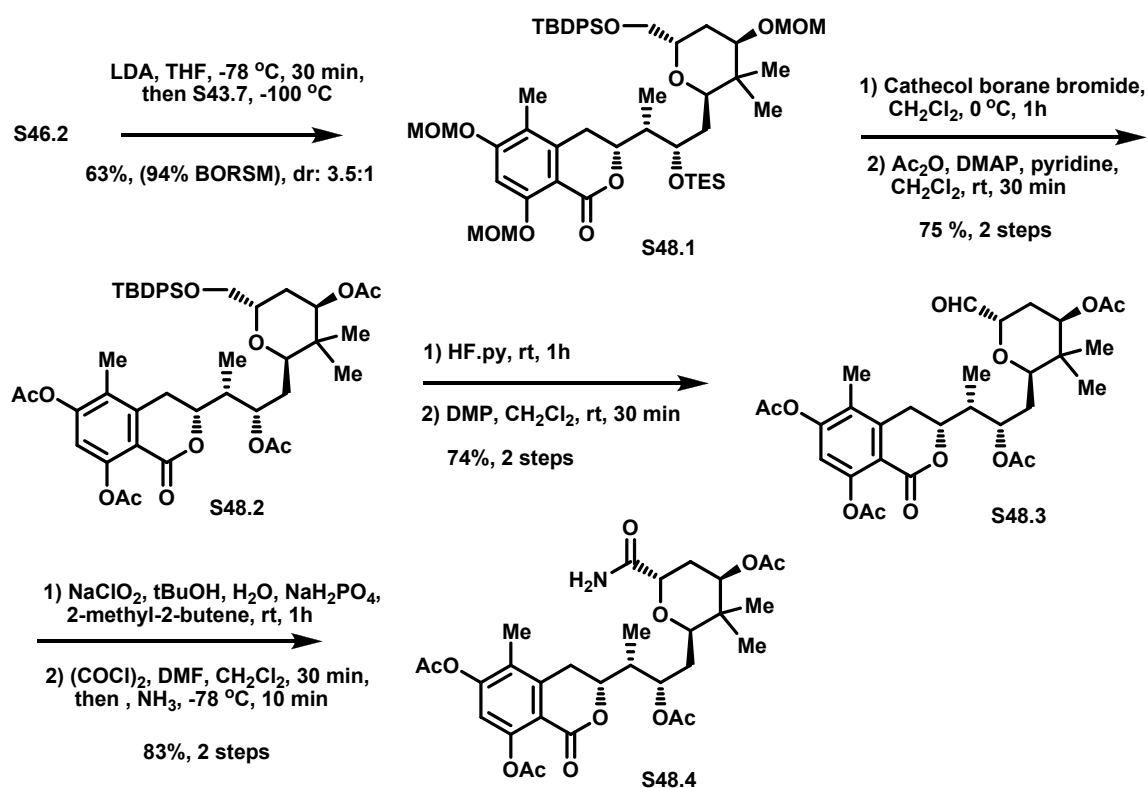
Scheme 47 Anion Formation from Arene S42.2



To couple **S47.2** and **S43.7** in the real system, the anion generated from **S44.2** by treatment with LDA at -78 °C was slowly added to the precooled aldehyde (**S43.7**) solution in THF. The inverse and slow addition of *O*-toluate carbanion was preferred to

diminish the side product, which formed from the addition of carbanion to the corresponding lactone product (**S48.1**). The coupling reaction gave **S48.1** as the major product predicted according to the Felkin-Ahn model in a ratio of 3.5 to 1 (64% yield, 94% brsm). Gratifyingly, the formation of the dihydroisocoumarin ring from the coupling of the pentasubstituted arene **S47.2** and complex aldehyde **S43.7** represented the most sophisticated example to date. Removal of all MOM and TES protecting groups followed by acetylation furnished **S48.2** in 75% yield over 2 steps.²⁴ Cleavage of the TBDPS group and then oxidation gave the aldehyde (**S48.3**) in 74% yield after 2 steps. Oxidation of **S48.3** to a carboxylic acid and then amidation gave rise to amide **S48.4**, which has identical ¹H, ¹³C NMR and optical rotation to the earlier data reported by De Brabander. The formal synthesis of psymberin was accomplished.²⁵

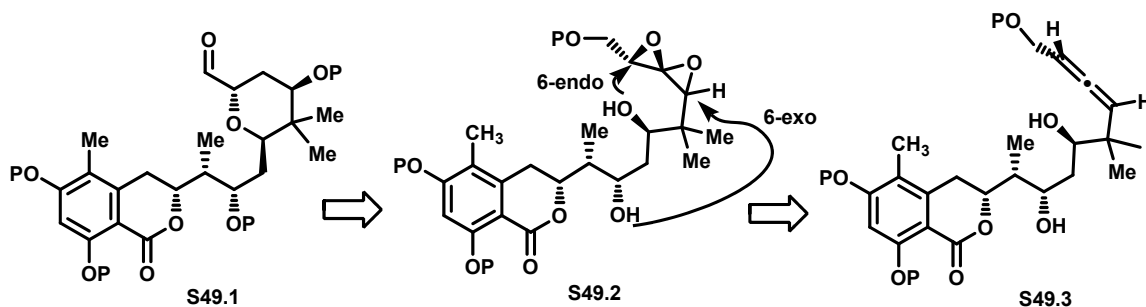
Scheme 48 Completion of Formal Synthesis



IV. Spirodiepoxides in Psymberin Synthesis: 2nd generation

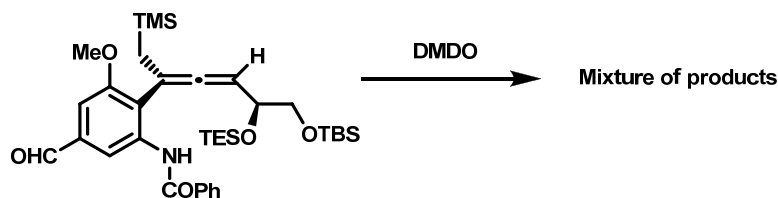
The synthesis of the right segment of psymberin was accomplished in 25 steps from known aldehyde (**S33.1**, Scheme 33). Our novel strategy demonstrated the oxidation of comparatively complex allene chemo-, regio-, and stereoselectively. The facile intramolecular opening of the resulting SDE to form six-membered cyclic ether represented the first application in the synthesis of complex molecules. Moreover, construction of a dihydroisocoumarin ring from complex partners proved to be an elegant and efficient method. In light of these promising results, the synthesis of **S49.1** was envisioned from the SDE (**S49.2**) derived from oxidation of a more functionalized allene **S49.3** (Scheme 49). This would enable us to reach the target more directly and advance our understanding of the functional and protecting group compatibility of SDE chemistry. Moreover, the trend for the preference of epoxide opening has been studied in detail and found to be 5-exo>6-exo>6-endo. However, the trend for SDE cyclization has not been well established. Therefore, the oxidation of **S49.3** and exo vs endo opening in the presence of multiple hydroxyl groups is of interest. In the case of allene **S49.3**, it would be expected that 6-endo mode would be favorable over the neopentyl-like 6-exo cyclization despite the fact that 6-exo is more preferable in unbiased epoxide systems. The competition between the two modes, which could lead to complex mixtures of products, could be resolved if one of the hydroxyl groups was protected.

Scheme 49 Synthetic Strategy for 2nd Generation



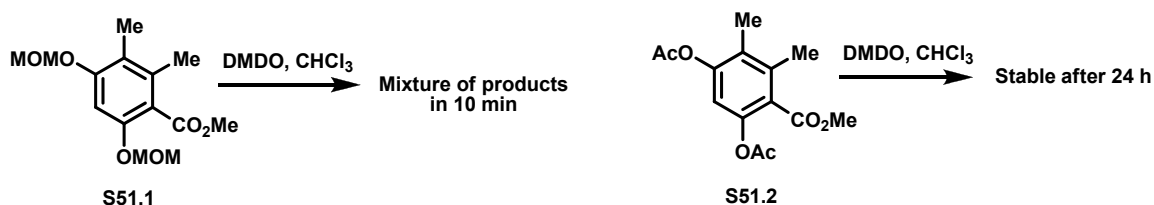
In related synthetic studies toward FR900482 mitomicinoids, the Williams group found that oxidation of the complex allene with DMDO gave several products, presumably due to deterioration of arene moiety.^{3a}

Scheme 50 DMDO Oxidation of Allene in FR Synthesis



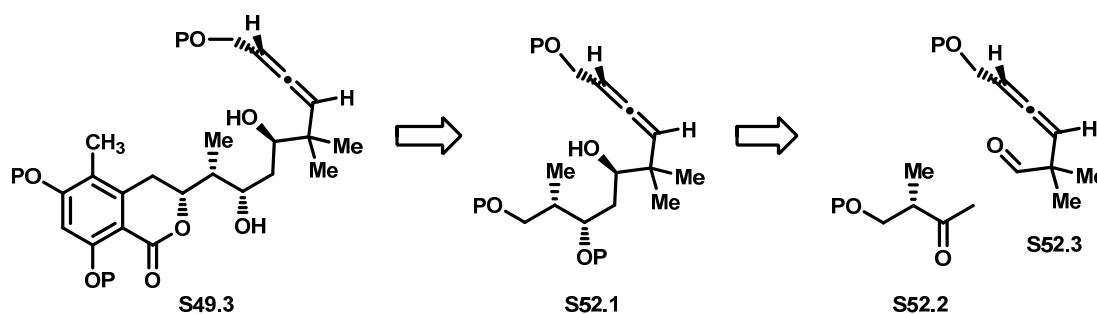
In order to prevent this problem for allene **S49.3**, the stability of arenes with MOM (**S51.1**) and acetate (**S51.2**) protecting groups under oxidation conditions were tested (Scheme 51). When **S51.1** was treated with DMDO, many products were observed within 10 min. However, **S51.2** was stable even after 24 hours. This different behavior could be reasoned from the nature of protecting groups, where an electron withdrawal acetate group could decrease the reactivity of an otherwise electron rich arene toward DMDO.²⁶

Scheme 51 Stability of Arenes



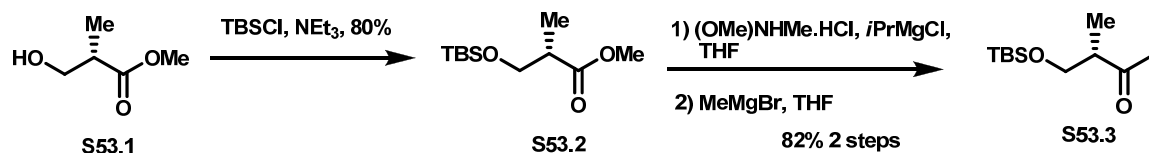
It was observed that PMB and Bn protecting groups may be cleaved under oxidation conditions. Therefore, this problem as well as protecting group compatibility prompted us to revise the second generation synthesis of psymberin. Our interest was to prepare an allene without an arene unit, which may not cause the above-mentioned problems. We envisioned that allene (**S49.3**) would be accessed from **S52.1**, which could be prepared from two simpler units; the allenyl aldehyde (**S52.3**) and a ketone (**S52.3**). Coupling of the two units could be achieved via the Paterson aldol condition.²⁷ The reagent controlled reduction of a ketone followed by selective protection of the hydroxyl group would generate the allene, ready for DMDO oxidation.

Scheme 52 Revised 2nd generation Strategy



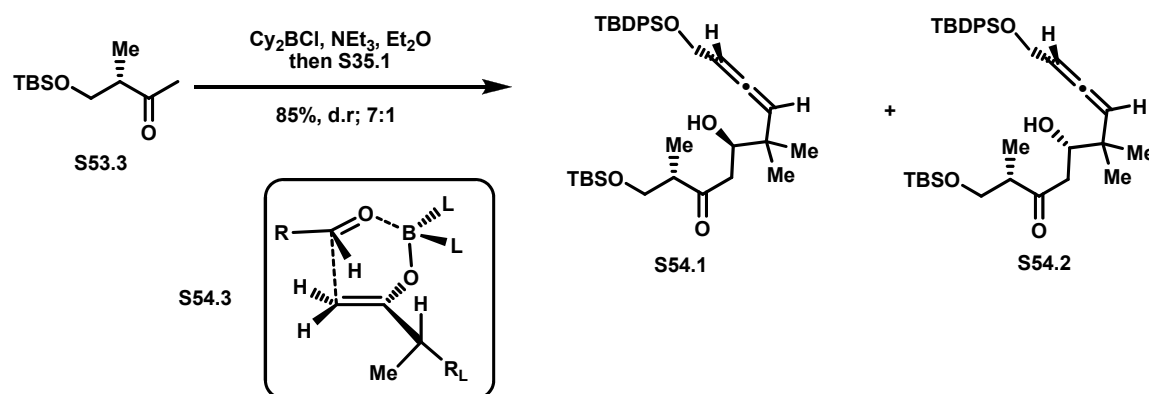
The known ketone (**S53.3**) was prepared in 3 steps from the chiral methyl ester (**S53.1**). TBS protection gave **S53.2**, which was converted to a Weinreb amide and then ketone (**S53.3**) in 82% yield after 2 steps (Scheme 53).

Scheme 53 Synthesis of Ketone S53.3



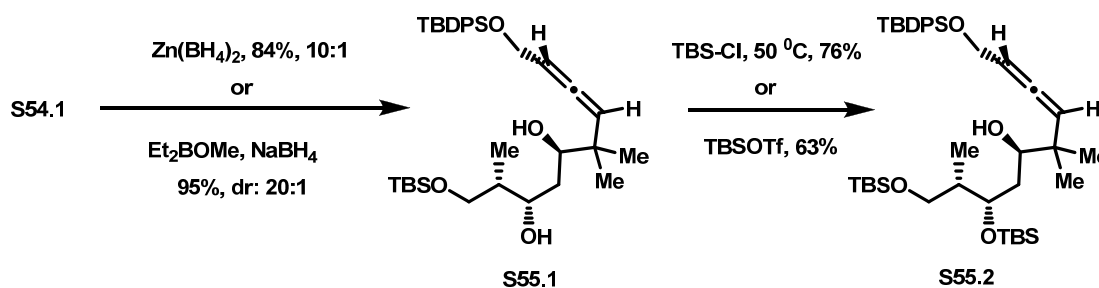
After a solution of **S53.3** in diethyl ether was treated with NEt_3 and Cy_2BCl at low temperature, a solution of allene aldehyde (**S37.1**, Scheme 37) in the same solvent was added to the reaction mixture at -78°C . The resultant alcohols were separated by FCC, providing the major product (**S54.1**) in 74% yield, and **S54.2** in 11% yield (dr; 7:1). The high selectivity of the substrate directed aldol reaction using an achiral borane reagent has been explained with a transition state model (**S54.3**) by the Paterson group. In the proposed chair-like transition state, the large R group of a ketone is positioned in such a way as to minimize destabilizing steric interactions.²⁵ The efficiency and reliability of the reaction was shown in the synthesis of complex molecules by the same group.^{25c} In order to ensure that the major product had desired configuration, the reaction was repeated with a chiral borane reagent providing **S54.1** as major product with a higher selectivity (<20:1), albeit in lower yield (30%).

Scheme 54 Paterson Aldol Reaction



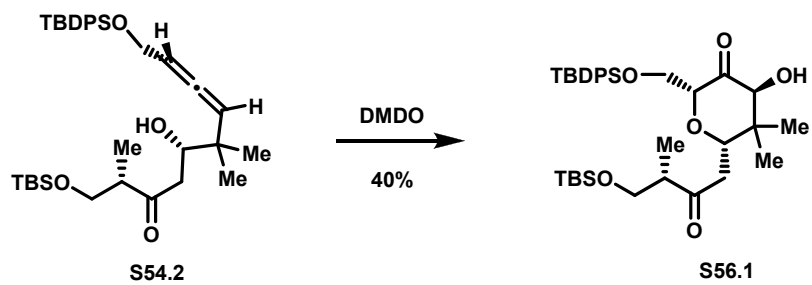
For the substrate directed asymmetric reduction of ketone **S54.1**, two different conditions were applied to provide 1,3 syn diol (Scheme 53). Treatment of **S54.1** with $(\text{Et})_2\text{BOMe}$ and NaBH_4 gave **S55.1** in higher yield and ratio (95%, dr:20:1) than ZnBH_4 (84%, 10:1). The hydroxyl group distal to the neopentyl center in **S55.1** was selectively protected with either TBSOTf or alternatively with TBSCl to yield **S55.2**. Yields were not optimized.

Scheme 55 Asymmetric Reduction of Hydroxyl Ketone



Unfortunately, the oxidation of **S55.2** with DMDO gave rise to a mixture of products. Even though the electron spray mass spectroscopy indicates the molecular ion peak corresponding to the desired product, it was very difficult to isolate out from the reaction mixture. Also, addition of MeOH and inverse addition did not work. Likewise, the oxidation of **S54.1**, structurally similar to **S55.2**, produced the same result. However, the oxidation of **S54.2**, epimeric to **S54.1**, furnished the cyclic ether ring (**S56.1**) in 40% yield. The product was fully characterized. Separation and characterization of products from DMDO oxidation of **S55.2** and **S54.1** would enable us to rationalize the behavior of the two similar allene **S54.1** and **S54.2**, but it was a very difficult process. This route was not further pursued because of these unexpected results.

Scheme 56 DMDO Oxidation of Allenes



REFERENCES

1) (a) Crandall, J. K.; Machleder, W. H., *J. Am. Chem. Soc.* **1968**, *90*, 7292. (b) Crandall, J. K.; Machleder, W. H.; Thomas, M. J., *J. Am. Chem. Soc.*, **1968**, *90*, 7346. (c) Crandall, J. K.; Machleder, W. H. *J. Am. Chem. Soc.* **1968**, *90*, 7347. (d) Crandall, J. K.; Machleder, W. H. *J. Het. Chem.* **1969**, *6*, 777. (e) Crandall, J. K.; Conover, W. W.; Komin, J. B.; Machleder, W. H. *J. Org. Chem.* **1974**, *39*, 1723. (f) Crandall, J. K.; Batal, D. J. *J. Org. Chem.* **1988**, *53*, 1338. (g) Crandall, J. K.; Batal, D. J. *Tetrahedron Lett.* **1988**, *29*, 4791. (h) Crandall, J. K.; Rambo, E. *J. Org. Chem.* **1990**, *55*, 5929. (i) Crandall, J. K.; Batal, D. J.; Sebesta, D. P.; Ling, F. *J. Org. Chem.* **1991**, *56*, 1153. (j) Crandall, J. K.; Batal, D. J.; Lin, F.; Riex, T.; Nadol, G. S.; Ng, R. A. *Tetrahedron* **1992**, *48*, 1427. (k) Crandall, J. K.; Rambo, E. *Tetrahedron Lett.* **1994**, *35*, 1489. (l) Crandall, J. K.; Reix, T. *Tetrahedron Lett.* **1994**, *35*, 2513. (l) Crandall, J. K.; Rambo, E. *Tetrahedron* **2002**, 7027. See also: (m) Reeves, W. P.; Stroebel, G. G. *Tetrahedron Lett.* **1971**, *12*, 2946. (n) Greibrokk, T.; Skattebol, L. *Acta Chem. Scand.* **1973**, *27*, 1421. (o) Boeseken, J., *Rec. Trav. Chim. Pays-Bas.* **1935**, *54*, 657. (p) Pansevich-Kolyada; Idelchik, Z. B.; *J. Gen. Chem. USSR*, **1954**, *24*, 1601. (r) Rameshkumar, C.; Xiong, H.; Tracey, M. R.; Berry, C. R.; Yao, L. J.; Hsung, R. P. *J. Org. Chem.* **2002**, *67*, 1339.

2) Baldwin, J. E. *J. Chem. Soc. Chem. Comm.* **1976**, 734.

3) (a) Wang, Z.; Shangguan, N.; Cusick, J. R.; Williams, L. J. *Synlett*, **2008**, *2*, 213–216. (b) Lotesta, S. D.; Hou, Y.; Williams, L. J. *Org. Lett.* **2007**, *9*, 869. (c) Lotesta, S. D.; Kiren, S. K.; Sauers, R. R.; Williams, L. J. *Angew. Chem. Int. Ed.* **2007**, *46*, 15. (d) Shangguan, N.; Kiren, S.; Williams, L. J. *Org. Lett.* **2007**, *9*, 1093. (e) Ghosh, P.; Lotesta, S. D.; Williams, L. J. *J. Am. Chem. Soc.* **2007**, *129*, 2438. (f) Katukojvala, S.; Barlett, K. N.; Lotesta, S. D.; Williams, L. J. *J. Am. Chem. Soc.* **2004**, *126*, 15348, and references cited therein.

4) Yamamoto, H.; Tsuda, M.; Sakaguchi, S.; Ishi, Y. *J. Org. Chem.* **1997**, *62*, 7174 and references cited therein.

5) For preparation of DMDO in acetone see: (a) Murray, R. W.; Jeyaraman, R. *J. Org. Chem.* **1985**, *50*, 2847. For preparation of DMDO in chloroform see: (b) Gilbert, M.; Ferrer, M.; Sanchez-Baeza, F.; Messeguer, A. *Tetrahedron*, **1997**, *53*, 8643. (c) Ferrer, M.; Gilbert, M.; Sandez-Baeza, F.; Messeguer, A. *Tetrahedron Lett.*, **1996**, *37*, 3585.

6) Cusick, J.; Williams, L. J. Unpublished results.

7) Myers, A.G.; Zheng, B. *J. Am. Chem. Soc.* **1996**, *118*, 4492.

8) Corey, E. J.; Fuchs, P. L. *Tetrahedron Lett.* **1972**, *36*, 3769-3772.

9) Roth, G. J.; Liepold, B.; Mueller, S.G.; Bestmann, H. J. *Synthesis*, **2004**, *1*, 59.

10) Nahm, S.; Weinreb, S. M. *Tetrahedron Lett.* **1981**, *22*, 3815.

-
- 11) Matsumura, K.; Hashiguchi, S.; Ikariya, T.; Noyori, R. *J. Am. Chem. Soc.* **1997**, *119*, 8738.
- 12) (a) Corey, E.J.; Bakshi, R.K.; Shibata, S. *J. Am. Chem. Soc.*, **1987**, *109*, 1797.
(b) Corey, E. J.; Helal C. J. *Angew. Chem., Int. Ed. Engl.*, **1998**, *37*, 1986–2012.
- 13) Murray, R. W., Singh, M. *J. Org. Chem.* **1993**, *58*, 5076-5080.
- 14) Evans, D.; Clark, J.; Metternich, R.; Novack, V.; Sheppard, G. *J. Am. Chem. Soc.* **1990**, *112*, 866.
- 15) Kim, S.; Ko, H.; Lee, T.; Kim, D. *J. Org. Chem.* **2005**, *70*, 5756.
- 16) Evans, D. A.; Takacs, J. M.; McGee, L. R.; Ennis, M. D.; Mathre, D. J. Bartolli, L. *Pure & Appl. Chem.* **1981**, *53*, 1109-1127.
- 17) Evans, D. A.; Bender, S. L.; Morris, J. *J. Am. Chem. Soc.* **1988**, *110*, 2506-2526.
- 18) (a) Hauser, F.M.; Rhee, R. *Synthesis*, **1977**, *4*, 245. (b) Hauser, F. M; Rhee, R.; Prasanna, S. *Synthesis* **1980**, *1*, 72. (c) F. J. Leeper and J. Staunton, *J. Chem. Soc. Chem. Commun.*, **1979**, *5*, 205. (d) Ward, R.A.; Procter, G. *Tetrahedron* **1995**, *51*, 12301. (e) Barber, J. A.; Staunton, J.; Wilkinson, M. R. *J. Chem. Soc. Perkin Trans. I*, **1986**, 2101.
- 19) (a) Chevenier, E.; Lucatelli, C.; Pandya, U.; Wang, W.; Gimbert, Y.; Greence A. E. *Synlett*. **2004**, *15*, 2693. (b) Zhang, Z.; Yu, B. *J. Org. Chem.* **2003**, *68*, 6309-6313.
- 20) Doering, W.; Beringer, F.M. *J. Am. Chem. Soc.* **1949**, *71*, 2221.
- 21) Nelson, P.H.; Nelson J. T. *Synthesis* **1992**, *12*, 1287.
- 22) Mendelson, W. L.; Hayden, S. *Synth. Comm.* **1996**, *26*, 603.
- 23) Robertson, A., Whalley, W. B. *J. Chem. Soc.* **1949**, 3033.
- 24) Cao, B.; Park, H.; Joullie, M. *J. Am. Chem. Soc.* **2002**, *124*, 520.
- 25) Shangguang, N.; Kiren, S.; Williams, L. *J. Org. Lett.* **2007**, *9*, 1093-1096.
- 26) (a) Murray, R. W. *Chem. Rev.* **1989**, *89*, 1187. (b) Marples, B. A.; Muxworthy, J. P.; Baggeley, K. H. *Synlett* **1992**, 646. (c) Csuk, R.; Dörr, P. *Tetrahedron* **1994**, *50*, 983.
- 27) (a) Pateson, I.; Goodman, J. M.; Isaka, M. *Tett. Lett.* **1989**, *30*, 7121. (b) Pateson, I.; Oballa, R. M. *Tett. Lett.* **1997**, *47*, 8241. (c) Yeung, K.-S.; Paterson, I. *Chem. Rev.* **2005**, *105*, 4237-4313

Chapter IV

Direct Carbinolamide Synthesis

I. Introduction

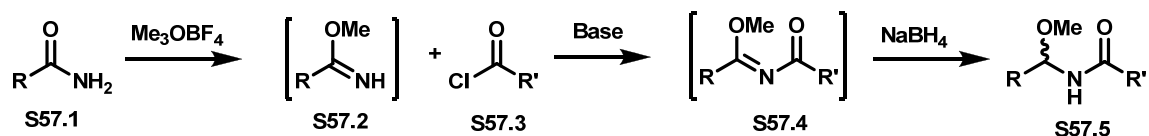
The elegant synthesis of both the core ring with the application of SDE and the dihydroisocoumarin ring were accomplished in order to reach the target molecule, psymberin. These novel and flexible strategies could also enable us to synthesize analogs and hybrid structures of psymberin. The last synthetic challenge posed by this complex molecule is to construct, efficiently and stereoselectively, the unique *O*-alkyl carbinolamide functional group (Figure 2, p2). Presumably, this group plays a significant role in the biological activity of the pederin family members. A probable mechanism for the biological action is eliminative cleavage of the C-O bond giving rise to an acylimine which could act as an alkylating agent.

In chapter 2 the synthetic strategies for the fragments of the pederin family members were discussed. These fragments are bridged by the *O*-alkyl carbinolamide. There are several creative methods reported for the construction of this motif. Among them, the Matsumoto and Roush methods, which are the most widely used, will be discussed in this chapter. In addition, the Huang group recently reported the total synthesis of psymberin and their approach will be mentioned here. Our group devised a different approach to build this highly sensitive motif and is applying it to the synthesis of analogs.

In the late 80's, the Matsumoto group developed an outstanding strategy to form

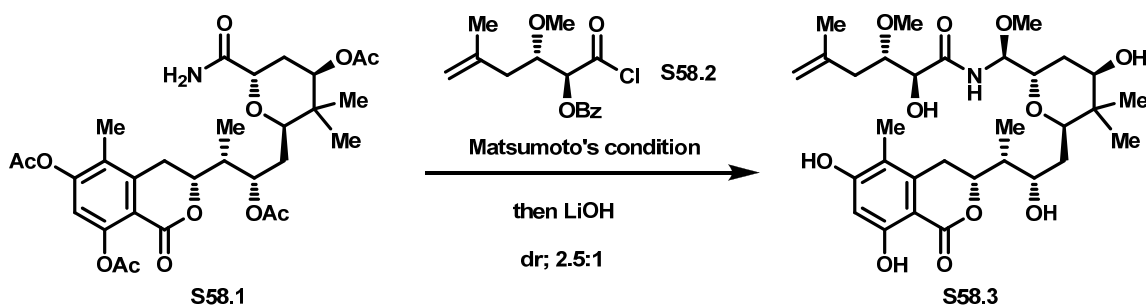
O-methyl carbinolamides, which was demonstrated in the first total synthesis of pederin. In this strategy, an amide (**S57.1**) is treated with trimethyloxonium tetrafluoroborate to give rise to an imidate (**S57.2**), which is subjected to an acyl chloride (**S57.3**) and a base to afford *N*-acyl imidate (**S57.4**). The resulting **S57.4** is readily reduced in situ with NaBH₄ in alcoholic solvents to the carbinolamide (**S57.5**). Although studies for the model and real systems afforded the motif in high yields, this approach suffered from poor stereoselectivity in product formation. For example, the pederin was obtained in a 1:3 ratio (desired:undesired) after the employment of this strategy in their total synthesis. Nevertheless, this synthetic method has been employed by several other groups to achieve both the synthesis of pederin and its analogs.

Scheme 57 The Matsumoto Strategy



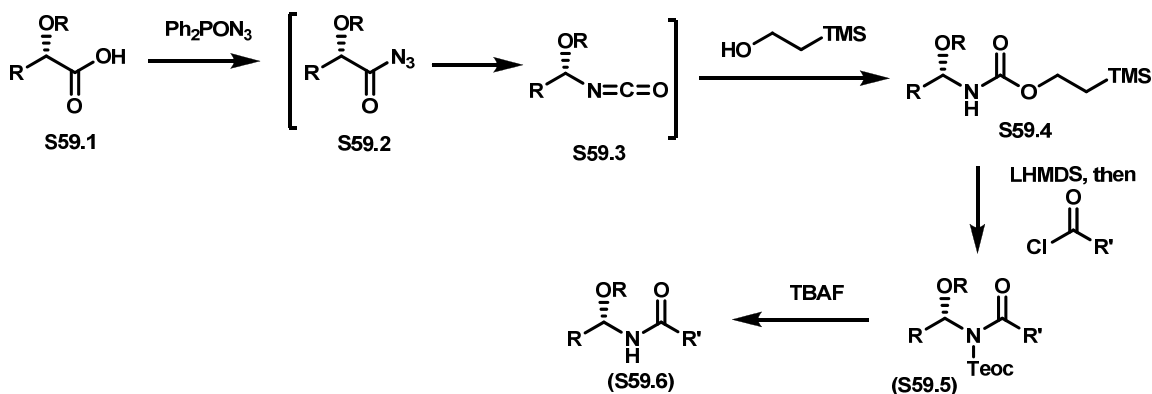
The De Brabander group recently applied the Matsumoto method in the total synthesis of psymberin. They prepared the amide (**S58.1**) and acyl chloride (**S58.2**) partners and combined them under the Matsumoto condition to get *O*-methyl protected carbinolamide. Albeit capricious, they found that polyvinyl pyridine base appeared to be uniquely effective among amine bases. After basic hydrolysis of the acetate and benzoate protecting groups, they obtained the natural product (**S58.3**) and its epimer in a 2.5 to 1 ratio. The yield was 56% based on recovered **S58.1**.

Scheme 58 The De Brabander Synthesis of Psymberin



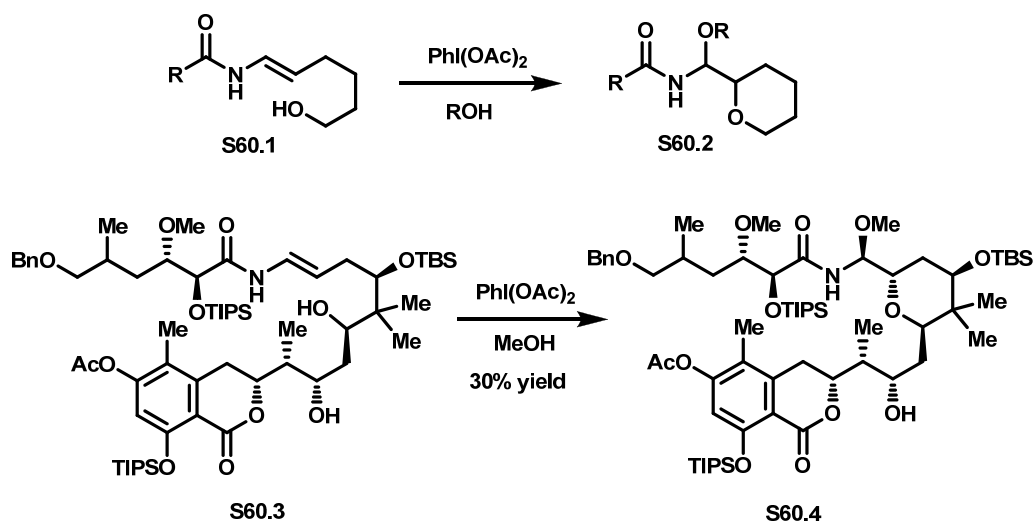
Another creative strategy was developed by the Roush group and employed in their total synthesis of mycalamide A. In this strategy, **S59.1** was converted to a carbamate (**S59.3**) through Curtius rearrangement of **S59.2** with diphenylphosphoryl azide in the presence of TMS ethanol. The resulting **S59.4** was then deprotonated with base and captured with an acyl chloride to give an *N*-acyl product (**S59.5**). Exposure of **S59.5** to the TBAF removed the trimethylsilylethoxy carbonyl (Teoc) group to readily afford the desired functionality (**S59.6**). The most striking feature of this method is complete stereocontrol. No epimerization is observed under the reaction conditions. Several other groups have applied this method successfully in the synthesis of the pederin family members.

Scheme 59 The Roush Strategy



The Huang group developed an interesting method for the motif and applied it to the synthesis of psymberin. They converted an *N*-acyl enamine (**S60.1**) to the corresponding pyran (**S60.2**) using $\text{PhI}(\text{OAc})_2$ as oxidant in a single step. They also investigated the likely mechanism of the reaction during the optimization and reported two possible pathways to product formation. For the synthesis of psymberin, they prepared precursor **S60.3** and treated it with the oxidant, which afforded a total yield of 72% of isolated products. The desired product (**S60.4**) was isolated in 30% yield among the four diastereomers. After protecting group manipulations and double bond formation in the acyclic side chain (5 steps), they completed the total synthesis of the natural product. Although this transformation leads to product formation very quickly, the selectivity is poor. Additionally, the reaction conditions may not be suitable for some functional groups, e.g. other C-C double bonds.

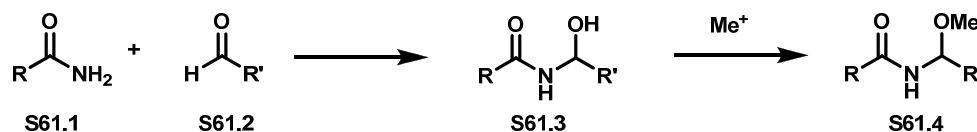
Scheme 60 The Huang Strategy



II. Direct Aldehyde-Amide Coupling

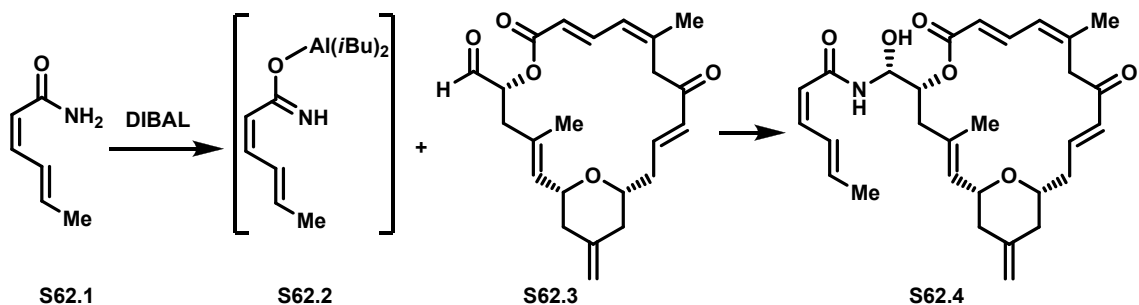
We completed a formal synthesis of psymberin. To complete total synthesis we could apply the Matsumoto coupling. However, the reported approaches to *O*-methyl carbinolamide formation require multi-step processes. We felt that a direct method that leads to formation of the motif stereoselectively is necessary. We envisioned that the desired motif would be accessible from methylation of a carbinolamide (**S61.3**), which would be in turn derived from a direct coupling of an amide (**S61.1**) and an aldehyde (**S61.2**). In the literature, direct coupling of two partners had been reported, but it was limited to only electron poor aldehydes and required relatively harsh conditions.¹ There are also indirect approaches reported for the motif formation.²

Scheme 61 Direct Aldehyde-Amide Coupling



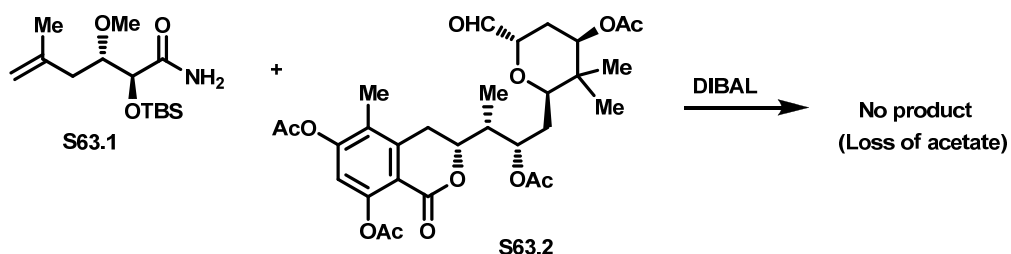
During the total synthesis of zampanolide, the Hoyer group disclosed an approach that involved coupling an aldehyde (**S62.3**) with the metal imidate (**S62.2**) derived from an amide (**S62.1**) and DIBAL (Scheme 62).³ This reaction was the first example of the direct coupling of two partners under mild conditions. However, they obtained a mixture of products (**S62.4**) in a ratio of 1: 1 and no yield was reported.

Scheme 62 The Hoye Synthesis of Zampanolide



We anticipated that the complex aldehyde (**S63.2**) could be coupled with the complex amide (**S63.1**) under the same conditions to afford the corresponding carbinolamide. Unfortunately, the reaction failed to give the desired product. Consequently, we studied this reaction in more detail in terms of generality, reliability, and efficiency. In addition, the stereoselectivity issue must also be addressed.

Scheme 63 Direct Coupling of Amide S63.1 and S63.3



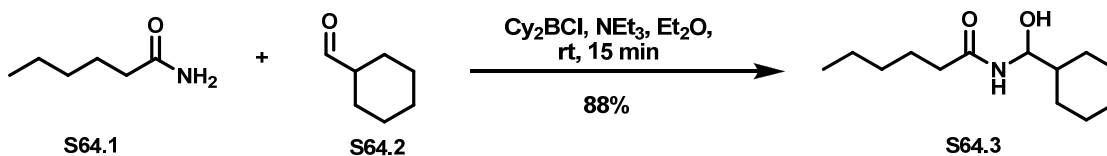
In principle, addition of an amide anion to an aldehyde represents a type of aldol reaction, which is one of the most studied reactions in organic chemistry. Aldol reactions have been efficiently and reliably applied in complex synthesis and provided stereoselective product formation under reagent or substrate controlled reaction conditions.⁴ The enolates can be formed with different metals such as Li, B, Ti, Sn. Hence, we expected that different metal imidates could be generated from amides

coupled with aldehydes to provide carbinolamides. Boron imidates represent an alternative approach.

III. Results for Boron Imidates with Aldehydes

We applied the Paterson aldol reaction conditions to couple hexanamide (**S64.1**) and cyclohexanecarbaldehyde (**S64.2**).⁵ Thus, **S64.1** (1.2 eq) was taken up in diethyl ether (0.2 M) and NEt₃ (2.0 eq) was then added. After cooling to 0 °C, dicyclohexylboron chloride (1.3 eq, 1.0 M in hexane) was added. The heterogeneous mixture was stirred for 15 min and then **S64.2** (1.0 eq) was added. After 30 minutes the reaction was quenched with a mixture of MeOH/phosphate buffer (ph=7.40)/H₂O₂ (30%). Isolation and purification gave the carbinolamide (**S64.3**) in 88% yield.


Scheme 64 Simple Aldehyde and Amide Coupling



Presumably, boron imidate formation takes place under the reaction conditions and then couples the aldehyde. We then turned our attention to optimize product formation. In table 2, the yields were given with different equivalents of amide (**T2.1**), aldehyde (**T3.2**), Cy₂BCl, and NEt₃. Using either a slight excess of the imidate or aldehyde gave the same yield (entry 1-3 and 7). Finally, the yield did not change with excess imidate (entry 4, 5 and 6). As a result, entry 1 and 7 gave the optimal conditions. The solvent Et₂O was found to be a good choice since CH₂Cl₂, THF, and CH₃CN gave

the yields of 75%, 54%, 23%, respectively. Also, using the $(n\text{Bu})_2\text{BOTf}$ for imidate formation did not improve the yield.

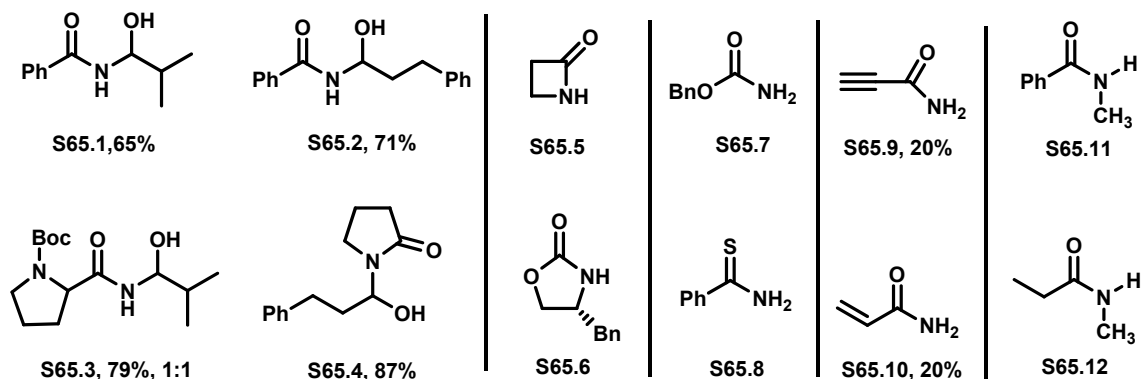
Table 2 Optimization of Coupling Reaction



Entry	T2.1	T2.2	Cy ₂ BCl	NEt ₃	T2.3
1	1.2 eq	1.0 eq	1.2 eq	2.0 eq	84%
2	1.2 eq	1.0 eq	1.5 eq	2.0 eq	84%
3	1.4 eq	1.0 eq	1.1 eq	2.0 eq	78%
4	1.5 eq	1.0 eq	1.5 eq	2.0 eq	83%
5	2.0 eq	1.0 eq	2.0 eq	2.0 eq	82%
6	2.5 eq	1.0 eq	2.5 eq	3.0 eq	77%
7	1.0 eq	1.5 eq	1.05 eq	2.0 eq	84%

Several aldehydes and amides were coupled. The findings are tabulated in Scheme 65. The primary amides coupled readily with an aldehyde to give the carbinolamides (**S65.1**, **S65.2**, **S65.3**) in moderate yields. Interestingly, the cyclic amides (**S65.5**, **S65.6**) appeared to be unreactive, while the five-membered cyclic amide (**S65.4**) furnished the product in 87%. Also, carbamate (**S65.7**) and thioamide (**S65.9**) did not provide product. Unsaturated amides (**S65.9** and **S65.10**) were found to form the carbinolamide, albeit in low yields (less than 20%). Moreover, products formation was traceable on TLC for secondary amides (**S65.11** and **S65.12**), but the isolation was difficult since they reformed the starting materials during column separation.

Scheme 65 Examples of Aldehyde-Amide Coupling



We also investigated stereoselective carbinolamide formation. For this matter, (-)-(Ipc)₂BCl was used for coupling of the amide (**T2.1**) and the aldehyde (**T2.2**).⁶ The reaction yield of the coupling was 87% after isolation of product (**T2.3**). Chiral HPLC analysis indicated that the enantiomeric excess of the reaction was 18%. The product was column chromatographed a second time to determine if epimerization occurred during column purification, but the ee was the same as before. The reaction was carried out by using Cy₂BCl at low temperatures such as -78, -40 and -20°C. Unfortunately, no product formation was observed.

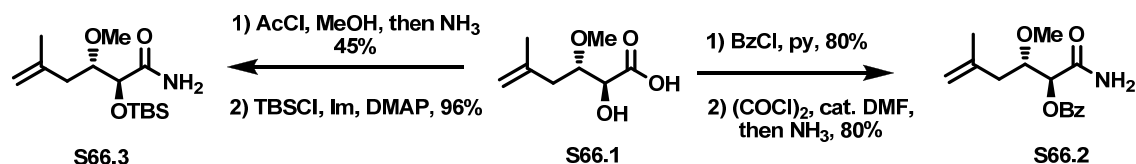
Much more research needs to be done to fully understand this reaction. In a reagent controlled aldol reactions, it is known that the selectivity results from the formation of a chair-like Zimmerman-Traxler transition state.⁶ It is likely that this reaction follows the same mechanism.

IV. Complex Amide and Aldehyde Coupling: Analogs

We wanted to prepare analogs of psymberin to understand its mode of biological action. In addition, we wanted to investigate our new coupling reaction. The complex

amides (**S66.2** and **S66.3**) were prepared from the hydroxyl carboxylic acid (**S66.1**) in 2 steps.

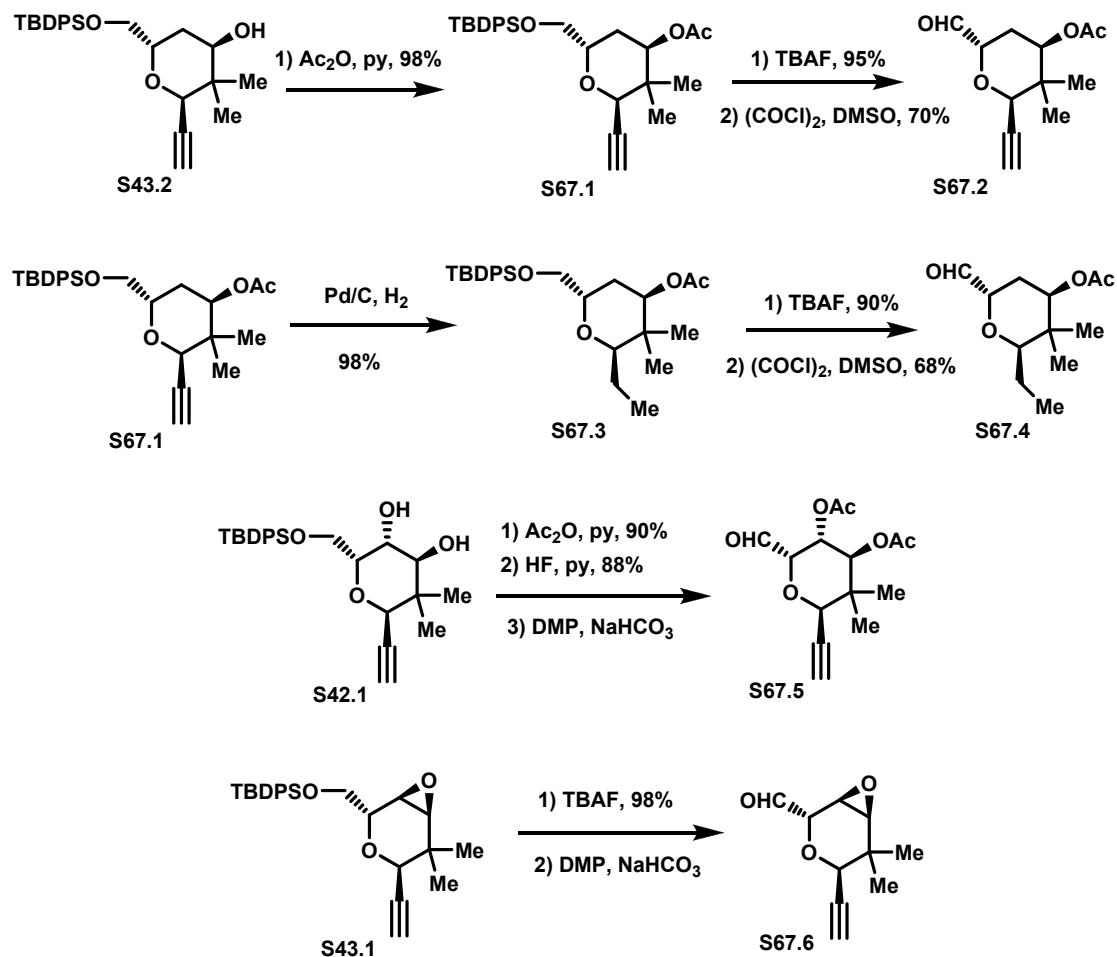
Scheme 66 Preparation of Complex Amides



The preparation of complex aldehydes starts with the alcohol (**S43.2**), which was first protected as the acetate to afford **S67.1**. Then, deprotection of TBDPS followed by oxidation under Swern conditions gave rise to aldehyde **S67.2**. Similarly, reduction of the alkyne (**S67.1**), deprotection of TBDPS and then oxidation under Swern conditions yielded aldehyde **S67.4**. Interestingly, the coupling constant analysis indicated that the aldehyde group is positioned axially in **S67.2** and equatorially in **S67.4**, which may lead to differences in reactivity. In particular, the aldehyde (**S67.4**) would be useful as both it and **S63.2** contains a similar chain on the pyran ring.

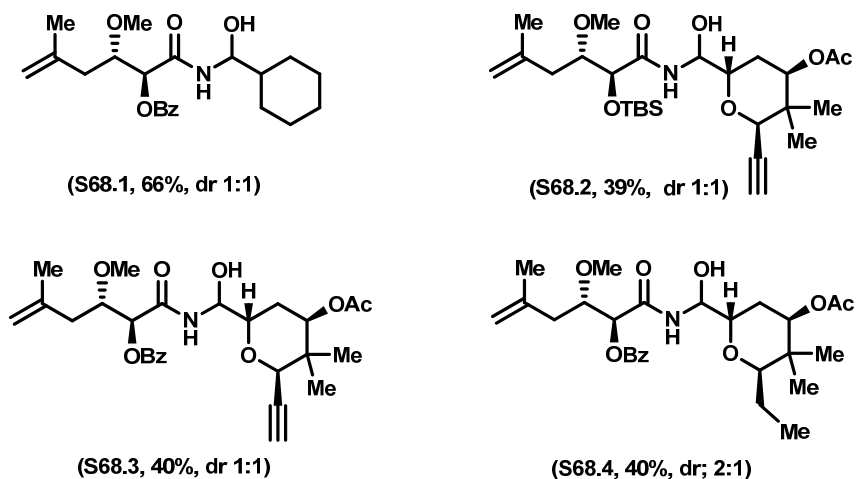
For the preparation of aldehyde **S67.5**, the diol (**S42.1**) was first protected as the diacetate, deprotected with TBAF and then oxidized with DMP. The epoxide **S43.1** is deprotected with TBAF and oxidized to the aldehyde (**S67.6**). Both aldehydes were prone to β -elimination under oxidizing conditions. Therefore, they were used immediately after they were formed.

Scheme 67 Complex Aldehydes Preparation



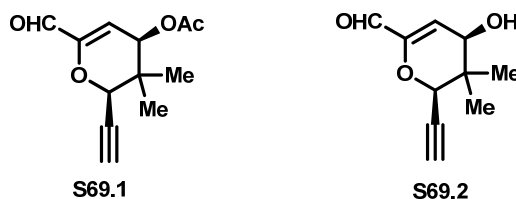
The findings from coupling of complex amides and aldehydes are given in Scheme 68. The union of the complex amide with cyclohexanecarbaldehyde efficiently took place under our conditions to give a mixture of separable carbinolamides (**S68.1**) in 66% yield (dr 1:1). Amides **S66.2** and **S66.3** coupled with the aldehyde **S67.2** with almost the same yield (**S68.2** and **S68.3**), indicating no effect from the protecting groups. Similarly no significant influence was observed from the pyran side chain (**S68.4**).

Scheme 68 Examples of Complex Amide and Aldehyde Coupling



The pyran aldehydes (**S67.5** and **S67.6**) failed to give the corresponding carbinolamides under the coupling conditions. Instead of addition, β -elimination in the aldehydes took place to form compounds **S69.1** and **S69.2**. The Rawal group reported the same type of decomposition of similar aldehydes.⁷ Compound **S69.1** was further treated with the imidate formed from the amide, but no product was observed.

Scheme 69 Elimination Products

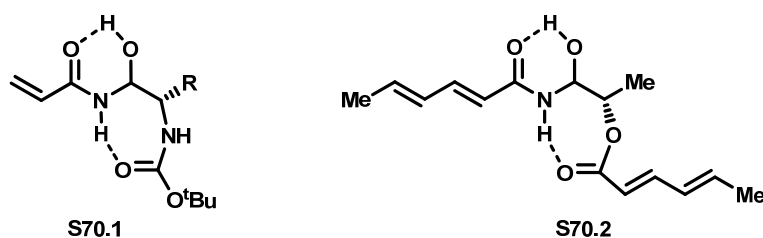


V. Stability of Carbinolamides

It is reported that the carbinolamides are inherently unstable functional groups and readily decompose to amide and aldehyde. However, the Porco and Bussolari groups

demonstrated that certain carbinolamides (**S70.1** and **S70.2**, Scheme 70) were unexpectedly stable, and even isolable by chromatography.⁸ They proposed that the stability of these molecules resulted from extended hydrogen bonding, provided by a heteroatom positioned appropriately to act as a hydrogen bond acceptor. The Porco group showed experimentally that there was an interaction between the carbonyl group and the amide hydrogen, and they suggested that this is necessary for the stability.^{10b} The presence of this interaction was supported by ¹H NMR since the peak exhibited by the hydrogen bonded NH appears at more downfield than that of the non-hydrogen bonded NH. Additionally, the stability of zampanolide (**S62.4**) was rationalized by invoking an intramolecular hydrogen-bond network, similar to **S70.2**.⁹

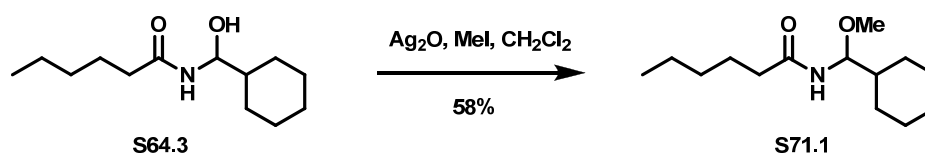
Scheme 70 Stable Carbinolamides



Although the hydrogen bond network is apparent in **S70.1** and **S70.2**, it has not been established as necessary. We believe this notion must be reevaluated based on the results we obtained during the application of our new condition for carbinolamide syntheses. We were able to isolate, characterize and manipulate the carbinolamides, which were devoid of hydrogen bonding interactions. Particularly, **S64.3**, **T2.3**, **S65.1**, **S65.2** and **S65.4** derived from simple aldehydes and amides exhibited unexpected stability under the reaction conditions, and accommodated aqueous work-up, flash column chromatography, routine handling, and storage. Moreover, the Smith group

demonstrated *O*-alkylation of the zamponilide carbinolamide did not any reduce the stability of the product.¹¹ Similarly, we methylated the carbinolamide **S64.3**, and not surprisingly isolated the stable **S71.1** (Scheme 71), which lacks of the stabilizing hydrogen bonding network. In light of these results, carbinolamides appear intrinsically stable, even in the absence of the intramolecular stabilizing interactions.

Scheme 71 Methylation of the Carbinolamide S64.3



VI. Scope of the Boron Imidates

Normally, an amide could couple with an aldehyde either under harsh condition or when the aldehyde is electron poor. We demonstrated that the nucleophilicity of an amide increases when it is transformed to an imidate since the union with aldehydes took place smoothly under mild conditions. Likewise, we wanted to investigate the coupling of boron imidates with different electrophiles, which may lead to a variety of nitrogen containing functionality. For this purposes, the boron imidates were treated with such electrophiles as benzyl bromide, allyl tosylate, benzenesulfonyl chloride, benzoyl chloride, phenyl isocyanate, styrene as well as Micheal acceptors like cyclohexenone, 1-nitrocyclohexene and phenyl vinyl sulfone. Unfortunately, all were nonreactive to a boron imidate. Apparently, the nucleophilicity of a boron imdate too low to react with these electrophiles.

In order to increase of imidate nucleophilicity we tried borane reagents with

electron drawing groups like pinacol borane chloride and. But, the reactivity of the imidate was not improved. We turned our focus to the imidates of different metals. We tried AlMe_2Cl , AgOTf , $\text{Sc}(\text{OTf})_3$, SnCl_4 , $\text{Zn}(\text{OTf})_2$, $\text{MgBr}_2\cdot\text{OEt}_2$. Unfortunately, all of these attempts failed to increase the yield of the carbinolamide product.

REFERENCE

- 1) (a) Zoller, U.; Ben-Ishai, D. *Tetrahedron* **1975**, *31*, 863. (b) Zaugg, H. E. *Synthesis* **1984**, 85. (c) Lokensgard, J. P.; Fischer, J. W.; Bartz, J. W. *J. Org. Chem.* **1985**, *50*, 5609.
- 2) (a) Katritzky, A. R.; Fan, W.-Q.; Black, M.; Pernak, J. *J. Org. Chem.* **1992**, *57*, 547. (b) Johnson, A. P.; Luke, R. W.; Steele, R. W.; Boa, A. N. *J. Chem. Soc., Perkin Trans. I* **1996**, 883.
- 3) Hoye, T. R.; Hu, M. *J. Am. Chem. Soc.* **2003**, *125*, 9576.
- 4) For reviews see: (a) Evans, D. A.; Nelson, J. V.; Taber, T. R. "Stereoselective Aldol Condensations," in *Topics in Stereochemistry*, New York, 1982; Vol. 13, p. 2. (b) Mukaiyama, T. "The Directed Aldol Reaction," in *Organic Reactions*, New York, 1982; Vol. 28, p 203.
- 5) For review see; Cowden C.; Paterson, I. *Org. React.* **1997**, *51*, 1.
- 6) Zimmerman, H. E.; Traxler, M. D. *J. Am. Chem. Soc.* **1957**, *79*, 1920.
- 7) Sohn, J.-H, Waizumi, N.; Zhong, H. M.; Rawal, V. H. *J. Am. Chem. Soc.* **2006**, *127*, 7290.
- 8) (a) Bussolari, J. C.; Beers, K.; Lalan, P.; Murray, W. V.; Gauthier, D.; McDonnell, P. *Chem. Lett.* **1998**, 787. (b) Porco, J. A. Jr.; Troast, D. M.; *Org. Lett.* **2002**, *4*, 991.
- 9) Smith, A, B, III; Safonov, I. G.; Corbett, R. M. *J. Am. Chem. Soc.* **2001**, *123*, 12426.

Chapter V

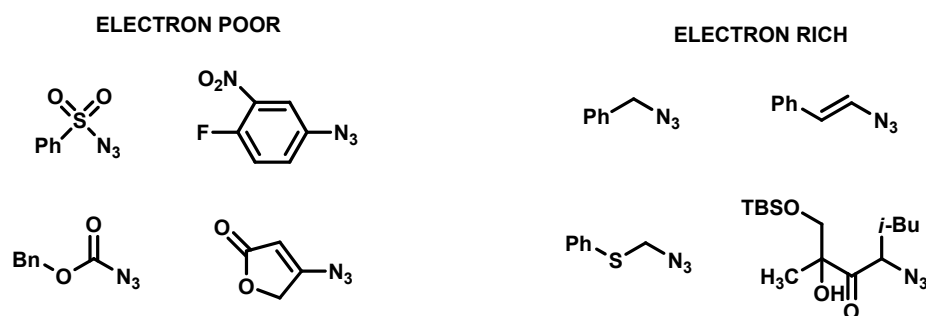
Metal Promoted Thioacid-Azide Coupling

I. Introduction

Our group investigated the reaction of thioacid-azide coupling, which gives an amide.¹ The amidation was shown to be effective in water and organic solvents. Moreover, the reaction was applied to a variety of thioacids and azides to obtain simple and complex amides, which were difficult to obtain by using conventional methods.^{1a}

The reactivity of amidation depends on the electronic character of azides. The coupling of thioacids with electron poor azides approaches the ideal reaction profile, including short, room temperature reactions that give near quantitative yields, while electron rich azides require higher temperatures and longer reaction times. Some representative examples of both azides are given in Scheme 72.

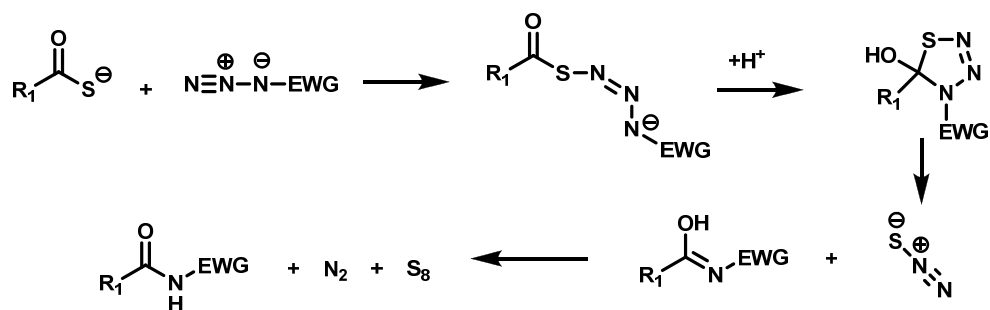
Scheme 72 Examples of Electron Rich and Poor Azides



The experimental and computational data revealed two reaction pathways.^{1d} For electron poor azides, it is a stepwise process, initially forming a nitrogen-sulfur bond, a

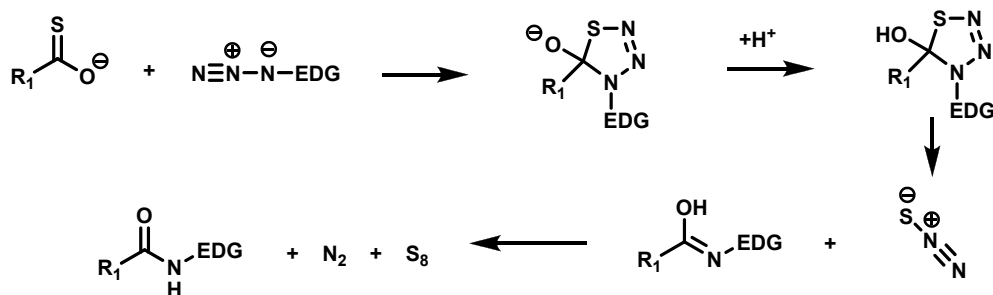
carbon-nitrogen bond forms in a separate step to give the thiatriazoline intermediate after protonation. The thiatriazoline intermediate decomposes to the amide product, nitrogen and sulfur via retro-[3+2] cycloaddition.

Scheme 73 Mechanism for Electron Withdrawing Azides



For electron rich substrates, it is a concerted process: carbon-nitrogen and sulfur-nitrogen bond formation takes place in a single step by anion-accelerated [3+2] cycloaddition. This gives rise to the anion, after which protonation forms a thiatriazoline intermediate, which gives the amide product along with nitrogen and sulfur through the same mechanism.

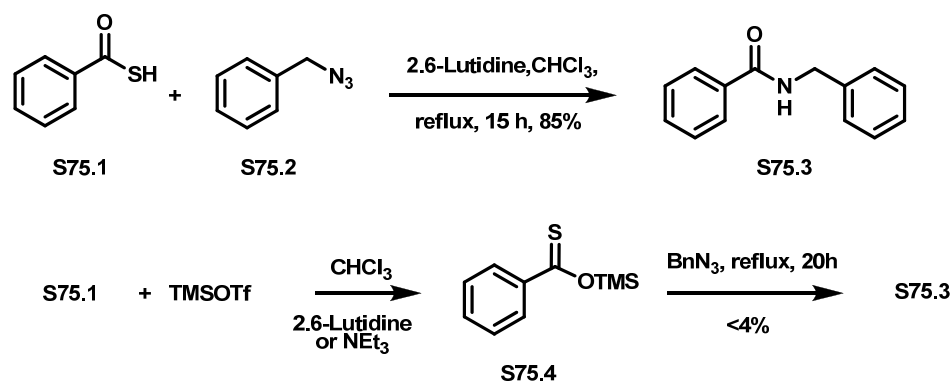
Scheme 74 Mechanism for Electron Rich Azides



We hypothesized that a suitable metal would promote the reaction of electron rich azides with thioacids, as there is literature precedent that a metal can accelerate the [3+2]

cycloaddition.² Our goal was to facilitate the coupling of electron rich azides at room temperature in a conveniently short timeframe. We selected benzyl azide (**S75.2**) and thiobenzoic acid (**S75.1**) as our test substrates. Benzyl azide is a good model of electron rich primary azides and thiobenzoic acid is a good model of thioacids. Under the original conditions developed by our group, this reaction required 15 hours in refluxing chloroform to form the amide (**S75.3**) in 85% yield. Addition of trimethyl silyl triflate to thiobenzoic acid and triethyl amine or 2,6-lutidine effected complete conversion to trimethyl silyl thionobenzoate (**S75.4**). The silylation could be conveniently followed by ¹³C-NMR. Thus, the 190 ppm signal apparent for thiobenzoic acid disappeared and a new signal at 213 ppm became evident within minutes. Subsequent treatment of thiobenzoic acid with benzyl azide failed to give rise to the corresponding amide (**S75.3**) product at room temperature with no measurable improvement at 60 °C (<4% after 20 hrs).

Scheme 75 Coupling of Thioacid and Thionoester with Azide



The Wong group found that the amidation reaction could be promoted in the presence of RuCl₃ and 2,6-Lutidine under mild conditions.³ They showed the coupling of thioacetic acid with a limited set of electron rich azides to furnish acetamide products. We applied the same amidation conditions to our substrates; thiobenzoic acid and benzyl

azide. However, it provided the product in just 14% yield. Moreover, we examined RuCl_3 promoted coupling of thiobenzoic acid with **S75.1** and **S75.4** (thionoester) in the absence of base, but the yields were 27% and 14%, respectively. Therefore, we believe that RuCl_3 may not be the best choice for a metal promoter and also that these conditions are not general for thioacid and azide couplings. We thus screened Lewis acids in search of a promoter that would induce amidation within hours at room temperature.

During the initial investigations, the thionoester derived from thiobenzoic acid was used since the carbon sulfur double bond could function as a dipolarophile in [3+2] cycloaddition reaction. Our findings are tabulated in Table 3. We set out with the copper metals as they are known to facilitate the cycloaddition reaction of azides.⁴ Unfortunately, they furnished the product in very low yields (entry 1 to 11), even in the presence of a ligand (entry 7 and 8). Similarly, most of the metals we tried did not provide the product (entry 12 to 24). In contrast, iron (II) chloride along with such bases as DMAP and 2,6 Lutidine gave **S75.3** in promising yields. However, the yields were not improved in the presence of different bases and with different stoichiometric amounts of starting materials.

Table 3 Screening of Metal Promoter

Entry	Solvent	S75.4 (eq)	BnN ₃ (eq)	Metal (1.0 eq)	Base	Yield (%)	Time (h)
1	CH ₂ Cl ₂	1.0	1.0	CuSCN	no	8.3	20
2	CH ₂ Cl ₂	1.0	1.0	CuCN	no	0	20
3	CH ₃ CN	1.0	0.5	CuI (0.5 eq)	no	10.2	20
4	CH ₂ Cl ₂	1.0	1.0	CuBr	no	6.3	20
5	CH ₂ Cl ₂	1.0	1.0	CuCl	no	9.5	20
6	CH ₂ Cl ₂	1.0	1.0	CuOTf·Toluene	no	6.3	20
7	CH ₂ Cl ₂	1.0	1.0	CuI	F ₅ -PhSH(1.0)	3.2	20
8	CH ₂ Cl ₂	1.0	1.0	CuOTf	F ₅ -PhSH(1.0)	2.1	20
9	CH ₂ Cl ₂	1.0	1.0	Cu(OTf) ₂	no	0	20
10	CH ₂ Cl ₂	1.0	1.0	Cu(di-Mebbiq) ₂ ·BF ₄	no	10	20
11	CH ₂ Cl ₂	1.0	1.0	Cu(CH ₃ CN) ₄ ·PF ₄	no	0	20
12	Et ₂ O	1.0	0.5	Zn(OTf) ₂ (0.5 eq)	no	0	20
13	Et ₂ O	1.0	0.5	SnCl ₂ (0.5 eq)	no	0	20
14	CH ₂ Cl ₂	1.0	1.0	AgOTf	no	0	20
16	CH ₂ Cl ₂	1.0	1.0	Ag(CH ₃ CN) ₄ ·BF ₄	no	0	20
17	CH ₂ Cl ₂	1.0	1.0	Pd(OAc) ₂	no	0	20
18	CH ₂ Cl ₂	1.0	1.0	Pd(OAc) ₂	Pyridine(1.0)	0	20
19	CH ₂ Cl ₂	1.0	1.0	AlCl ₃	no	0	20
20	CH ₂ Cl ₂	1.0	1.0	BF ₃ OEt ₂	no	0	20
21	CH ₂ Cl ₂	1.0	1.0	NiCl ₂	no	0	20
22	CH ₂ Cl ₂	1.0	1.0	Cp ₂ Fe	no	0	20
23	CH ₂ Cl ₂	1.0	1.0	Fe(acac) ₃	no	0	20
24	CH ₂ Cl ₂	1.0	1.0	Fe(acac) ₃	Pyridine(1.0)	0	20
25	CH ₂ Cl ₂	1.0	1.0	FeCl ₂ (1.0)	DMAP(1.0)	32	6
26	CH ₂ Cl ₂	1.0	1.0	FeCl ₂ (1.0)	Lutidine(1.0)	41	6

The findings from the iron (III) chloride are given in Table 4. We obtained 35% yield with 0.5 equivalent of the metal (entry 1), which was improved to 52% in the presence of DMAP (0.5 eq) after screening many different bases (entry 2). This was the highest yield up to this point. We proceeded to optimize the reaction by changing the amount of the substrates. Doubling the amount of either the thionoester (**S75.4**) or the

benzyl azide did not affect the yield (entry 3 and 4). Using 1.0 equivalent of both metal and base increased the yield slightly (entry 4). The largest increase in yield occurred when using 2.0 equivalents of both FeCl_3 and DMAP (entry 6). Under these conditions, doubling the amount of the azide afforded the highest yield (82%) in the shortest time (entry 7). Methylene chloride was used as solvent for all presented data.

Table 4 Results from Iron (III) Chloride and Thionoester Coupling

Entry	S75.4 (eq)	BnN ₃	Metal (eq)	Base (eq)	Yield (%)	Time (h)
1	1.0	1.0	$\text{FeCl}_3(0.5)$	no	35	7
2	1.0	1.0	$\text{FeCl}_3(0.5)$	DMAP (0.5)	52	7
3	2.0	1.0	$\text{FeCl}_3(0.5)$	DMAP (0.5)	50	7
4	1.0	2.0	$\text{FeCl}_3(0.5)$	DMAP (0.5)	42	7
5	1.0	1.0	$\text{FeCl}_3(1.0)$	DMAP (1.0)	56	6
6	1.0	1.0	$\text{FeCl}_3(2.0)$	DMAP (2.0)	71	3
7	1.0	2.0	$\text{FeCl}_3(2.0)$	DMAP (2.0)	82	3

All the attempts to further improve the yield of the optimized condition (Table 4 entry 7) such as using other solvents (THF, Et_2O , CH_3CN), changing the order of addition of substrates, and altering concentration were not satisfactory. In addition, longer reaction times did not provide higher yields. The best time of the reaction was found to be 3 h since the yields were 48% and 62% after 1h and 2h, respectively.

We also applied these conditions (Table 4, entry 7) to thiobenzoic acid in order to see the effect of thionoester on the reaction. Virtually the same yield was obtained when 2.0 equivalents of both FeCl_3 and DMAP were used for the coupling of the azide with thiobenzoic acid (Table 5, entry 1). The increased amount of metal and azide did not influence the yield significantly (entry 2 and 3). Interestingly, it was found that DMAP plays a critical role in the amidation, since almost no product formation was observed in

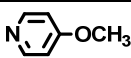
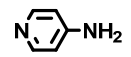
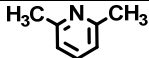
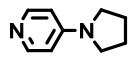
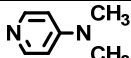
its absence. Therefore, we turned our attention to other bases to understand the role of a base in the coupling.

Table 5 Results from Iron (III) Chloride and Thioacid Coupling

Entry	S75.1 (eq)	BnN ₃ (eq)	FeCl ₃ (eq)	DMAP (eq)	Yield (%)	Time (h)
1	1.0	2.0	2.0	2.0	78	3
2	1.0	2.0	3.0	3.0	77	3
3	1.0	2.0	4.0	4.0	74	3
4	1.0	2.0	2.0	no	0	18
5	1.0	1.0	0.5	no	9	22

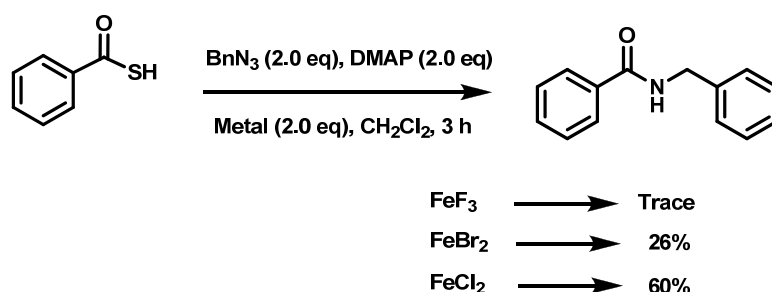
We focused on the pyridines bearing electron donating groups since they resemble DMAP in terms of electronic structure. The results are given in Table 6. The yields for each thiobenzoic acid (**S75.1**) and thionoester (**S75.4**) were obtained by using 2.0 equivalents of both FeCl₃ and base in 3 h. Interestingly, the methoxy (entry 1), amino (entry 2) and dimethyl (entry 3) substituents provided very low yields for the coupling of both **S75.1** and **S75.4**. However, the pyrrolidine group on pyridine (entry 4) gave rise to the amide in almost the same yield as DMAP.

Table 6 Results from Using Different Bases

Entry	Bases	S75.1 (% yield)	S75.4 (% yield)
1		26	9
2		27	trace
3		trace	trace
4		72	72
5		78	82

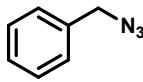
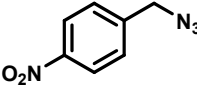
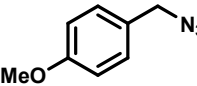
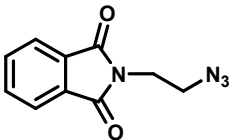
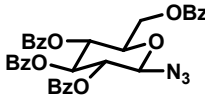
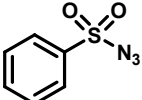
We also tested different iron halides under the reoptimized conditions (Scheme 76). For this purpose, FeCl_2 , FeBr_2 , and FeF_3 were applied to the model system in presence of DMAP. The iron (III) fluoride and iron (II) bromide furnished the product in low yields, while iron (II) chloride gave a modest yield (60%).

Scheme 76 Results for Different Iron Halides



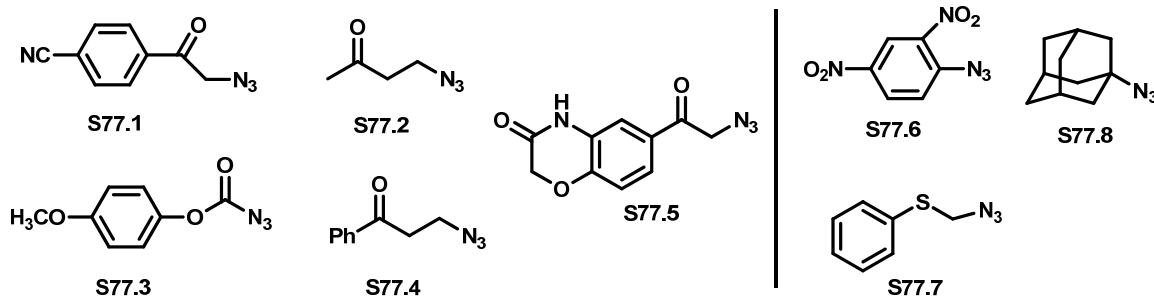
Iron (III) chloride and DMAP appear to be a good system for the amidation. Therefore, the optimized condition was applied to a variety of thioacids and azides. For this study, the azides were prepared from the corresponding halides (see table 7 and Scheme 77) and thiobenzoic acid and thioacetic acid were applied as the other coupling partner. The results for some azides are given in table 7. The coupling of the benzyl azide with thioacetic acid furnished the corresponding amide in 62% yield (entry 1). Likewise, substituted benzyl azides formed the products in moderate yields (entry 2 and 3). The imide substituted primary azide also provided the amides (entry 4). The thionoester (**S75.4**) gave rise to the amides with the electron rich and poor azides (entry 5 and 6), albeit in low yields.

Table 7 Results from Thioacid-Azide Coupling

$\text{R}-\text{C}(=\text{O})\text{SH} + \text{R}'-\text{N}_3 \xrightarrow[\text{CH}_2\text{Cl}_2, \text{rt}, 3\text{h}]{\text{FeCl}_3, \text{DMAP}} \text{R}-\text{C}(=\text{O})\text{NHR}'$ <p>R = -Ph, -CH₃</p>			
Entry	R'-N ₃	R=-Ph	R=-CH ₃
1		81%	62%
2		66%	73%
3		67%	67%
4		80%	60%
		S75.4	
5		13%	-
6		25%	-

We prepared the azides shown in Scheme 77, since the corresponding amines could not easily lead to amides by conventional methods. Unfortunately, the optimized condition resulted in decomposition of azides **S77.1**, **S77.2**, **S77.3**, and **S77.4**. **S77.5** was not reactive even after longer reaction times. The azides **S77.6**, **S77.7**, and **S77.8** coupled to **S75.4**, but the yields were very low (<5%).

Scheme 77 The Azides Failed to Couple

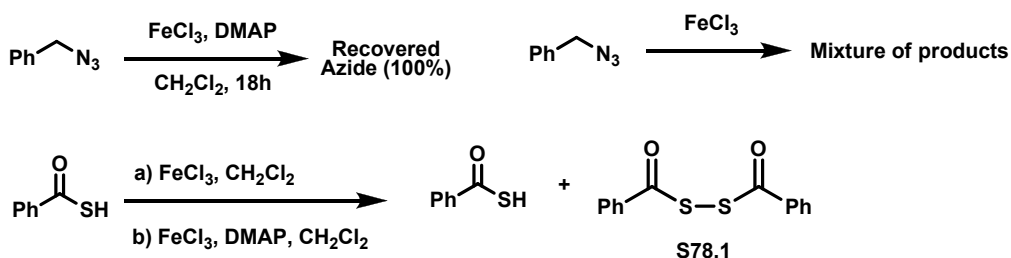


II. Discussions for the Mechanism of Thioacid-Azide Coupling

Although our findings were not generally applicable, we were still interested in the likely mechanism of the coupling reaction which gives a good yield for certain substrates. We carried out some control reactions. Benzyl amine was not observed. Although reduction of benzyl azide is possible, it is not observed when the benzyl azide is exposed to iron (III) chloride and DMAP (Scheme 78). If benzyl amine is formed, it must be rapidly converted into another substance.

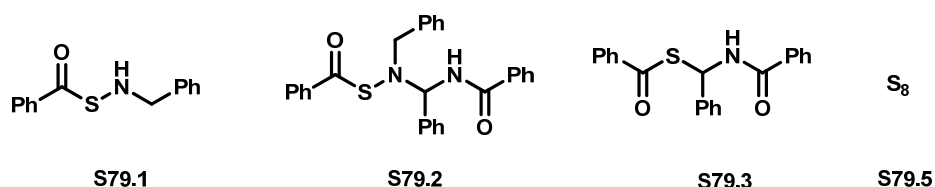
We checked the stability of benzyl azide and thiobenzoic acid under the reaction conditions (Scheme 78). The benzyl azide decomposed upon treatment with iron (III) chloride, yet it survived in presence of FeCl_3 and DMAP. We also observed the same pattern for the azides in Scheme 76. Similarly, the thiobenzoic acid was observed to form the dimer (S78.1) slowly over time when treated with either FeCl_3 or FeCl_3 and DMAP.

Scheme 78 Control Reactions for Azide and Thioacid



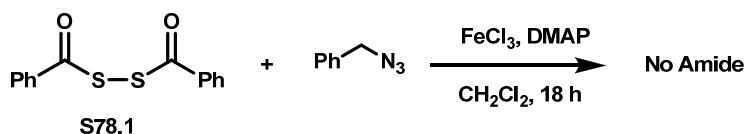
During the optimization studies, we observed by-product formation along with the major amide product. Interestingly, when the yield of the amide (**S75.3**) jumps from 35% (Table 4, entry 1) to 82% (Table 4, entry 7), the side product formation was significantly diminished. The yields for **S79.1**, **S79.2**, and **S79.3** were less than 5% when the highest yield for **S75.3** was obtained. The structure of these side products was identified in order to investigate their possible relevance to the mechanism of the coupling (Scheme 79). **S79.1** and **S79.2** were crystallized and structural proof was accomplished by X-ray crystallography. Sulfur (**S79.5**) was identified by melting point measurement, while the usual spectroscopic methods used for **S79.3**. In addition to these side products, dimer formation (**S78.1**) was detected for all data in Table 4 and 5.

Scheme 79 Side and by-Products from Amidation



We checked the importance of the dimer (**S78.1**), since it forms immediately upon mixing the substrates (Scheme 78). **S78.1** and the benzyl azide were exposed to the metal and base. No amide formation was detected after 18 h (Scheme 80).

Scheme 80 Dimer and Benzyl Azide

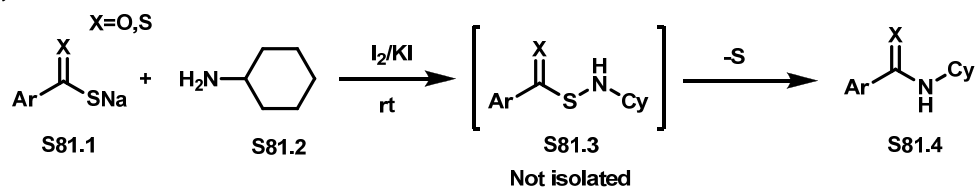


We noted that both **S79.1** and amide (**S75.3**) form almost simultaneously under

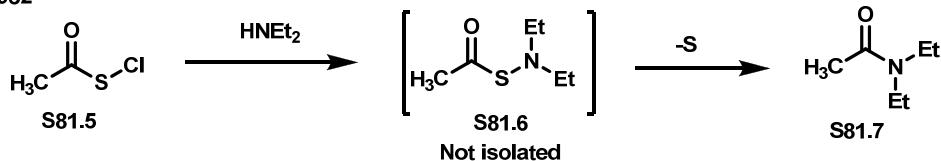
the amidation reaction conditions. Therefore, we next focused on **S79.1**. A literature search revealed interesting information about molecules of this sort (Scheme 81). The Alliger group obtained amide (**S81.4**, X=O) or thioamide (**S81.4**, X=S) and sulfur from oxidative coupling of thioacid (X=O) or dithioacid (X=S) salts with cyclohexylamine (**S81.2**).⁵ They postulated that the reaction proceeded through the unstable *N*-cyclohexyl-*S*-aroylhydrosulfamine (**S81.3**). Moreover, the Bohme group reported amide (**S81.7**) and sulfur formation from the reaction of **S81.5** with diethylamine, which presumably resulted from immediate decomposition of unstable intermediate **S81.6**.⁶ They also obtained similar results for piperidine and aniline. The Raasch group showed that stable *S*-aroylhydrosulfamines (**S81.10**) could be prepared by mixing sodium salts of both thioacids (**S81.8**) and hydroxylamine-*O*-sulfonate (**S81.9**).⁷ Their conditions corroborate the reported instability of both *N*-alkyl-*S*-aroylhydrosulfamines (**S81.3**) and *S*-acylhydrosulfamines (**S81.6**) (see intermediates **S81.13** and **S81.16**). They speculated that the decomposition of *S*-aroylhydrosulfamines to an amide and sulfur could involve a bimolecular process, forming a cyclic intermediate or transition state (**S82.1**). The more basic *N*-alkyl derivatives could readily lead to similar transition states, causing the observed instability of *N*-alkyl-*S*-hydrosulfanamines (**S81.3**, **S81.6**, and **S81.16**). Furthermore, they rationalized the stability of *S*-aroylhydrosulfamines (**S81.8**), in contrast to their aliphatic analogs (**S81.5**, **S81.15**), due to the additional resonance conjugation (**S82.2**).

Scheme 81 Stable and Unstable Hydrosulfamines

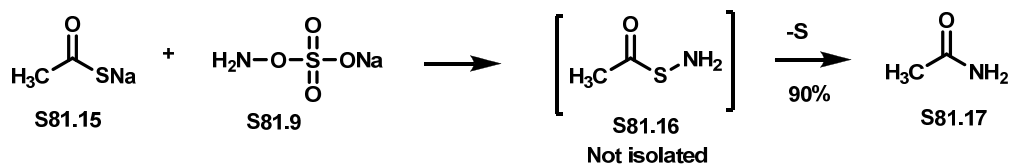
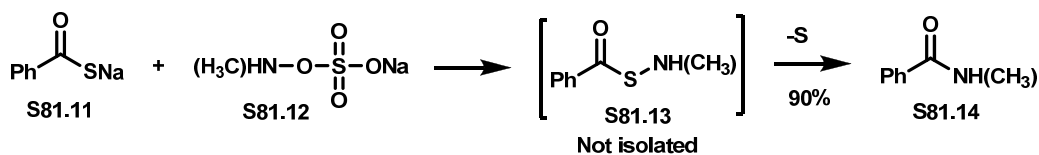
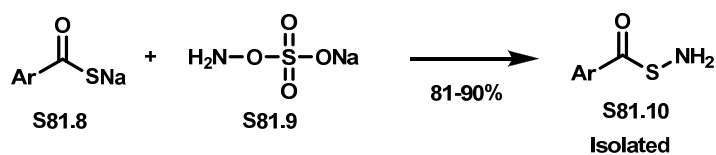
Alliger, 1949



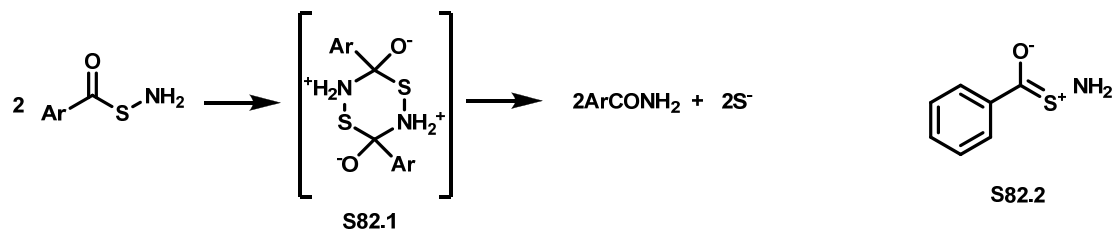
Bohme, 1952



Raasch, 1972



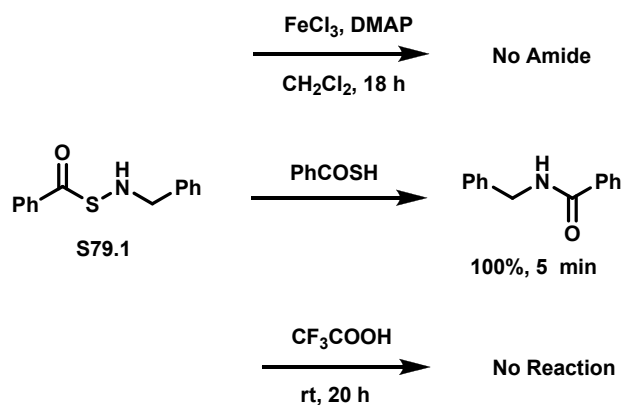
Scheme 82 The Mechanism for Decomposition S-Aroylhydrosulfamines



Much of the work presented in Scheme 81 and 82 is speculative. Our work may

serve to clarify some of these notions. The side product **S79.1** is very closely related to the putatively unstable *N*-alkyl-*S*-aroylhydrosulfamines, but it was isolated without decomposition. Control reactions done on **S79.1** reveal other significant information. Exposure of **S79.1** to the metal and base gave no amide, while treatment with the thiobenzoic acid furnished quantitatively the amide product in five minutes. Sulfur formation was also observed as reported. Moreover, the rapid formation of the same amide and sulfur was detected on treatment with thioacetic acid. In addition, the **S79.1** was unexpectedly found to be stable to the trifluoroacetic acid, in contrast to the thioacid derivatives.

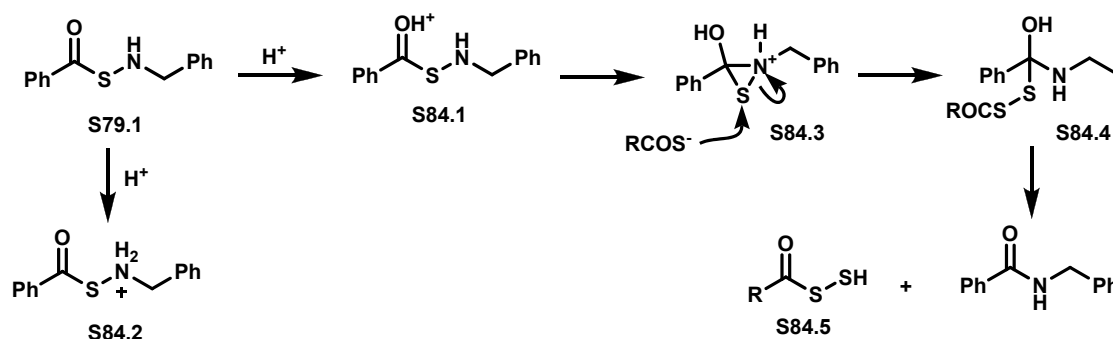
Scheme 83 Control Reactions on Side Product S79.1



The cyclic intermediate (**S82.1**) was proposed by Raasch. However, performing a crossover experiment between two stable *S*-aroylhydrosulfamines, which decompose at about same rates would distinguish unimolecular and bimolecular process. As indicated in Scheme 84, a unimolecular process could also be speculated for decomposition of similar molecules. Both thiaacid and trifluoroacetic acid could protonate two basic sites on **S79.1**, which could lead to either **S84.1** or **S84.2**. In principle, both trifluoroacetic and

thiobenzoic acid could lead to **S84.3**. The opening of **S84.4** likely would not be facile for trifluoroacetic acid due to the low nucleophilicity of the trifluoroacetate anion. A thiocarboxylate could give **S84.4**, which could give rise to the amide and **S84.5**. **S84.5** decomposes to the observed the dimer (**S78.1**) and sulfur products. However, this mechanism is unnecessarily complex. Another alternative is that **S84.2** is attacked by thiobenzoic acid to give **S78.1** directly. This species is a very potent acylating agent, as is **S84.5**. Amines react almost instantaneously with such thioanhydrides. This accounts for very rapid conversion of **S79.1** to amide (Scheme 83), avoids unlikely events such as **S84.1**→**S84.3**, and most of the speculative notions of Alliger, Bohme and Raasch. Although we did not observe benzyl amine in our reaction, it would be expected to form only in trace quantity before rapidly reacting with **S78.1** to give the amide product.

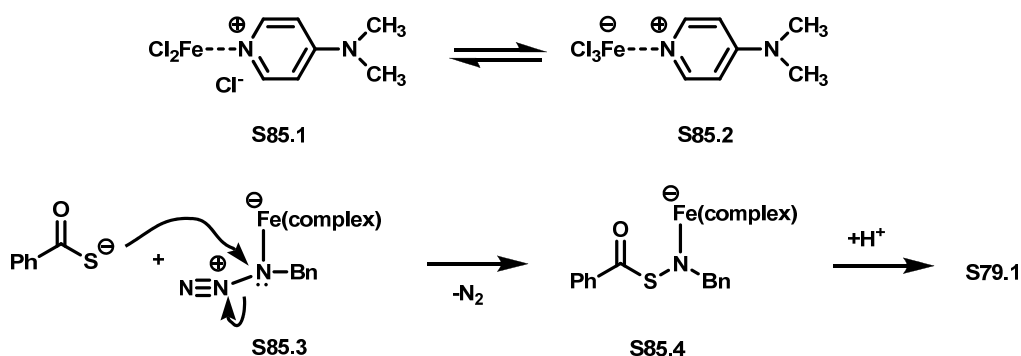
Scheme 84 The Proposed Mechanism of Amide Formation from S79.1



Although iron (III) chemistry is complex, and ascertaining the precise mechanism of amidation is beyond the scope of these studies, several observations are noteworthy. The iron (III) chloride and DMAP combination could have a substantial effect on the formation of **S79.1**, since all the metals in Table 3 and all bases in Table 6, except for entry 4, failed to couple. The promoter and base could give rise to complex structures

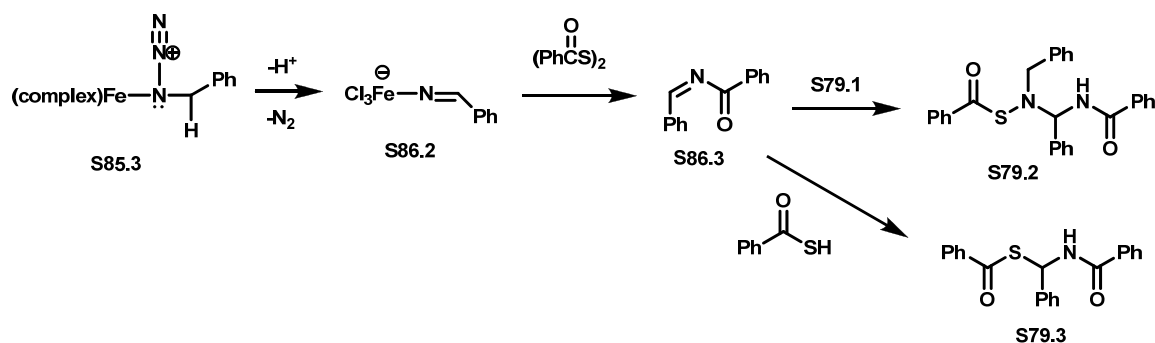
S85.1 and **S85.2**. An iron complex could coordinate to the internal or to the terminal azide nitrogen and form, for example, **S85.3**, either of which could facilitate attack of thiobenzoate. Sulfur-nitrogen bond formation could take place simultaneously with loss of nitrogen, which would lead to formation of the **S79.1**.

Scheme 85 The Mechanism for the Formation of S79.1



We were also curious about side products **S79.2** and **S79.3** since they diminish as formation of the major amide product increases. Based on their structure, it is reasonable to speculate that they are formed from a different pathway than **S79.1**, which could likely involve the highly reactive intermediate **S86.3** (Scheme 86). Nucleophiles readily add to the similar electrophiles.⁸ In this case the nucleophiles are the **S79.1** and the thiobenzoate anion. A plausible mechanism for formation of **S86.3** is by rearrangement of the azide. The same type of intermediate as **S86.2** was also invoked by the Kerr group earlier.⁹ Nucleophilic addition of **S79.1** to or thiobenzoic acid **S86.3** would provide **S79.2** and **S79.3**.

Scheme 86 The Formation of the Intermediate S86.3



In contrast to the reported instability, the metal promoted amidation revealed a stable intermediate (S79.1 and S79.2). Although amide product formation was unambiguously established from S79.1 upon treatment with thiobenzoic acid, it has not been established as the major path by which the amide product is formed. Indeed, it is speculative to indicate that similar mechanism could take place for the thioacid-azide coupling, as opposed to the reported mechanisms.¹ Nevertheless, this mechanism could be considered as an alternative pathway for amide formation.

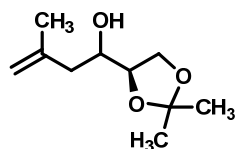
REFERENCES

- 1) (a) Shangguan, N.; Katukojvala, S.; Williams, L. J. *J. Am. Chem. Soc.* **2003**, *125*, 7754 (b) Kolakowski, R. V.; Shangguan, N.; Williams, L. J. *Tetrahedron Lett.*, **2006**, 47(7), 1163-1166. (c) Barlett, K. N.; Kolakowski, R. V.; Katukojvala, S.; Williams, L. J. *Org. Lett.*, **2006**, 8, 823-826. (d) Kolakowski, R. V.; Shangguan, N.; Sauers, R. R.; Williams, L. J. *J. Am. Chem. Soc.*, **2006**, *128*, 5695-5702.
- 2) W. Lwowski, in *1,3-Dipolar Cycloaddition Chemistry, Vol. 1* (Ed. A. Padwa) **1984**, pp. 621–634 (Wiley: NewYork, NY).
- 3) Fazio, F.; Wong, C.-H. *Tett. Lett.* **2003**, *44*, 9083-9085.
- 4) a) Rostovtev, V. V.; Green, J. G.; Fokin, V. V.; Sharpless, K. B. *Angew. Chem. Int. Ed.* **2002**, *41*, 2596-2599. b) Tornøe, C. W.; Christensen, C.; Meldal, M. *J. Org. Chem.* **2002**, *67*, 3057-3064.
- 5) Alliger, G.; Smith, G. E. P. Jr.; Carr, E. L.; Stevens, H. P. *J. Org. Chem.* **1949**, *42*, 7296.
- 6) Bohme, H.; Clement, M. *Justus Liebegs Ann. Chem.* **1952**, *61*, 576.
- 7) Raasch, M. S. *J. Org. Chem.* **1972**, *24*, 3820.
- 8) Gizecki, P.; Dhal, R.; Poulard, C.; Gosselin, P.; Dujardin, G. *J. Org. Chem.* **2003**, *68*, 4338-4344.
- 9) Barrett, I. C.; Langille, J. D.; Kerr, M. A. *J. Org. Chem.* **2000**, *65*, 6268-6269.

EXPERIMENTAL

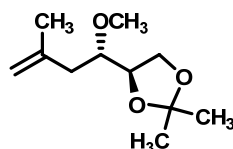
General: Starting materials, reagents and solvents were purchased from commercial suppliers (Aldrich, Fischer, Advanced ChemTech) and used without further purification unless otherwise stated. All reactions were conducted in oven-dried (135 °C) glassware under an inert atmosphere of argon. The progress of reactions was monitored by silica gel thin layer chromatography (tlc) plates (mesh size 60Å with fluorescent indicator, Sigma-Aldrich), visualized under UV and charred using cerium or anisaldehyde stain. Products were purified by flash column chromatography (FCC) on 120-400 mesh silica gel (Fisher). Infrared (FTIR) spectra were recorded on an ATI Mattson Genesis Series FT-Infrared spectrophotometer. Proton nuclear magnetic resonance spectra (^1H NMR) were recorded on either a Varian-300 instrument (300 MHz) or a Varian-400 instrument (400 MHz) unless otherwise stated. Chemical shifts are reported in ppm relative to residual CHCl_3 signal. Data is reported as follows: chemical shift, integration, multiplicity (s=singlet, d=doublet, t=triplet, q=quartet, br=broad, m=multiplet), and coupling constants (Hz). Carbon nuclear magnetic resonance spectra (^{13}C NMR) were recorded on either a Varian-300 instrument (75 MHz) or a Varian-400 instrument (100 MHz) unless otherwise stated. Optical rotations were recorded at 25 °C using the sodium D line (589 nm), on a Perkin-Elmer 241 polarimeter. Mass spectra were recorded on a Finnigan LCQ-DUO mass spectrometer.

CHAPTER 1

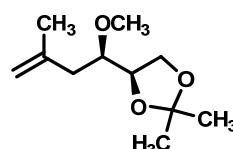


anti (S1.3): α OH
 syn (S1.4): β OH

To a solution of methallylmagnesium chloride in THF (0.0375 mole, 0.8 M) at -78°C was added slowly a solution of protected glyceraldeyhde **S1.1** (0.025 mole, 3.25g) in THF (62.5 ml) down the inside of the flask. The reaction mixture was allowed to warm to room temperature, and stirred for additional 4 h. The mixture was then cooled to -78°C , quenched with saturated NH_4Cl solution, extracted with Et_2O , and dried over Na_2SO_4 . Solvent was evaporated and the residue was purified by FCC using hexane:acetone (15:1) as eluent to give **5** and **6** as a colorless oil (3.4g, 74%). The ratio anti:syn alcohol was 4:3, as determined by $^1\text{H-NMR}$. R_F 0.22 (15:1-hexane:acetone); IR $\nu_{\text{max}}(\text{neat})/\text{cm}^{-1}$ 3475, 3057, 2986, 1648, 1067; δ_{H} (400 MHz, CDCl_3) 4.86-4.85 (2H, brs), 4.79-4.78 (2H, brs), 4.04-3.65 (8H, m), 2.29-2.05 (6H, m), 1.75 (6H, brs) 1.42-1.40 (6H, s), 1.35-1.34 (6H, s); δ_{C} (100 MHz, CDCl_3) 141.9 (s), 141.7 (s), 113.57 (t), 113.50 (t), 109.3 (s), 109.0 (s), 78.6 (d), 78.3 (d), 69.8 (d), 68.8 (d), 65.9 (t), 65.3 (t), 42.0 (q), 41.7 (q), 26.5 (two signals, q), 25.27 (q), 25.25 (q), 22.4 (t), 22.3 (t); m/z (ESIMS) found: 187 ($\text{M}+1$) $^{+}$; calcd: 187.



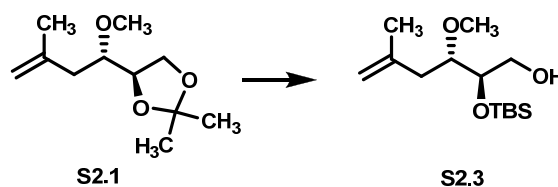
Anti (S2.1)



Syn (S2.2)

The mixture of **S1.3** and **S1.4** (1.25g, 6.7mmol) was dissolved in THF (12 ml), and cooled to 0 °C. NaH (484 mg, 12.1 mmol, 60% dispersion in mineral oil) was added and the mixture was stirred for 15 min. To this CH₃I (1.90 g, 0.84 ml, 13.4 mmol) was added and the mixture was allowed to warm to room temperature and stirred over 12 h. The reaction mixture was quenched with sat. NH₄Cl, extracted with Et₂O and dried over Na₂SO₄. After removing the solvent *in vacuo*, the residue was purified by FCC using with hexane:acetone (70:1) as eluent to give 657 mg (49%) *anti* isomer **S2.1** and 523 mg (39%) *syn* isomer **S2.2** as colorless oils (total yield 93%). **Anti isomer S2.1**; R_F 0.44 (40:1-hexane:acetone); $[\alpha]_D^{22} +19.0$ (c 4.52, CHCl₃); IR $\nu_{\max}(\text{neat})/\text{cm}^{-1}$ 3076, 2985, 1647, 1104; δ_{H} (400 MHz, CDCl₃) 4.82-4.79 (1H, brs), 4.789-4.786 (1H, brs) , 4.08-4.00 (2H, m), 3.90-3.87 (1H, m), 3.47-3.44 (1H, m), 3.44 (3H, s), 2.30-2.15 (2H, m), 1.79 (3H, s), 1.42 (3H,s), 1.34 (3H, s); δ_{C} (100 MHz, CDCl₃) 142.2 (s), 112.9 (t), 108.9 (s), 79.7 (q), 77.4 (d), 65.7 (t), 58.5 (d), 39.3 (q), 26.3 (q), 25.2 (q), 22.7 (t); *m/z* (ESIMS) found: 201 (M+1)⁺; calcd: 201.

Syn isomer S2.2; R_F 0.27 (40:1-hexane:acetone); $[\alpha]_D^{22} +9.7$ (c 0.72, CHCl₃); IR $\nu_{\max}(\text{neat})/\text{cm}^{-1}$ 3076, 2985, 1647, 1107; δ_{H} (400 MHz, CDCl₃) 4.82 (1H, brs), 4.78 (1H, brs), 4.19-4.14 (1H, m), 3.992 (1H, dd, J=6.8, 8.4), 3.70-3.66 (1H, m), 3.46 (3H, m), 3.41-3.36 (1H, m), 2.73 (2H, d, J=5.6), 1.79 (3H, s), 1.43 (3H, s), 1.36 (3H, s); δ_{C} (100 MHz, CDCl₃) 142.1 (s), 112.9 (t), 109.1 (s), 80.3 (q), 77.6 (d), 65.7 (t), 58.3 (d), 38.5 (q), 26.4 (q), 25.2 (q), 22.8 (t); *m/z* (ESIMS) found: 201 (M+1)⁺; calcd: 201.

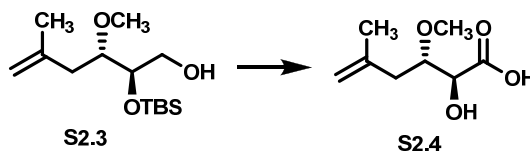


The protected diol **S2.1** (627 mg, 3.1 mmol) was stirred in 6.5 ml of AcOH:H₂O mixture (4:1) for 20 h at room temperature. The reaction mixture was concentrated and purified by FCC using with hexane:acetone (5:1) as eluent to afford 461 mg (93%) diol as a colorless oil. R_F 0.10 (5:1-hexane:acetone); $[\alpha]_D^{22}$ +22.5 (c 1.42, CHCl₃); IR $\nu_{\max}(\text{neat})/\text{cm}^{-1}$ 3395, 3086, 2935, 1649, 1101; δ_H (400 MHz, CDCl₃) 4.83 (1H, brs), 4.79 (1H, brs), 3.57-3.68 (3H, m), 3.52-3.48 (1H, m), 3.41 (3H, s), 3.00 (2H, brs), 2.364-2.328 (1H, m), 2.203-2.206 (1H, m), 1.78 (3H, s); δ_C (100 MHz, CDCl₃) 142.2 (s), 113.2 (t), 81.7 (q), 72.4 (d), 63.1 (t), 58.3 (d), 38.7 (q), 22.7 (t); m/z (ESIMS) found: 183 (M+23)⁺; calcd: 183.

To a solution of diol (205 mg, 1.28 mmol) in DMF (4 ml) was added imidazole (262 mg, 3.84 mmol) and TBSCl (503 mg, 3.33 mmol). The reaction mixture was stirred overnight, and then diluted with H₂O. The solution was extracted with Et₂O, dried over Na₂SO₄. After removing the solvent in vacuo, the residue was purified by FCC using hexane:acetone (40:1) as eluent to give 437 mg (88%) bis-[TBS] ether as a colorless oil. R_F 0.93 (40:1-hexane:acetone); $[\alpha]_D^{22}$ -8.7 (c 6.06, CHCl₃); IR $\nu_{\max}(\text{neat})/\text{cm}^{-1}$ 3076, 2955, 1650, 1183, 1082; δ_H (300 MHz, CDCl₃) 4.79 (1H, brs), 4.80 (1H, brs), 4.77 (1H, brs), 3.82-3.77 (1H, m), 3.56 (2H, d, J=5.7 Hz), 3.47-3.42 (1H, m), 3.38 (3H, s), 2.25 (2H, d, J=6.9 Hz), 1.77 (3H, s), 0.90 (9H, s), 0.89 (9H, s), 0.06 (6H, s), 0.07 (6H, s); δ_C (75 MHz, CDCl₃) 143.6 (s), 112.1 (t), 81.3 (q), 74.5 (d), 64.6 (t), 58.3 (d), 38.7 (q), 26.3

(q), 26.2 (q), 23.1 (t), 18.6 (s), 18.5 (s), -4.1 (q), -4.3 (q), -4.9 (q), -5.0 (q); m/z (ESIMS) found: 411 ($M+23$)⁺; calcd: 411.

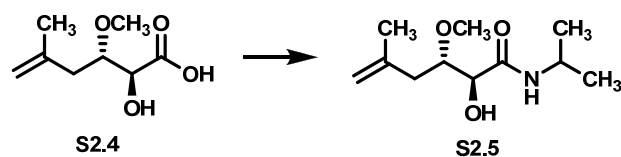
To a solution of bis-[TBS] ether (440 mg, 1.13 mmol) in THF (3.6 ml) in a plastic vial was added pyridine (0.60 ml) and HF-pyridine (0.1 ml of a 65-70% solution of HF in pyridine). The mixture was stirred 22 h, then diluted with Et₂O and washed with 0.5 M HCl solution. The aqueous layer was re-extracted with Et₂O. The combined organic layers were washed with saturated CuSO₄·H₂O and dried over NaSO₄. After removing the solvent, the residue was purified by FCC using hexane:acetone (20:1) as eluent to give 226 mg (73%) mono-alcohol **S2.3** as a colorless oil. R_F 0.24 (20:1-hexane:acetone); $[\alpha]_D^{22} +5.4$ (c 2.98, CHCl₃); IR ν_{max} (neat)/cm⁻¹ 3456, 3076, 2930, 1649, 1112; δ_H (400 MHz, CDCl₃) 4.81 (1H, brs), 4.79 (1H, brs) 3.73-3.60 (3H, m), 3.43 (3H, s), 3.41-3.39 (1H, m), 2.29-2.15 (3H, m), 0.9 (9H, s), 0.09 (6H, s); δ_C (100 MHz, CDCl₃) 142.9 (s), 112.9 (t), 82.1 (q), 74.5 (d), 64.1 (t), 59.3 (d), 40.4 (q), 26.1 (q), 23.1 (t), 18.4 (s), -4.0 (q), -4.1 (q); m/z (ESIMS) found: 275 ($M+1$)⁺; calcd: 275.



A solution of oxalyl chloride (0.19 ml, 2.18 mmol) in CH₂Cl₂ (7 ml) was cooled down to -78 °C. DMSO (0.340 ml, 4.79 mmol) was syringed in one portion and stirred for 15 min. Then the alcohol **S2.3** (396 mg, 1.45 mmol) dissolved in CH₂Cl₂ (7 ml) was added slowly. After 30 min Et₃N (1,026 ml, 7.4 mmol) was added after which the cooling bath was replaced by an ice bath. Stirring was continued for 20 min, and then diluted with

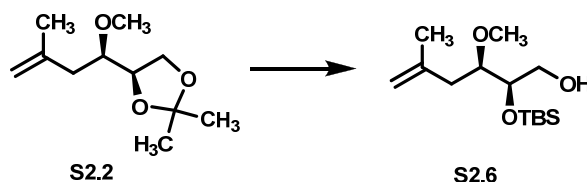
CH₂Cl₂ and H₂O. Extraction with CH₂Cl₂ and drying over Na₂SO₄ furnished 386 mg (98%) aldehyde. $[\alpha]_D^{22}$ -27.6 (c 0.98, CHCl₃); IR $\nu_{\max}(\text{neat})/\text{cm}^{-1}$ 3069, 2955, 2858, 1733, 1647, 1109; δ_{H} (400 MHz, CDCl₃) 9.59 (1H, d, J=1.1 Hz) 4.82 (2H, brs), 4.13 (1H, dd, J=2.4, 1.1 Hz), 3.60 (1H, dt, J=7.0, 2.4 Hz), 3.61 (3H, s), 2.33-2.21 (2H, m), 0.93 (9H, s), 0.08 (6H, d, J=8.2 Hz); δ_{C} (75 MHz, CDCl₃) 203.4 (s), 141.4 (s), 114.8 (t), 83.0 (q), 78.7 (d), 58.1 (d), 38.8 (q), 26.0 (q), 22.9 (t), 18.5 (s), -4.4 (q), -4.5 (q); m/z (ESIMS) found: 273 (M+1)⁺; calcd: 273.

A solution of aldehyde (150 mg, 0.55 mmol) in 12.5 ml tBuOH-H₂O (3.5:1) was cooled to 0 °C, to which was added NaH₂PO₄·H₂O (137 mg, 0.99 mmol), 2-methyl-2-butene (10 mmol, 5.2 ml from 2 M solution in THF) and NaClO₂ (122 mg, 1.35 mmol). The cooling bath was removed after 5 min and stirring was continued for 2 h. The mixture was concentrated, diluted with H₂O, acidified with 1 N HCl until pH 2-3 was reached, and then extracted with Et₂O (5×). The organic extract was washed with brine and dried over Na₂SO₄. After removing the solvent in vacuo, the residue was purified by FCC (50% hexane:acetone and 1% AcOH) to furnish 80 mg (84%) carboxylic acid **S2.4** as a colorless oil. R_{F} 0.34 (1:1:0.01-hexane:acetone:acetic acid); $[\alpha]_D^{22}$ +18.6 (c 0.86, CHCl₃); IR $\nu_{\max}(\text{neat})/\text{cm}^{-1}$ 3600-2500, 3395, 3077, 2936, 1732, 1651, 1105; δ_{H} (300 MHz, CDCl₃) 4.87 (1H, brs), 4.84 (1H, brs), 4.40 (1H, d, J=3.9 Hz), 3.76-3.71 (1H, m), 3.48 (3H, s), 2.46-2.29 (2H, m), 1.79 (3H, s); δ_{C} (75 MHz, CDCl₃) 175.1 (s), 141.4 (s), 114.0 (t), 81.4 (q), 71.3 (d), 58.3 (d), 37.8 (q), 23.0 (t); m/z (ESIMS) found: 197 (M+23)⁺; calcd: 197.



To a solution of 2-hydroxy-carboxylic acid **S2.4** (43.5 mg, 0.25 mmol), catalytic amount of DMAP (~1 mg), and pyridine (43 μ l, 0.53 mmol) was added TMSCl (68 μ l, 0.53 mmol) dropwise. The reaction was stirred at room temperature for 3 h. The reaction was cooled to 0 $^{\circ}$ C and catalytic DMF (1 drop) was added followed by oxalyl chloride (25 μ l, 0.28 mmol). The reaction mixture was stirred for 30 min at 0 $^{\circ}$ C and then 30 min at room temperature. After cooling the mixture to 0 $^{\circ}$ C, a solution of isopropyl amine (43 μ l, 0.5 mmol) in pyridine (121 μ l, 1.5 mmol) was added and the reaction was allowed to warm to room temperature and stir for 2 h. Citric acid (111.3 mg, 0.53 mmol) was dissolved in methanol (1 ml) and added to the reaction. After 45 min, the mixture was poured into a separatory funnel and diluted with ethyl acetate. The organic phase was washed with 1 N HCl and the aqueous wash was back extracted with ethyl acetate. The combined organic layers were washed with a saturated bicarbonate solution followed by brine and dried over Na_2SO_4 . After removing the solvent, the residue was purified by FCC using hexane:acetone (5:1) as eluent to furnish 27 mg (50%) amide **S2.5** as a white solid. For crystallization, 1 mg of purified compound **S2.5** was dissolved in 1 ml of CH_2Cl_2 , and then almost 1 ml of hexane was added until turbidity appeared. Colorless crystals were obtained in next day. R_F 0.36 (5:1-hexane:acetone); $[\alpha]_D^{22}$ -24.2 (c 0.99, CHCl_3); IR (KBr) 3391, 3285, 3077, 2974, 1650, 1648, 1104; δ_H (300 MHz, CD_3OD) 4.76 (1H, s), 4.73 (1H, s), 4.26 (1H, d, $J=3$ Hz), 4.00 (1H, m, $J=6.6$ Hz), 3.66 (1H, dt, $J=9.3, 3.0$), 3.38 (3H, s), 2.27 (1H, ddd, $J=14, 9.3, 0.6$), 2.05 (1H, dd, $J=14, 3.6$), 1.73 (3H, s), 1.56 (6H, dd, $J=6.6, 4.5$ Hz); (75 MHz, CDCl_3) 172.3 (s), 142.6 (s), 111.7 (t), 81.4 (q), 71.2 (d),

56.5 (d), 41.1 (d), 37.2 (q), 21.8 (t), 21.48 (q), 21.43 (q); m/z (ESIMS) found: 216 (M+1)⁺; calcd: 216.

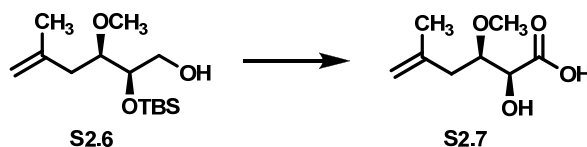


The protected diol **S2.2** (627 mg, 3.1 mmol) was stirred in 6.5 ml of AcOH:H₂O mixture (4:1) for 20 h at room temperature. The reaction mixture was concentrated and purified by FCC using hexane:acetone (5:1) as eluent to afford 436 mg (88%) diol as a colorless oil. R_F 0.08 (5:1-hexane:acetone); $[\alpha]_D^{22}$ -29.2 (c 0.24, CHCl₃); IR ν_{\max} (neat)/cm⁻¹ 3076, 2985, 1647, 1107; δ_H (400 MHz, CDCl₃) 4.82 (1H, brs), 4.78 (1H, brs), 4.19-4.14 (1H, m), 3.992 (1H, dd, J=6.8, 8.4), 3.70-3.66 (1H, m), 3.46 (3H, m), 3.41-3.36 (1H, m), 2.73 (2H, d, J=5.6), 1.79 (3H, s), 1.43 (3H, s), 1.36 (3H, s); δ_C (100 MHz, CDCl₃) 142.0 (s), 113.4 (t), 79.9 (q), 72.7 (d), 64.0 (t), 57.9 (d), 38.1 (q), 22.8 (t); m/z (ESIMS) found: 201 (M+1)⁺; calcd: 201.

To a solution of the above diol (205 mg, 1.28 mmol) in DMF (4 ml) was added imidazole (262 mg, 3.84 mmol) and TBSCl (503 mg, 3.33 mmol). The reaction mixture was stirred overnight and then diluted with H₂O, extracted with Et₂O, and dried over Na₂SO₄. After removing the solvent in vacuo, the residue was purified by FCC using hexane:acetone (40:1) as eluent to give 457 mg (92%) bis-TBS ether as a colorless oil. R_F 0.93 (40:1-hexane:acetone); [α]_D²² +5.6 (c 0.90, CHCl₃); IR ν_{max} (neat)/cm⁻¹ 3076, 2955, 1648, 1111; δ_{H} (400 MHz, CDCl₃) 4.79 (1H, brs), 4.76 (1H, brs), 3.80-3.72 (2H, m), 3.53-3.49 (1H, m), 3.43-3.40 (1H, m), 3.40 (3H, s), 2.330 (1H, dd, J=14.4, 2.8), 2.10 (1H, dd, J=14.4,

9.2), 0.90 (18H, s), 0.09 (6H, s), 0.06 (6H, brs); δ_C (400 MHz, $CDCl_3$) 143.8 (s), 112.2 (t), 80.8 (q), 74.1 (d), 64.2 (t), 58.6 (d), 38.0 (q), 26.2 (q), 26.1 (q), 22.9 (t), 18.5 (s), 18.3 (s), -3.9 (q), -4.5 (q), -5.0 (q), -5.1 (q); m/z (ESIMS) found: 411 ($M+23$)⁺; calcd: 411.

To a solution of bis-TBS ether (440 mg, 1.13 mmol) in THF (3.6 ml) in a plastic vial was added pyridine (0.60 ml) and HF-pyridine (0.1 ml of a 65-70% solution of HF in pyridine). The mixture was stirred 22 h, then diluted with Et₂O and washed with 0.5 M HCl solution. The aqueous layer was re-extracted with Et₂O. The combined organic layers were washed with saturated CuSO₄·H₂O and dried over NaSO₄. After removing the solvent, the residue was purified by FCC using hexane:acetone (20:1) as eluent to give 229 mg (74%) alcohol **12** as a colorless oil. R_F 0.24 (20:1-hexane:acetone); [α]²²_D +3.3 (c 1.80, CHCl₃); IR ν_{max}(neat)/cm⁻¹ 3461, 3076, 2930, 1647, 1107; (400 MHz, CDCl₃) 4.80 (1H, brs), 4.77 (1H, brs), 3.93-3.89 (1H, m), 3.72-3.68 (1H, m), 3.58-3.54 (1H, m), 3.43-3.418 (1H, m), 3.410 (3H, s), 2.36 (1H, d, J=14.4 Hz), 2.24 (1H, brs), 2.12 (1H, dd, J=14.4, 9.6 Hz), 1.77 (3H, s), 0.90 (9H, s), 0.11 (6H, s); δ_C (100 MHz, CDCl₃) 143.3 (s), 112.5 (t), 82.3 (q), 71.9 (d), 63.8 (t), 58.7 (d), 37.8 (q), 26.1 (q), 23.1 (t), 18.4 (s), -4.2 (q); *m/z* (ESIMS) found: 275 (M+1)⁺; calcd: 275.

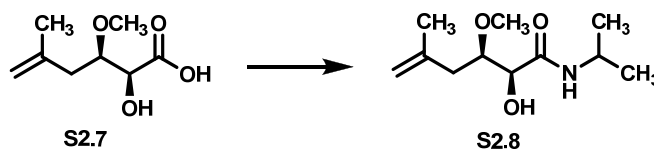


A solution of oxalyl chloride (0.19 ml, 2.18 mmol) in CH₂Cl₂ (7 ml) was cooled down to -78 °C. DMSO (0.340 ml, 4.79 mmol) was syringed in one portion and stirred for 15 min. Then the alcohol **S2.6** (396 mg, 1.45 mmol) dissolved in CH₂Cl₂ (7 ml) was added

slowly. After 30 min Et₃N (1,026 ml, 7.4 mmol) was added after which the cooling bath was replaced by an ice bath. Stirring was continued for 20 min, and then diluted with CH₂Cl₂ and H₂O. Extraction with CH₂Cl₂ and drying over Na₂SO₄ furnished 386 mg (98%) aldehyde. $[\alpha]_D^{22}$ -5.9 (c 1.18, CHCl₃); IR $\nu_{\max}(\text{neat})/\text{cm}^{-1}$ 3078, 2932, 2858, 1736, 1648, 1099; δ_{H} (400 MHz, CDCl₃) 9.69 (1H, d, J=1.2 Hz), 4.79 (1H, brs), 4.75 (1H, brs), 4.07 (1H, dd, J=3.9, 1.2 Hz), 3.66-3.61 (1H, m), 3.35 (3H, s), 2.34-2.29 (1H, m), 2.24-2.17 (1H, m), 0.91 (9H, s), 0.05 (6H, d, J=7.6 Hz); δ_{C} (75 MHz, CDCl₃) 203.7 (s), 142.2 (s), 113.1 (t), 81.5 (q), 78.7 (d), 58.7 (d), 38.4 (q), 26.1 (q), 23.1 (t), 18.6 (s), -4.1 (q), -4.6 (q); m/z (ESIMS) found: 273 (M+1)⁺; calcd: 273.

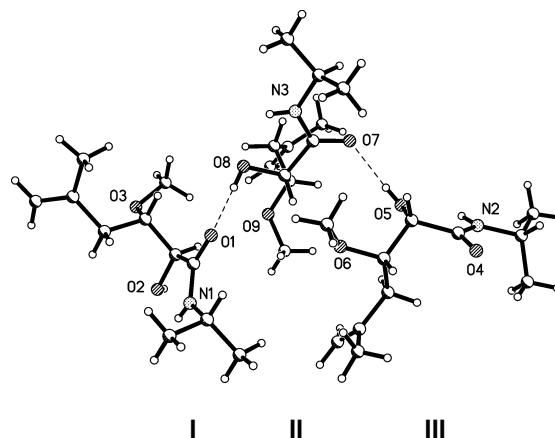
A solution of aldehyde (150 mg, 0.55 mmol) in 12.5 ml of tBuOH-H₂O (3.5:1) was cooled to 0 °C and added NaH₂PO₄·H₂O (137 mg, 0.99 mmol), 2-methyl-2-butene (10 mmol, 5.2 ml from 2 M solution in THF) and NaClO₂ (122 mg, 1.35 mmol). The cooling bath was removed after 5 min and stirring was continued for 2 h. The mixture was concentrated, diluted with H₂O, and then 1 N HCl was added until pH 2-3 was reached. The mixture was extracted with Et₂O (5×), and the combined organic extract was washed with brine and dried over Na₂SO₄. After removing the solvent in vacuo, the residue was purified by FCC (50% hexane:acetone and 1% AcOH) to furnish 77 mg (80%) carboxylic acid **S2.7** as a colorless oil. R_{F} 0.34 (1:1:0.01-hexane:acetone:acetic acid); $[\alpha]_D^{22}$ +6.0 (c 1.16, CHCl₃); IR $\nu_{\max}(\text{neat})/\text{cm}^{-1}$ 3600-2600, 3346, 3076, 2936, 1732, 1650, 1089; δ_{H} (300 MHz, CDCl₃) 4.87 (1H, brs), 4.84 (1H, brs), 4.21 (1H, s), 3.83 (1H, t, J=7.2 Hz), 3.40 (3H, s), 2.38 (2H, d, J=7.2 Hz); (75 MHz, CDCl₃) 177.3 (s), 141.3 (s), 114.3 (t),

80.2 (q), 71.3 (d), 58.5 (d), 38.2 (q), 23.1 (t); m/z (ESIMS) found: 197 ($M+23$)⁺; calcd: 197.



To a solution of 2-hydroxy-carboxylic acid **S2.7** (43.5 mg, 0.25 mmol), catalytic amount of DMAP, and pyridine (43 μ l, 0.53 mmol) was added TMSCl (68 μ l, 0.53 mmol) dropwise. The reaction was stirred at room temperature for 3 h. The reaction was cooled to 0 °C and catalytic amount of DMF (1 drop) was added followed by oxalyl chloride (25 μ l, 0.28 mmol). The reaction mixture was stirred for 30 min at 0 °C and then 30 min at room temperature. After cooling the mixture to 0 °C, a solution of isopropyl amine (43 μ l, 0.5 mmol) in pyridine (121 μ l, 1.5 mmol) was added and the reaction was allowed to warm to room temperature and stir for 2 h. Citric acid (111.3 mg, 0.53 mmol) was dissolved in methanol (1 ml) and added to the reaction. After 45 min, the mixture was poured into a separatory funnel and diluted with ethyl acetate. The organic phase was washed with 1 N HCl and the aqueous wash was back extracted with ethyl acetate. The combined organic layers were washed with a saturated bicarbonate solution followed by brine and dried over Na₂SO₄. After removing the solvent, the residue was purified by FCC using hexane:acetone (5:1) as eluent to furnish 29 mg (54%) amide **S2.8** as a colorless oil. M.p. 62-63 °C; R_F 0.36 (5:1-hexane:acetone); $[\alpha]_D^{22}$ -26.7 (c 2.32, CHCl₃); IR ν_{max} (neat)/cm⁻¹ 3390, 3340, 3076, 2971, 1650, 1090; δ_H (300 MHz, CD₃OD) 4.84-4.83 (1H, brs), 4.81-4.80 (1H, brs), 4.02 (1H, m, J=6.6 Hz), 3.90 (1H, d, J=1.8 Hz), 3.83-3.77 (1H, m), 3.33 (3H, s), 2.40-2.26 (2H, m), 1.80 (3H, s), 1.17 (6H, dd, J=6.6, 2.4 Hz); (75

MHz, CDCl₃) 173.4 (s), 142.2 (s), 112.6 (s), 80.2 (q), 72.2 (d), 57.8 (d), 41.2 (d), 38.6 (q), 21.8 (t), 21.5 (q), 21.4 (q); *m/z* (ESIMS) found: 216 (M+1)⁺; calcd: 216.

Crystal Structure: Three Conformers of **S2.5**.

Empirical formula	C ₁₁ H ₂₁ N O ₃	
Formula weight	215.29	
Temperature	1	00(2) K
Wavelength	0.71073 Å	
Crystal system	Hexagonal	
Space group	P6(1)	
Unit cell dimensions	a = 11.3849(3) Å	∠ = 90°.
	b = 11.3849(3) Å	∠ = 90°.
	c = 51.704(3) Å	∠ = 120°.
Volume	5803.8(4) Å ³	
Z	18	
Density (calculated)	1.109 Mg/m ³	
Absorption coefficient	0.080 mm ⁻¹	
F(000)	2124	

Crystal size	.22 x 0.20 x 0.10 mm ³
Theta range for data collection	2.07 to 28.37°.
Index ranges	-15≤h≤15, -15≤k≤15, -68≤l≤68
Reflections collected	61964
Independent reflections	9635 [R(int) = 0.0454]
Completeness to theta = 28.37°	99.6 %
Absorption correction	Semi-empirical from equivalents
Max. and min. transmission	0.9999 and 0.8502
Refinement method	Full-matrix least-squares on F ²
Data / restraints / parameters	9635 / 1 / 440
Goodness-of-fit on	F21.036
Final R indices [I>2sigma(I)]	R1 = 0.0464, wR2 = 0.1110
R indices (all data)	R1 = 0.0561, wR2 = 0.1164
Absolute structure parameter	0.1(6)
Largest diff. peak and hole	0.580 and -0.202 e.Å ⁻³

Table 2. Atomic coordinates ($\times 10^4$) and equivalent isotropic displacement parameters ($\text{\AA}^2 \times 10^3$) for **S2.5**. U(eq) is defined as one third of the trace of the orthogonalized U^{ij} tensor.

	x	y	z	U(eq)
N(1)	2766(2)	-3690(2)	-649(1)	25(1)
O(1)	2163(1)	-4572(1)	-1051(1)	30(1)
O(2)	4219(1)	-1200(1)	-815(1)	26(1)
O(3)	5189(1)	-860(1)	-1356(1)	27(1)
C(1)	6842(2)	-2111(2)	-1273(1)	38(1)

C(2)	6368(3)	-3265(4)	-1454(1)	62(1)
C(3)	8190(3)	-1026(3)	-1259(1)	66(1)
C(4)	5799(2)	-2152(2)	-1084(1)	29(1)
C(5)	4621(2)	-2098(2)	-1216(1)	24(1)
C(6)	4321(2)	-891(2)	-1558(1)	32(1)
C(7)	3583(2)	-2158(2)	-1016(1)	23(1)
C(8)	2774(2)	-3585(2)	-905(1)	24(1)
C(9)	2033(2)	-4977(2)	-510(1)	30(1)
C(10)	3032(3)	-5254(2)	-368(1)	45(1)
C(11)	1004(2)	-4943(2)	-328(1)	44(1)
N(2)	-6455(2)	-7779(2)	-1251(1)	29(1)
O(4)	-6295(2)	-9292(1)	-993(1)	33(1)
O(5)	-3923(2)	-6477(2)	-1367(1)	36(1)
O(6)	-2013(1)	-6609(1)	-1017(1)	32(1)
C(12)	-2712(2)	-5598(2)	-573(1)	32(1)
C(13)	-1985(2)	-4274(2)	-527(1)	41(1)
C(14)	-2712(2)	-6623(2)	-390(1)	37(1)
C(15)	-3593(2)	-6131(2)	-808(1)	32(1)
C(16)	-3418(2)	-7193(2)	-958(1)	27(1)
C(17)	-1612(2)	-7571(2)	-1079(1)	40(1)
C(18)	-4263(2)	-7612(2)	-1207(1)	29(1)
C(19)	-5767(2)	-8312(2)	-1141(1)	27(1)
C(20)	-7907(2)	-8299(2)	-1209(1)	32(1)
C(21)	-8174(3)	-7971(3)	-937(1)	44(1)
C(22)	-8398(2)	-7685(2)	-1412(1)	40(1)
N(3)	-380(2)	-6569(2)	-1821(1)	26(1)
O(7)	-2138(1)	-6241(2)	-1735(1)	32(1)
O(8)	1325(1)	-4582(1)	-1535(1)	26(1)
O(9)	658(1)	-2516(1)	-1381(1)	30(1)
C(23)	205(2)	-1862(2)	-1926(1)	28(1)
C(24)	-986(2)	-2381(2)	-2105(1)	42(1)
C(25)	892(3)	-580(2)	-1847(1)	43(1)
C(26)	571(2)	-2895(2)	-1834(1)	26(1)
C(27)	-73(2)	-3521(2)	-1573(1)	24(1)
C(28)	12(2)	-2813(2)	-1135(1)	34(1)
C(29)	-15(2)	-4815(2)	-1517(1)	24(1)

C(30)	-939(2)	-5941(2)	-1703(1)	24(1)
C(31)	-1128(2)	-7738(2)	-1993(1)	30(1)
C(32)	-109(2)	-7844(2)	-2166(1)	40(1)
C(33)	-1970(3)	-9018(2)	-1838(1)	46(1)

Table 3. Bond lengths [Å] and angles [°] for **S2.5**.

N(1)-C(8)	1.328(2)	C(11)-H(11A)	0.9800
N(1)-C(9)	1.463(2)	C(11)-H(11B)	0.9800
N(1)-H(1N)	0.76(2)	C(11)-H(11C)	0.9800
O(1)-C(8)	1.238(2)	N(2)-C(19)	1.332(2)
O(2)-C(7)	1.414(2)	N(2)-C(20)	1.468(3)
O(2)-H(2O)	0.78(3)	N(2)-H(2N)	0.84(2)
O(3)-C(5)	1.422(2)	O(4)-C(19)	1.235(2)
O(3)-C(6)	1.426(2)	O(5)-C(18)	1.416(2)
C(1)-C(3)	1.411(4)	O(5)-H(5O)	0.76(3)
C(1)-C(2)	1.480(4)	O(6)-C(17)	1.419(2)
C(1)-C(4)	1.519(3)	O(6)-C(16)	1.424(2)
C(2)-H(2A)	0.9800	C(12)-C(13)	1.329(3)
C(2)-H(2B)	0.9800	C(12)-C(15)	1.501(3)
C(2)-H(2C)	0.9800	C(12)-C(14)	1.501(3)
C(3)-H(3A)	0.9500	C(13)-H(13A)	0.9500
C(3)-H(3B)	0.9500	C(13)-H(13B)	0.9500
C(4)-C(5)	1.532(3)	C(14)-H(14A)	0.9800
C(4)-H(4A)	0.9900	C(14)-H(14B)	0.9800
C(4)-H(4B)	0.9900	C(14)-H(14C)	0.9800
C(5)-C(7)	1.545(2)	C(15)-C(16)	1.531(3)
C(5)-H(5)	1.0000	C(15)-H(15A)	0.9900
C(6)-H(6A)	0.9800	C(15)-H(15B)	0.9900
C(6)-H(6B)	0.9800	C(16)-C(18)	1.533(3)
C(6)-H(6C)	0.9800	C(16)-H(16)	1.0000
C(10)-H(10A)	0.9800	C(17)-H(17A)	0.9800
C(10)-H(10B)	0.9800	C(17)-H(17B)	0.9800
C(10)-H(10C)	0.9800	C(17)-H(17C)	0.9800

C(18)-C(19)	1.523(3)	C(29)-H(29)	1.0000
C(18)-H(18)	1.0000	C(31)-C(33)	1.514(3)
C(20)-C(22)	1.515(3)	C(31)-C(32)	1.518(3)
C(20)-C(21)	1.522(3)	C(31)-H(31)	1.0000
C(20)-H(20)	1.0000	C(32)-H(32A)	0.9800
C(21)-H(21A)	0.9800	C(32)-H(32B)	0.9800
C(21)-H(21B)	0.9800	C(32)-H(32C)	0.9800
C(21)-H(21C)	0.9800	C(33)-H(33A)	0.9800
C(22)-H(22A)	0.9800	C(33)-H(33B)	0.9800
C(22)-H(22B)	0.9800	C(33)-H(33C)	0.9800
C(22)-H(22C)	0.9800	C(8)-N(1)-C(9)	123.74(16)
N(3)-C(30)	1.322(2)	C(8)-N(1)-H(1N)	117.4(18)
N(3)-C(31)	1.466(2)	C(9)-N(1)-H(1N)	118.9(18)
N(3)-H(3N)	0.83(2)	C(7)-O(2)-H(2O)	105(2)
O(7)-C(30)	1.241(2)	C(5)-O(3)-C(6)	112.56(14)
O(8)-C(29)	1.414(2)	C(3)-C(1)-C(2)	124.2(2)
O(8)-H(8O)	0.80(3)	C(3)-C(1)-C(4)	119.1(2)
O(9)-C(28)	1.425(2)	C(2)-C(1)-C(4)	116.6(2)
O(9)-C(27)	1.426(2)	C(1)-C(2)-H(2A)	109.5
C(23)-C(25)	1.328(3)	C(1)-C(2)-H(2B)	109.5
C(23)-C(24)	1.498(3)	H(2A)-C(2)-H(2B)	109.5
C(23)-C(26)	1.507(3)	C(1)-C(2)-H(2C)	109.5
C(24)-H(24A)	0.9800	H(2A)-C(2)-H(2C)	109.5
C(24)-H(24B)	0.9800	H(2B)-C(2)-H(2C)	109.5
C(24)-H(24C)	0.9800	C(1)-C(3)-H(3A)	120.0
C(25)-H(25A)	0.9500	C(1)-C(3)-H(3B)	120.0
C(25)-H(25B)	0.9500	H(3A)-C(3)-H(3B)	120.0
C(26)-C(27)	1.531(2)	C(1)-C(4)-C(5)	113.65(15)
C(26)-H(26A)	0.9900	C(1)-C(4)-H(4A)	108.8
C(26)-H(26B)	0.9900	C(5)-C(4)-H(4A)	108.8
C(27)-C(29)	1.536(2)	C(1)-C(4)-H(4B)	108.8
C(27)-H(27)	1.0000	C(5)-C(4)-H(4B)	108.8
C(28)-H(28A)	0.9800	H(4A)-C(4)-H(4B)	107.7
C(28)-H(28B)	0.9800	O(3)-C(5)-C(4)	107.05(15)
C(28)-H(28C)	0.9800	O(3)-C(5)-C(7)	110.16(13)
C(29)-C(30)	1.525(2)	C(4)-C(5)-C(7)	111.49(14)

O(3)-C(5)-H(5)	109.4	C(19)-N(2)-C(20)	123.60(17)
C(4)-C(5)-H(5)	109.4	C(19)-N(2)-H(2N)	112.7(15)
C(7)-C(5)-H(5)	109.4	C(20)-N(2)-H(2N)	123.6(15)
O(3)-C(6)-H(6A)	109.5	C(18)-O(5)-H(5O)	113(2)
O(3)-C(6)-H(6B)	109.5	C(17)-O(6)-C(16)	114.05(15)
H(6A)-C(6)-H(6B)	109.5	C(13)-C(12)-C(15)	121.0(2)
O(3)-C(6)-H(6C)	109.5	C(13)-C(12)-C(14)	121.8(2)
H(6A)-C(6)-H(6C)	109.5	C(15)-C(12)-C(14)	117.17(18)
H(6B)-C(6)-H(6C)	109.5	C(12)-C(13)-H(13A)	120.0
O(2)-C(7)-C(8)	110.57(14)	C(12)-C(13)-H(13B)	120.0
O(2)-C(7)-C(5)	111.78(14)	H(13A)-C(13)-H(13B)	120.0
C(8)-C(7)-C(5)	109.85(14)	C(12)-C(14)-H(14A)	109.5
O(2)-C(7)-H(7)	108.2	C(12)-C(14)-H(14B)	109.5
C(8)-C(7)-H(7)	108.2	H(14A)-C(14)-H(14B)	109.5
C(5)-C(7)-H(7)	108.2	C(12)-C(14)-H(14C)	109.5
O(1)-C(8)-N(1)	123.40(16)	H(14A)-C(14)-H(14C)	109.5
O(1)-C(8)-C(7)	120.34(15)	H(14B)-C(14)-H(14C)	109.5
N(1)-C(8)-C(7)	116.26(15)	C(12)-C(15)-C(16)	113.95(16)
N(1)-C(9)-C(10)	109.68(17)	C(12)-C(15)-H(15A)	108.8
N(1)-C(9)-C(11)	109.91(17)	C(16)-C(15)-H(15A)	108.8
C(10)-C(9)-C(11)	111.98(18)	C(12)-C(15)-H(15B)	108.8
N(1)-C(9)-H(9)	108.4	C(16)-C(15)-H(15B)	108.8
C(10)-C(9)-H(9)	108.4	H(15A)-C(15)-H(15B)	107.7
C(11)-C(9)-H(9)	108.4	O(6)-C(16)-C(15)	107.36(15)
C(9)-C(10)-H(10A)	109.5	O(6)-C(16)-C(18)	110.51(15)
C(9)-C(10)-H(10B)	109.5	C(15)-C(16)-C(18)	111.20(15)
H(10A)-C(10)-H(10B)	109.5	O(6)-C(16)-H(16)	109.2
C(9)-C(10)-H(10C)	109.5	C(15)-C(16)-H(16)	109.2
H(10A)-C(10)-H(10C)	109.5	C(18)-C(16)-H(16)	109.2
H(10B)-C(10)-H(10C)	109.5	O(6)-C(17)-H(17A)	109.5
C(9)-C(11)-H(11A)	109.5	O(6)-C(17)-H(17B)	109.5
C(9)-C(11)-H(11B)	109.5	H(17A)-C(17)-H(17B)	109.5
H(11A)-C(11)-H(11B)	109.5	O(6)-C(17)-H(17C)	109.5
C(9)-C(11)-H(11C)	109.5	H(17A)-C(17)-H(17C)	109.5
H(11A)-C(11)-H(11C)	109.5	H(17B)-C(17)-H(17C)	109.5
H(11B)-C(11)-H(11C)	109.5	O(5)-C(18)-C(19)	109.30(15)

O(5)-C(18)-C(16)	111.34(16)	H(24A)-C(24)-H(24B)	109.5
C(19)-C(18)-C(16)	110.03(15)	C(23)-C(24)-H(24C)	109.5
O(5)-C(18)-H(18)	108.7	H(24A)-C(24)-H(24C)	109.5
C(19)-C(18)-H(18)	108.7	H(24B)-C(24)-H(24C)	109.5
C(16)-C(18)-H(18)	108.7	C(23)-C(25)-H(25A)	120.0
O(4)-C(19)-N(2)	122.99(18)	C(23)-C(25)-H(25B)	120.0
O(4)-C(19)-C(18)	121.53(16)	H(25A)-C(25)-H(25B)	120.0
N(2)-C(19)-C(18)	115.47(17)	C(23)-C(26)-C(27)	112.58(15)
N(2)-C(20)-C(22)	108.20(17)	C(23)-C(26)-H(26A)	109.1
N(2)-C(20)-C(21)	111.08(17)	C(27)-C(26)-H(26A)	109.1
C(22)-C(20)-C(21)	111.25(17)	C(23)-C(26)-H(26B)	109.1
N(2)-C(20)-H(20)	108.8	C(27)-C(26)-H(26B)	109.1
C(22)-C(20)-H(20)	108.7	H(26A)-C(26)-H(26B)	107.8
C(21)-C(20)-H(20)	108.8	O(9)-C(27)-C(26)	106.79(14)
C(20)-C(21)-H(21A)	109.5	O(9)-C(27)-C(29)	110.44(14)
C(20)-C(21)-H(21B)	109.5	C(26)-C(27)-C(29)	112.01(14)
H(21A)-C(21)-H(21B)	109.5	O(9)-C(27)-H(27)	109.2
C(20)-C(21)-H(21C)	109.5	C(26)-C(27)-H(27)	109.2
H(21A)-C(21)-H(21C)	109.5	C(29)-C(27)-H(27)	109.2
H(21B)-C(21)-H(21C)	109.5	O(9)-C(28)-H(28A)	109.5
C(20)-C(22)-H(22A)	109.5	O(9)-C(28)-H(28B)	109.5
C(20)-C(22)-H(22B)	109.5	H(28A)-C(28)-H(28B)	109.5
C(22)-H(22B)	109.5	C(28)-H(28C)	109.5
C(20)-C(22)-H(22C)	109.5	H(28A)-C(28)-H(28C)	109.5
H(22A)-C(22)-H(22C)	109.5	H(28B)-C(28)-H(28C)	109.5
H(22B)-C(22)-H(22C)	109.5	O(8)-C(29)-C(30)	110.03(14)
C(30)-N(3)-C(31)	123.65(16)	O(8)-C(29)-C(27)	111.52(15)
C(30)-N(3)-H(3N)	115.4(15)	C(30)-C(29)-C(27)	110.03(14)
C(31)-N(3)-H(3N)	120.9(15)	O(8)-C(29)-H(29)	108.4
C(29)-O(8)-H(8O)	105.6(18)	C(30)-C(29)-H(29)	108.4
C(28)-O(9)-C(27)	114.03(14)	C(27)-C(29)-H(29)	108.4
C(25)-C(23)-C(24)	122.81(19)	O(7)-C(30)-N(3)	123.28(17)
C(25)-C(23)-C(26)	121.40(19)	O(7)-C(30)-C(29)	121.19(16)
C(24)-C(23)-C(26)	115.78(17)	N(3)-C(30)-C(29)	115.53(15)
C(23)-C(24)-H(24A)	109.5	N(3)-C(31)-C(33)	110.66(16)
C(23)-C(24)-H(24B)	109.5	N(3)-C(31)-C(32)	108.06(17)

C(33)-C(31)-C(32)	112.22(18)	C(32)-C(31)-H(31)	108.6
N(3)-C(31)-H(31)	108.6	C(33)-C(31)-H(31)	108.6
H(32B)-C(32)-H(32C)	109.5	C(31)-C(32)-H(32A)	109.5
C(31)-C(33)-H(33A)	109.5	C(31)-C(32)-H(32B)	109.5
C(31)-C(33)-H(33B)	109.5	H(32A)-C(32)-H(32B)	109.5
H(33A)-C(33)-H(33B)	109.5	H(33B)-C(33)-H(33C)	109.5
C(31)-C(33)-H(33C)	109.5	C(31)-C(32)-H(32C)	109.5
H(33A)-C(33)-H(33C)	109.5	H(32A)-C(32)-H(32C)	109.5

Table 4. Anisotropic displacement parameters ($\text{\AA}^2 \times 10^3$) for Sezgin's Amide. The anisotropic displacement factor exponent takes the form: $-2\pi^2 [h^2 a^{*2} U^{11} + \dots + 2 h k a^* b^* U^{12}]$

	U11	U22	U33	U23	U13	U12
N(1)	28(1)	18(1)	25(1)	-1(1)	-3(1)	8(1)
O(1)	38(1)	24(1)	25(1)	-2(1)	-10(1)	12(1)
O(2)	31(1)	20(1)	27(1)	-1(1)	-1(1)	13(1)
O(3)	27(1)	28(1)	25(1)	7(1)	-2(1)	12(1)
C(1)	50(1)	58(1)	29(1)	10(1)	6(1)	43(1)
C(2)	66(2)	103(2)	49(2)	-31(2)	-17(1)	66(2)
C(3)	77(2)	91(2)	70(2)	44(2)	49(2)	73(2)
C(4)	35(1)	39(1)	23(1)	1(1)	-2(1)	24(1)
C(5)	30(1)	24(1)	21(1)	0(1)	-2(1)	15(1)
C(6)	37(1)	33(1)	25(1)	7(1)	-3(1)	15(1)
C(7)	25(1)	23(1)	24(1)	2(1)	-3(1)	14(1)
C(8)	25(1)	25(1)	25(1)	1(1)	-5(1)	15(1)
C(9)	36(1)	22(1)	24(1)	2(1)	-7(1)	8(1)
C(10)	55(1)	33(1)	48(1)	2(1)	-13(1)	23(1)
C(11)	40(1)	45(1)	37(1)	7(1)	6(1)	13(1)
N(2)	34(1)	27(1)	32(1)	2(1)	1(1)	19(1)
O(4)	37(1)	27(1)	43(1)	5(1)	4(1)	21(1)
O(5)	41(1)	45(1)	33(1)	13(1)	11(1)	29(1)
O(6)	32(1)	34(1)	36(1)	4(1)	6(1)	22(1)

C(12)	28(1)	36(1)	33(1)	-4(1)	7(1)	17(1)
C(13)	43(1)	37(1)	45(1)	-7(1)	3(1)	21(1)
C(14)	34(1)	37(1)	31(1)	1(1)	1(1)	11(1)
C(15)	35(1)	36(1)	33(1)	-2(1)	3(1)	22(1)
C(16)	27(1)	27(1)	29(1)	2(1)	4(1)	15(1)
C(17)	48(1)	46(1)	41(1)	14(1)	14(1)	36(1)
C(18)	37(1)	33(1)	27(1)	2(1)	3(1)	24(1)
C(19)	34(1)	27(1)	26(1)	-4(1)	-1(1)	20(1)
C(20)	33(1)	31(1)	36(1)	-1(1)	-2(1)	20(1)
C(21)	47(1)	62(2)	39(1)	2(1)	4(1)	38(1)
C(22)	40(1)	45(1)	43(1)	-2(1)	-7(1)	28(1)
N(3)	26(1)	28(1)	23(1)	-3(1)	-4(1)	14(1)
O(7)	23(1)	40(1)	33(1)	-5(1)	-2(1)	15(1)
O(8)	26(1)	35(1)	21(1)	-1(1)	-5(1)	17(1)
O(9)	35(1)	31(1)	22(1)	-4(1)	-1(1)	15(1)
C(23)	35(1)	37(1)	21(1)	6(1)	7(1)	23(1)
C(24)	47(1)	51(1)	38(1)	-1(1)	-10(1)	32(1)
C(25)	49(1)	33(1)	49(1)	5(1)	0(1)	22(1)
C(26)	29(1)	31(1)	23(1)	0(1)	1(1)	19(1)
C(27)	26(1)	29(1)	21(1)	-1(1)	1(1)	17(1)
C(28)	44(1)	43(1)	24(1)	-3(1)	1(1)	29(1)
C(29)	26(1)	29(1)	17(1)	-1(1)	-1(1)	15(1)
C(30)	25(1)	27(1)	20(1)	2(1)	1(1)	13(1)
C(31)	35(1)	33(1)	25(1)	-6(1)	-6(1)	19(1)
C(32)	53(1)	44(1)	30(1)	-6(1)	-2(1)	31(1)
C(33)	49(1)	33(1)	40(1)	-7(1)	0(1)	8(1)

Table 5. Hydrogen coordinates ($\times 10^4$) and isotropic displacement parameters ($\text{\AA}^2 \times 10^3$) for S2.5.

	x	y	z	U(eq)
H(1N)	3180(20)	-3040(20)	-572(5)	26(6)

H(2O)	4120(30)	-590(30)	-854(5)	39
H(2A)	7134	-3161	-1558	94
H(2B)	5672	-3283	-1568	94
H(2C)	5983	-4115	-1356	94
H(3A)	8860	-1006	-1372	79
H(3B)	8427	-315	-1138	79
H(4A)	6255	-1375	-964	35
H(4B)	5430	-2994	-981	35
H(5)	4156	-2877	-1338	29
H(6A)	3478	-1008	-1483	49
H(6B)	4112	-1649	-1675	49
H(6C)	4776	-37	-1655	49
H(7)	2939	-1943	-1107	28
H(9)	1535	-5718	-639	36
H(10A)	3525	-4539	-239	67
H(10B)	3676	-5269	-492	67
H(10C)	2541	-6134	-280	67
H(11A)	389	-4745	-427	66
H(11B)	1478	-4237	-197	66
H(11C)	482	-5825	-243	66
H(2N)	-5960(20)	-7080(20)	-1338(5)	27(5)
H(5O)	-3400(30)	-6370(30)	-1469(6)	54
H(13A)	-2018	-3650	-644	50
H(13B)	-1432	-3953	-377	50
H(14A)	-2241	-6169	-230	55
H(14B)	-2246	-7056	-470	55
H(14C)	-3649	-7313	-350	55
H(15A)	-3385	-5362	-925	39
H(15B)	-4554	-6538	-755	39
H(16)	-3709	-8011	-847	32
H(17A)	-2076	-8057	-1237	59
H(17B)	-1854	-8219	-936	59
H(17C)	-629	-7103	-1106	59
H(18)	-4080	-8264	-1304	35
H(20)	-8403	-9306	-1231	38
H(21A)	-7745	-6986	-917	67

H(21B)	-7794	-8329	-810	67
H(21C)	-9153	-8388	-910	67
H(22A)	-8173	-7873	-1584	60
H(22B)	-7955	-6702	-1386	60
H(22C)	-9383	-8082	-1397	60
H(3N)	430(20)	-6280(20)	-1787(4)	23(5)
H(8O)	1590(30)	-4510(20)	-1389(6)	37(7)
H(24A)	-1198	-1660	-2138	63
H(24B)	-1772	-3157	-2025	63
H(24C)	-766	-2664	-2268	63
H(25A)	634	51	-1905	51
H(25B)	1641	-295	-1733	51
H(26A)	1570	-2456	-1819	31
H(26B)	270	-3625	-1965	31
H(27)	-1041	-3742	-1573	29
H(28A)	58	-3571	-1056	51
H(28B)	-940	-3059	-1156	51
H(28C)	473	-2013	-1023	51
H(29)	-349	-5116	-1336	28
H(31)	-1750	-7571	-2104	36
H(32A)	577	-7890	-2060	59
H(32B)	330	-7046	-2279	59
H(32C)	-578	-8665	-2273	59
H(33A)	-2583	-8890	-1723	69
H(33B)	-1369	-9215	-1734	69
H(33C)	-2502	-9776	-1955	69

Table 6. Torsion angles [°] for **S2.5**.

C(3)-C(1)-C(4)-C(5)	118.5(2)	O(3)-C(5)-C(7)-O(2)	-68.37(17)
C(2)-C(1)-C(4)-C(5)	-63.6(2)	C(4)-C(5)-C(7)-O(2)	50.33(19)
C(6)-O(3)-C(5)-C(4)	158.44(15)	O(3)-C(5)-C(7)-C(8)	168.50(13)
C(6)-O(3)-C(5)-C(7)	-80.17(18)	C(4)-C(5)-C(7)-C(8)	-72.80(18)
C(1)-C(4)-C(5)-O(3)	-60.1(2)	C(9)-N(1)-C(8)-O(1)	-0.3(3)
C(1)-C(4)-C(5)-C(7)	179.36(16)	C(9)-N(1)-C(8)-C(7)	179.42(16)

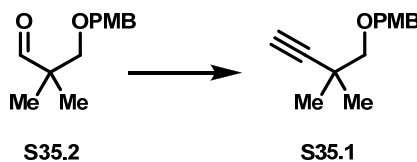
O(2)-C(7)-C(8)-O(1)	-178.54(16)	C(16)-C(18)-C(19)-N(2)	125.03(17)
C(5)-C(7)-C(8)-O(1)	-54.7(2)	C(19)-N(2)-C(20)-C(22)	-165.93(18)
O(2)-C(7)-C(8)-N(1)	1.8(2)	C(19)-N(2)-C(20)-C(21)	71.7(2)
C(5)-C(7)-C(8)-N(1)	125.62(17)	C(25)-C(23)-C(26)-C(27)	84.4(2)
C(8)-N(1)-C(9)-C(10)	116.0(2)	C(24)-C(23)-C(26)-C(27)	-94.6(2)
C(8)-N(1)-C(9)-C(11)	-120.5(2)	C(28)-O(9)-C(27)-C(26)	166.84(15)
C(13)-C(12)-C(15)-C(16)	132.0(2)	C(28)-O(9)-C(27)-C(29)	-71.14(19)
C(14)-C(12)-C(15)-C(16)	-49.3(2)	C(23)-C(26)-C(27)-O(9)	-74.13(19)
C(17)-O(6)-C(16)-C(15)	160.62(16)	C(23)-C(26)-C(27)-C(29)	164.85(15)
C(17)-O(6)-C(16)-C(18)	-77.95(19)	O(9)-C(27)-C(29)-O(8)	-64.58(18)
C(12)-C(15)-C(16)-O(6)	-54.6(2)	C(26)-C(27)-C(29)-O(8)	54.30(19)
C(12)-C(15)-C(16)-C(18)	-175.62(16)	O(9)-C(27)-C(29)-C(30)	173.03(13)
O(6)-C(16)-C(18)-O(5)	-62.05(19)	C(26)-C(27)-C(29)-C(30)	-68.09(19)
C(15)-C(16)-C(18)-O(5)	57.1(2)	C(31)-N(3)-C(30)-O(7)	-3.5(3)
O(6)-C(16)-C(18)-C(19)	176.61(14)	C(31)-N(3)-C(30)-C(29)	175.57(16)
C(15)-C(16)-C(18)-C(19)	-64.3(2)	O(8)-C(29)-C(30)-O(7)	-174.06(16)
C(20)-N(2)-C(19)-O(4)	-0.5(3)	C(27)-C(29)-C(30)-O(7)	-50.8(2)
C(20)-N(2)-C(19)-C(18)	-179.27(17)	O(8)-C(29)-C(30)-N(3)	6.8(2)
O(5)-C(18)-C(19)-O(4)	-176.30(17)	C(27)-C(29)-C(30)-N(3)	130.08(16)
C(16)-C(18)-C(19)-O(4)	-53.7(2)	C(30)-N(3)-C(31)-C(33)	-77.7(2)
O(5)-C(18)-C(19)-N(2)	2.5(2)	C(30)-N(3)-C(31)-C(32)	159.02(17)

Table 7. Hydrogen bonds for **S2.5** [\AA and $^\circ$].

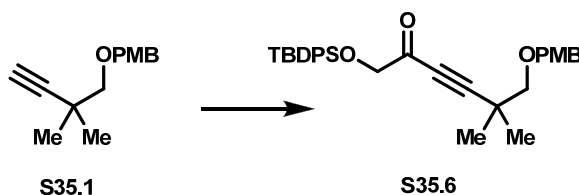
D-H...A	d(D-H)	d(H...A)	d(D...A)	$\angle(\text{DHA})$
O(2)-H(2O)...O(4)#1	0.78(3)	1.91(3)	2.6795(18)	171(3)
O(5)-H(5O)...O(7)	0.76(3)	1.94(3)	2.696(2)	175(3)
O(8)-H(8O)...O(1)	0.80(3)	1.88(3)	2.6726(18)	172(2)

Symmetry transformations used to generate equivalent atoms: #1 $x+1, y+1, z$

CHAPTER 3

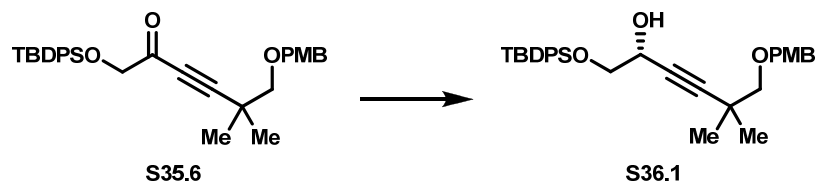


To a solution of K_2CO_3 (24.8 g, 180 mmol), TsN_3 (15.3 g, 78 mmol) in 400 mL was syringed dimethyl-(2-oxapropyl) phosphonate (10.6 mL, 78 mmol) at rt. After stirring for 2 h, a solution of aldehyde **S35.2** (13.3 g, 60 mmol) in 80 mL of MeOH was added. Stirring continued for 20 h, the mixture was concentrated under reduced pressure and then diluted with distilled water. The mixture was extracted with Et_2O and dried over Na_2SO_4 . Purification by FCC using ethyl acetate / hexane (1:20) afforded 11.4 g (85%) alkyne **S35.1** as a colorless oil. IR $\nu_{\text{max}}(\text{neat})/\text{cm}^{-1}$ 3290, 2970, 2934, 2100, 1612, 1586, 1513; ^1H NMR (400 MHz, CDCl_3) 7.28 (2H, d, $J = 8.4$ Hz), 6.88 (2H, d, $J = 8.4$ Hz), 4.54 (2H, s), 3.80 (3H, s), 3.29 (2H, s), 2.12 (1H, s), 1.23 (3H, s); ^{13}C NMR (75 MHz, CDCl_3) 161.8, 159.1, 130.5, 129.1, 113.7, 90.3, 73.0, 68.1, 55.2, 32.2, 26.0. m/z (ESIMS) calculated for $\text{C}_{14}\text{H}_{18}\text{O}_2\text{Na} [\text{MNa}]^+$ 241.12, found: 241.1.

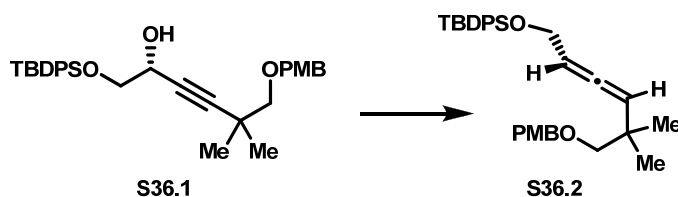


To a solution of alkyne **S35.1** (200 mg, 0.9 mmol) in THF was added 0.4 mL $n\text{-BuLi}$ (2.5M) at -78°C . After warming to 0°C and stirring for 30 min, the reaction mixture was cooled to -78°C and a solution of weinreb amide **S35.5** in THF was added slowly.

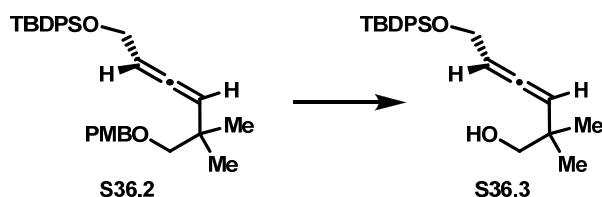
Stirring continued for 2h at -20 °C and the mixture was quenched with NH₄Cl solution. The mixture was extracted with CH₂Cl₂. The combined organic extracts were dried over Na₂SO₄ and concentrated under reduced pressure. The residue was purified by FCC (silica gel, ethyl acetate/hexane 1:10) to give 400 mg product **S35.6** (85%) as a colorless oil. IR ν_{max} (neat)/cm⁻¹ 3068, 2950, 2925, 2200, 1696, 1673, 1612, 1513, 1427, 1110, 702; ¹H NMR (300 MHz, CDCl₃) 7.70-7.67 (4H, m), 7.44-7.35 (6H, m), 7.23 (2H, d, J= 5.4 Hz), 6.85 (2H, d, J= 5.4 Hz), 4.48 (2H, s), 4.29 (2H, s), 3.80 (3H, s), 3.3 (2H, s), 1.25 (6H, s), 1.09 (9H, s); *m/z* (ESIMS) calculated for C₃₂H₃₈O₄SiNa [MNa]⁺ 537.24, found: 537.3.



To a solution of Noyori catalyst in 3 mL iPrOH was added a solution of ketone **S35.6** (372 mg, 1.00 mmol) in 3 mL iPrOH. The mixture was stirred for 30 min, then was concentrated in vacuo. Purification of the residue by FCC using hexane/ethyl acetate (1:10) furnished 362 mg (97%) alcohol **S36.1** as a colorless oil. $[\alpha]_D^{25} = -9.6$ ($c = 0.83$, CHCl_3); IR $\nu_{\text{max}}(\text{neat})/\text{cm}^{-1}$ 3448, 3070, 2955, 2930, 2238, 1612, 1513, 1427, 1247, 1112, 702; ^1H NMR (300 MHz, CDCl_3) 7.71-7.65 (4H, m), 7.45-7.35 (6H, m), 7.24 (2H, d, $J = 5.4$ Hz), 6.84 (2H, d, $J = 5.4$ Hz), 4.49-4.45 (3H, m), 3.80-3.66 (4H, m), 1.20 (6H, s), 1.06 (9H, s); m/z (ESIMS) calculated for $\text{C}_{32}\text{H}_{40}\text{O}_4\text{SiNa}$ $[\text{MNa}]^+$ 539.26, found: 539.4..

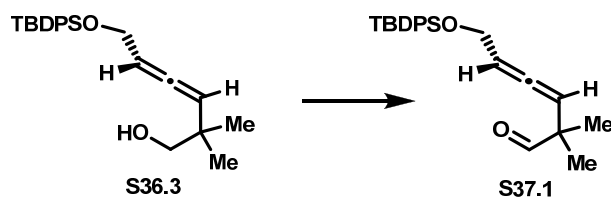


A solution of PPh_3 (249 mg, 0.95 mmol) in 2 mL THF was cooled to $-15\text{ }^\circ\text{C}$ and was added DIAD (192 mg, 0.95 mmol). The mixture was stirred for 10 min then a solution of alcohol **S36.1** (300 mg, 0.63 mmol) in 2 mL THF was added. After 10 min, NBSH (206 mg, 0.95 mmol) in 1 mL THF was added at $-15\text{ }^\circ\text{C}$. Stirring continued after warming to rt for 12 h. The solvent was removed under vacuum and the crude was directly purified by FCC (silica gel, hexane/ethyl acetate 1:15) to afford allene **S36.2** (201 mg, 61%) as a colorless oil. $[\alpha]_D^{25} = -35.7$ ($c = 1.82$, CHCl_3); IR $\nu_{\text{max}}(\text{neat})/\text{cm}^{-1}$ 3070, 2958, 2930, 1962, 1612, 1513, 1112, 702; ^1H NMR (300 MHz, CDCl_3) 7.73-7.67 (4H, m), 7.42-7.26 (6H, m), 7.23 (2H, d, $J = 5.7$ Hz), 6.86 (2H, d, $J = 5.7$ Hz), 5.35-5.22 (2H, m), 4.43 (2H, s), 4.20 (2H, dd, $J = 2.7, 6.0$), 3.80 (3H, s), 3.15 (2H, s) 1.04 (9H, s), 1.02 (3H, s), 1.01 (3H, s); m/z (ESIMS) calculated for $\text{C}_{32}\text{H}_{40}\text{O}_3\text{SiNa}$ $[\text{MNa}]^+$ 523.26, found: 523.3.

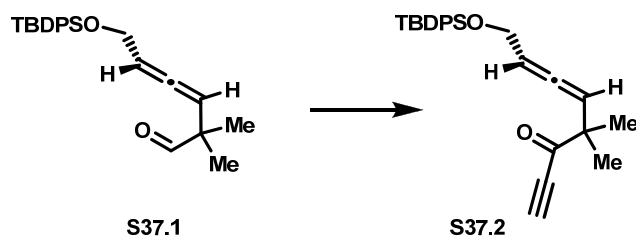


To a solution of allene **S36.2** (6.25 g, 12.4) in CH_2Cl_2 (80 mL) was added buffer (8 mL, $\text{pH} = 7.40$) and cooled to $0\text{ }^\circ\text{C}$. DDQ was added to the mixture and stirred for 30 min. The reaction mixture was quenched with NaHCO_3 , diluted with H_2O , extracted with CH_2Cl_2 and dried over Na_2SO_4 . Solvent was evaporated and the residue was treated with excess amount of NaBH_4 in MeOH to remove the resulting anisaldehyde. The mixture was

quenched with saturated NH_4Cl solution, extracted with CH_2Cl_2 and purified by FCC using hexane/ethyl acetate (20:1) as eluent to furnish alcohol **S36.3** (4.65 g, 98%) as a colorless oil. IR $\nu_{\text{max}}(\text{neat})/\text{cm}^{-1}$ 3419, 3071, 2959, 2930, 2858, 1962, 1471, 1427, 1112, 702; ^1H NMR (400 MHz, CDCl_3) 7.70-7.68 (4H, m), 7.45-7.36 (6H, m), 5.36-5.31 (1H, m), 5.17-5.14 (1H, m), 4.20-4.17 (2H, m), 3.42 (1H, d, $J=10.8$ Hz), 3.31 (1H, d, $J=10.8$ Hz), 1.05 (9H, s), 1.01 (6H, s); ^{13}C NMR (100 MHz) 201.9, 135.7, 133.6, 129.9, 127.9, 100.9, 93.7, 71.5, 62.0, 37.7, 26.9, 25.1, 24.9, 19.4; m/z (ESIMS) calculated for $\text{C}_{24}\text{H}_{32}\text{O}_3\text{Na} [\text{MNa}]^+$ 403.2, found: 403.3.

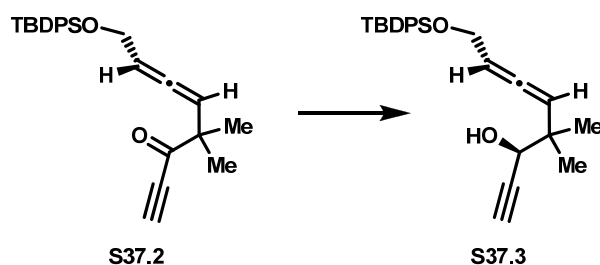


A solution of alcohol **S36.3** (6.4 g, 16.8 mmol) in CH_2Cl_2 (100 mL) was treated with Dess-Martin periodinone at room temperature. After stirring for 2 h, the mixture was quenched with a 2:1 (v/v) mixture of saturated NaHCO_3 and saturated $\text{Na}_2\text{S}_2\text{O}_3$ and extracted with CH_2Cl_2 . The combined organic extracts were dried over Na_2SO_4 and solvent was removed in vacuo. Purification by FCC using hexane/ethyl acetate as eluent furnished aldehyde **S37.1** (5.4 g, 85%) as a colorless oil.

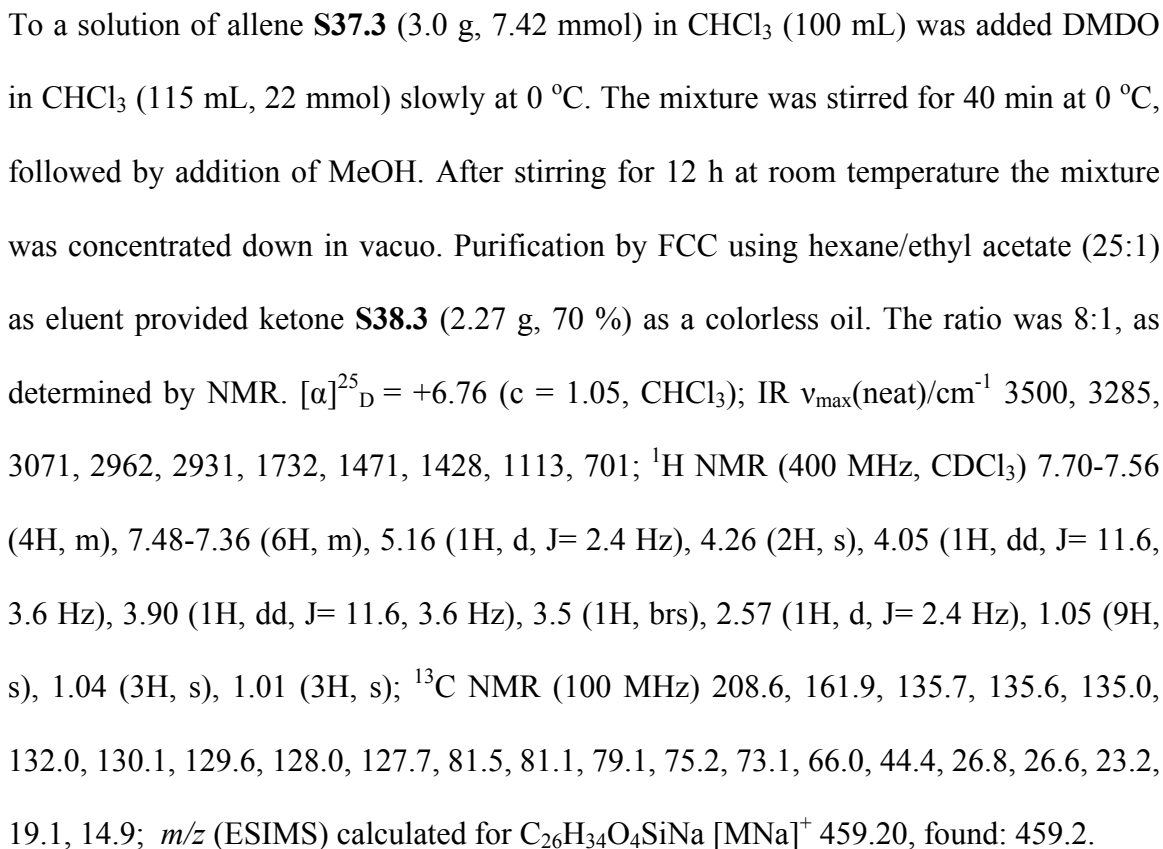


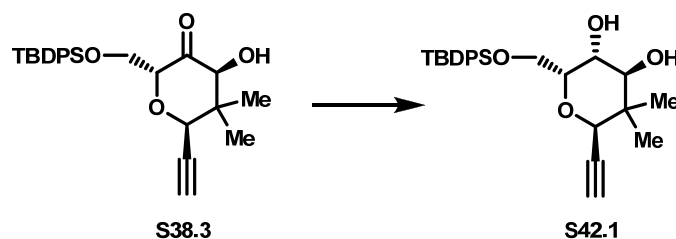
To the solution of aldehyde **S37.1** (5.2 g, 13.7 mmol) in THF (80 mL) at -78°C was

added the ethynyl magnesium bromide solution slowly. After stirring for 5 min, the reaction mixture was placed in refrigerator for 12 h. The mixture was quenched with saturated NH_4Cl at cold temperature, extracted with CH_2Cl_2 and then dried over Na_2SO_4 . The crude alcohol was dissolved in CH_2Cl_2 (100 mL) and treated with Dess-Martin periodinone (8.2 g, 19.3 mmol) at room temperature. The mixture was stirred for 30 min and then quenched with a 2:1 (v/v) mixture of saturated NaHCO_3 and saturated $\text{Na}_2\text{S}_2\text{O}_3$. The aqueous phase was extracted with CH_2Cl_2 and dried over Na_2SO_4 . Evaporation of the solvent and then purification by FCC using hexane/ethyl acetate (20:1) as eluent afforded ketone **S37.2** (4.9 g, 89% over two steps) as a colorless oil. IR $\nu_{\text{max}}(\text{neat})/\text{cm}^{-1}$ 3269, 3071, 2961, 2931, 2091, 1964, 1680, 1464, 1427, 1112, 702; ^1H NMR (400 MHz, CDCl_3) 7.68-7.66 (4H, m), 7.42-7.35 (6H, m), 5.48-5.43 (1H, m), 5.35-5.32 (1H, m), 4.24-4.22 (2H, m), 3.13 (1H, s), 1.27 (6H, s), 1.04 (9H, s); ^{13}C NMR (100 MHz) 203.3, 190.3, 135.7, 133.7, 129.9, 127.9, 97.6, 95.2, 80.8, 79.8, 61.9, 48.5, 27.0, 24.1, 23.8, 19.4; m/z (ESIMS) calculated for $\text{C}_{26}\text{H}_{30}\text{O}_2\text{SiNa}$ $[\text{MNa}]^+$ 425.19, found: 425.2.

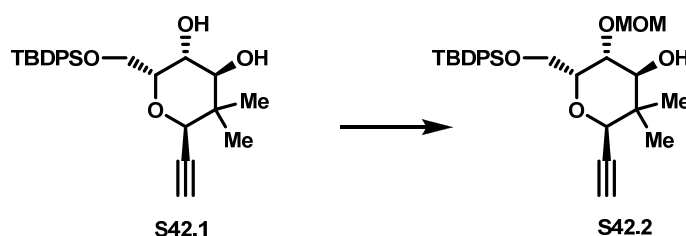


A solution of S-(CBS) (2.6 g, 9.32 mmol) in THF (40 mL) at $-30\text{ }^{\circ}\text{C}$ was treated with $\text{BH}_3\cdot\text{SMe}_2$ (4.66 mL, 9.32 mmol). After stirring for 15 min, a solution of allene **S37.2** (3.57 g, 8.80 mmol) in THF was added over the course of 10 min. The reaction mixture was stirred for 1 h and quenched with MeOH. The mixture was concentrated down and purified by FCC using hexane/ethyl acetate (1:30) as eluent to furnish alcohol **S37.3**.

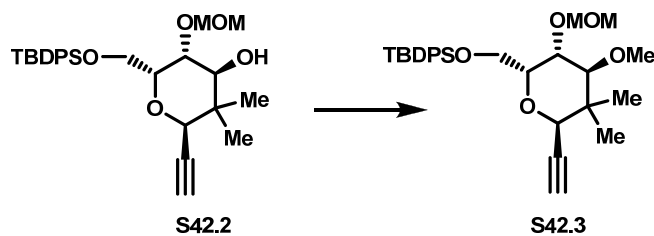




To a solution of ketone **S38.3** (2.03 g, 4.6 mmol) and $\text{Me}_4\text{NBH}(\text{OAc})_3$ (6.12 g, 23.3 mmol), in CH_3CN (40 mL) at -40°C was added acetic acid (10.0 mL). After 5 min, the reaction mixture was warmed to -20°C and kept at -20°C for 48 h. The mixture was quenched with saturated NaHCO_3 at cold temperature, extracted with CH_2Cl_2 and dried over Na_2SO_4 . Solvent was removed in vacuo and then the crude was purified by FCC using hexane/ethyl acetate (1:2) as eluent to give diol **S42.1** (1.50 g, 74 %) as a white foam. $[\alpha]_D^{25} = +25.0$ ($c = 1.00$, CHCl_3); IR $\nu_{\text{max}}(\text{neat})/\text{cm}^{-1}$ 3436, 3304, 3071, 2960, 2931, 1723, 1471, 1427, 1113, 702; ^1H NMR (400 MHz, CDCl_3) 7.72-7.69 (4H, m), 7.44-7.39 (6H, m), 4.30 (1H, d, $J = 2.4$ Hz), 4.2 (1H, q, $J = 5.2$ Hz), 4.07 (1H, dd, $J = 11.2, 4.8$ Hz), 4.00-3.92 (2H, m), 3.55 (1H, d, $J = 8$ Hz), 2.48 (1H, d, $J = 2.4$ Hz), 1.10 (6H, s), 1.07 (9H, s); ^{13}C NMR (75 MHz) 135.8, 132.6, 130.1, 128.0, 80.5, 76.7, 75.2, 73.7, 71.4, 70.7, 63.2, 56.8, 39.9, 27.2, 24.3, 19.5; m/z (ESIMS) calculated for $\text{C}_{32}\text{H}_{40}\text{O}_3\text{SiNa}$ $[\text{MNa}]^+$ 461.21, found: 461.3.

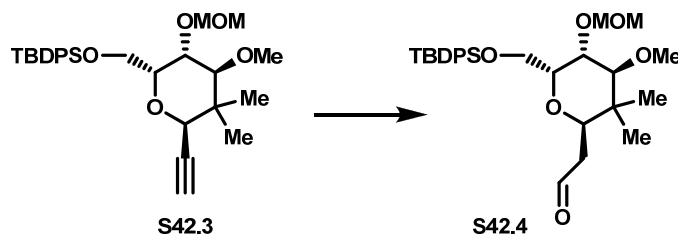


To a solution of diol **S42.1** (94 mg, 0.215 mmol) in 5.0 mL THF (containing trace water) at 0 °C was added NaH (60% of suspension in mineral oil, 45 mg, 1.125 mmol). After stirring for 5 min, MOMCl (52 mg, 0.65 mmol) was added dropwise. The reaction flask was kept in an ice bath for 10 min and then the ice bath was removed. After stirring for another 30 min, the reaction was quenched with NH₄Cl solution and extracted with CH₂Cl₂. The combined organic extracts were dried over Na₂SO₄ and concentrated under reduced pressure. The residue was purified by FCC (silica gel, ethyl acetate/hexane 1:4) to give 62 mg compound **S42.2** (60%) as a colorless oil. $[\alpha]_D^{25} = +39.8$ ($c = 1.33$, CHCl₃); ¹H NMR (400 MHz, CDCl₃) 7.22(4H, m), 7.41 (6H, m), 4.66 (1H, d, $J = 6.8$ Hz), 4.63 (1H, d, $J = 6.8$ Hz), 4.43 (1H, d, $J = 2.0$ Hz), 4.17 (1H, m), 3.94 (2H, m), 3.71 (1H, dd, $J = 6.4, 8.8$ Hz), 3.60 (1H, dd, $J = 2.8, 8.8$ Hz), 3.35 (3H, s), 3.14 (1H, br), 2.47 (1H, d, $J = 2.0$ Hz), 1.11 (3H, s), 1.07 (12H, s); ¹³C NMR (100 MHz, CDCl₃) 136.0, 135.9, 133.4, 133.3, 130.0, 130.0, 128.0, 127.9, 98.2, 80.6, 78.9, 75.5, 74.7, 74.5, 70.7, 62.0, 56.3, 40.4, 27.1, 27.0, 23.8, 19.3, 15.4; IR ν max (neat) /cm⁻¹ 3464, 3293, 3068, 3040, 1471, 1428, 1111. m/z (ESIMS) calculated for C₂₈H₃₈O₅SiNa [MNa]⁺ 505.24, found: 505.4.



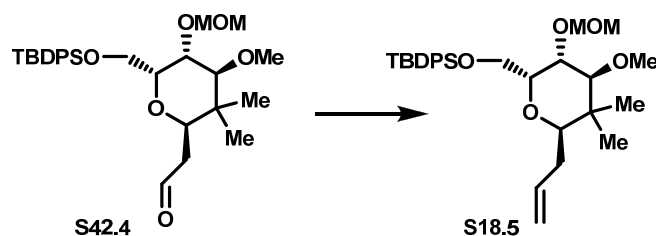
To a solution of compound **S42.2** (48 mg, 0.100 mmol) in 1.0 mL THF at 0 °C was added NaH (60% of suspension in mineral oil, 20 mg, 0.500 mmol). After stirring for 5 min, MeI (284 mg, 2.00 mmol) was added. The reaction flask was kept in an ice bath for 5 min and then the ice bath was removed. After stirring for another 1 h, the reaction was

quenched with NH_4Cl solution and extracted with CH_2Cl_2 . The combined organic extracts were dried over Na_2SO_4 and concentrated under reduced pressure. The residue was purified by FCC (silica gel, ethyl acetate/hexane 1:10) to give 49 mg compound **S42.3** (99%) as a colorless oil. $[\alpha]_D^{25} = +16.2$ ($c = 0.35$, CHCl_3); ^1H NMR (300 MHz, CDCl_3) 7.73 (m, 4H), 7.40 (m, 6H), 4.71 (d, 1H, $J = 6.6$ Hz) 4.61 (d, 1H, $J = 6.6$ Hz), 4.51 (d, 1H, $J = 1.5$ Hz), 4.11 (dd, 1H, $J = 4.8, 10.5$ Hz), 3.95 (dd, 2H, $J = 3.9, 4.5$ Hz), 3.85 (dd, 1H, $J = 6.0, 8.4$ Hz), 3.50 (s, 3H), 3.28 (m, 4H), 2.43 (d, 1H, $J = 2.1$ Hz) 1.07 (s, 9H), 1.05 (s, 6H). ^{13}C NMR (100 MHz, CDCl_3) 136.0, 135.9, 133.3, 133.2, 130.0, 129.9, 128.0, 127.9, 97.5, 85.2, 80.7, 75.1, 74.2, 71.3, 63.0, 61.6, 56.0, 40.9, 27.05, 24.2, 19.3, 16.6; IR ν_{max} (neat) / cm^{-1} 3289, 3072, 3048, 1471, 1428, 1112. m/z (ESIMS) calculated for $\text{C}_{29}\text{H}_{40}\text{O}_5\text{SiNa}$ $[\text{MNa}]^+$ 519.25, found: 519.4.



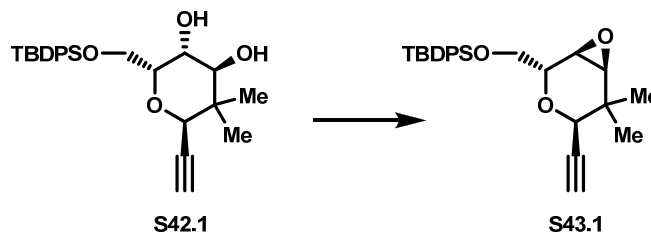
To a solution of BH_3/THF (0.3 mL, 1.0 M) at 0°C was added 2-methyl-2-butene in THF (0.25 mL, 2.0 M). After stirring for 20 min, alkyne **S42.3** (33 mg, 0.066 mmol) in 1 mL THF was added. The reaction was kept at 0°C for 30 min and then 0.2 mL 3 M NaOH solution and 0.2 mL H_2O_2 was added. After stirring for another 15 min at 0°C , the reaction mixture was diluted with distilled water and extracted with CH_2Cl_2 . The combined organic extracts were dried over Na_2SO_4 and concentrated under reduced pressure. The residue was purified by FCC (silica gel, ethyl acetate/hexane 1:8) to give 28 mg compound **S42.4** (82%) as a colorless oil. $[\alpha]_D^{25} = +16.7$ ($c = 0.30$, CHCl_3); ^1H

NMR (400 MHz, CDCl_3) 9.78 (dd, 1H, $J = 1.6, 2.4$ Hz), 7.73 (m, 4H), 7.41 (m, 6H) 4.66 (d, 1H, $J = 6.8$ Hz), 4.53 (d, 1H, $J = 6.8$ Hz), 4.27 (dd, 1H, $J = 2.8, 10.4$ Hz), 4.08 (dd, 1H, $J = 6.4, 11.2$ Hz), 3.99 (td, 1H, $J = 2.8, 6.8$ Hz), 3.84 (m, 1H), 3.51 (s, 3H), 3.29 (d, 1H, $J = 9.6$ Hz), 3.17 (s, 3H), 2.46 (ddd, 1H, $J = 2.8, 10.8, 16.0$ Hz) 2.35 (m, 1H), 1.07 (s, 9H), 0.96 (s, 3H), 0.89 (s, 3H). ^{13}C NMR (100 MHz, CDCl_3) 202.4, 136.0, 135.9, 133.3, 133.2, 130.0, 129.9, 128.0, 127.9, 97.2, 85.5, 80.7, 75.6, 73.9, 62.4, 62.0, 55.8, 43.5, 31.8, 27.0, 23.5, 19.3, 14.7; IR ν_{max} (neat)/ cm^{-1} 3068, 3043, 1728, 1471, 1427, 1112; m/z (ESIMS) calculated for $\text{C}_{30}\text{H}_{45}\text{O}_7\text{SiNa}$ $[\text{MNaMeOH}]^+$ 569.29, found: 569.4.

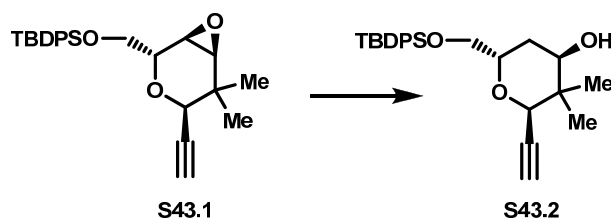


To a solution of $\text{Ph}_3\text{PCH}_3\text{Br}$ (54 mg, 0.151 mmol) in 0.3 mL THF at 0 °C was added BuLi in THF (0.05 mL, 2.5 M) dropwise. After stirring for 30 min, aldehyde **S42.4** (20 mg, 0.04 mmol) in 0.3 mL THF was added. The reaction was allowed to warm to room temperature and stirred for 1.5 h, then it was quenched with NH_4Cl solution and extracted with CH_2Cl_2 . The combined organic extracts were dried over Na_2SO_4 and concentrated under reduced pressure. The residue was purified by FCC (silica gel, ethyl acetate/hexane 1:8) to give 15 mg compound **S18.5** (75%) as colorless oil. $[\alpha]_{\text{D}}^{25} = +16.7$ ($c = 0.38$, CHCl_3); ^1H NMR (400 MHz, CDCl_3) 7.75 (m, 4H), 7.38 (m, 6H) 5.98 (m, 1H), 5.11 (dd, 1H, $J = 1.6, 17.2$ Hz), 5.03 (d, 1H, $J = 10.4$ Hz), 4.60 (dd, 2H, $J = 6.4, 50$ Hz), 4.04 (dd, 1H, $J = 6.4, 13.2$ Hz), 3.84 (m, 1H), 3.71 (m, 1H), 3.50 (s, 3H), 3.18 (m, 4H), 2.18 (m, 2H), 1.06 (s, 9H), 0.97 (s, 3H), 0.89 (s, 3H); ^{13}C NMR (100 MHz, CDCl_3)

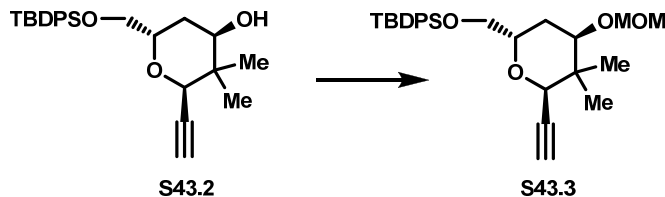
137.3, 136.0, 136.0, 133.5, 133.4, 129.9, 129.8, 127.9, 127.8, 115.8, 97.2, 86.0, 78.1, 75.9, 62.2, 62.0, 55.7, 41.3, 33.8, 27.0, 23.6, 19.3, 14.3; IR ν_{\max} (neat)/ cm^{-1} 3072, 3048, 2888, 2855, 1638, 1471, 1427, 1389, 1360, 1147, 1112, 1037, 1021, 915, 825; m/z (ESIMS) calculated for $\text{C}_{30}\text{H}_{44}\text{O}_5\text{SiNa}$ $[\text{MNa}]^+$ 535.29, found: 535.4.



To a solution of diol **S42.1** (1.14 g, 2.6 mmol) in THF (20 mL, containing trace amount of water) at 0 °C was added NaH (832 mg, 10.4 mmol, 60% dispersion in mineral oil) and the mixture was stirred for 10 min. To this was added a solution of TsCl in 6mL THF and 200 μL H_2O . After stirring for 30 min, the mixture was quenched with saturated NH_4Cl , extracted with CH_2Cl_2 and dried over Na_2SO_4 . Solvent was removed and then the crude was purified by FCC using hexane/ethyl acetate (20:1) as eluent to furnish epoxide **S43.1** (760 mg, 70%) as a colorless oil. $[\alpha]_D^{25} = -8.9$ ($c = 1.23$, CHCl_3); IR ν_{\max} (neat)/ cm^{-1} 3285, 3071, 2960, 2930, 1471, 1427, 1113, 702; ^1H NMR (400 MHz, CDCl_3) 7.71-7.68 (4H, m), 7.50-7.40 (6H, m), 4.26 (1H, t, $J = 4.4$ Hz), 4.20 (1H, 2.4 Hz), 3.95-3.87 (1H, m), 3.38 (1H, d, $J = 4.0$ Hz), 3.00 (1H, d, $J = 4.0$ Hz), 2.51 (1H, d, $J = 2.4$ Hz), 1.24 (3H, s), 1.18 (3H, s), 1.09 (9H, s); ^{13}C NMR (100 MHz) 135.6, 133.1, 129.9, 127.8, 80.1, 75.7, 70.7, 70.2, 64.9, 58.4, 53.1, 33.4, 26.8, 24.2, 21.6, 19.2; m/z (ESIMS) calculated for $\text{C}_{26}\text{H}_{32}\text{O}_3\text{Si Na}$ $[\text{MNa}]^+$ 443.20, found: 443.3.



To a solution of epoxide **S43.1** (0.61 mg, 1.45 mmol) in Et₂O (10 mL) at 0 °C was added DIBAL (4.35 mL, 4.35 mmol) at one portion. After 10 min, the reaction mixture was quenched with saturated Rochelle's salt and diluted with Et₂O. The resulting biphasic solution was stirred for 1 h. The layers were separated, and then the aqueous layer was extracted with Et₂O and dried over Na₂SO₄. Solvent was concentrated in vacuo and the crude was purified by FCC using hexane/ethyl acetate (10:1) as eluent to afford alcohol **S43.2** (489 mg, 80%) as a colorless oil. $[\alpha]_D^{25} = +2.44$ ($c = 0.41$, CHCl₃); IR $\nu_{\text{max}}(\text{neat})/\text{cm}^{-1}$ 3454, 3285, 3070, 2957, 2930, 1472, 1427, 1112, 702; ¹H NMR (400 MHz, CDCl₃) 7.69-7.67 (4H, m), 7.41-7.38 (6H, m), 4.40-4.20 (2H, m), 3.75 (2H, d, $J = 4.8$ Hz), 2.60-2.59 (1H, m), 2.38 (1H, d, $J = 8.4$ Hz), 2.04-1.97 (1H, m), 1.71-1.66 (1H, m); m/z (ESIMS) calculated for C₂₆H₃₄O₃SiNa [MNa]⁺ 445.22, found: 445.3.



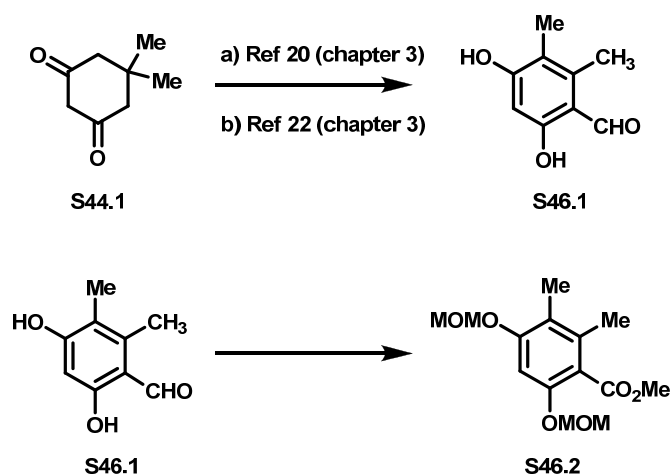
To a solution of alcohol **S43.2** (360 mg, 0.85 mmol) in DMF (10 mL) at 0 °C was added Hunig's base (1.5 mL, 8.53 mmol) followed by MOMCl (0.65 mL, 8.53 mmol). The reaction mixture was stirred for 24 h at room temperature, and then quenched with saturated NH₄Cl solution. The resulting mixture was extracted with CH₂Cl₂. The organic layers were washed with H₂O, dried over Na₂SO₄ and concentrated under reduced

pressure under reduced pressure in vacuo. The crude was purified by FCC using ethyl acetate/hexane (1:20) to give product **S43.3** as a colorless oil (390 mg, 97%). $[\alpha]_D^{25} = +0.91$ (c = 1.10, CHCl₃); IR $\nu_{\text{max}}(\text{neat})/\text{cm}^{-1}$ 3288, 3071, 2949, 2930, 1472, 1428, 1042, 702; ¹H NMR (400 MHz, CDCl₃) 7.70-7.67 (4H, m), 7.41-7.39 (6H, m), 4.70 (1H, d, J = 6.8 Hz), 4.60 (1H, d, J = 7.2 Hz), 4.22-4.18 (2H, m), 3.74 (2H, J = 9.2 Hz), 3.55-3.52 (1H, m), 3.38 (3H, s), 1.94-1.89 (2H, m), 1.10 (3H, s), 1.07 (9H, s), 1.06 (3H, s); ¹³C NMR (100 MHz) 135.7, 133.4, 129.7, 127.7, 95.9, 81.3, 77.8, 74.0, 71.7, 70.4, 65.9, 55.5, 37.9, 28.3, 26.8, 24.7, 19.2, 18.8; *m/z* (ESIMS) calculated for C₂₈H₃₈O₄SiNa [MNa]⁺ 489.24, found: 489.3.



To the 2-methyl-2-butene (2.30 mL of 2 M solution in THF, 4.60 mmol) cooled to 0 °C was added $\text{BH}_3 \cdot \text{SMe}_2$ (1.15 mL of 1M solution in THF, 2.30 mmol) dropwise. The ice-bath was removed and the mixture was stirred for 1 h. The reaction mixture was cooled to 0 °C, to which was added a solution of alkyne **S43.3** (356 mg, 0.76 mmol) in THF slowly. The mixture was stirred for 30 min at room temperature and cooled back to 0 °C. The reaction mixture was quenched with a precooled solution of 4 mL of 3N NaOH and 1.4 mL of 30% H_2O_2 dropwise. The resulting mixture was stirred for 30 min at room temperature, then and extracted with CH_2Cl_2 . The organic layers were dried over Na_2SO_4 and concentrated under reduced pressure under reduced pressure in vacuo. The crude was purified by FCC using hexane/ethyl acetate (15:1) to furnish aldehyde **S43.4** (282 mg,

76%) as a colorless oil. $[\alpha]_D^{25} = +7.14$ ($c = 0.84$, CHCl_3); IR $\nu_{\text{max}}(\text{neat})/\text{cm}^{-1}$ 3071, 2949, 2931, 2888, 2857, 1728, 1472, 1428, 1112, 702; ^1H NMR (400 MHz, CDCl_3) 9.72 (1H, dd, $J = 1.6, 3.6$ Hz), 4.68 (1H, d, $J = 5.2$ Hz), 4.59 (1H, d, $J = 5.2$ Hz), 4.04-3.96 (2H, m), 3.78-3.67 (2H, m), 2.85-2.77 (1H, m), 2.44 (1H, qd, $J = 1, 17.6$ Hz), 1.94-1.88 (1H, m), 1.81-1.74 (1H, m); ^{13}C NMR (100 MHz) 202.5, 135.6, 133.3, 129.7, 127.7, 95.9, 78.2, 75.0, 70.0, 65.5, 55.6, 43.4, 37.4, 28.2, 26.8, 24.4, 19.1, 17.0; m/z (ESIMS) calculated for $\text{C}_{28}\text{H}_{40}\text{O}_5\text{SiNa}$ $[\text{MNa}]^+$ 507.25, found: 507.3.



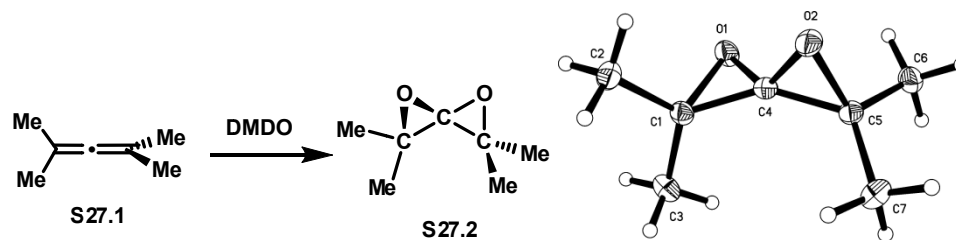
To a solution of aldehyde **S46.1** (1.65g, 9.96 mmol) in DMF (12 ml) at 0 °C was added Hunig's base (5.2 ml, 29.9 mmol) and MOMCl (2.27 ml, 29.9 mmol). After stirring for 20 h at room temperature, the reaction mixture was quenched with saturated NH_4Cl and then extracted with CH_2Cl_2 . The extracts were dried over Na_2SO_4 and concentrated in vacuo. The crude was passed through a pad of silica gel and used for next step without further purification.

A solution of aldehyde (2.4 mg, 9.4 mmol) in 120 ml $t\text{BuOH-H}_2\text{O}$ (1:1) was cooled to 0 °C, to which was added $\text{NaH}_2\text{PO}_4\cdot\text{H}_2\text{O}$ (3.38 g, 28.2 mmol), 2-methyl-2-butene (12.1 ml

from 2 M solution in THF, 28.2 mmol) and NaClO₂ (3.18 g, 28.2 mmol). After stirring for 4 h, the mixture was concentrated down, extracted with EtOAc and dried over Na₂SO₄. The crude was passed through a pad of silica gel and used for next step without further purification.

A solution of acid (2.48 g, 9.2 mmol) in THF (25 ml) was treated with PPh₃ (4.82 g, 18.4 mmol) and MeOH (1.8 ml, 46 mmol) which was then cooled to 0 °C. DIAD (3.72 g, 18.4 mmol) was added to reaction mixture. After stirring for 12 h, the mixture was diluted with H₂O and extracted with CH₂Cl₂. The organic extracts were dried over Na₂SO₄ and concentrated down under reduced pressure. The crude was purified by FCC using hexane:ethyl acetate (10:1) as eluent to furnish ester **S46.2** (2.43 g, 86% over 3 steps) as yellowish oil. IR $\nu_{\text{max}}(\text{neat})/\text{cm}^{-1}$ 2952, 2913, 2827, 1731, 1597, 1481, 1436, 1271, 1153, 923; ¹H NMR (400 MHz, CDCl₃) 6.77 (1H, s), 5.17 (2H, s), 5.13 (2H, s), 3.89 (3H, s), 3.46 (6H, s), 2.18 (3H, s), 2.11 (3H, s); ¹³C NMR (100 MHz) 169.4, 156.5, 152.6, 135.6, 120.1, 119.5, 100.2, 95.3, 94.9, 56.4, 56.3, 52.3, 17.2, 11.6; *m/z* (ESIMS) calculated for C₁₄H₂₀O₆Na [MNa]⁺ 307.2, found: 307.2.

Crystal structure of Spirodiepoxide



Empirical formula	C7 H12 O2	
Formula weight	128.17	
Temperature	100(2) K	
Wavelength	0.71073 Å	
Crystal system	Tetragonal	
Space group	I4(1)/a	
Unit cell dimensions	$a = 10.7367(6) \text{ Å}$	$\square = 90^\circ$.
	$b = 10.7367(6) \text{ Å}$	$\square = 90^\circ$.
	$c = 25.6705(15) \text{ Å}$	$\square = 90^\circ$.
Volume	$2959.2(8) \text{ Å}^3$	
Z	16	
Density (calculated)	1.151 Mg/m^3	
Absorption coefficient	0.083 mm^{-1}	
F(000)	1120	
Crystal size	$.60 \times .51 \times .10 \text{ mm}^3$	
Theta range for data collection	$2.06 \text{ to } 30.50^\circ$.	

Index ranges	-15<= <i>h</i> <=14, -15<= <i>k</i> <=15, -36<= <i>l</i> <=36
Reflections collected	17976
Independent reflections	2270 [R(int) = 0.0280]
Completeness to $\theta = 30.50^\circ$	100.0 %
Absorption correction	Semi-empirical from equivalents
Max. and min. transmission	0.9999 and 0.8614
Refinement method	Full-matrix least-squares on F^2
Data / restraints / parameters	2270 / 0 / 130
Goodness-of-fit on F^2	1.004
Final R indices [$I > 2\sigma(I)$]	R1 = 0.0436, wR2 = 0.1058
R indices (all data)	R1 = 0.0520, wR2 = 0.1128
Largest diff. peak and hole	0.503 and -0.150 e. \AA^{-3}

Table 2. Atomic coordinates ($\times 10^4$) and equivalent isotropic displacement parameters ($\text{\AA}^2 \times 10^3$) for spirodiepoxide. $U(\text{eq})$ is defined as one third of the trace of the orthogonalized U^{ij} tensor.

	x	y	z	$U(\text{eq})$
O(1)	6904(1)	5028(1)	806(1)	20(1)
O(2)	7527(1)	4403(1)	1695(1)	20(1)
C(1)	8314(1)	4994(1)	767(1)	16(1)
C(2)	8816(1)	3740(1)	621(1)	22(1)
C(3)	8875(1)	6102(1)	501(1)	22(1)
C(4)	7640(1)	5140(1)	1250(1)	15(1)
C(5)	7494(1)	5814(1)	1733(1)	16(1)
C(6)	6240(1)	6316(1)	1879(1)	22(1)
C(7)	8602(1)	6375(1)	1999(1)	22(1)

Table 3. Bond lengths [Å] and angles [°] for spirodiepoxide.

O(1)-C(4)	1.3934(10)	C(3)-H(3B)	0.962(16)
O(1)-C(1)	1.5168(10)	C(3)-H(3C)	0.946(14)
O(2)-C(4)	1.3932(10)	C(4)-C(5)	1.4440(12)
O(2)-C(5)	1.5177(10)	C(5)-C(7)	1.4975(12)
C(1)-C(4)	1.4455(12)	C(5)-C(6)	1.4986(12)
C(1)-C(3)	1.4978(12)	C(6)-H(6A)	0.959(14)
C(1)-C(2)	1.4981(12)	C(6)-H(6B)	0.944(16)
C(2)-H(2A)	0.961(14)	C(6)-H(6C)	0.974(14)
C(2)-H(2B)	0.959(17)	C(7)-H(7A)	0.960(15)
C(2)-H(2C)	0.976(14)	C(7)-H(7B)	0.960(17)
C(3)-H(3A)	0.952(14)	C(7)-H(7C)	0.963(13)
C(4)-O(1)-C(1)	59.38(5)	O(1)-C(4)-C(5)	133.29(7)
C(4)-O(2)-C(5)	59.30(5)	O(2)-C(4)-C(1)	133.25(7)
C(4)-C(1)-C(3)	120.41(8)	O(1)-C(4)-C(1)	64.56(6)
C(4)-C(1)-C(2)	119.46(8)	C(5)-C(4)-C(1)	147.79(7)
C(3)-C(1)-C(2)	117.10(8)	C(4)-C(5)-C(7)	120.46(8)
C(4)-C(1)-O(1)	56.05(5)	C(4)-C(5)-C(6)	119.47(8)
C(3)-C(1)-O(1)	114.37(7)	C(7)-C(5)-C(6)	117.06(8)
C(2)-C(1)-O(1)	113.42(7)	C(4)-C(5)-O(2)	56.05(5)
C(1)-C(2)-H(2A)	108.6(8)	C(7)-C(5)-O(2)	114.41(7)
C(1)-C(2)-H(2B)	110.0(8)	C(6)-C(5)-O(2)	113.37(7)
H(2A)-C(2)-H(2B)	107.2(12)	C(5)-C(6)-H(6A)	108.9(8)
C(1)-C(2)-H(2C)	111.3(8)	C(5)-C(6)-H(6B)	110.5(8)
H(2A)-C(2)-H(2C)	109.5(11)	H(6A)-C(6)-H(6B)	106.5(12)
H(2B)-C(2)-H(2C)	110.1(12)	C(5)-C(6)-H(6C)	110.9(8)
C(1)-C(3)-H(3A)	110.0(8)	H(6A)-C(6)-H(6C)	110.3(11)
C(1)-C(3)-H(3B)	110.0(9)	H(6B)-C(6)-H(6C)	109.6(11)
H(3A)-C(3)-H(3B)	110.7(12)	C(5)-C(7)-H(7A)	109.8(8)
C(1)-C(3)-H(3C)	108.5(9)	C(5)-C(7)-H(7B)	110.0(9)
H(3A)-C(3)-H(3C)	109.6(12)	H(7A)-C(7)-H(7B)	111.4(13)
H(3B)-C(3)-H(3C)	108.0(12)	C(5)-C(7)-H(7C)	108.2(8)
O(2)-C(4)-O(1)	124.93(7)	H(7A)-C(7)-H(7C)	109.6(12)
O(2)-C(4)-C(5)	64.65(6)	H(7B)-C(7)-H(7C)	107.8(12)

Table 4. Anisotropic displacement parameters ($\text{\AA}^2 \times 10^3$) for spirodiepoxide. The anisotropic displacement factor exponent takes the form: $-2\pi^2 [h^2 a^{*2} U^{11} + \dots + 2 h k a^* b^* U^{12}]$

	U ¹¹	U ²²	U ³³	U ²³	U ¹³	U ¹²
O(1)	12(1)	30(1)	18(1)	-3(1)	-1(1)	-1(1)
O(2)	29(1)	12(1)	18(1)	1(1)	2(1)	-1(1)
C(1)	12(1)	19(1)	17(1)	-1(1)	-1(1)	0(1)
C(2)	21(1)	21(1)	24(1)	-7(1)	2(1)	1(1)
C(3)	18(1)	24(1)	24(1)	5(1)	4(1)	1(1)
C(4)	14(1)	14(1)	17(1)	1(1)	-1(1)	-1(1)
C(5)	19(1)	12(1)	17(1)	1(1)	1(1)	0(1)
C(6)	21(1)	21(1)	24(1)	-2(1)	6(1)	0(1)
C(7)	23(1)	19(1)	24(1)	-4(1)	-5(1)	1(1)

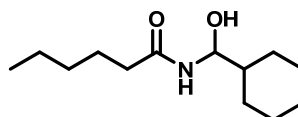
Table 5. Hydrogen coordinates ($\times 10^4$) and isotropic displacement parameters ($\text{\AA}^2 \times 10^3$) for spirodiepoxide.

	x	y	z	U(eq)
H(2A)	9702(13)	3741(13)	676(6)	30(3)
H(2B)	8678(13)	3586(13)	258(7)	32(3)
H(2C)	8436(13)	3081(13)	829(6)	31(3)
H(3A)	8498(13)	6847(13)	626(6)	31(3)
H(3B)	8775(13)	6031(13)	130(6)	30(3)
H(3C)	9738(13)	6118(13)	575(6)	29(3)
H(6A)	6238(13)	7201(13)	1827(5)	27(3)
H(6B)	6081(13)	6184(13)	2237(6)	30(3)
H(6C)	5586(12)	5928(13)	1672(5)	29(3)
H(7A)	9352(13)	5997(13)	1871(6)	33(4)
H(7B)	8527(14)	6279(14)	2370(7)	34(4)
H(7C)	8612(12)	7254(13)	1924(5)	26(3)

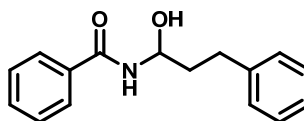
Table 6. Torsion angles [°] for spirodiepoxide.

C(4)-O(1)-C(1)-C(3)	-111.40(8)
C(4)-O(1)-C(1)-C(2)	110.76(8)
C(5)-O(2)-C(4)-O(1)	-126.48(9)
C(5)-O(2)-C(4)-C(1)	147.10(10)
C(1)-O(1)-C(4)-O(2)	-126.39(9)
C(1)-O(1)-C(4)-C(5)	147.04(10)
C(3)-C(1)-C(4)-O(2)	-144.50(9)
C(2)-C(1)-C(4)-O(2)	15.23(13)
O(1)-C(1)-C(4)-O(2)	115.03(10)
C(3)-C(1)-C(4)-O(1)	100.47(8)
C(2)-C(1)-C(4)-O(1)	-99.80(8)
C(3)-C(1)-C(4)-C(5)	-31.55(18)
C(2)-C(1)-C(4)-C(5)	128.19(13)
O(1)-C(1)-C(4)-C(5)	-132.02(15)
O(2)-C(4)-C(5)-C(7)	100.49(8)
O(1)-C(4)-C(5)-C(7)	-144.42(9)
C(1)-C(4)-C(5)-C(7)	-31.59(18)
O(2)-C(4)-C(5)-C(6)	-99.72(8)
O(1)-C(4)-C(5)-C(6)	15.37(13)
C(1)-C(4)-C(5)-C(6)	128.20(13)
O(1)-C(4)-C(5)-O(2)	115.09(10)
C(1)-C(4)-C(5)-O(2)	-132.08(15)
C(4)-O(2)-C(5)-C(7)	-111.44(8)
C(4)-O(2)-C(5)-C(6)	110.80(8)

CHAPTER 4

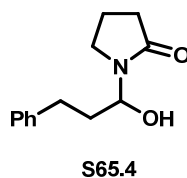
**S64.3**

To a solution of hexanamide (75mg, 0.65 mmol) in 3 mL Et₂O was added NEt₃ (101 mg, 1.0 mmol) and the mixture was cooled to 0 °C. To this was added Cy₂BCl in hexane (0.75 mmol, 1.0 M) in one portion. After stirring at this temperature for 30 min, aldehyde (56 mg, 0.5 mmol) was added dropwise to the reaction mixture. The mixture was stirred for 30 min and quenched with MeOH, phosphate buffer (pH=7.4) and 30% H₂O₂. The resulting mixture was stirred for 30 min and extracted with CH₂Cl₂. The combined organic extracts were dried over Na₂SO₄ and concentrated under reduced pressure. The residue was purified by FCC (silica gel, ethyl acetate/hexane 1:3) to give **S64.3** (100.6 mg, 88%) as white solid. IR ν max (neat)/cm⁻¹ 3246, 3068, 1645, 1553, 1026; ¹H NMR (300MHz, CDCl₃) 6.28 (d, 1H, J= 7.8 Hz), 5.06 (dd, 1H, J=7.8, 7.5Hz), 4.27 (br, 1H), 2.16 (t, 1H, J= 7.5Hz), 0.98-1.89 (m, 17H), 0.87 (t, 3H, J = 6.6 Hz); ¹³C NMR (75MHz, CDCl₃) 174.5, 77.7, 42.5, 37.1, 31.8, 28.5, 28.4, 26.6, 26.1, 26.0, 25.6, 22.7, 14.3; *m/z* (ESIMS) calculated for C₁₃H₂₅NO₂Na [MNa]⁺ 250.18, found: 250.2.

**S65.2**

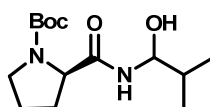
A solution of benzamide (73 mg, 0.6 mmol) was treated with NEt₃ (0.140 ml, 1.0 mmol) and cooled to 0 °C. To this was added Cy₂BCl (0.65 mmol, 1M in Hexane), and then the

mixture was stirred for 30 min at room temperature. Then aldehyde (0.074 ml, 0.5 mmol) was added to reaction mixture. After the mixture was stirred for 30 min, the regular workup was applied. The crude product was purified by FCC (silica gel, hexane/ethyl acetate 2/1) to yield 90 mg (71%) of **S65.2** as a white solid. IR ν max (neat)/cm⁻¹ 3415, 3328, 3313, 3055, 3029, 2963, 2946, 1643, 1527, 1029; ¹H NMR (400MHz, CDCl₃) 7.61-7.59 (2H, m), 7.53-7.48 (1H, m), 7.42-7.39 (2H, m), 7.34-7.30 (2H, m), 7.27-7.22 (3H, m), 6.57-6.55 (1H, d, J=6.4), 5.55-5.50 (1H, m), 3.88 (1H, d, J=2.8), 2.97-2.90 (1H, m), 2.83-2.76 (1H, m), 2.20-2.01 (2H, m); ¹³C NMR (100 MHz, CDCl₃) 168.5, 141.2, 133.6, 132.2, 128.9, 128.8, 128.7, 127.1, 126.4, 75.0, 36.4, 31.1; *m/z* (ESIMS) calculated for C₁₆H₁₇NO₂Na [MNa]⁺ 278.12, found: 278.0.



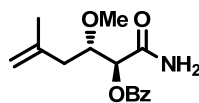
A solution of amide (204 mg, 2.4 mmol) was treated with NEt₃ (0.42 ml, 3.0 mmol) and cooled to 0 °C. To this was added Cy₂BCl (2.4 mmol, 1M in Hexane), and then the mixture was stirred for 30 min at room temperature. Then aldehyde (0.293 ml, 2.0 mmol) was added to reaction mixture. After the mixture was stirred for 30 min, the regular workup was applied. The crude product was purified by FCC (silica gel, hexane/ethyl acetate 2/1) to yield 381 mg (87 %) of **S65.4** as colorless oil. IR ν max (neat)/cm⁻¹ 3348, 3026, 2951, 2917, 1667, 1494, 1422. 1289; ¹H NMR (400MHz, CDCl₃) 7.29-7.26 (2H, m), 7.21-7.16 (3H, m), 5.52-5.48 (1H, m), 4.04 (1H, d, J=4.4), 3.58-3.52 (1H, m), 3.32-3.26 (1H, m), 2.80-2.73 (1H, m), 2.63-2.55 (1H, m), 2.42-2.28 (2H, m), 2.11-1.18 (4H, m); ¹³C NMR (100 MHz, CDCl₃) 176.4, 141.3, 128.68, 128.61, 126.2, 75.19, 42.01, 35.2,

32.0, 31.8, 18.3; m/z (ESIMS) calculated for $C_{13}H_{17}NO_2Na$ $[MNa]^+$ 242.12, found: 242.0.



S65.3

A solution of amide (170 mg, 0.79 mmol) was treated with NEt_3 (0.180 ml, 0.158 mmol) and cooled to 0 °C. To this was added Cy_2BCl (0.85 mmol, 1M in Hexane), and then the mixture was stirred for 30 min at room temperature. Then aldehyde (170 mg, 0.66 mmol) was added to reaction mixture. After the mixture was stirred for 30 min, the regular workup was applied. The crude product was purified by FCC (silica gel, hexane/ethyl acetate 2/1) to yield 150 mg (79%) of **S65.3** as a white solid. IR ν max (neat)/ cm^{-1} 3426, 3301, 2973, 2931, 2880, 1670, 1547, 1415, 1165; 1H NMR (500MHz, $CDCl_3$) 7.83-7.71 (1H, m), 5.08-5.05 (2H, m), 4.30-4.20 (2H, m), 3.46-3.25 (6H, m), 2.50- 1.80 (10H, m), 1.47 (18H, s), 1.00-0.94 (12H, m); ^{13}C NMR (125 MHz, $CDCl_3$) 173.337, 173.336, 156.359, 156.351, 80.889, 80.876, 78.728, 78.728, 59.975, 59.945, 47.384, 47.295, 32.665, 32.665, 28.567, 28.567, 27.906, 27.251, 24.774, 23.979, 17.724, 17.612; m/z (ESIMS) calculated for $C_{14}H_{26}N_2O_4Na$ $[MNa]^+$ 309.18, found: 309.1.

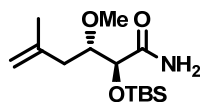


S66.2

A solution of α -hydroxycarboxylic acid (275 mg, 1.58 mmol) in CH_2Cl_2 (10 ml) was cooled to 0 °C and treated with $BzCl$ (0.37 ml, 3.16 mmol) and pyridine (0.32 ml, 3.95 mmol). After stirring for 1 h, the reaction was quenched with saturated NH_4Cl solution

and acidified with 3N HCl until pH 2-3. The mixture was extracted with CH₂Cl₂ and dried over Na₂SO₄. After removing the solvent in vacuo, the residue was purified by FCC (50% hexane:ethyl acetate and 1% AcOH) to furnish 350 mg (80%) a benzoyl protected carboxylic acid as a colorless oil.

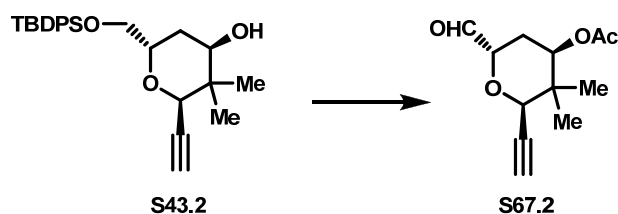
To a solution of benzoyl protected carboxylic acid (290 mg, 1.04 mmol) in toluene (10 ml) was added oxallyl chloride (0.272 ml, 3.12 mmol) and catalytic amount DMF. After stirring for 20 min at room temperature, the mixture was cooled to -78 °C and exposed to NH₃ gas for 2 min. Stirring continued for 10 min and then the reaction was quenched with 3N HCl until pH 2-3. The mixture was extracted with CH₂Cl₂ (5×), and the combined organic extract was washed with brine and dried over Na₂SO₄. After removing the solvent in vacuo, the residue was purified by FCC using hexane:ethyl acetate (3:1) as eluate to furnish 220 mg (80%) S66.2 as a colorless oil. IR ν max (neat)/cm⁻¹ 3448, 3334, 3182, 3074, 2978, 2936, 1727, 1692, 1600, 1451, 1267, 1111; ¹H NMR (500MHz, CDCl₃) 8.09-8.07 (2H, m), 7.63-7.60 (1H, m), 7.50-7.47 (2H, m), 6.22 (1H, brs), 5.98 (1H, brs), 5.74 (1H, d, J=3.5), 4.86 (1H, s), 4.83 (1H, s), 3.46 (3H, s), 2.47-2.36 (2H, m), 1.80 (3H, s); ¹³C NMR (125 MHz, CDCl₃) 170.7, 165.2, 141.9, 133.9, 130.0, 129.3, 128.9, 113.9, 79.9, 73.4, 58.3, 38.6, 22.8; *m/z* (ESIMS) calculated for C₁₄H₂₆N₂O₄Na [MNa]⁺ 309.18, found: 309.1. *m/z* (ESIMS) calculated for C₁₅H₁₉NO₄Na [MNa]⁺ 300.12, found: 299.4.



S66.3

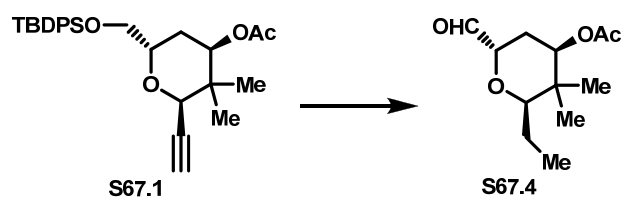
To a solution of α -hydroxylamide (60 mg, 0.34 mmol) in DMF (4 ml) was added TBSCl

(102.6 mg, 0.68 mmol) and DMAP (83 mg, 0.68 mg). After stirring for 1 h, the reaction was quenched with saturated NH_4Cl solution and extracted with CH_2Cl_2 . After removing the solvent in vacuo, the residue was purified by FCC using hexane:ethyl acetate (1:1) as eluate to furnish 94 mg (96%) **S66.2** as a colorless oil. IR ν_{max} (neat)/ cm^{-1} 3467, 3264, 3141, 2953, 2932, 1694, 1657, 1252, 1109; ^1H NMR (400MHz, CDCl_3) 6.53 (1H, brs), 6.11 (1H, brs), 4.69 (1H, s), 4.65 (1H, s), 3.57-3.56 (1H, m), 3.29 (3H, s), 2.23-2.17 (1H, m), 2.01- 1.96 (1H, m), 1.64 (3H, s), 0.83 (9H, s), 0.04 (3H, s), 0.00 (3H, s); ^{13}C NMR (100 MHz, CDCl_3) 175.3, 142.6, 112.7, 81.9, 74.1, 58.0, 37.6, 26.0, 22.8, 18.3, -4.3, -5.3; m/z (ESIMS) calculated for $\text{C}_{14}\text{H}_{29}\text{NO}_3\text{NaSi}$ $[\text{MNa}]^+$ 310.18, found: 310.2.



To a solution of alcohol (110 mg, 0.26 mmol) in pyridine (5 ml) was added Ac_2O (0.5 ml, 5.2 mmol) at rt. After 12 h, the mixture was quenched with saturated NaHCO_3 and extracted with CH_2Cl_2 . The combined organic extracts were washed with 1 N HCl solution and dried over Na_2SO_4 . The crude was passed through a pad of silica gel and used for next step without further purification.

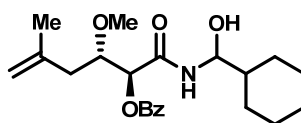
A solution of acetate protected alcohol (118 mg, 0.25 mmol) in THF (3 ml) was treated with TBAF (1.00 mmol, 1.0 M in THF) at rt. The reaction mixture was quenched with H_2O after 3 h, and extracted with CH_2Cl_2 . The organic extracts were dried over Na_2SO_4 and concentrated down under reduced pressure. The residue was purified by FCC (silica gel, ethyl acetate/hexane 1:3) to give **S67.2** (53 mg, 90%, over 2 steps) as colorless oil.



A solution of TBDPS protected pyran ring in THF (3 ml) was treated with TBAF and stirred for 3 h. The reaction was diluted with water and extracted with CH₂Cl₂. The

extracts were dried over Na_2SO_4 . After removal of solvent, the residue was purified by FCC (silica gel, ethyl acetate/hexane 1:4) to give 35 mg compound (88%, over 2 steps) as colorless oil.

To a solution of oxalyl chloride (0.021 ml, 0.23 mmol) in CH_2Cl_2 (1 ml) at $-78\text{ }^\circ\text{C}$ was added DMSO (0.033 ml, 0.47 mmol) slowly. After stirring for 15 min at that temperature, a solution of alcohol (35.0 mg, 0.15 mmol) in CH_2Cl_2 was injected to the mixture. After 20 min, NEt_3 (0.173 ml, 1.25 mmol) was added to reaction mixture. Stirring continued at $-78\text{ }^\circ\text{C}$ for 5 min, and then ice-bath was removed. After stirring at rt for 20 min, the mixture was quenched with sat NH_4Cl . The resulting mixture was extracted with CH_2Cl_2 and dried over Na_2SO_4 . The residue was purified by FCC (silica gel, ethyl acetate/hexane 1:3) to give **S67.4** (23.5 mg, 68%) as colorless oil. IR ν_{max} (neat)/ cm^{-1} 2969, 2929, 2876, 1745, 1728, 470, 1368, 1235, 1110; ^1H NMR (300 MHz, CDCl_3) 9.80 (1H, s), 4.53 (1H, dd, $J=11.4, 4.8$), 4.26 (1H, dd, $J=6.9, 2.4$), 3.10, (1H, dd, $J=9.6, 2.7$), 2.28 (1H, dd, $J=13.2, 2.4$), 2.06 (3H, s), 1.91-1.81 (1H, m), 1.40-1.50 (2H, m), 1.06 (3H, t, $J=9.6$), 0.93 (3H, s), 0.81 (3H, s); 203.7, 170.4, 83.6, 74.1, 37.9, 25.9, 23.0, 22.0, 21.2, 13.9, 11.7; m/z (ESIMS) calculated for $\text{C}_{12}\text{H}_{20}\text{O}_4\text{Na}$ $[\text{MNa}]^+$ 251.1, found: 251.1



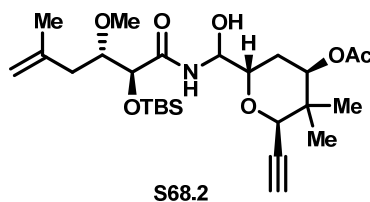
S68.1

To a solution of amide (100.0 mg, 0.35 mmol), in 3 ml of Et_2O was added NEt_3 (100 ml, 0.70 mmol) and the mixture was cooled to $0\text{ }^\circ\text{C}$. To this was added Cy_2BCl in hexane (0.52 mmol, 1.0 M) in one portion. After stirring at $0\text{ }^\circ\text{C}$ for 30 min, aldehyde (32.5 mg, 0.29 mmol) was added to the reaction mixture. The mixture was stirred for 30 min and

quenched with MeOH, phosphate buffer (pH=7.4) and 30% H₂O₂. The resulting mixture was stirred for 30 min and extracted with CH₂Cl₂. The combined organic extracts were dried over Na₂SO₄ and concentrated under reduced pressure. The residue was purified by FCC (silica gel, ethyl acetate/hexane 1:3) to give product (74 mg, 66%, dr=1:1 determined by HNMR).

Isomer A; IR ν max (neat)/cm⁻¹ 3433, 3358, 3073, 2927, 2853, 1728, 1671, 1520, 1451, 1263, 1111, 711; ¹H NMR (500MHz, CDCl₃) 8.08 (2H, d, J=7.5 Hz), 7.63 (1H, t, J=7.5 Hz), 7.50 (2H, t, J=7.5 Hz), 6.76 (1H, d, J=7.5 Hz), 5.66 (1H, d, J=4.0 Hz), 5.12 (1H, t, J=7.5 Hz), 4.86 (1H, s), 4.83 (1H, s), 3.97-3.94 (1H, m), 3.46 (3H, s), 3.45 (1H, bs), 2.44-2.38 (2H, m), 1.82-1.63 (7H, m), 1.25-0.96 (7H, m); ¹³C NMR (125 MHz, CDCl₃) 169.4, 165.2, 141.8, 134.0, 130.0, 129.2, 128.9, 113.7, 79.9, 77.8, 73.8, 58.3, 42.1, 38.7, 28.09, 28.02, 26.4, 25.84, 25.78, 22.9; *m/z* (ESIMS) calculated for C₁₃H₂₅NO₂Na [MNa]⁺ 412.1, found: 412.1.

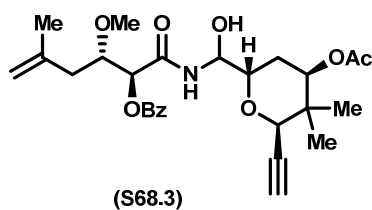
Isomer B; IR ν max (neat)/cm⁻¹ 3427, 3369, 3073, 2928, 2853, 1727.6, 1673, 1527, 1451, 1265, 1114, 710; ¹H NMR (500MHz, CDCl₃) 8.07 (2H, d, J=7.5 Hz), 7.63 (1H, t, J=7.5 Hz), 7.50 (2H, t, J=7.5 Hz), 6.79 (1H, d, 8 Hz), 5.66 (1H, d, J=4 Hz), 5.15 (1H, t, J=7.5 Hz), 4.85 (1H, s), 4.82 (1H, s), 3.95-3.92 (1H, m), 3.46 (3H, s), 3.36 (1H, bs), 2.43-2.32 (2H, m), 1.86-1.66 (7 H, m), 1.28-1.04 (7H, m); ¹³C NMR (125 MHz, CDCl₃) 169.2, 165.1, 141.8, 133.9, 130.0, 129.2, 128.9, 113.7, 79.9, 77.8, 73.7, 58.4, 42.2, 38.8, 28.16, 28.11, 26.4, 25.92, 25.82, 22.9; *m/z* (ESIMS) calculated for C₁₃H₂₅NO₂Na [MNa]⁺ 412.1, found: 412.1.



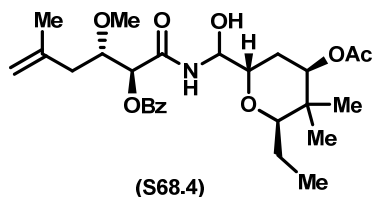
To a solution of **S66.3** (17.5 mg, 0.06 mmol) in 1 ml of Et₂O was added NEt₃ (14 ml, 0.10 mmol) the mixture was cooled to 0 °C. To this was added Cy₂BCl in hexane (0.075 ml, 1.0 M) in one portion. After stirring at 0 °C for 30 min, a solution of **S67.2** (10 mg, 0.04 mmol) in 0.4 ml of Et₂O was added to the reaction mixture. The mixture was stirred for 30 min at room temperature and quenched with MeOH, phosphate buffer (pH=7.4) and 30% H₂O₂. The resulting mixture was stirred for 30 min and extracted with CH₂Cl₂. The combined organic extracts were dried over Na₂SO₄ and concentrated under reduced pressure. The residue was purified by FCC (silica gel, ethyl acetate/hexane 1:5) to give product (8 mg, 40%, dr; 1:1 by HNMR).

Isomer A; ¹H NMR (500MHz, CDCl₃) 7.60 (1H, brs), 5.27-5.23 (1H, m), 4.90-4.89 (1H, m), 4.80 (1H, s), 4.77 (1H, s), 4.39 (1H, d, J=2.0 Hz), 4.24-4.20 (2H, m), 3.77 (1H, d, J=4.5 Hz), 3.71-3.68 (1H, m), 3.41 (3H, s), 2.50 (1H, d, J=2.0 Hz), 2.32-2.28 (2H, m), 2.09 (3H, s), 1.87-1.85 (2H, m), 1.75 (3H, s), 1.14 (3H, s), 1.04 (3H, s), 0.96 (9H, s), 0.16 (3H, s), 0.11 (3H, s).

Isomer B; ¹H NMR (500MHz, CDCl₃) 7.81(1H, brs), 5.28-5.25 (1H, m), 4.95-4.94 (1H, m), 4.79 (1H, s), 4.76 (1H, s), 4.40 (1H, d, J=2.0 Hz), 4.40 (1H, d, J=1.5 Hz), 4.33 (1H, d, J= 2.0 Hz), 4.15 (1H, d, J=11 Hz), 3.72-3.69 (1H, m), 3.41(3H, s), 3.09 (1H, d, J=6.0 Hz), 2.46 (1H, d, J=2.0 Hz), 2.33-2.28 (1H, m), 2.24-2.18 (1H, m), 2.09 (3H, s), 1.74 (3H, s), 1.68 (3H, s), 1.04 (3H ,s), 0.98 (3H, s), 0.16 (3H, s), 0.12 (3H, s).



To a solution of **S66.2** (36.5 mg, 0.13 mmol) in 1 ml of Et₂O was added NEt₃ (14 ml, 0.10 mmol) the mixture was cooled to 0 °C. To this was added Cy₂BCl in hexane (0.075 ml, 1.0 M) in one portion. After stirring at 0 °C for 30 min, a solution of **S67.2** (20 mg, 0.09 mmol) in 0.4 ml of Et₂O was added to the reaction mixture. The mixture was stirred for 30 min at room temperature and quenched with MeOH, phosphate buffer (pH=7.4) and 30% H₂O₂. The resulting mixture was stirred for 30 min and extracted with CH₂Cl₂. The combined organic extracts were dried over Na₂SO₄ and concentrated under reduced pressure. The residue was purified by FCC (silica gel, ethyl acetate/hexane 1:5) to give a mixture of inseparable products (18 mg, 40%, dr; 1:1 by HNMR).



To a solution of **S66.2** (11.0 mg, 0.063 mmol) in 1 ml of Et₂O was added NEt₃ (14 ml, 0.10 mmol) the mixture was cooled to 0 °C. To this was added Cy₂BCl in hexane (0.075 ml, 1.0 M) in one portion. After stirring at 0 °C for 30 min, a solution of **S67.4** (20 mg, 0.09 mmol) in 0.4 ml of Et₂O was added to the reaction mixture. The mixture was stirred for 30 min at room temperature and quenched with MeOH, phosphate buffer (pH=7.4) and 30% H₂O₂. The resulting mixture was stirred for 30 min and extracted with CH₂Cl₂. The combined organic extracts were dried over Na₂SO₄ and concentrated under reduced

pressure. The residue was purified by FCC (silica gel, ethyl acetate/hexane 1:5) to give a mixture of inseparable products (9 mg, 40%, dr; 2:1 by HNMR).

CHAPTER 5

General procedure for thionoesters:

A solution of thiobenzoic acid in CH_2Cl_2 (~0.2 M) was treated with NEt_3 and then cooled to 0 °C. This mixture was charged with TMSOTf and stirred for 10 min in ice bath. Then, FeCl_3 , a base (if necessary) and an azide was added. The mixture was stirred for indicated time at room temperature, quenched with saturated NaHCO_3 and extracted with dichloromethane. The extractions were dried over Na_2SO_4 and evaporate under vacuum. The crude was purified by FCC using Hex to give the corresponding amide product.

Genereal procedure for thioacids:

A solution of thioacid in CH_2Cl_2 (~0.2 M) was exposed to FeCl_3 , a base (if necessary) and an azide and the mixture was stirred for indicated time at room temperature. The reaction quenched with saturated NaHCO_3 and extracted with dichloromethane. The extractions were dried over Na_2SO_4 and evaporate under vacuum. The crude was purified by FCC to give the corresponding amide products.

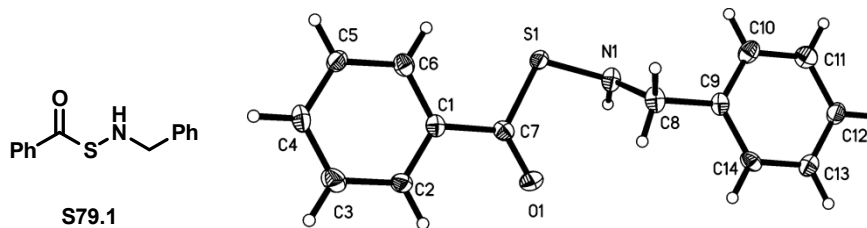
Characterization of Side Products:

S79.1: m.p.= 41-42 °C. ^1H NMR (400 MHz, DMSO) 7.82-7.79 (2H, m), 7.70-7.66 (1H, m), 7.56-7.52 (2H, m), 7.37-7.23 (5H, m), 5.27 (1H, t, $J=4.8$ Hz), 4.11 (2H, d, $J=4.8$ Hz). ^{13}C NMR (100 MHz, DMSO) 198.0, 139.8, 135.3, 134.4, 129.7, 128.7, 128.6, 127.6, 126.5, 55.1. IR ν_{max} (KBr pellet, cm^{-1}) 3304, 3023, 2923, 2864, 2804, 1651, 1442.5, 1199, 1042, 907. m/z (ESIMS) calculated for $\text{C}_{14}\text{H}_{13}\text{NOS}$ $[\text{MH}]^+$ 244.07, found: 244.1.]

S79.2: m.p.= 108-109 °C. ^1H NMR (400 MHz, DMSO) 9.20 (1H, d, $J=8.4$ Hz), 7.98 (2H, d, $J=7.2$ Hz), 7.67-7.24 (18H, m), 6.57-6.55 (1H, d, $J=8.4$ Hz), 4.46 (2H, dd, $J=70, 14$ Hz). ^{13}C NMR (125 MHz, CHCl_3) 202.3, 166.9, 138.6, 137.6, 134.8, 134.3, 134.1, 131.9, 129.08, 129.04, 128.93, 128.91, 128.6, 128.5, 128.2, 127.7, 127.5, 127.2, 73.3, 60.0. IR ν_{max} (KBr pellet, cm^{-1}) 3328, 3056, 3025, 2917, 2857, 1658, 1595, 1575, 1511, 1479, 1203, 900. m/z (ESIMS) calculated for $\text{C}_{28}\text{H}_{24}\text{N}_2\text{O}_2\text{S}$ $[\text{MNa}]^+$ 475.16, found: 475.2].

S79.3: m.p.= 158-160 °C. ^1H NMR (400 MHz, DMSO) 9.68 (1H, d, $J=9.2$ Hz), 7.94-7.89 (4H, m), 7.72-7.68 (1H, m), 7.58-7.32 (10H, m), 7.12 (1H, d, $J=9.2$ Hz). ^{13}C NMR (100 MHz, DMSO) 191.9, 166.3, 139.1, 136.7, 134.1, 132.2, 129.0, 128.9, 128.4, 127.70, 127.5, 127.52, 127.50, 127.0, 57.07. IR ν_{max} (KBr pellet, cm^{-1}) 3283, 3054, 2920, 1671, 1626, 1509, 1480, 1201, 903. m/z (ESIMS) calculated for $\text{C}_{21}\text{H}_{17}\text{NO}_2\text{S}$ $[\text{MNa}]^+$ 370.1, found: 370.0].

All the azides in table 7 and Scheme 77 as well as the corresponding amides in table 7 are known compounds. The characterization data for the dimer **S78.1** were also reported in literature.

Crystal Structure: **S79.1**

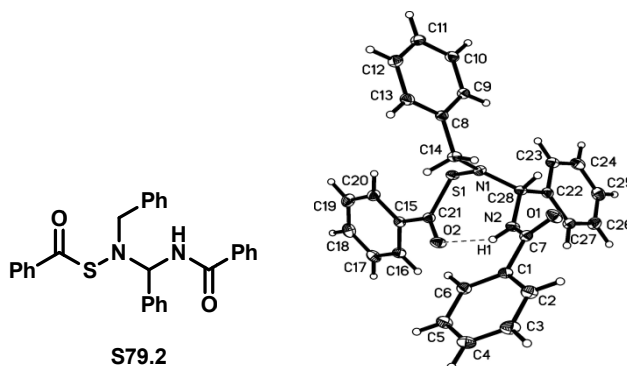
Empirical formula	C ₁₄ H ₁₃ N O S	
Formula weight	243.31	
Temperature	100(2) K	
Wavelength	0.71073 Å	
Crystal system	Monoclinic	
Space group	P2(1)	
Unit cell dimensions	a = 8.0082(10) Å	□ = 90°.
	b = 5.3274(7) Å	□ = 96.577(2)°.
	c = 28.679(4) Å	□ = 90°.
Volume	1215.5(3) Å ³	
Z	4	
Density (calculated)	1.330 Mg/m ³	
Absorption coefficient	0.248 mm ⁻¹	
F(000)	512	
Crystal size	0.41 x 0.27 x 0.03 mm ³	
Theta range for data collection	2.56 to 30.54°.	
Index ranges	-11 ≤ h ≤ 11, -7 ≤ k ≤ 7, -41 ≤ l ≤ 40	

Reflections collected	13118
Independent reflections	3667 [R(int) = 0.0468]
Completeness to theta = 30.54°	98.3 %
Absorption correction	Semi-empirical from equivalents
Max. and min. transmission	0.9999 and 0.6353
Refinement method	Full-matrix least-squares on F ²
Data / restraints / parameters	3667 / 0 / 171
Goodness-of-fit on F ²	1.138
Final R indices [I>2sigma(I)]	R1 = 0.1508, wR2 = 0.3544
R indices (all data)	R1 = 0.1556, wR2 = 0.3564
Extinction coefficient	0.005(2)
Largest diff. peak and hole	1.270 and -1.695 e.Å ⁻³

Table. Preliminary bond lengths [Å] and angles [°] for **S79.1**.

S(1)-N(1)	1.664(5)	C(4)-H(4)	0.9300
S(1)-C(7)	1.770(6)	C(5)-C(6)	1.386(8)
N(1)-C(8)	1.469(8)	C(5)-H(5)	0.9300
N(1)-H(1)	0.87(7)	C(6)-H(6)	0.9300
O(1)-C(7)	1.210(7)	C(8)-C(9)	1.507(8)
C(1)-C(2)	1.391(8)	C(8)-H(8A)	0.9700
C(1)-C(6)	1.403(8)	C(8)-H(8B)	0.9700
C(1)-C(7)	1.492(8)	C(9)-C(14)	1.387(8)
C(2)-C(3)	1.388(8)	C(9)-C(10)	1.393(9)
C(2)-H(2)	0.9300	C(10)-C(11)	1.393(8)
C(3)-C(4)	1.381(9)	C(10)-H(10)	0.9300
C(3)-H(3)	0.9300	C(11)-C(12)	1.399(9)
C(4)-C(5)	1.382(9)	C(11)-H(11)	0.9300

C(12)-C(13)	1.389(9)	C(13)-H(13)	0.9300
C(12)-H(12)	0.9300	C(14)-H(14)	0.9300
C(13)-C(14)	1.395(8)		
N(1)-S(1)-C(7)	105.0(3)	N(1)-C(8)-H(8B)	109.7
C(8)-N(1)-S(1)	116.8(4)	C(9)-C(8)-H(8B)	109.7
C(8)-N(1)-H(1)	116(5)	H(8A)-C(8)-H(8B)	108.2
S(1)-N(1)-H(1)	107(4)	C(14)-C(9)-C(10)	119.1(5)
C(2)-C(1)-C(6)	119.9(5)	C(14)-C(9)-C(8)	119.7(5)
C(2)-C(1)-C(7)	119.0(5)	C(10)-C(9)-C(8)	121.2(6)
C(6)-C(1)-C(7)	121.1(5)	C(9)-C(10)-C(11)	120.6(6)
C(3)-C(2)-C(1)	119.8(6)	C(9)-C(10)-H(10)	119.7
C(3)-C(2)-H(2)	120.1	C(11)-C(10)-H(10)	119.7
C(1)-C(2)-H(2)	120.1	C(10)-C(11)-C(12)	120.1(6)
C(4)-C(3)-C(2)	120.4(6)	C(10)-C(11)-H(11)	120.0
C(4)-C(3)-H(3)	119.8	C(12)-C(11)-H(11)	120.0
C(2)-C(3)-H(3)	119.8	C(13)-C(12)-C(11)	119.2(6)
C(3)-C(4)-C(5)	120.0(6)	C(13)-C(12)-H(12)	120.4
C(3)-C(4)-H(4)	120.0	C(11)-C(12)-H(12)	120.4
C(5)-C(4)-H(4)	120.0	C(12)-C(13)-C(14)	120.4(6)
C(4)-C(5)-C(6)	120.7(6)	C(12)-C(13)-H(13)	119.8
C(4)-C(5)-H(5)	119.7	C(14)-C(13)-H(13)	119.8
C(6)-C(5)-H(5)	119.7	C(9)-C(14)-C(13)	120.6(5)
C(5)-C(6)-C(1)	119.3(6)	C(9)-C(14)-H(14)	119.7
C(5)-C(6)-H(6)	120.4	C(13)-C(14)-H(14)	119.7
C(1)-C(6)-H(6)	120.4	N(1)-C(8)-C(9)	109.8(5)
O(1)-C(7)-C(1)	122.4(6)	N(1)-C(8)-H(8A)	109.7
O(1)-C(7)-S(1)	121.2(5)	C(9)-C(8)-H(8A)	109.7
C(1)-C(7)-S(1)	116.3(4)		

Crystal Structure: **S79.2****Table 1.** Crystal data and structure refinement for **S79.2**.

Empirical formula	C ₁₄ H ₁₂ N O S _{0.50}	
Formula weight	226.28	
Temperature	100(2) K	
Wavelength	0.71073 Å	
Crystal system	Triclinic	
Space group	P-1	
Unit cell dimensions	$a = 10.3486(7)$ Å	$\alpha = 96.380(1)^\circ$.
	$b = 10.9537(7)$ Å	$\beta = 114.609(1)^\circ$.
	$c = 11.2778(7)$ Å	$\gamma = 99.450(1)^\circ$.
Volume	$1123.31(13)$ Å ³	
Z	4	
Density (calculated)	1.338 Mg/m ³	
Absorption coefficient	0.173 mm ⁻¹	
F(000)	476	
Crystal size	0.35 x 0.25 x 0.16 mm ³	

Theta range for data collection	2.03 to 30.55°.
Index ranges	-14≤h≤14, -15≤k≤15, -16≤l≤15
Reflections collected	13384
Independent reflections	6761 [R(int) = 0.0170]
Completeness to theta = 30.55°	98.2 %
Absorption correction	Semi-empirical from equivalents
Max. and min. transmission	0.9999 and 0.8445
Refinement method	Full-matrix least-squares on F ²
Data / restraints / parameters	6761 / 0 / 394
Goodness-of-fit on F ²	1.001
Final R indices [I>2sigma(I)]	R1 = 0.0431, wR2 = 0.1067
R indices (all data)	R1 = 0.0487, wR2 = 0.1106
Largest diff. peak and hole	0.629 and -0.327 e.Å ⁻³

Table 2. Atomic coordinates (x 10⁴) and equivalent isotropic displacement parameters (Å²x 10³) for Sezgin Side Product B. U(eq) is defined as one third of the trace of the orthogonalized U^{ij} tensor.

	x	y	z	U(eq)
S(1)	4245(1)	6744(1)	2733(1)	15(1)
N(1)	4792(1)	7694(1)	4198(1)	14(1)
O(1)	7888(1)	9502(1)	7614(1)	22(1)
N(2)	7371(1)	8183(1)	5693(1)	15(1)
O(2)	6558(1)	5813(1)	3968(1)	21(1)
C(1)	9026(1)	7763(1)	7797(1)	15(1)
C(2)	10082(1)	8315(1)	9093(1)	20(1)
C(3)	10968(2)	7611(1)	9879(1)	24(1)

C(4)	10803(1)	6348(1)	9380(1)	23(1)
C(5)	9771(1)	5795(1)	8086(1)	21(1)
C(6)	8885(1)	6502(1)	7297(1)	17(1)
C(7)	8046(1)	8564(1)	7038(1)	15(1)
C(8)	2564(1)	7238(1)	4556(1)	14(1)
C(9)	1903(1)	7944(1)	3618(1)	16(1)
C(10)	434(1)	7945(1)	3177(1)	19(1)
C(11)	-400(1)	7238(1)	3667(1)	21(1)
C(12)	254(1)	6548(1)	4620(1)	22(1)
C(13)	1724(1)	6544(1)	5060(1)	18(1)
C(14)	4171(1)	7240(1)	5070(1)	16(1)
C(15)	4888(1)	4625(1)	1811(1)	15(1)
C(16)	5921(1)	4212(1)	1470(1)	17(1)
C(17)	5459(2)	3238(1)	384(1)	21(1)
C(18)	3981(2)	2664(1)	-354(1)	24(1)
C(19)	2958(2)	3059(1)	-6(1)	24(1)
C(20)	3403(1)	4048(1)	1070(1)	19(1)
C(21)	5407(1)	5673(1)	2977(1)	15(1)
C(22)	6459(1)	9329(1)	3824(1)	14(1)
C(23)	5330(1)	9713(1)	2839(1)	17(1)
C(24)	5604(1)	10405(1)	1976(1)	21(1)
C(25)	7013(2)	10726(1)	2085(1)	23(1)
C(26)	8136(1)	10348(1)	3059(1)	22(1)
C(27)	7863(1)	9655(1)	3926(1)	18(1)
C(28)	6155(1)	8672(1)	4830(1)	14(1)

Table 3. Bond lengths [Å] and angles [°] for **S79.2**.

S(1)-N(1)	1.6670(10)	N(2)-C(28)	1.4603(14)
S(1)-C(21)	1.7774(12)	N(2)-H(1)	0.833(18)
N(1)-C(28)	1.4641(14)	O(2)-C(21)	1.2188(14)
N(1)-C(14)	1.4690(15)	C(1)-C(6)	1.3929(16)
O(1)-C(7)	1.2250(14)	C(1)-C(2)	1.3973(16)
N(2)-C(7)	1.3579(14)	C(1)-C(7)	1.5057(16)

C(2)-C(3)	1.3887(17)	C(15)-C(16)	1.3992(16)
C(2)-H(2)	0.966(19)	C(15)-C(21)	1.4865(15)
C(3)-C(4)	1.390(2)	C(16)-C(17)	1.3862(17)
C(3)-H(3)	0.98(2)	C(16)-H(16)	0.974(18)
C(4)-C(5)	1.3894(18)	C(17)-C(18)	1.3909(19)
C(4)-H(4)	0.964(17)	C(17)-H(17)	0.962(19)
C(5)-C(6)	1.3927(16)	C(18)-C(19)	1.387(2)
C(5)-H(5)	0.933(19)	C(18)-H(18)	0.936(18)
C(6)-H(6)	0.952(17)	C(19)-C(20)	1.3918(17)
C(8)-C(9)	1.3920(16)	C(19)-H(19)	0.985(19)
C(8)-C(13)	1.3956(16)	C(20)-H(20)	0.961(18)
C(8)-C(14)	1.5153(15)	C(22)-C(27)	1.3898(16)
C(9)-C(10)	1.3898(16)	C(22)-C(23)	1.4001(15)
C(9)-H(9)	0.927(18)	C(22)-C(28)	1.5193(16)
C(10)-C(11)	1.3865(18)	C(23)-C(24)	1.3880(17)
C(10)-H(10)	0.979(17)	C(23)-H(23)	0.969(17)
C(11)-C(12)	1.3873(19)	C(24)-C(25)	1.3921(19)
C(11)-H(11)	0.964(17)	C(24)-H(24)	0.939(18)
C(12)-C(13)	1.3909(17)	C(25)-C(26)	1.3867(19)
C(12)-H(12)	0.966(19)	C(25)-H(25)	0.947(19)
C(13)-H(13)	0.966(18)	C(26)-C(27)	1.3920(17)
C(14)-H(14A)	0.982(16)	C(26)-H(26)	0.966(18)
C(14)-H(14B)	0.983(17)	C(27)-H(27)	0.961(17)
C(15)-C(20)	1.3970(16)	C(28)-H(28)	0.991(15)
N(1)-S(1)-C(21)	107.46(5)	C(3)-C(2)-H(2)	120.6(11)
C(28)-N(1)-C(14)	116.96(9)	C(1)-C(2)-H(2)	118.9(11)
C(28)-N(1)-S(1)	123.10(8)	C(2)-C(3)-C(4)	119.98(12)
C(14)-N(1)-S(1)	116.40(8)	C(2)-C(3)-H(3)	121.9(11)
C(7)-N(2)-C(28)	122.78(10)	C(4)-C(3)-H(3)	118.1(11)
C(7)-N(2)-H(1)	118.4(12)	C(5)-C(4)-C(3)	120.02(12)
C(28)-N(2)-H(1)	115.9(12)	C(5)-C(4)-H(4)	119.8(10)
C(6)-C(1)-C(2)	119.22(11)	C(3)-C(4)-H(4)	120.1(10)
C(6)-C(1)-C(7)	123.45(10)	C(4)-C(5)-C(6)	119.97(12)
C(2)-C(1)-C(7)	117.27(10)	C(4)-C(5)-H(5)	120.9(11)
C(3)-C(2)-C(1)	120.43(12)	C(6)-C(5)-H(5)	119.1(11)

C(5)-C(6)-C(1)	120.37(11)	C(16)-C(17)-C(18)	120.35(12)
C(5)-C(6)-H(6)	118.8(10)	C(16)-C(17)-H(17)	120.6(11)
C(1)-C(6)-H(6)	120.7(10)	C(18)-C(17)-H(17)	119.0(11)
O(1)-C(7)-N(2)	122.92(11)	C(19)-C(18)-C(17)	120.22(12)
O(1)-C(7)-C(1)	121.21(10)	C(19)-C(18)-H(18)	119.3(11)
N(2)-C(7)-C(1)	115.86(10)	C(17)-C(18)-H(18)	120.4(11)
C(9)-C(8)-C(13)	118.58(11)	C(18)-C(19)-C(20)	120.06(12)
C(9)-C(8)-C(14)	121.80(10)	C(18)-C(19)-H(19)	122.4(11)
C(13)-C(8)-C(14)	119.59(10)	C(20)-C(19)-H(19)	117.5(11)
C(10)-C(9)-C(8)	120.82(11)	C(19)-C(20)-C(15)	119.69(11)
C(10)-C(9)-H(9)	118.6(11)	C(19)-C(20)-H(20)	121.7(11)
C(8)-C(9)-H(9)	120.6(11)	C(15)-C(20)-H(20)	118.6(11)
C(11)-C(10)-C(9)	120.29(11)	O(2)-C(21)-C(15)	122.78(10)
C(11)-C(10)-H(10)	120.8(10)	O(2)-C(21)-S(1)	123.80(9)
C(9)-C(10)-H(10)	118.9(10)	C(15)-C(21)-S(1)	113.30(8)
C(10)-C(11)-C(12)	119.34(11)	C(27)-C(22)-C(23)	118.85(11)
C(10)-C(11)-H(11)	119.9(10)	C(27)-C(22)-C(28)	121.41(10)
C(12)-C(11)-H(11)	120.8(10)	C(23)-C(22)-C(28)	119.50(10)
C(11)-C(12)-C(13)	120.46(12)	C(24)-C(23)-C(22)	120.69(11)
C(11)-C(12)-H(12)	120.3(11)	C(24)-C(23)-H(23)	119.1(10)
C(13)-C(12)-H(12)	119.2(11)	C(22)-C(23)-H(23)	120.2(10)
C(12)-C(13)-C(8)	120.49(11)	C(23)-C(24)-C(25)	120.04(12)
C(12)-C(13)-H(13)	119.0(11)	C(23)-C(24)-H(24)	121.9(11)
C(8)-C(13)-H(13)	120.5(11)	C(25)-C(24)-H(24)	118.0(11)
N(1)-C(14)-C(8)	112.67(9)	C(26)-C(25)-C(24)	119.51(12)
N(1)-C(14)-H(14A)	105.8(9)	C(26)-C(25)-H(25)	119.8(12)
C(8)-C(14)-H(14A)	110.5(9)	C(24)-C(25)-H(25)	120.6(12)
N(1)-C(14)-H(14B)	110.5(10)	C(25)-C(26)-C(27)	120.51(12)
C(8)-C(14)-H(14B)	109.6(10)	C(25)-C(26)-H(26)	120.5(10)
H(14A)-C(14)-H(14B)	107.6(13)	C(27)-C(26)-H(26)	119.0(10)
C(20)-C(15)-C(16)	120.16(11)	C(22)-C(27)-C(26)	120.40(11)
C(20)-C(15)-C(21)	121.24(10)	C(22)-C(27)-H(27)	120.7(10)
C(16)-C(15)-C(21)	118.60(10)	C(26)-C(27)-H(27)	118.9(10)
C(17)-C(16)-C(15)	119.52(11)	N(2)-C(28)-N(1)	111.35(9)
C(17)-C(16)-H(16)	121.0(11)	N(2)-C(28)-C(22)	113.72(9)
C(15)-C(16)-H(16)	119.5(11)	N(1)-C(28)-C(22)	112.04(9)

N(2)-C(28)-H(28)	105.7(9)	C(22)-C(28)-H(28)	107.6(9)
N(1)-C(28)-H(28)	105.9(9)		

Table 4. Anisotropic displacement parameters ($\text{\AA}^2 \times 10^3$) for **S79.2**. The anisotropic displacement factor exponent takes the form: $-2\pi^2 [h^2 a^{*2} U^{11} + \dots + 2 h k a^* b^* U^{12}]$

	U ¹¹	U ²²	U ³³	U ²³	U ¹³	U ¹²
S(1)	13(1)	16(1)	12(1)	0(1)	3(1)	5(1)
N(1)	13(1)	16(1)	12(1)	0(1)	6(1)	3(1)
O(1)	26(1)	18(1)	16(1)	0(1)	5(1)	10(1)
N(2)	14(1)	17(1)	13(1)	2(1)	4(1)	7(1)
O(2)	18(1)	22(1)	17(1)	-1(1)	2(1)	9(1)
C(1)	14(1)	18(1)	12(1)	3(1)	5(1)	5(1)
C(2)	20(1)	22(1)	14(1)	1(1)	4(1)	6(1)
C(3)	21(1)	32(1)	14(1)	3(1)	2(1)	9(1)
C(4)	21(1)	28(1)	20(1)	9(1)	6(1)	11(1)
C(5)	21(1)	20(1)	21(1)	6(1)	8(1)	9(1)
C(6)	17(1)	18(1)	15(1)	3(1)	5(1)	5(1)
C(7)	13(1)	16(1)	14(1)	3(1)	5(1)	2(1)
C(8)	14(1)	14(1)	15(1)	1(1)	7(1)	4(1)
C(9)	15(1)	15(1)	17(1)	2(1)	7(1)	3(1)
C(10)	16(1)	18(1)	21(1)	2(1)	5(1)	5(1)
C(11)	14(1)	20(1)	27(1)	0(1)	9(1)	4(1)
C(12)	20(1)	21(1)	29(1)	4(1)	15(1)	4(1)
C(13)	19(1)	18(1)	21(1)	5(1)	11(1)	6(1)
C(14)	14(1)	19(1)	15(1)	5(1)	7(1)	6(1)
C(15)	17(1)	14(1)	13(1)	2(1)	6(1)	4(1)
C(16)	18(1)	19(1)	16(1)	3(1)	8(1)	7(1)
C(17)	29(1)	20(1)	18(1)	4(1)	12(1)	11(1)
C(18)	32(1)	18(1)	18(1)	-1(1)	11(1)	4(1)
C(19)	22(1)	21(1)	21(1)	-3(1)	7(1)	-1(1)
C(20)	17(1)	19(1)	19(1)	1(1)	8(1)	2(1)
C(21)	15(1)	15(1)	15(1)	2(1)	7(1)	4(1)

C(22)	15(1)	13(1)	14(1)	1(1)	6(1)	4(1)
C(23)	17(1)	18(1)	17(1)	4(1)	7(1)	6(1)
C(24)	25(1)	21(1)	20(1)	8(1)	9(1)	10(1)
C(25)	30(1)	20(1)	24(1)	8(1)	15(1)	7(1)
C(26)	20(1)	21(1)	26(1)	4(1)	13(1)	3(1)
C(27)	16(1)	17(1)	19(1)	2(1)	7(1)	3(1)
C(28)	12(1)	15(1)	13(1)	2(1)	4(1)	5(1)

Table 5. Hydrogen coordinates ($\times 10^4$) and isotropic displacement parameters ($\text{\AA}^2 \times 10^3$) for **S79.2**.

	x	y	z	U(eq)
H(1)	7457(19)	7499(17)	5364(17)	24(4)
H(2)	10200(20)	9197(18)	9427(19)	33(5)
H(3)	11720(20)	7978(18)	10790(20)	35(5)
H(4)	11385(19)	5847(16)	9937(17)	23(4)
H(5)	9650(20)	4948(18)	7736(18)	30(5)
H(6)	8145(19)	6095(16)	6431(17)	23(4)
H(9)	2443(19)	8445(17)	3295(17)	26(4)
H(10)	5(18)	8464(16)	2530(17)	23(4)
H(11)	-1428(19)	7217(16)	3333(17)	24(4)
H(12)	-310(20)	6050(17)	4970(18)	30(5)
H(13)	2160(20)	6055(17)	5722(18)	29(4)
H(14A)	4743(17)	7813(15)	5940(16)	17(4)
H(14B)	4309(18)	6388(16)	5191(16)	19(4)
H(16)	6952(19)	4630(16)	1985(17)	27(4)
H(17)	6153(19)	2955(17)	124(18)	28(4)
H(18)	3669(19)	1999(17)	-1082(18)	29(4)
H(19)	1900(20)	2678(18)	-510(19)	35(5)
H(20)	2716(19)	4344(17)	1328(18)	27(4)
H(23)	4345(19)	9500(16)	2755(17)	22(4)
H(24)	4870(20)	10683(17)	1318(18)	28(4)

H(25)	7210(20)	11196(18)	1499(19)	33(5)
H(26)	9122(19)	10580(16)	3159(17)	25(4)
H(27)	8661(18)	9412(16)	4599(17)	23(4)
H(28)	6012(16)	9311(14)	5430(15)	13(3)

Table 6. Torsion angles [$^{\circ}$] for **S79.2**.

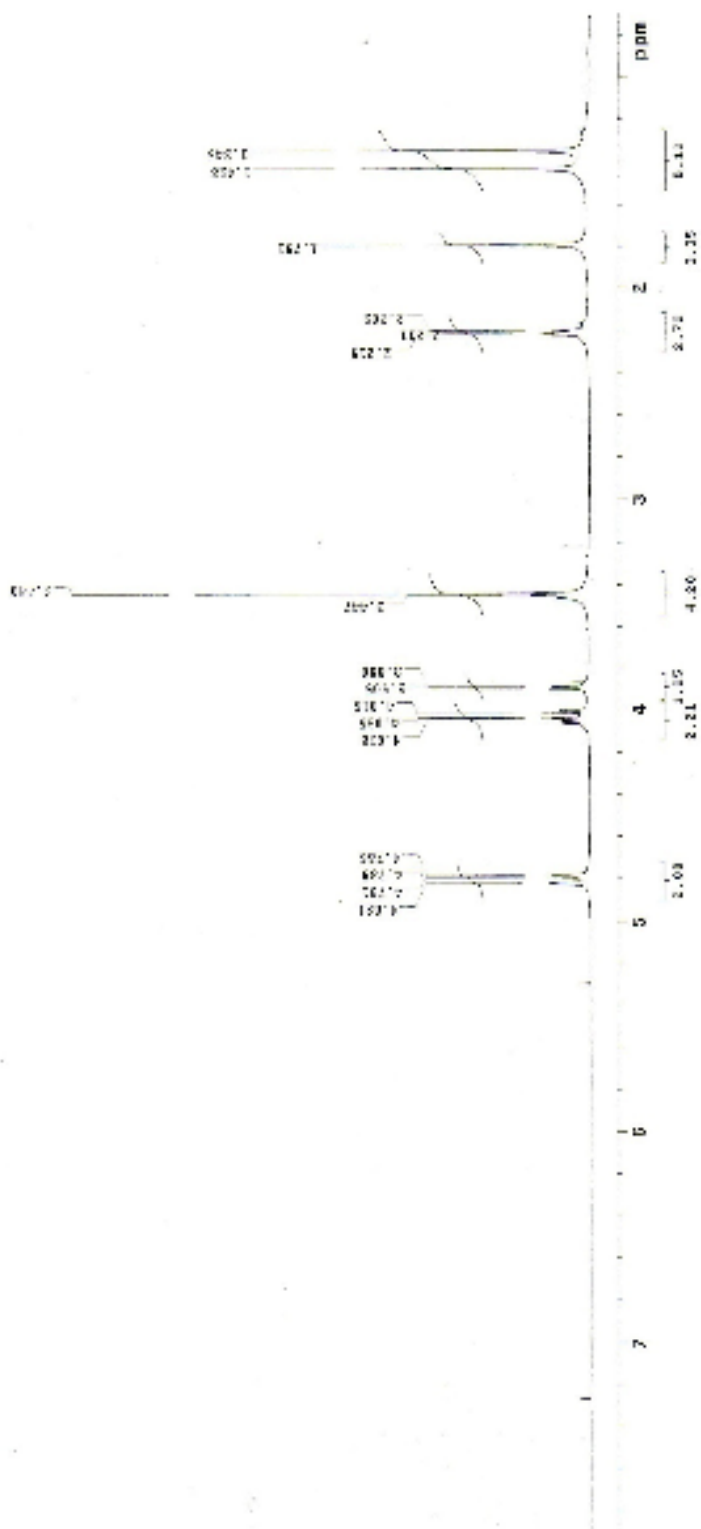
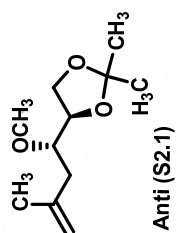
C(21)-S(1)-N(1)-C(28)	71.41(10)	C(20)-C(15)-C(16)-C(17)	0.80(18)
C(21)-S(1)-N(1)-C(14)	-86.70(9)	C(21)-C(15)-C(16)-C(17)	-179.83(11)
C(6)-C(1)-C(2)-C(3)	-0.80(19)	C(15)-C(16)-C(17)-C(18)	-0.76(18)
C(7)-C(1)-C(2)-C(3)	176.31(12)	C(16)-C(17)-C(18)-C(19)	-0.2(2)
C(1)-C(2)-C(3)-C(4)	-0.3(2)	C(17)-C(18)-C(19)-C(20)	1.2(2)
C(2)-C(3)-C(4)-C(5)	1.2(2)	C(18)-C(19)-C(20)-C(15)	-1.1(2)
C(3)-C(4)-C(5)-C(6)	-1.1(2)	C(16)-C(15)-C(20)-C(19)	0.13(18)
C(4)-C(5)-C(6)-C(1)	0.02(19)	C(21)-C(15)-C(20)-C(19)	-179.22(11)
C(2)-C(1)-C(6)-C(5)	0.92(18)	C(20)-C(15)-C(21)-O(2)	144.65(12)
C(7)-C(1)-C(6)-C(5)	-176.00(11)	C(16)-C(15)-C(21)-O(2)	-34.71(17)
C(28)-N(2)-C(7)-O(1)	-14.21(18)	C(20)-C(15)-C(21)-S(1)	-39.16(14)
C(28)-N(2)-C(7)-C(1)	166.22(10)	C(16)-C(15)-C(21)-S(1)	141.48(10)
C(6)-C(1)-C(7)-O(1)	157.20(12)	N(1)-S(1)-C(21)-O(2)	-14.09(12)
C(2)-C(1)-C(7)-O(1)	-19.78(17)	N(1)-S(1)-C(21)-C(15)	169.76(8)
C(6)-C(1)-C(7)-N(2)	-23.23(16)	C(27)-C(22)-C(23)-C(24)	0.19(17)
C(2)-C(1)-C(7)-N(2)	159.79(11)	C(28)-C(22)-C(23)-C(24)	174.70(11)
C(13)-C(8)-C(9)-C(10)	-0.91(17)	C(22)-C(23)-C(24)-C(25)	-0.10(19)
C(14)-C(8)-C(9)-C(10)	-178.89(11)	C(23)-C(24)-C(25)-C(26)	0.1(2)
C(8)-C(9)-C(10)-C(11)	-0.06(18)	C(24)-C(25)-C(26)-C(27)	-0.2(2)
C(9)-C(10)-C(11)-C(12)	1.20(19)	C(23)-C(22)-C(27)-C(26)	-0.28(17)
C(10)-C(11)-C(12)-C(13)	-1.36(19)	C(28)-C(22)-C(27)-C(26)	-174.68(11)
C(11)-C(12)-C(13)-C(8)	0.38(19)	C(25)-C(26)-C(27)-C(22)	0.29(19)
C(9)-C(8)-C(13)-C(12)	0.76(18)	C(7)-N(2)-C(28)-N(1)	-112.29(12)
C(14)-C(8)-C(13)-C(12)	178.78(11)	C(7)-N(2)-C(28)-C(22)	119.99(11)
C(28)-N(1)-C(14)-C(8)	130.18(10)	C(14)-N(1)-C(28)-N(2)	67.85(12)
S(1)-N(1)-C(14)-C(8)	-70.33(11)	S(1)-N(1)-C(28)-N(2)	-90.14(10)
C(9)-C(8)-C(14)-N(1)	-18.53(15)	C(14)-N(1)-C(28)-C(22)	-163.52(9)
C(13)-C(8)-C(14)-N(1)	163.52(10)	S(1)-N(1)-C(28)-C(22)	38.48(12)

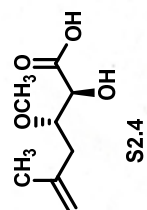
C(27)-C(22)-C(28)-N(2)	-12.87(15)	C(27)-C(22)-C(28)-N(1)	-140.24(11)
C(23)-C(22)-C(28)-N(2)	172.76(10)	C(23)-C(22)-C(28)-N(1)	45.40(14)

Table 7. Hydrogen bonds for **S79.2** [\AA and $^\circ$].

D-H...A	d(D-H)	d(H...A)	d(D...A)	$\angle(\text{DHA})$
N(2)-H(1)...O(2)	0.833(18)	2.080(18)	2.8339(13)	150.3(16)

NMR DATA




$$2.00 \times 10^{-2}$$

Pharmaceutical Expenditures 0.300

Advertiser: CIBC

2000 1001 1002 1003 1004 1005 1006 1007 1008 1009 1010 1011 1012 1013 1014 1015 1016 1017 1018 1019 1020 1021 1022 1023 1024 1025 1026 1027 1028 1029 1030 1031 1032 1033 1034 1035 1036 1037 1038 1039 1040 1041 1042 1043 1044 1045 1046 1047 1048 1049 1050 1051 1052 1053 1054 1055 1056 1057 1058 1059 1060 1061 1062 1063 1064 1065 1066 1067 1068 1069 1070 1071 1072 1073 1074 1075 1076 1077 1078 1079 1080 1081 1082 1083 1084 1085 1086 1087 1088 1089 1090 1091 1092 1093 1094 1095 1096 1097 1098 1099 1100 1101 1102 1103 1104 1105 1106 1107 1108 1109 1110 1111 1112 1113 1114 1115 1116 1117 1118 1119 1120 1121 1122 1123 1124 1125 1126 1127 1128 1129 1130 1131 1132 1133 1134 1135 1136 1137 1138 1139 1140 1141 1142 1143 1144 1145 1146 1147 1148 1149 1150 1151 1152 1153 1154 1155 1156 1157 1158 1159 1160 1161 1162 1163 1164 1165 1166 1167 1168 1169 1170 1171 1172 1173 1174 1175 1176 1177 1178 1179 1180 1181 1182 1183 1184 1185 1186 1187 1188 1189 1190 1191 1192 1193 1194 1195 1196 1197 1198 1199 1200 1201 1202 1203 1204 1205 1206 1207 1208 1209 1210 1211 1212 1213 1214 1215 1216 1217 1218 1219 1220 1221 1222 1223 1224 1225 1226 1227 1228 1229 1230 1231 1232 1233 1234 1235 1236 1237 1238 1239 1240 1241 1242 1243 1244 1245 1246 1247 1248 1249 1250 1251 1252 1253 1254 1255 1256 1257 1258 1259 1260 1261 1262 1263 1264 1265 1266 1267 1268 1269 1270 1271 1272 1273 1274 1275 1276 1277 1278 1279 1280 1281 1282 1283 1284 1285 1286 1287 1288 1289 1290 1291 1292 1293 1294 1295 1296 1297 1298 1299 1300 1301 1302 1303 1304 1305 1306 1307 1308 1309 1310 1311 1312 1313 1314 1315 1316 1317 1318 1319 1320 1321 1322 1323 1324 1325 1326 1327 1328 1329 1330 1331 1332 1333 1334 1335 1336 1337 1338 1339 1340 1341 1342 1343 1344 1345 1346 1347 1348 1349 1350 1351 1352 1353 1354 1355 1356 1357 1358 1359 1360 1361 1362 1363 1364 1365 1366 1367 1368 1369 1370 1371 1372 1373 1374 1375 1376 1377 1378 1379 1380 1381 1382 1383 1384 1385 1386 1387 1388 1389 1390 1391 1392 1393 1394 1395 1396 1397 1398 1399 1400 1401 1402 1403 1404 1405 1406 1407 1408 1409 1410 1411 1412 1413 1414 1415 1416 1417 1418 1419 1420 1421 1422 1423 1424 1425 1426 1427 1428 1429 1430 1431 1432 1433 1434 1435 1436 1437 1438 1439 1440 1441 1442 1443 1444 1445 1446 1447 1448 1449 1450 1451 1452 1453 1454 1455 1456 1457 1458 1459 1460 1461 1462 1463 1464 1465 1466 1467 1468 1469 1470 1471 1472 1473 1474 1475 1476 1477 1478 1479 1480 1481 1482 1483 1484 1485 1486 1487 1488 1489 1490 1491 1492 1493 1494 1495 1496 1497 1498 1499 1500 1501 1502 1503 1504 1505 1506 1507 1508 1509 1510 1511 1512 1513 1514 1515 1516 1517 1518 1519 1520 1521 1522 1523 1524 1525 1526 1527 1528 1529 1530 1531 1532 1533 1534 1535 1536 1537 1538 1539 1540 1541 1542 1543 1544 1545 1546 1547 1548 1549 1550 1551 1552 1553 1554 1555 1556 1557 1558 1559 1560 1561 1562 1563 1564 1565 1566 1567 1568 1569 1570 1571 1572 1573 1574 1575 1576 1577 1578 1579 1580 1581 1582 1583 1584 1585 1586 1587 1588 1589 1590 1591 1592 1593 1594 1595 1596 1597 1598 1599 1600 1601 1602 1603 1604 1605 1606 1607 1608 1609 1610 1611 1612 1613 1614 1615 1616 1617 1618 1619 1620 1621 1622 1623 1624 1625 1626 1627 1628 1629 1630 1631 1632 1633 1634 1635 1636 1637 1638 1639 1640 1641 1642 1643 1644 1645 1646 1647 1648 1649 1650 1651 1652 1653 1654 1655 1656 1657 1658 1659 1660 1661 1662 1663 1664 1665 1666 1667 1668 1669 1670 1671 1672 1673 1674 1675 1676 1677 1678 1679 1680 1681 1682 1683 1684 1685 1686 1687 1688 1689 1690 1691 1692 1693 1694 1695 1696 1697 1698 1699 1700 1701 1702 1703 1704 1705 1706 1707 1708 1709 1710 1711 1712 1713 1714 1715 1716 1717 1718 1719 1720 1721 1722 1723 1724 1725 1726 1727 1728 1729 1730 1731 1732 1733 1734 1735 1736 1737 1738 1739 1740 1741 1742 1743 1744 1745 1746 1747 1748 1749 1750 1751 1752 1753 1754 1755 1756 1757 1758 1759 1760 1761 1762 1763 1764 1765 1766 1767 1768 1769 1770 1771 1772 1773 1774 1775 1776 1777 1778 1779 1780 1781 1782 1783 1784 1785 1786 1787 1788 1789 1790 1791 1792 1793 1794 1795 1796 1797 1798 1799 1800 1801 1802 1803 1804 1805 1806 1807 1808 1809 1810 1811 1812 1813 1814 1815 1816 1817 1818

0941-18-6(10) 17M

$$d^2 \mathcal{L} / d\alpha^2 = 2\alpha \mathcal{L} = 2 \times 10^{-10} \text{ eV}^2$$
 $\lim_{t \rightarrow \infty} \|x(t) - x^*\| = 0$, where x^* is the optimal solution.

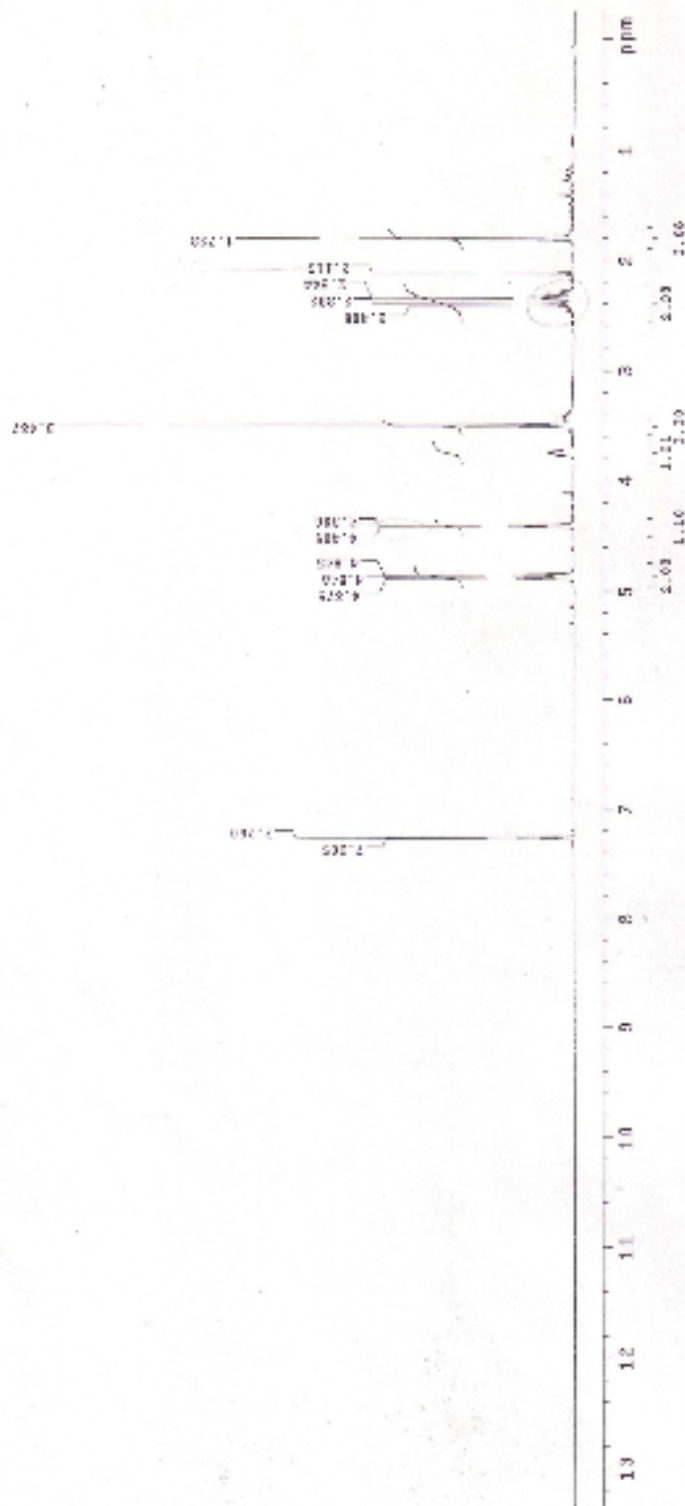
Suppl. 1000-7892 C06
Cat# A303-1 H2

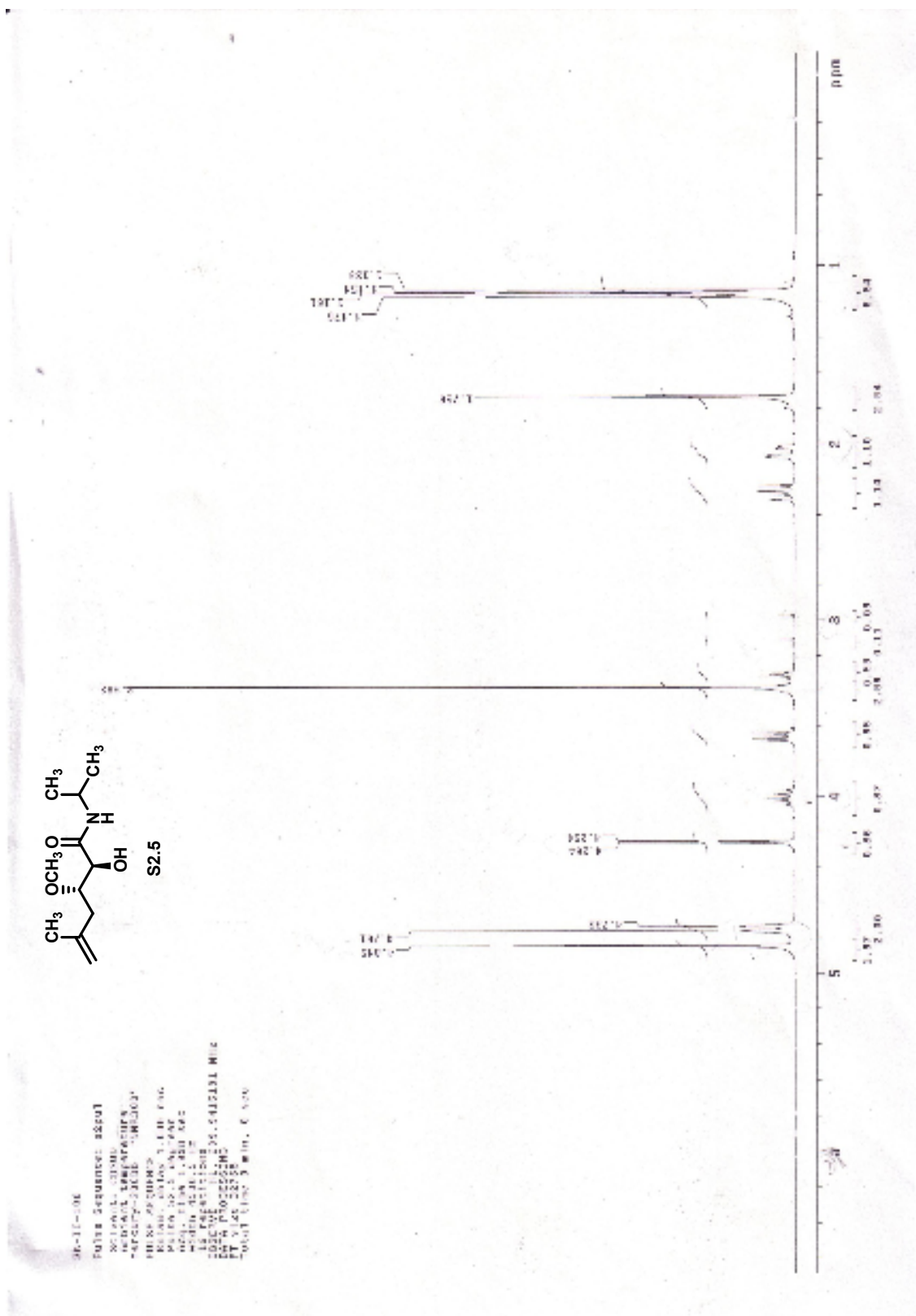
4401711 1969-52

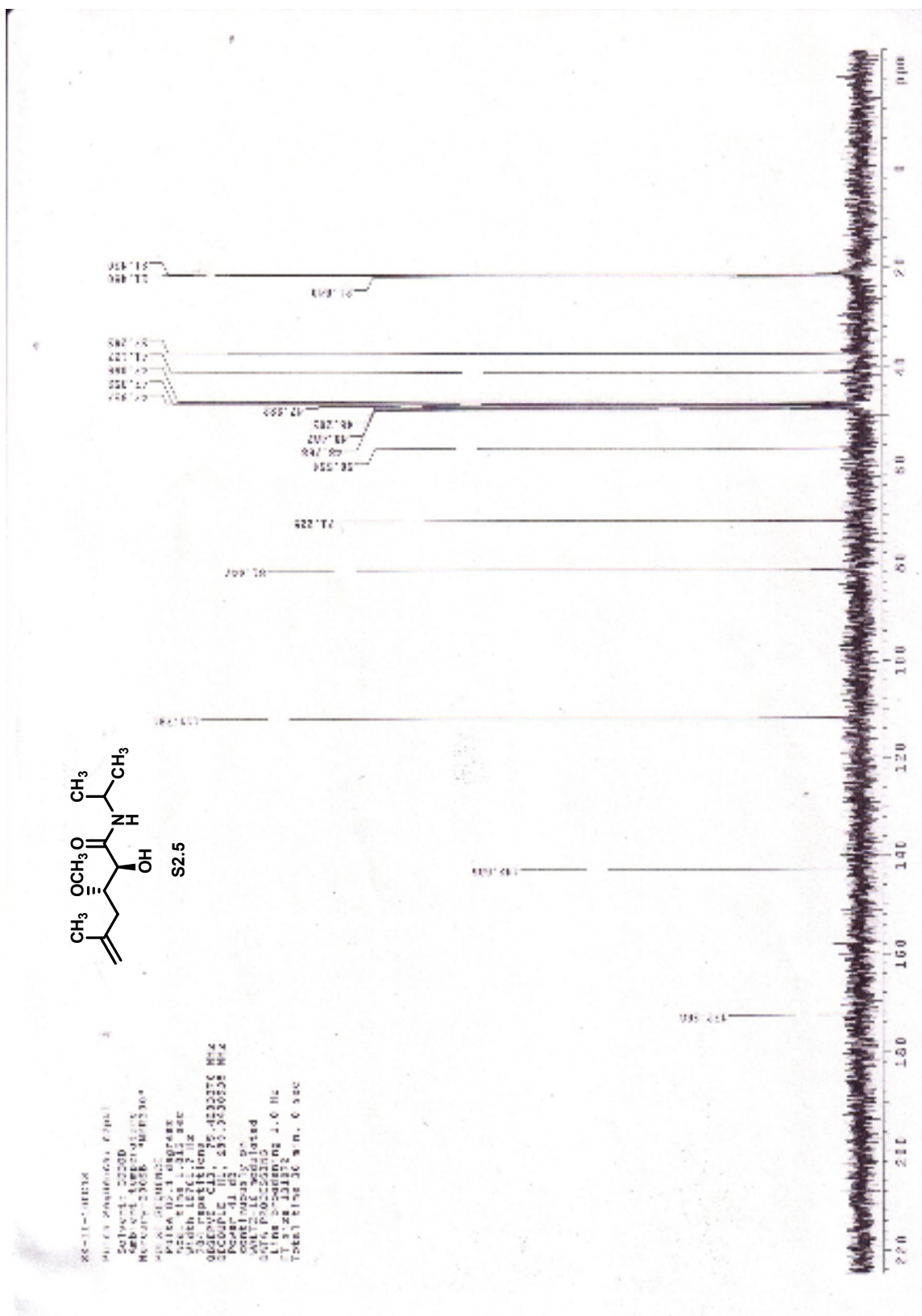
0528-2-2011 2011.04.20
0528-2-2011 2011.04.20

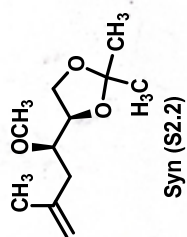
TEL: 0124 35760

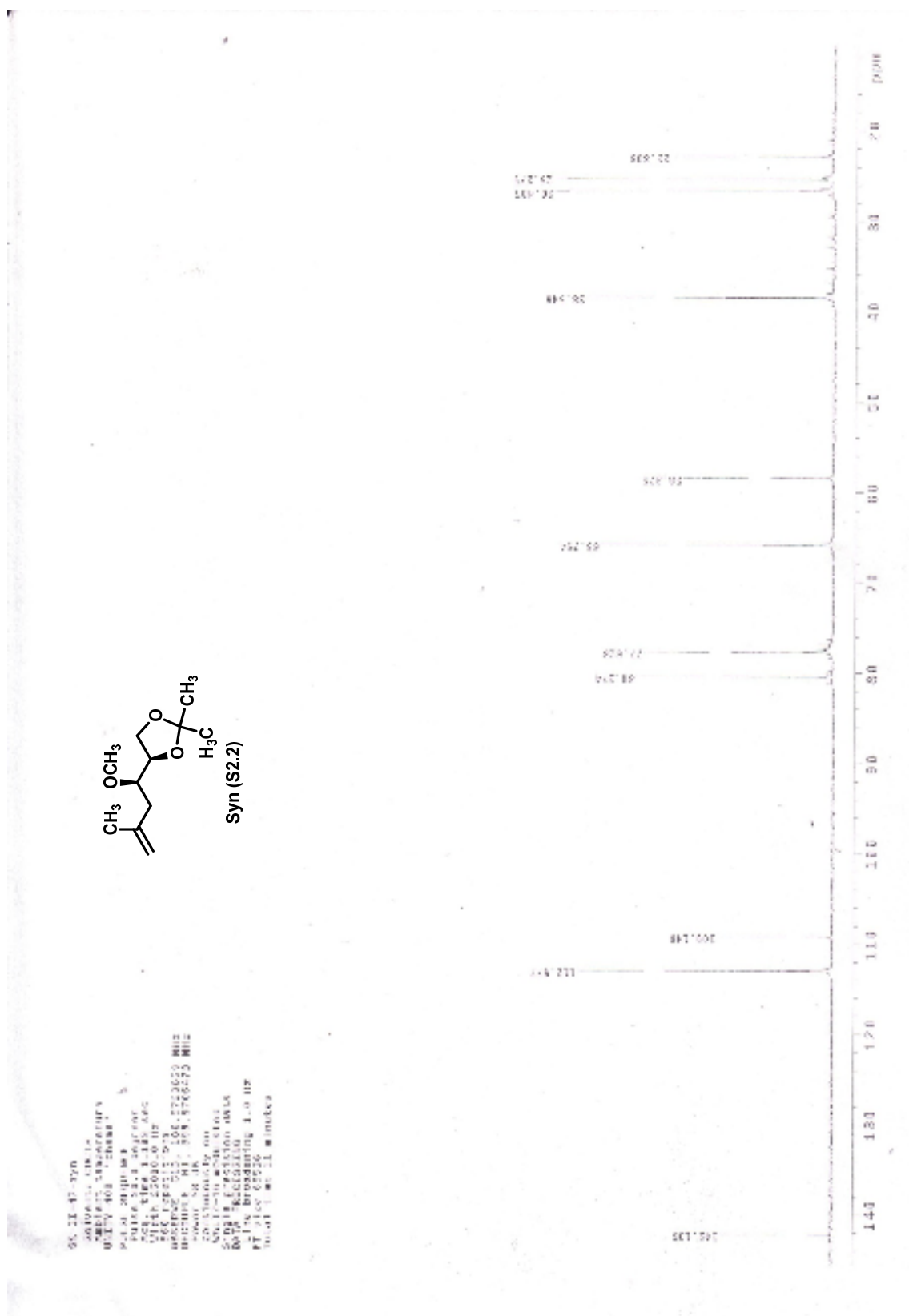
total time of 10 h, 45 min

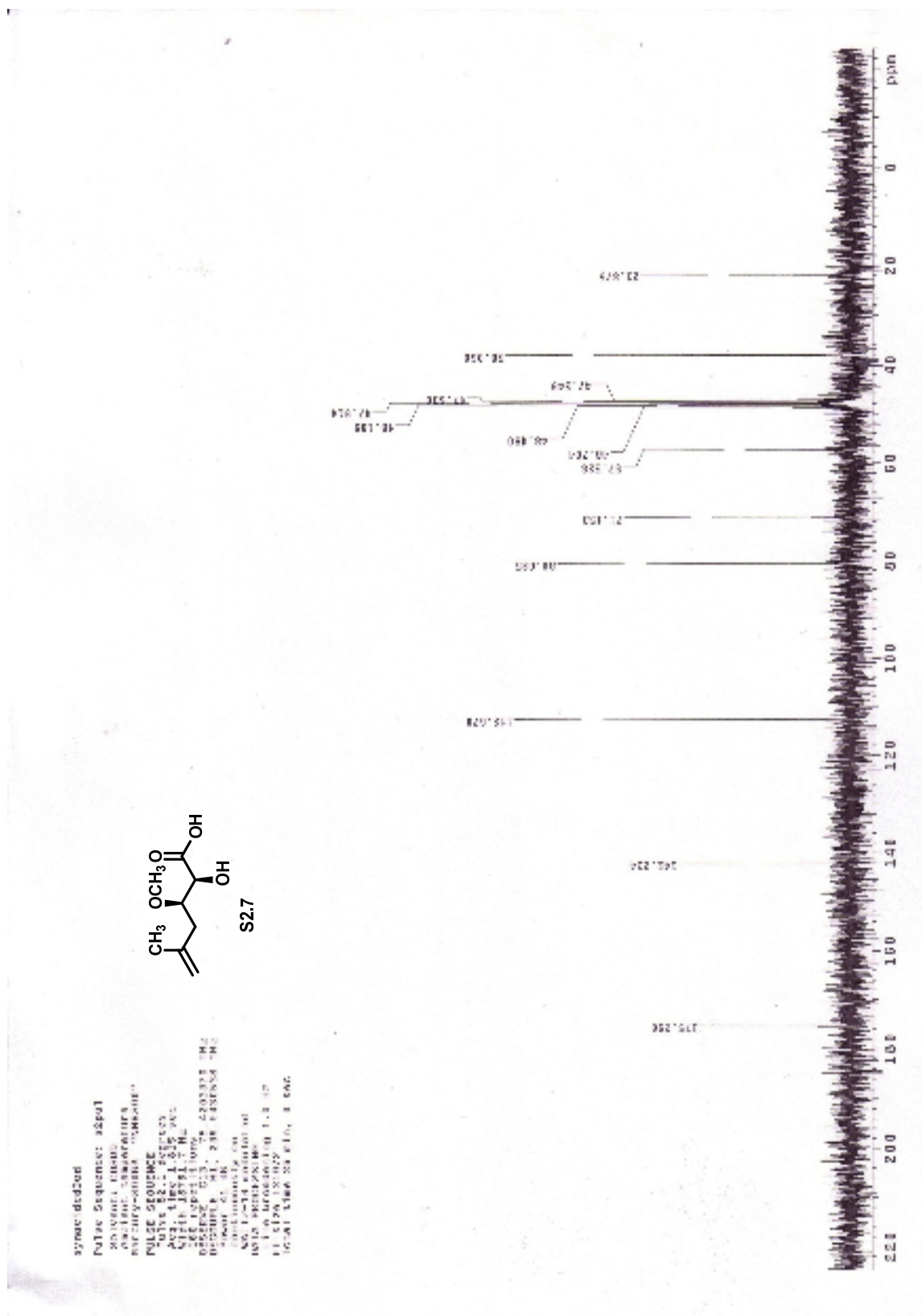


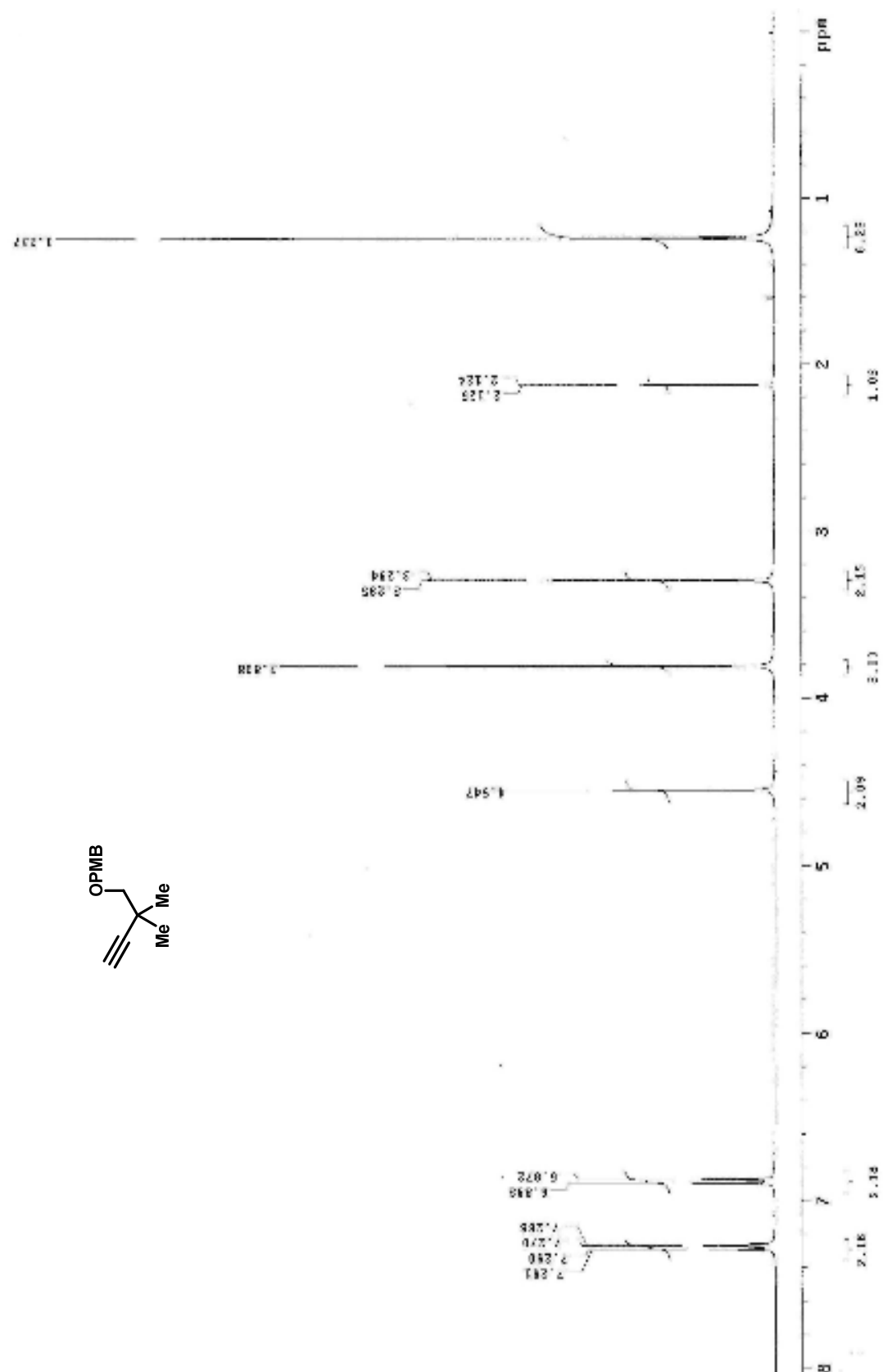


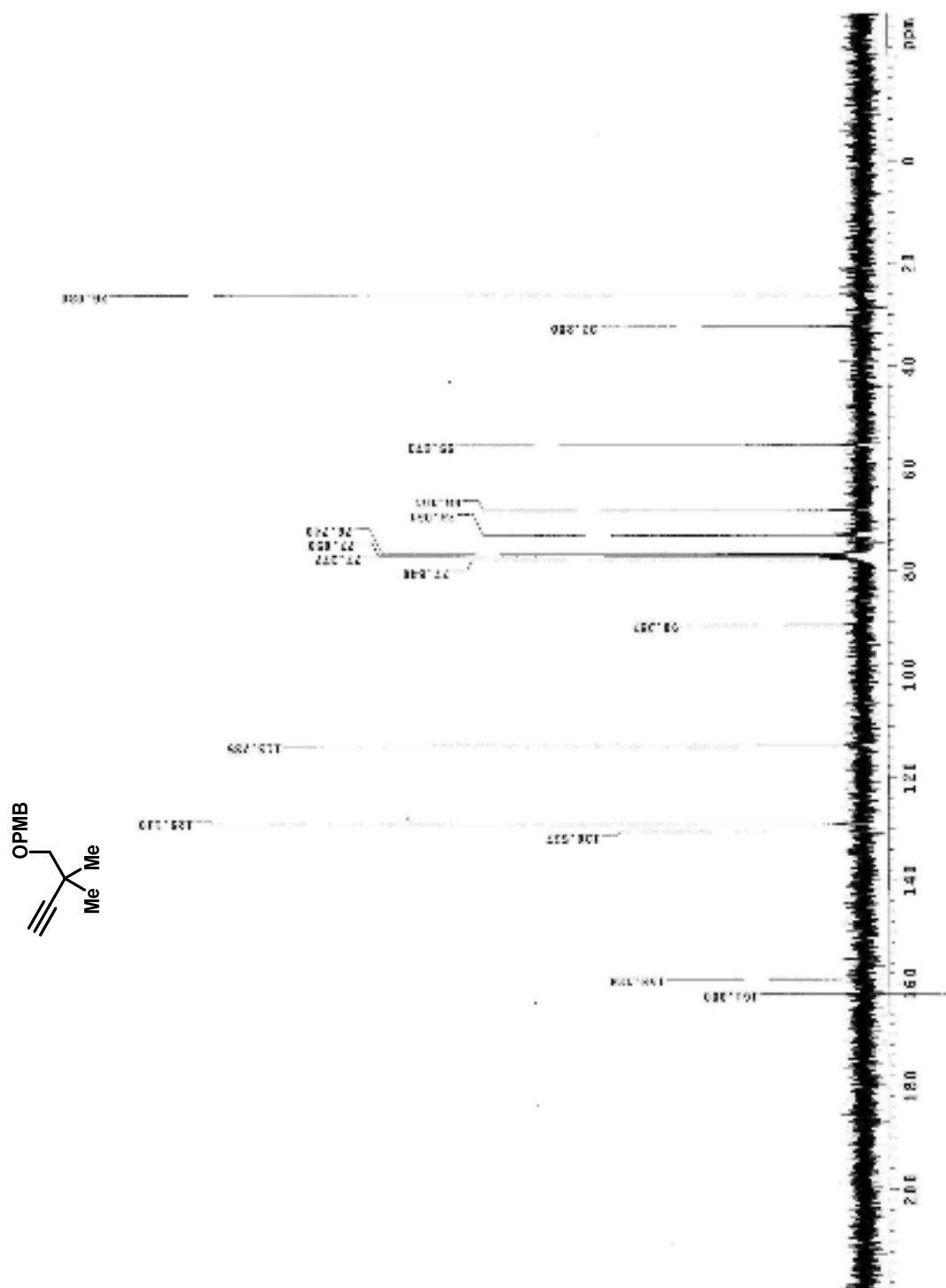


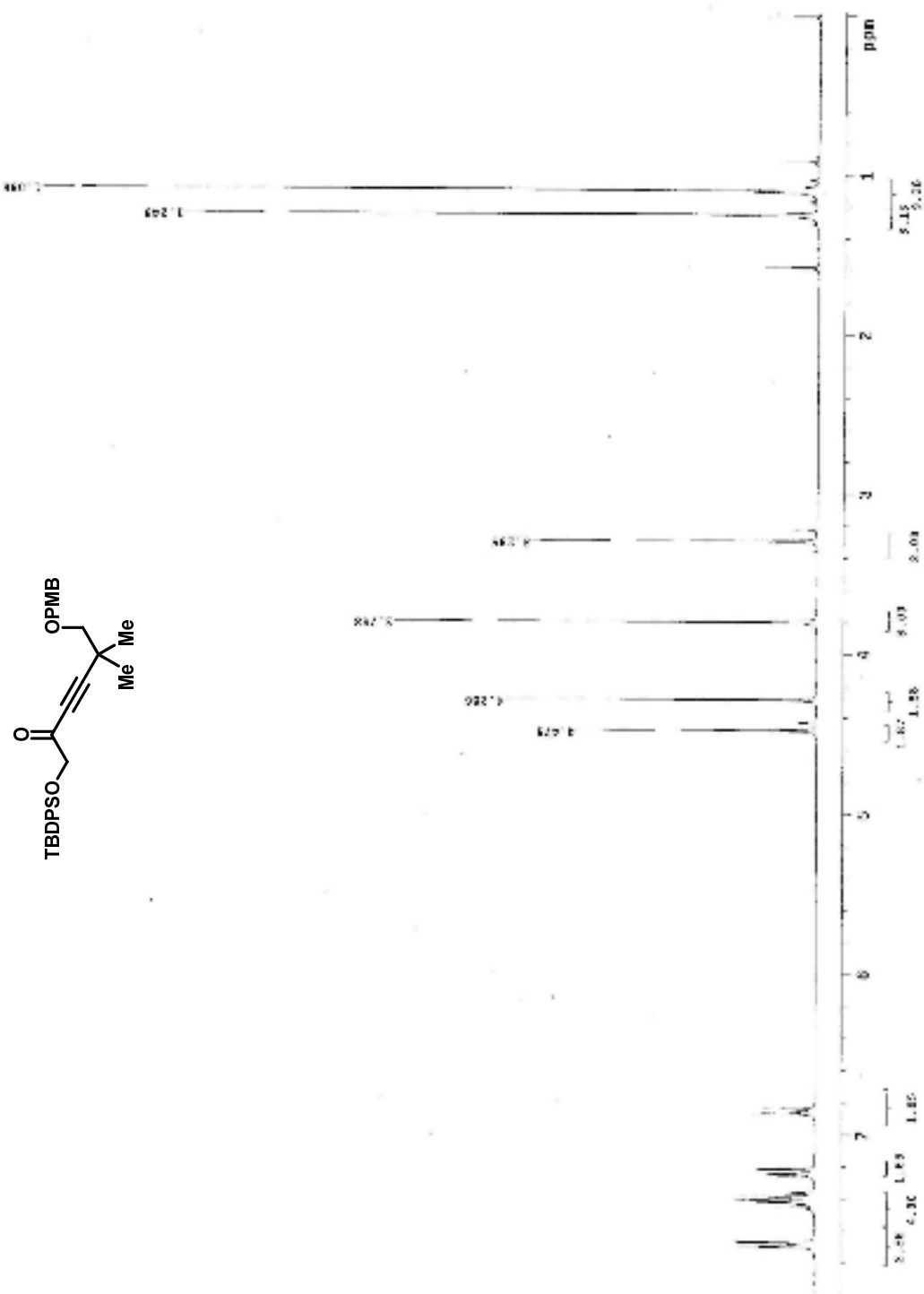
[illegible]

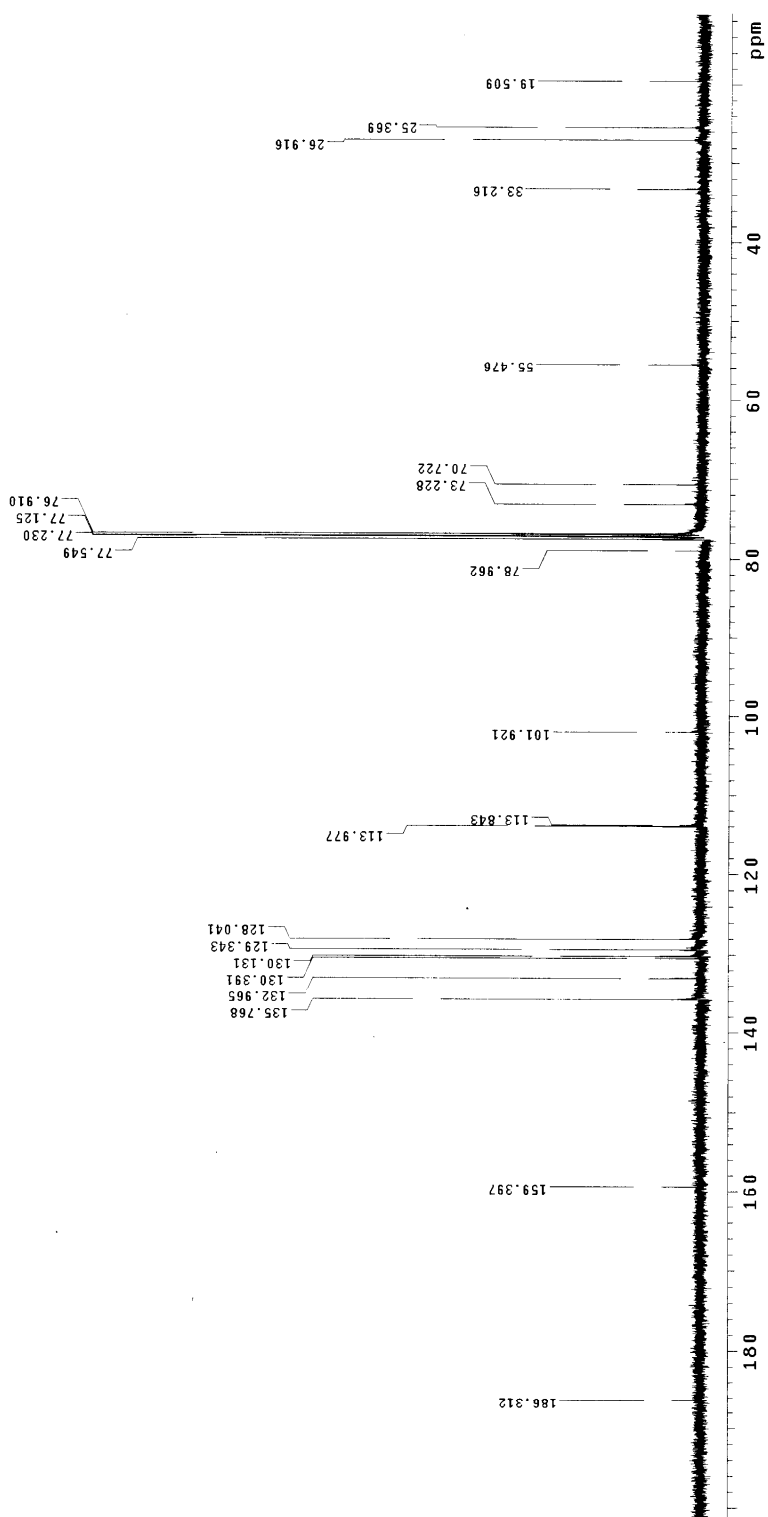
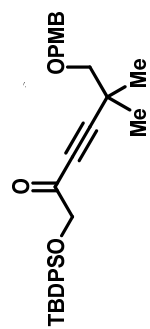


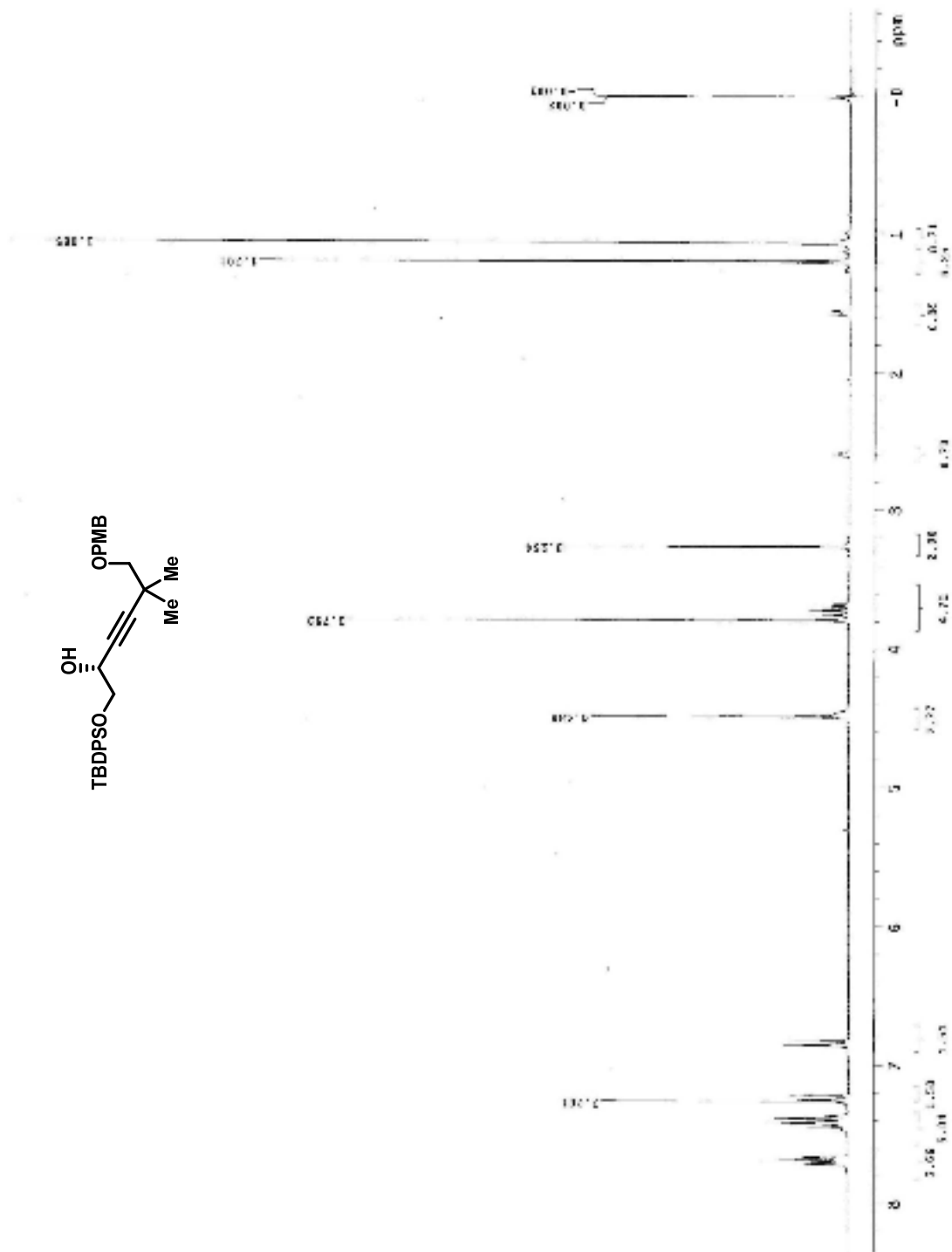
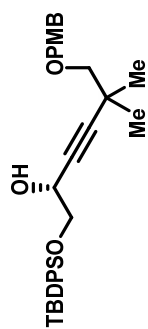


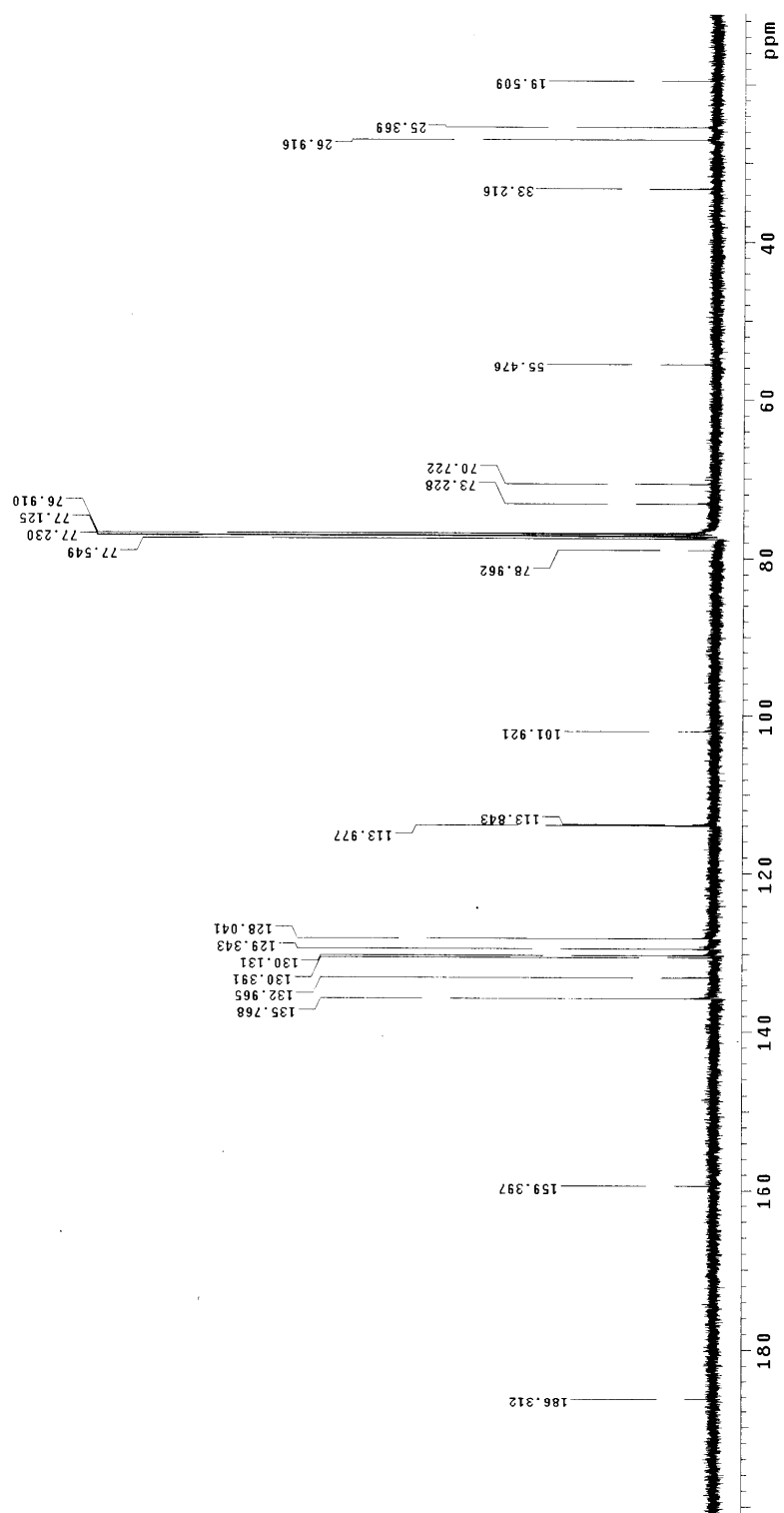
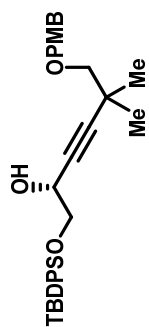












Std proton

File: Proton

Pulse Sequence: s2pul

Solvent: cdcl3

Temp: 25.0 C / 298.1 K

Operator: sezgink

VNMR-400 "nmr400.futgers.edu"

Relax. delay 1.000 sec

Pulse 45.0 degrees

Acq. time 2.049 sec

Width 6410.3 Hz

8

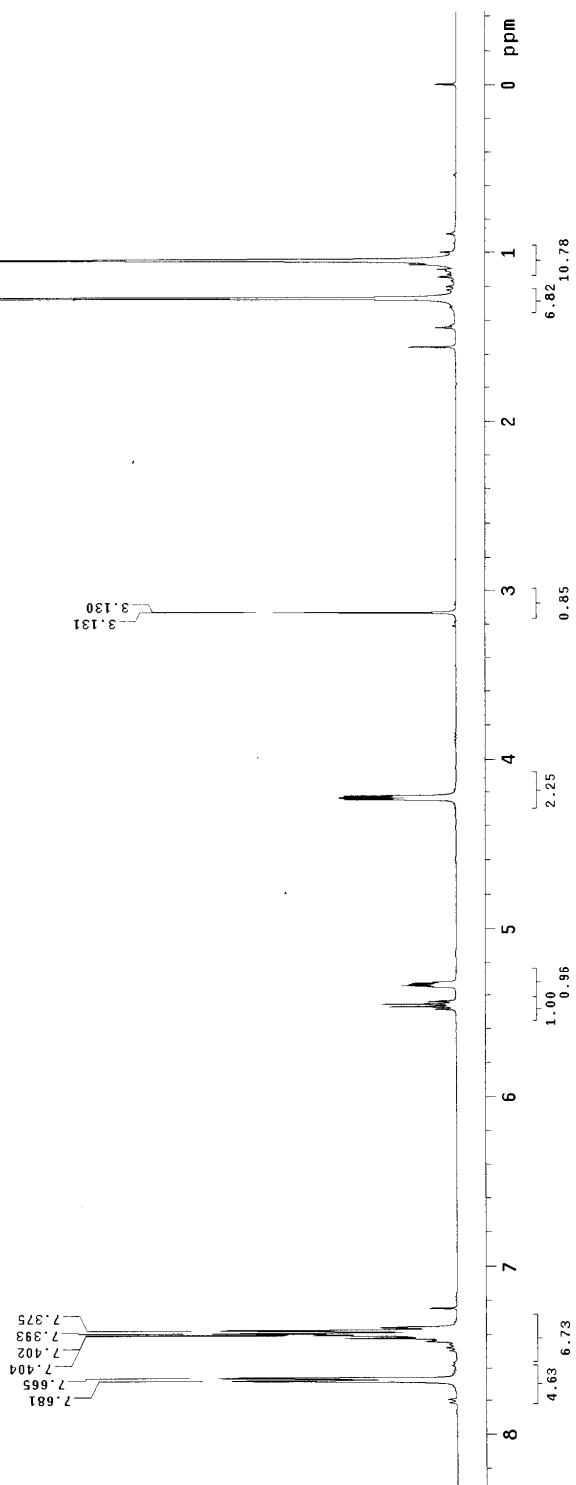
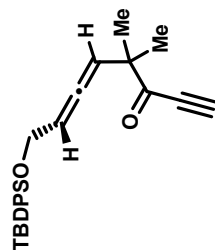
OBSERVE F1

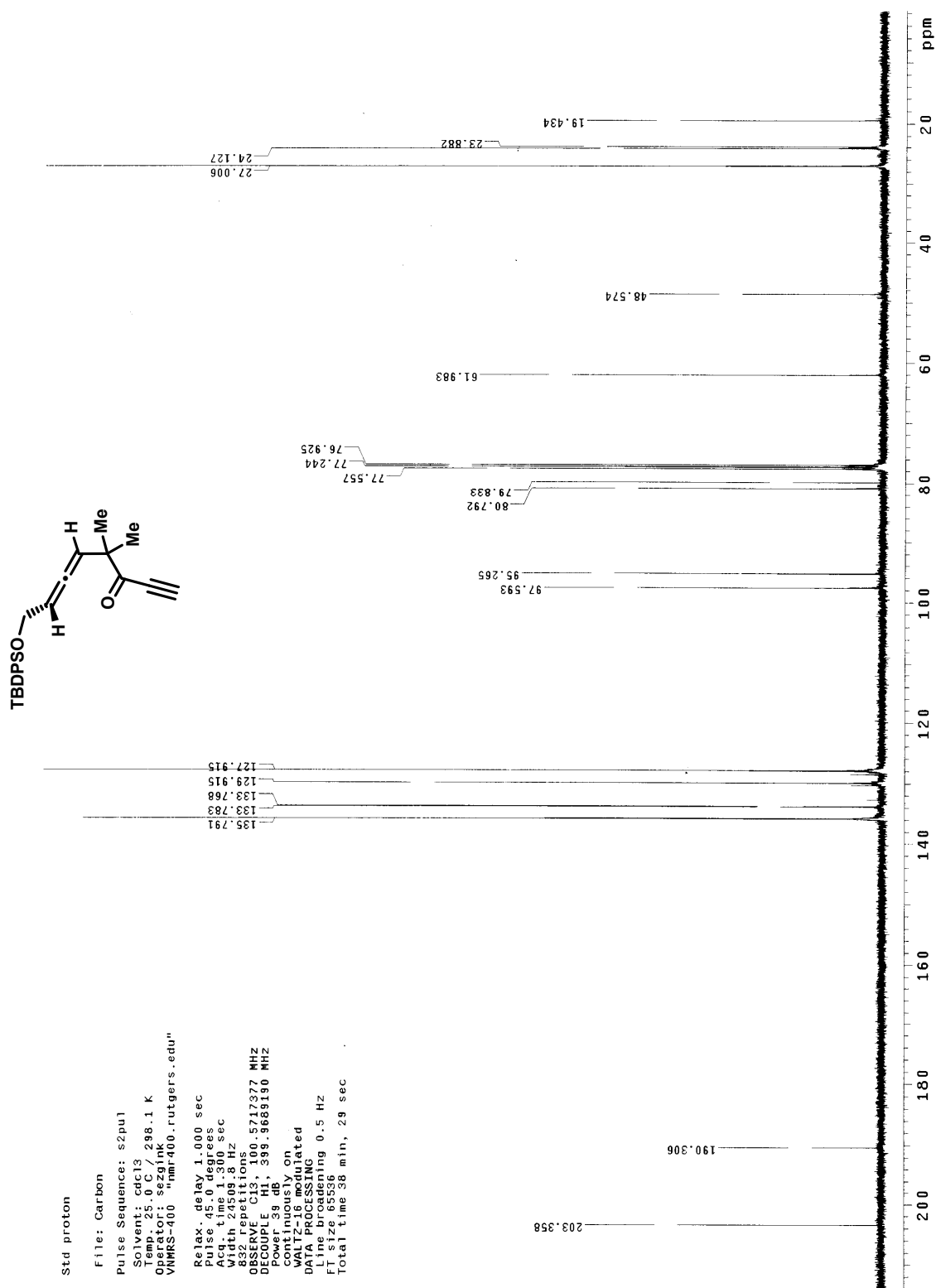
DATA PROCESSING

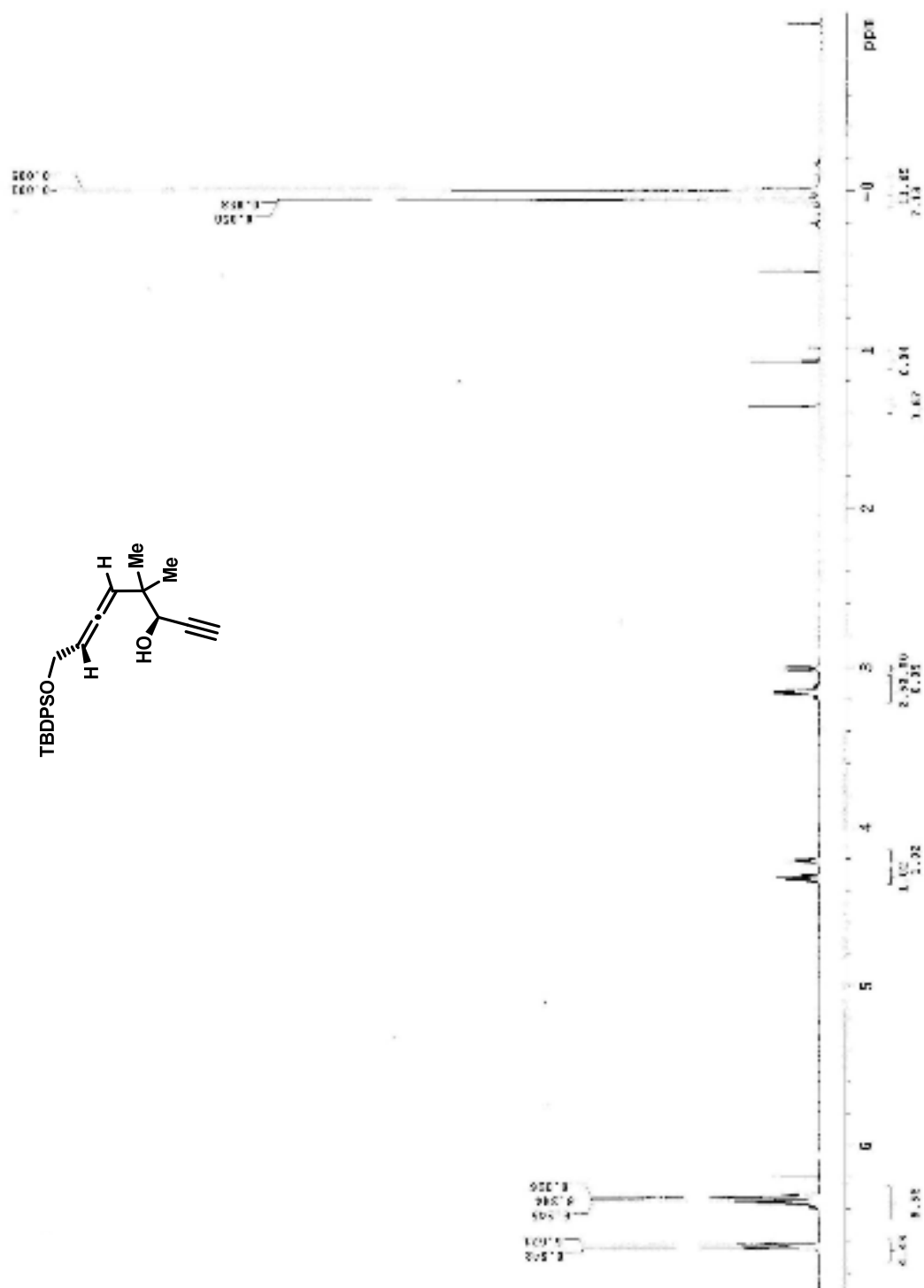
Line broadening 0.2 Hz

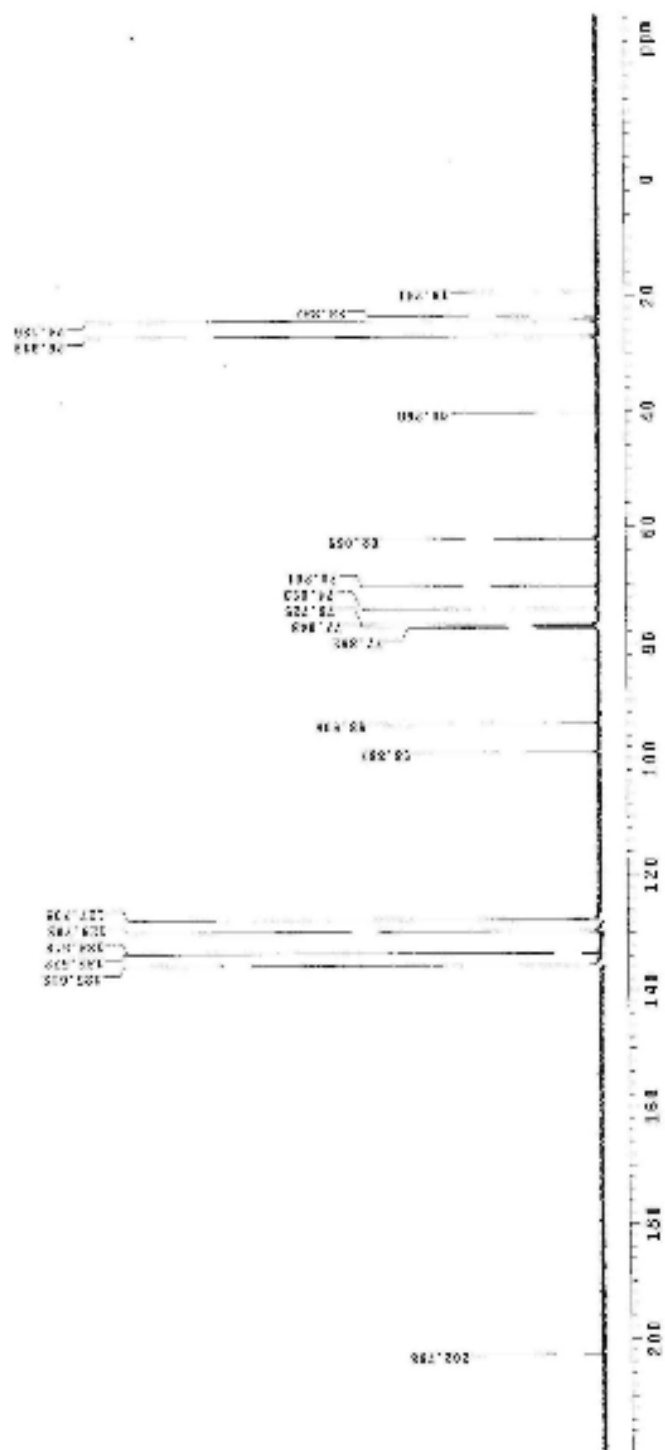
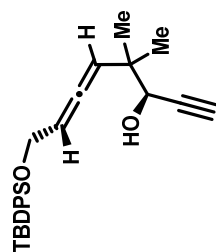
FT size 65536

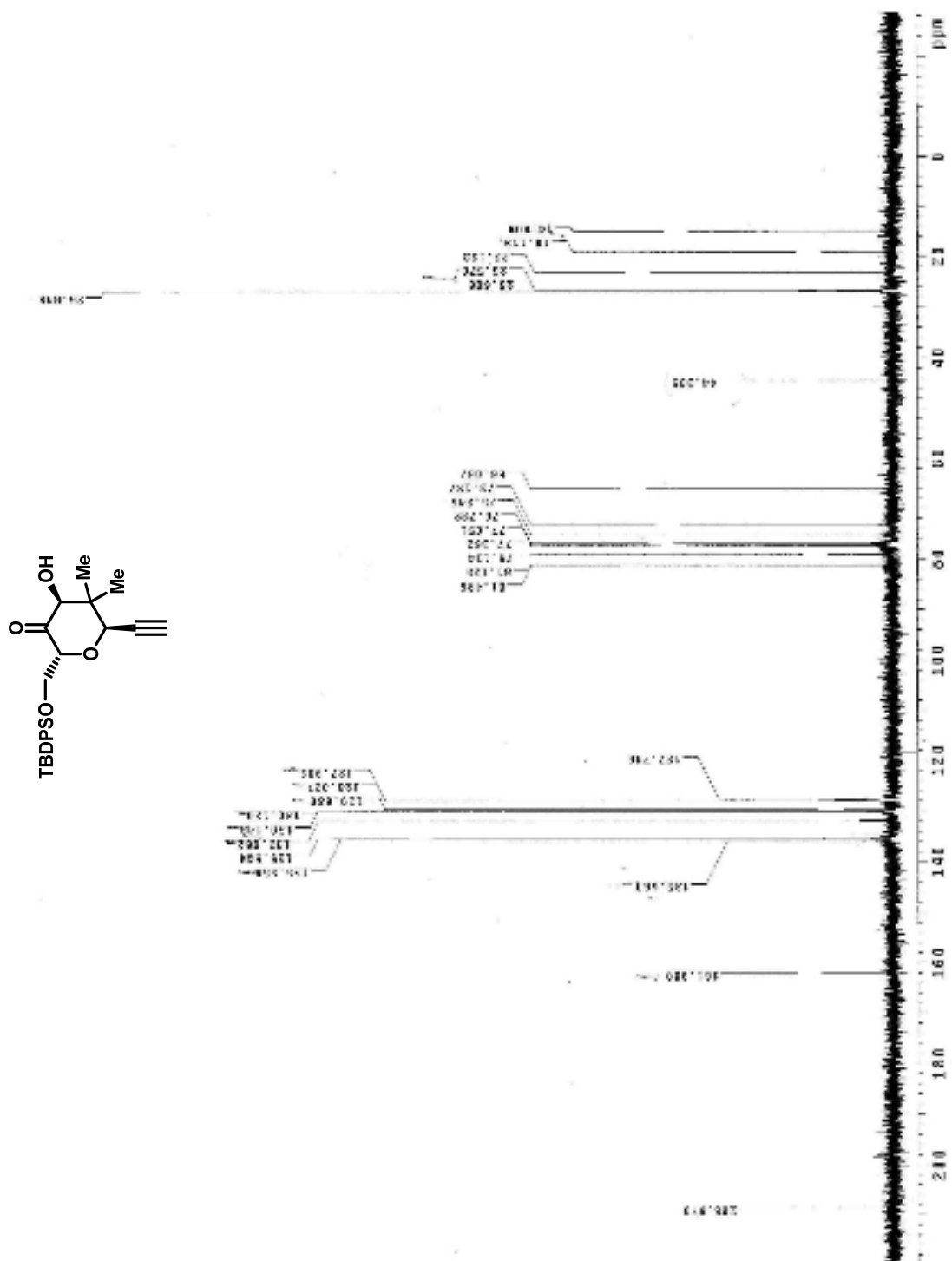
Total time 0 min, 30 sec

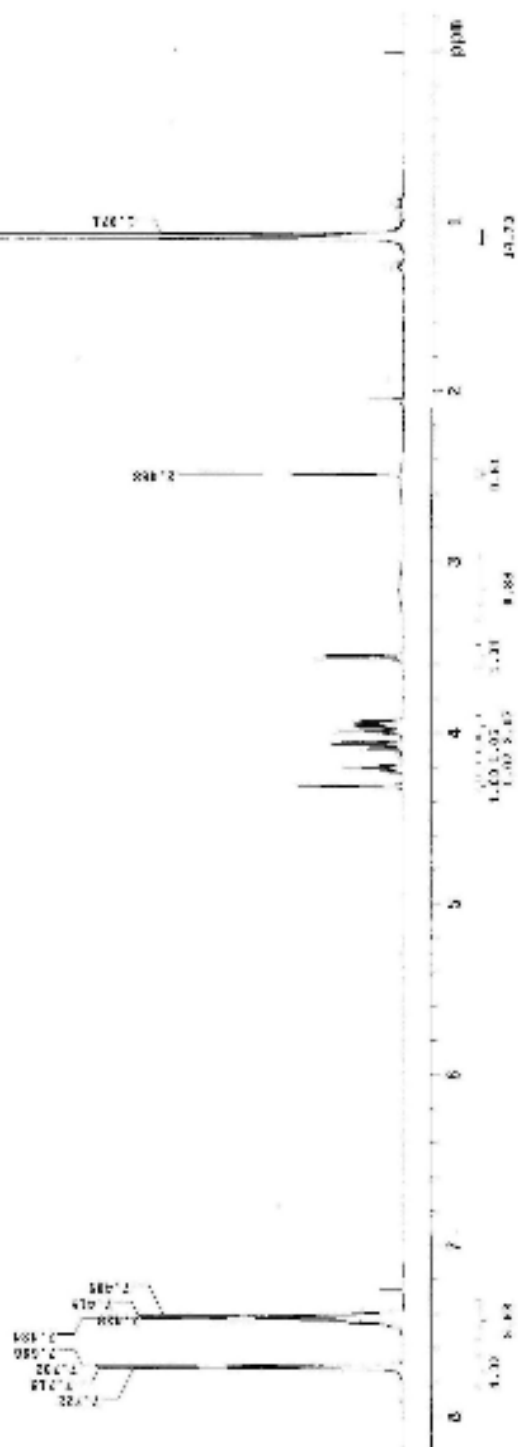
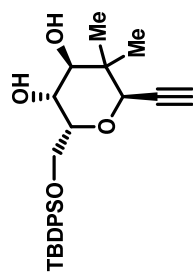


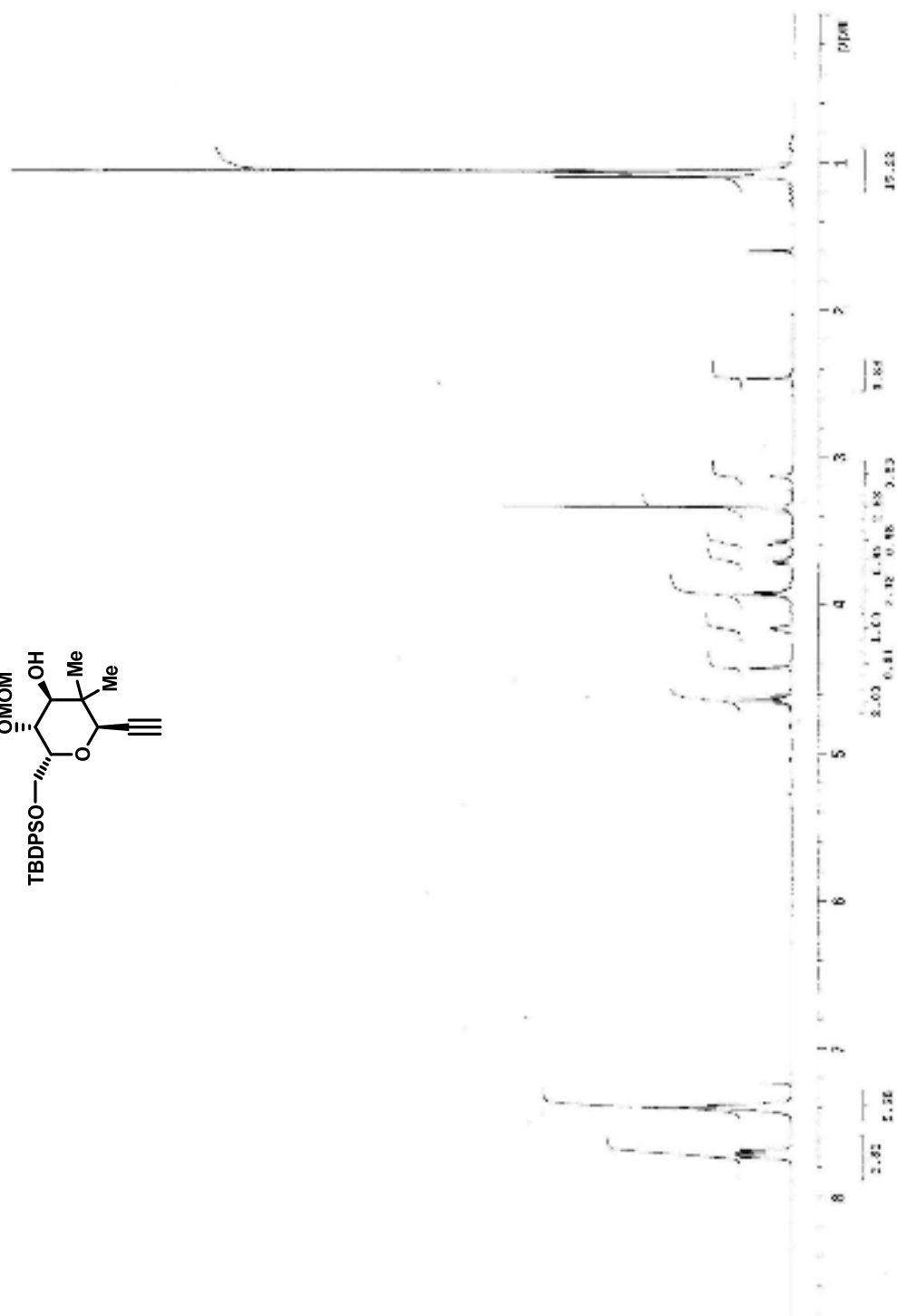
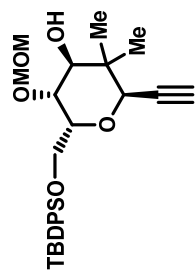




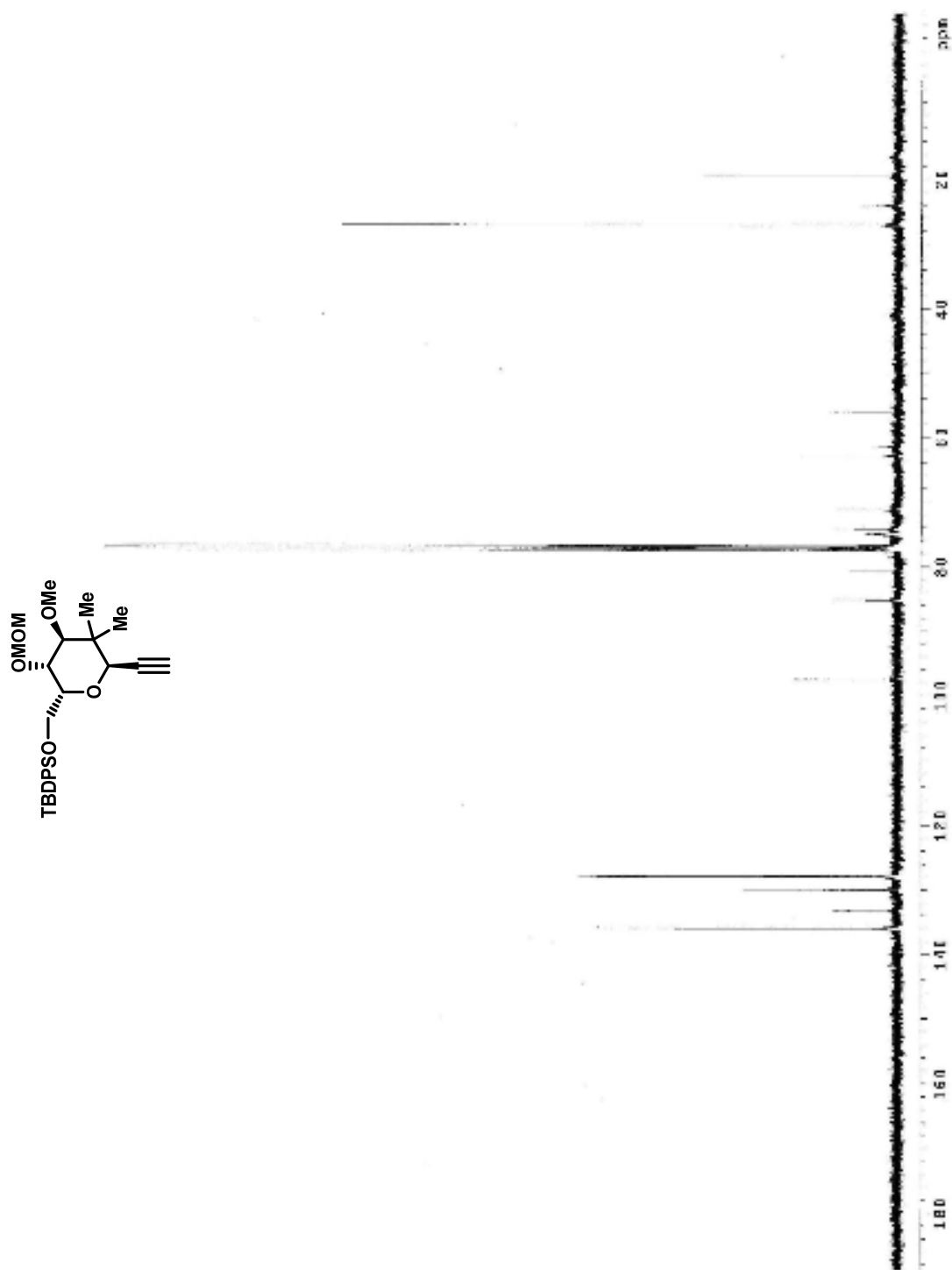


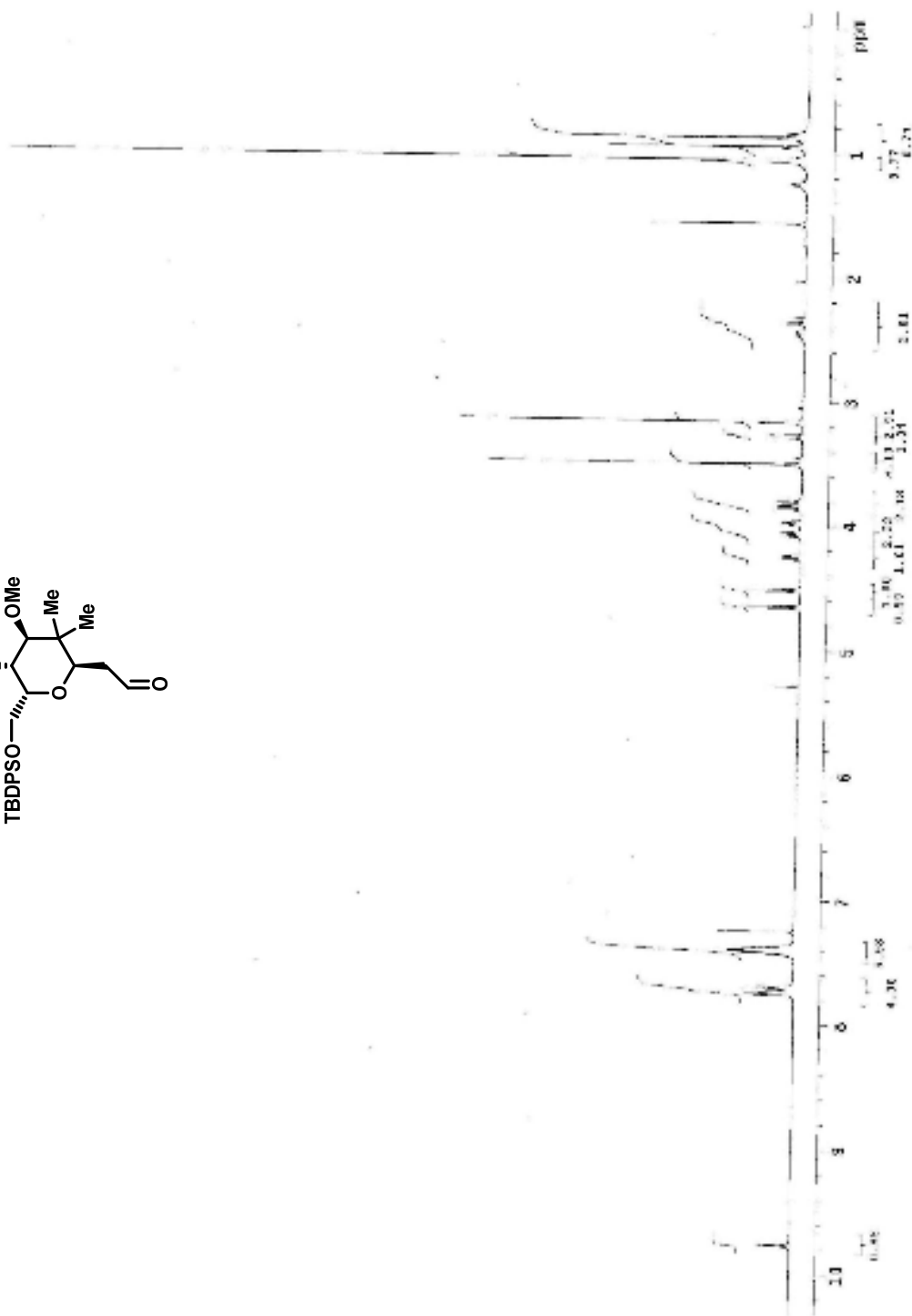
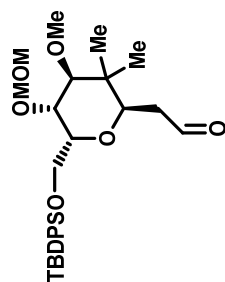


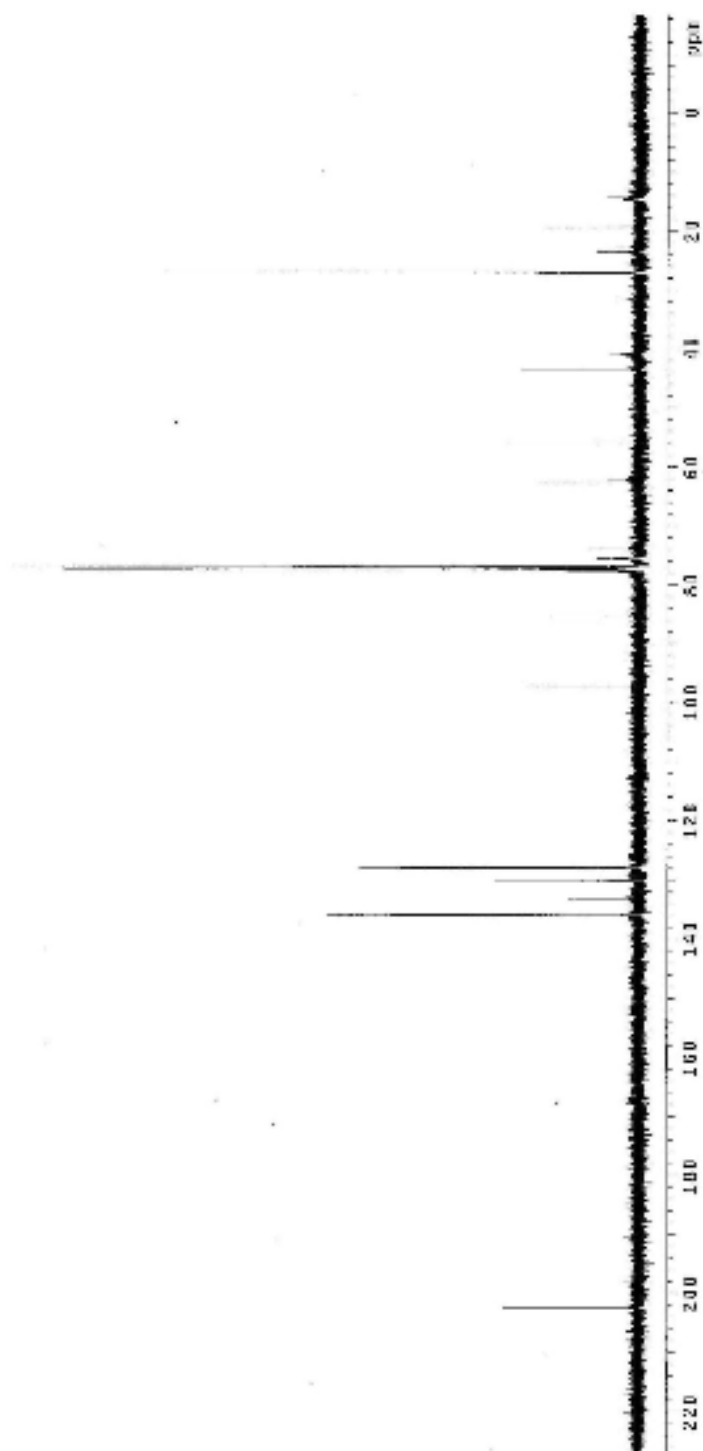
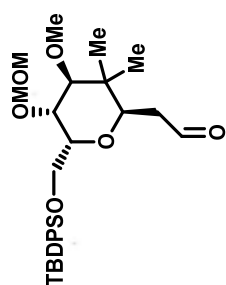


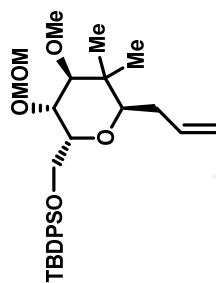


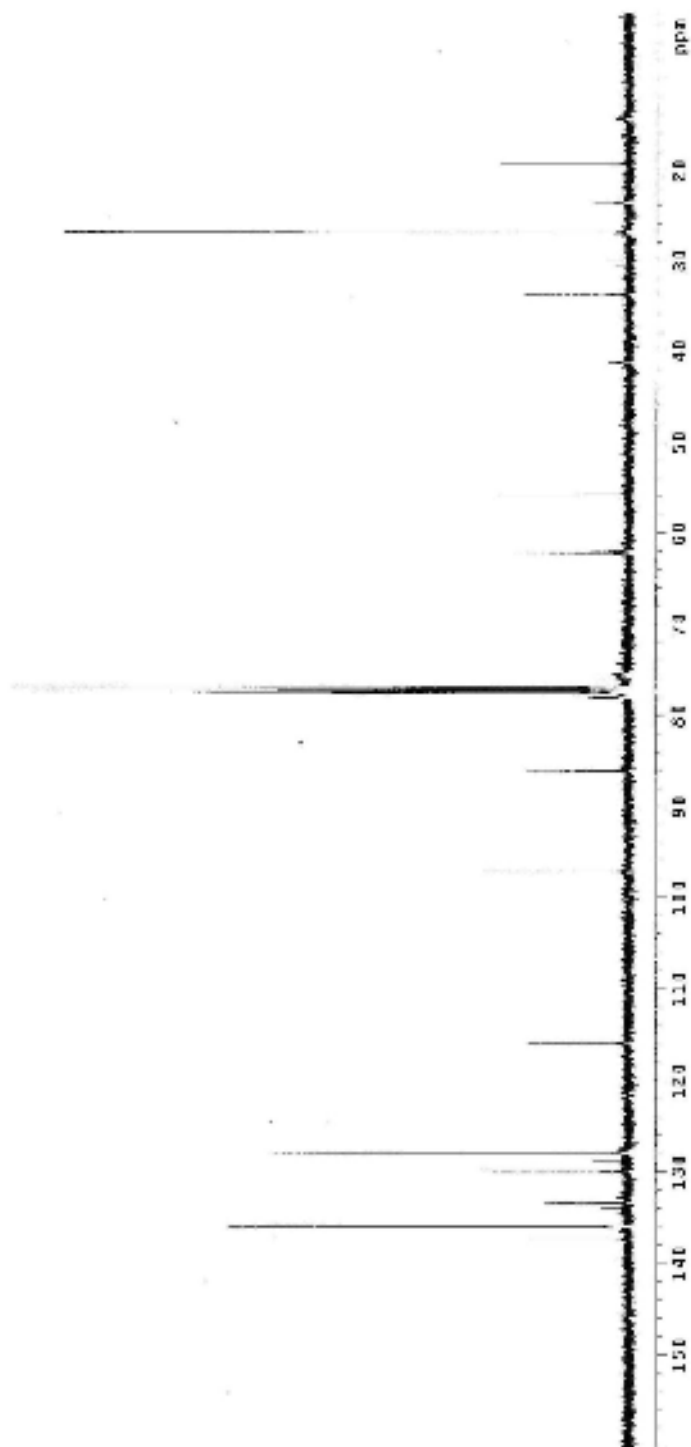
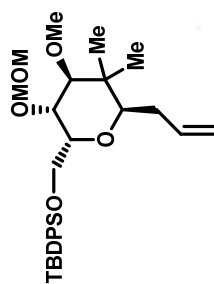


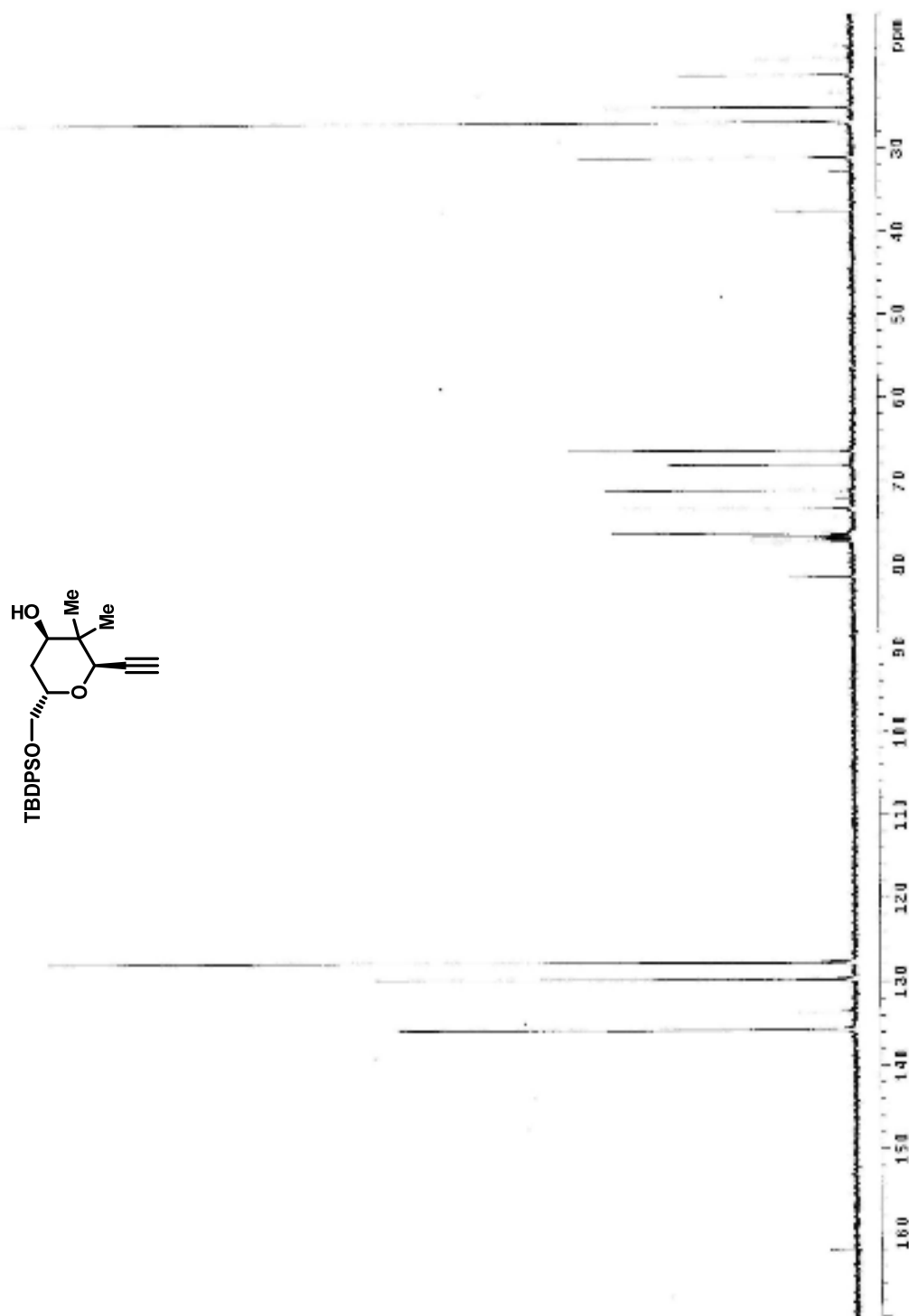


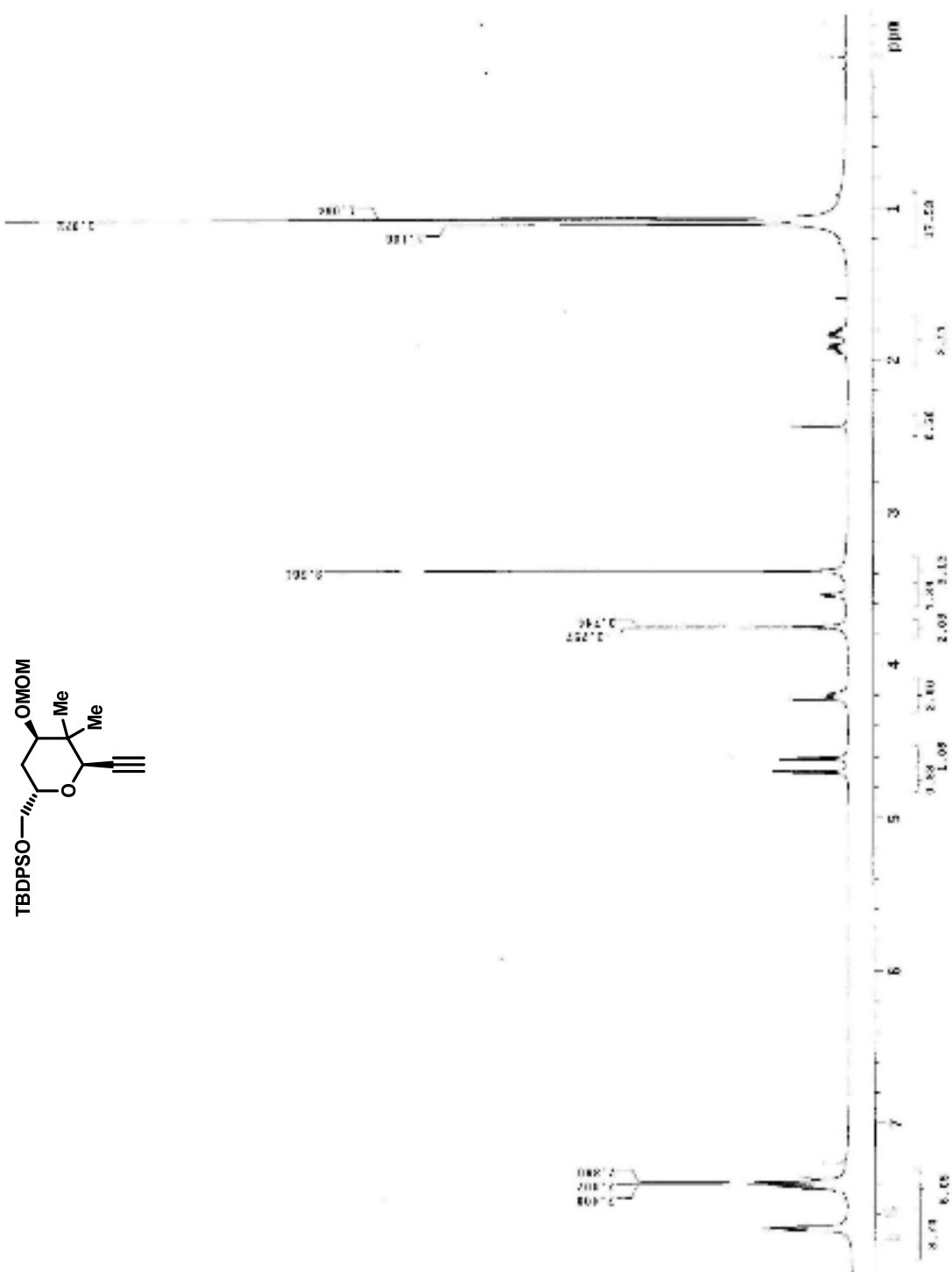


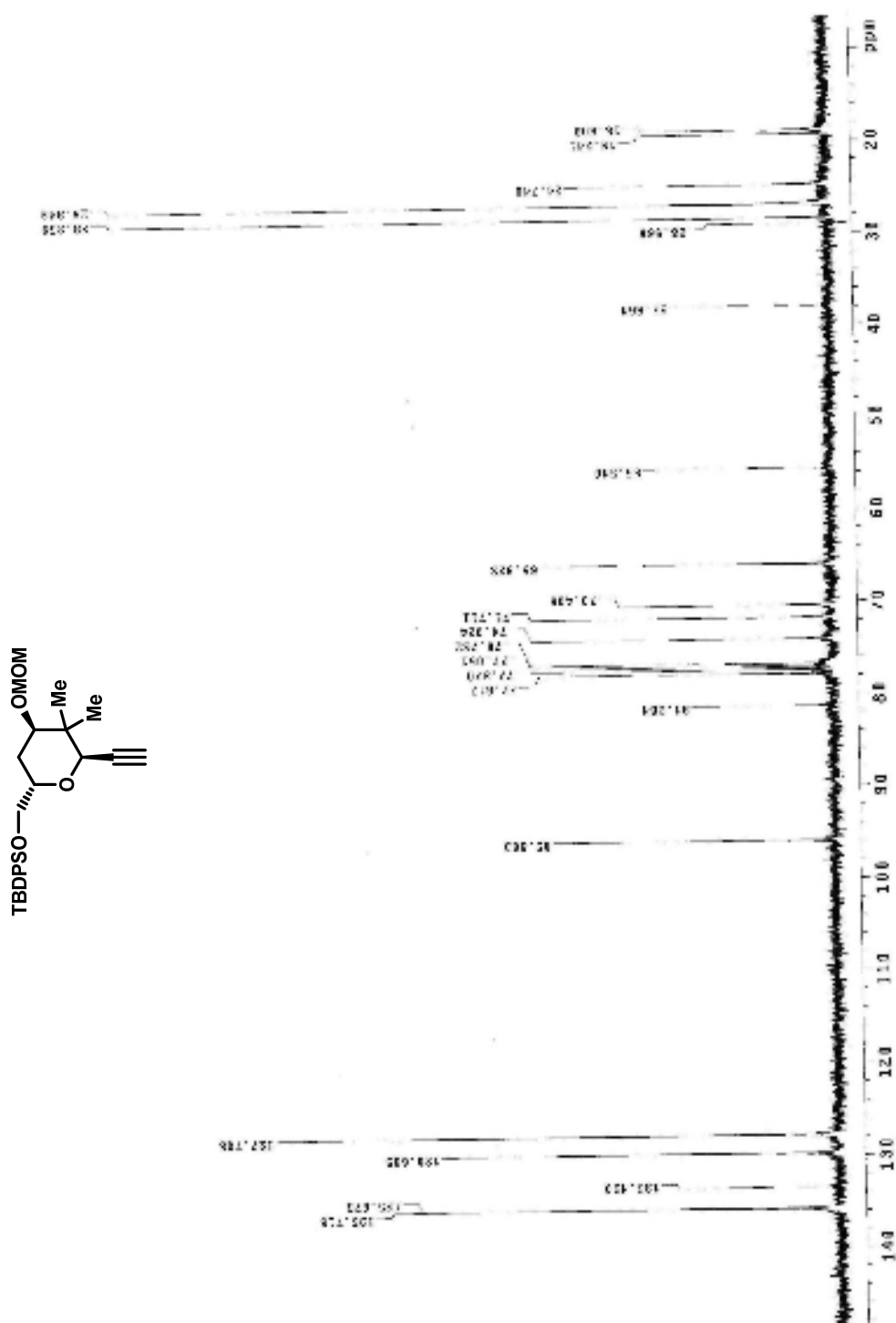




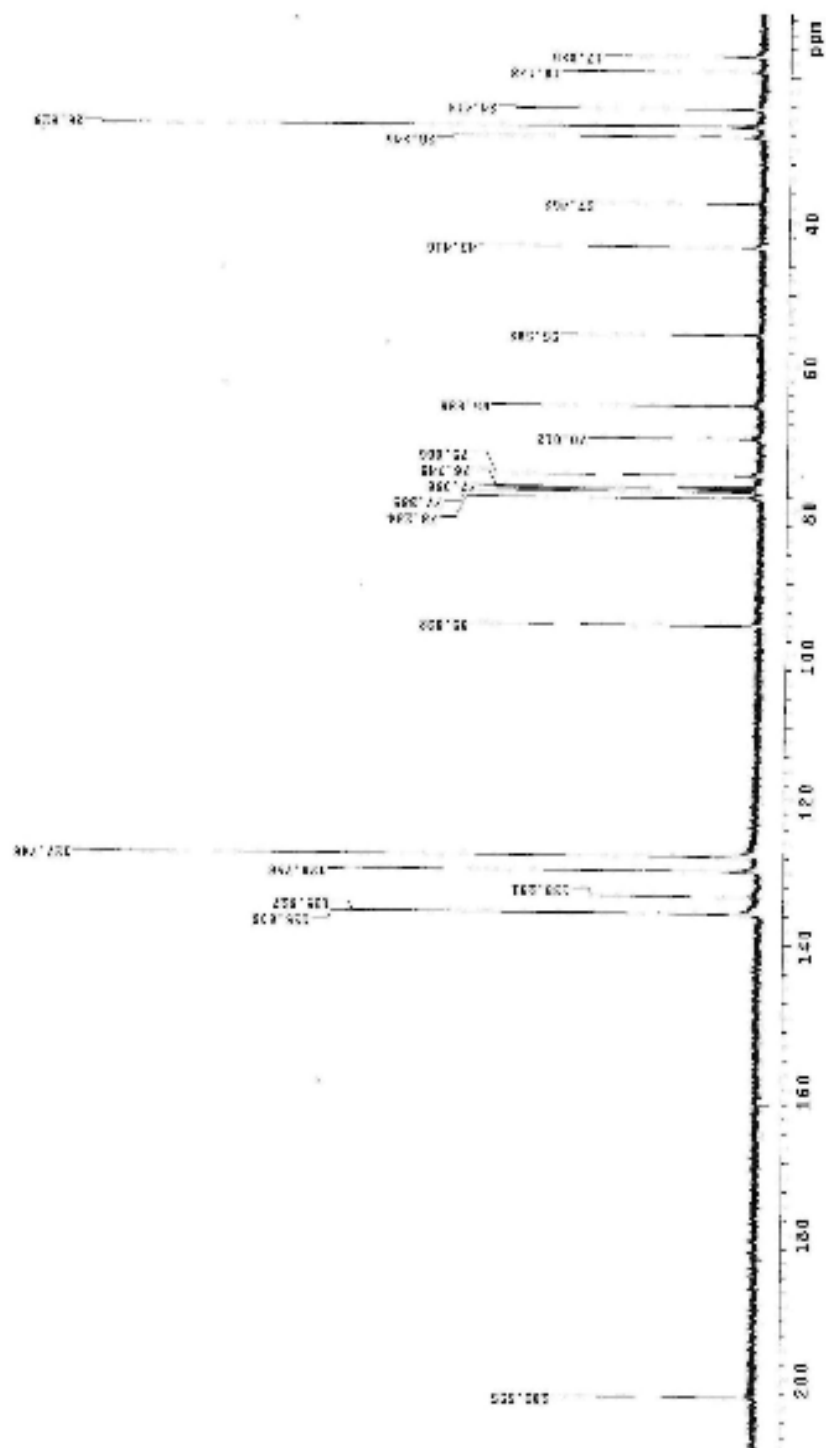
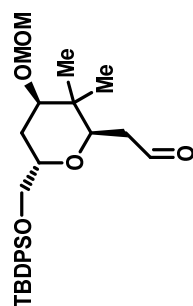












Std proton

File: Proton

Pulse Sequence: s2pu1

Solvent: cdcl3

Temp: 25.0 C / 298.1 K

Operator: sezgink

VNMRS-400 "nmr400.rutgers.edu"

Relax. delay 1.000 sec

Pulse 45.0 degrees

Acq. time 2.049 sec

Width 0.3 MHz

8 repetitions

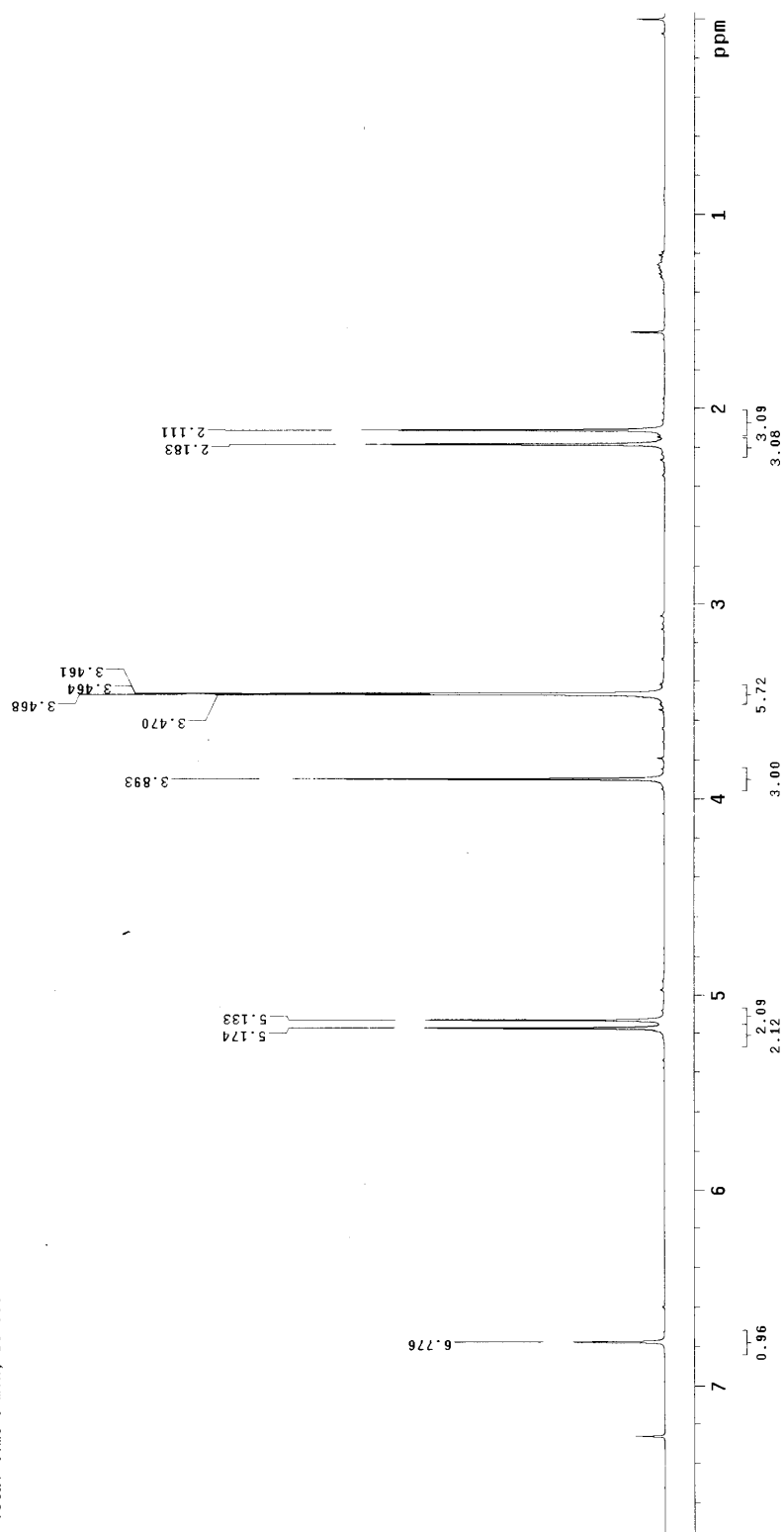
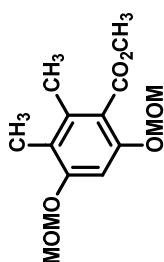
OBSERVE H1, 399.9669114 MHz

DATA PROCESSING

Line broadening 0.2 Hz

FT size 65536

Total time 0 min, 30 sec



C13

File: Carbon

Pulse Sequence: s2pu1

Solvent: cdcl3

Temp. 25.0 C / 298.1 K

Operator: sezgink

VNMR-400 "nmr400.rutgers.edu"

Relax. delay 1.000 sec

Pulse 45.0 degrees

Acq. time 1.300 sec

Width 24509.8 Hz

Spectrum 1000

OBSERVE C13, 100.571377 MHz

DECOUPLE H1, 399.9689190 MHz

Power 39 dB,

continuously on

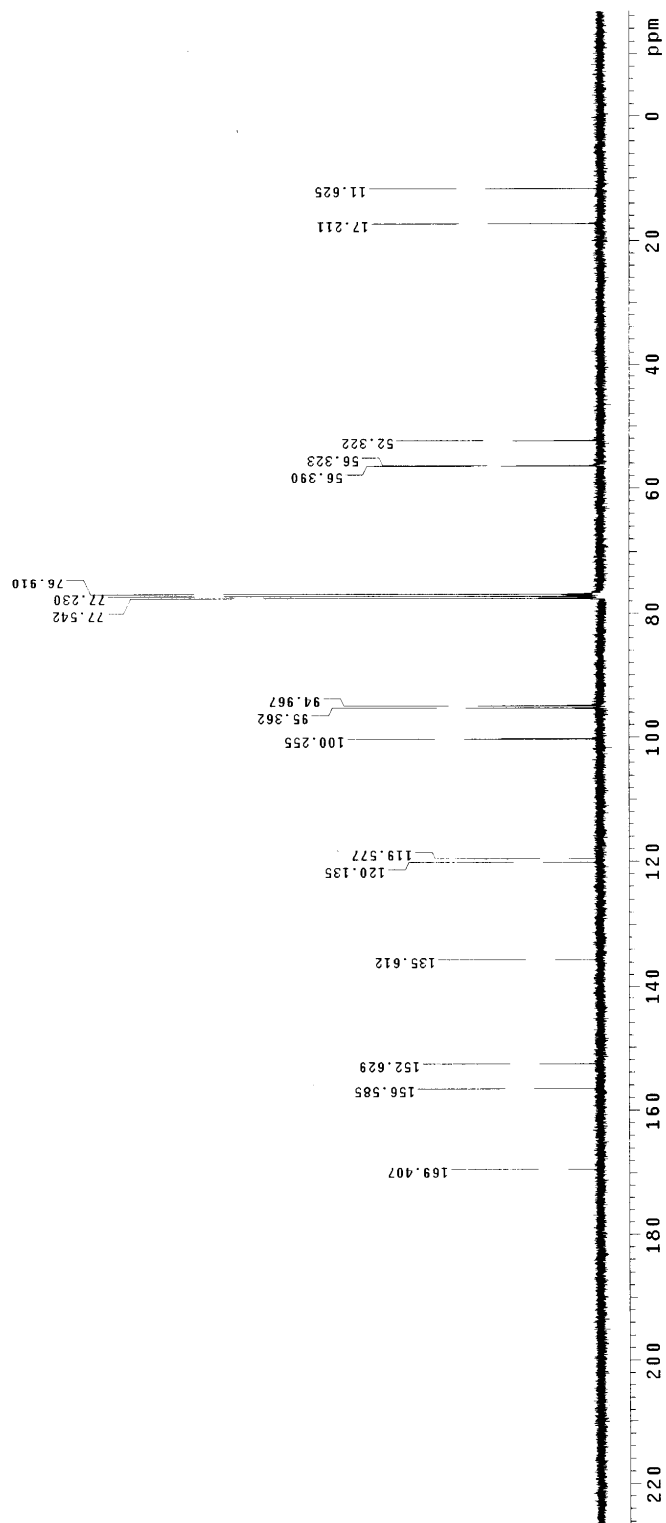
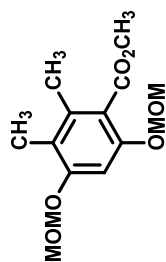
WALTZ-16 modulated

DATA PROCESSING

Line broadening 0.5 Hz

FT size 65536

Total time 19 min, 42 sec



51d proton

File: Proton

Pulse Sequence: zgpg30

Solvent: cdcl3

Temp: 25.0 C / 230.1 K

Operator: sxygink

UNMEX-SM 100130

Relax: delay 1.000 sec

Pulse: 125.0 deg

Acq. time 3.533 sec

Width 4013.2 Hz

K 100011000

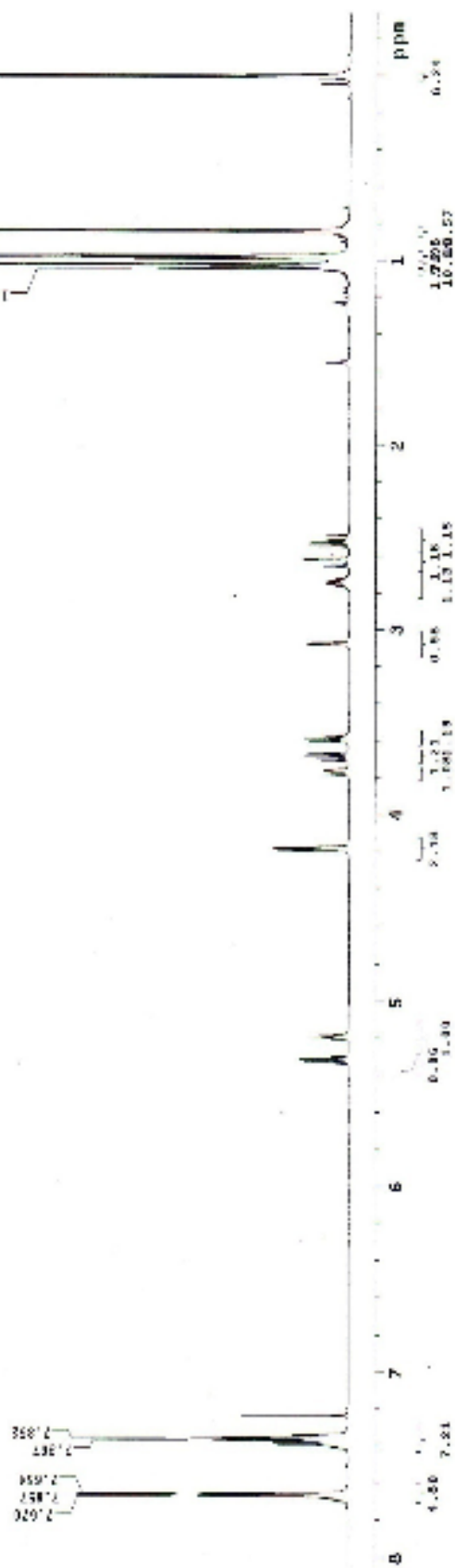
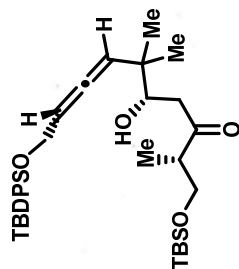
DESSKOR 400 MHz 499.780132 MHz

DELTA 100200000

DELTA 100200000

PT 11.45 6553

Total time 0 min, 30 sec



NAME: 070100

File: Carbon

Pulse Sequence: zgpg30

Solvent: cdcl3

Temp: 25.0 C / 240.1 K

Observed from: 1H

NAME: 070100

Relax: delay 1.000 sec

Relax: delay 1.000 sec

Relax: delay 1.000 sec

Relax: delay 1.000 sec

Relax: delay 1.000 sec

Relax: delay 1.000 sec

Relax: delay 1.000 sec

Relax: delay 1.000 sec

Relax: delay 1.000 sec

Relax: delay 1.000 sec

Relax: delay 1.000 sec

Relax: delay 1.000 sec

Relax: delay 1.000 sec

Relax: delay 1.000 sec

Relax: delay 1.000 sec

Relax: delay 1.000 sec

Relax: delay 1.000 sec

Relax: delay 1.000 sec

Relax: delay 1.000 sec

Relax: delay 1.000 sec

Relax: delay 1.000 sec

Relax: delay 1.000 sec

Relax: delay 1.000 sec

Relax: delay 1.000 sec

Relax: delay 1.000 sec

Relax: delay 1.000 sec

Relax: delay 1.000 sec

Relax: delay 1.000 sec

Relax: delay 1.000 sec

Relax: delay 1.000 sec

Relax: delay 1.000 sec

Relax: delay 1.000 sec

Relax: delay 1.000 sec

Relax: delay 1.000 sec

Relax: delay 1.000 sec

Relax: delay 1.000 sec

Relax: delay 1.000 sec

Relax: delay 1.000 sec

Relax: delay 1.000 sec

Relax: delay 1.000 sec

Relax: delay 1.000 sec

Relax: delay 1.000 sec

Relax: delay 1.000 sec

Relax: delay 1.000 sec

Relax: delay 1.000 sec

Relax: delay 1.000 sec

Relax: delay 1.000 sec

Relax: delay 1.000 sec

Relax: delay 1.000 sec

Relax: delay 1.000 sec

Relax: delay 1.000 sec

Relax: delay 1.000 sec

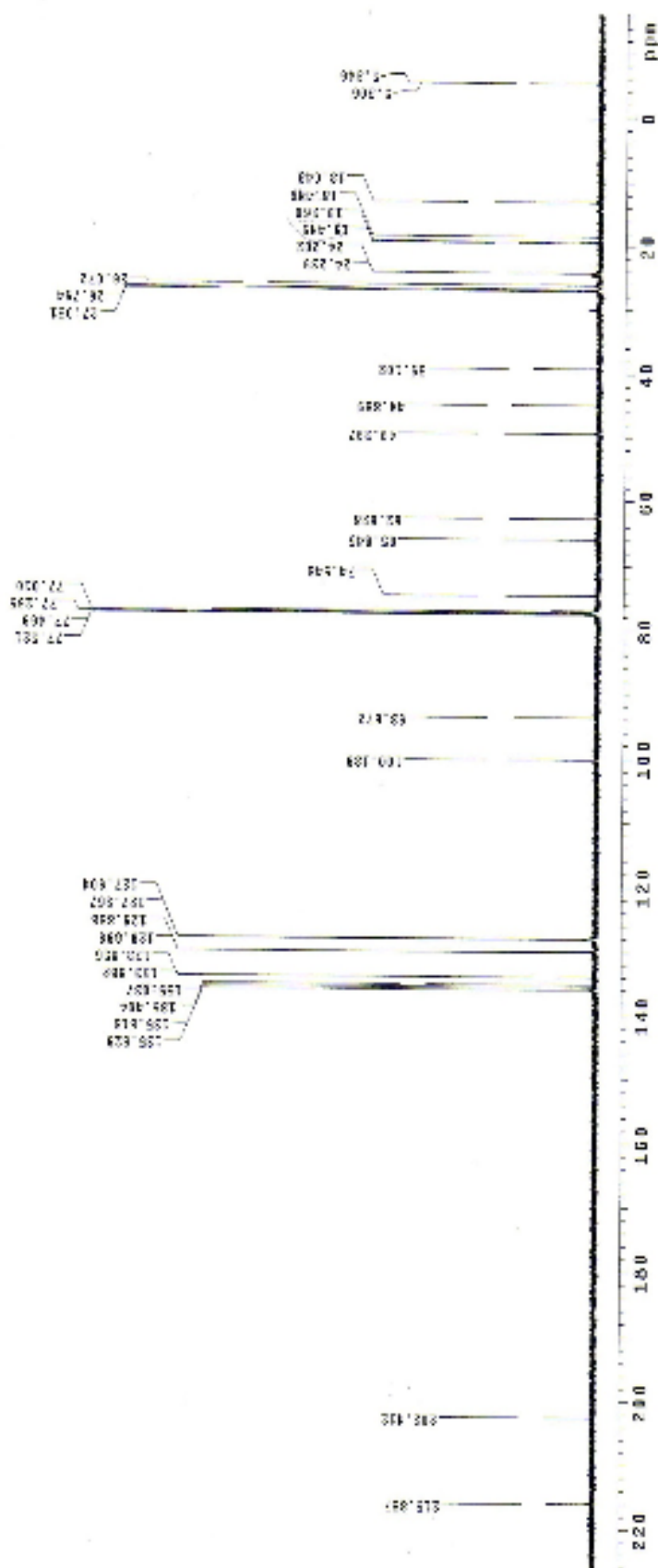
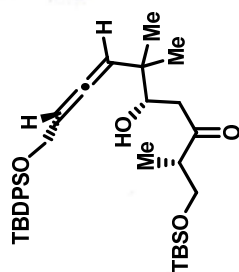
Relax: delay 1.000 sec

Relax: delay 1.000 sec

Relax: delay 1.000 sec

Relax: delay 1.000 sec

Relax: delay 1.000 sec



Sed proton

NAME: Proton

Pulse sequence: zgpg30

Solvent: CDCl₃

Temp: 25.0 C / 308.1 K

Circulation: 1.00000

GPMPS-0001: 1.00000-0.00000

Solve delay: 1.000 sec

Solve time: 1.000 sec

Solve width: 1.000 sec

Solve width: 1.000 sec

Solve width: 1.000 sec

Solve width: 1.000 sec

Solve width: 1.000 sec

Solve width: 1.000 sec

Solve width: 1.000 sec

Solve width: 1.000 sec

Solve width: 1.000 sec

Solve width: 1.000 sec

Solve width: 1.000 sec

Solve width: 1.000 sec

Solve width: 1.000 sec

Solve width: 1.000 sec

Solve width: 1.000 sec

Solve width: 1.000 sec

Solve width: 1.000 sec

Solve width: 1.000 sec

Solve width: 1.000 sec

Solve width: 1.000 sec

Solve width: 1.000 sec

Solve width: 1.000 sec

Solve width: 1.000 sec

Solve width: 1.000 sec

Solve width: 1.000 sec

Solve width: 1.000 sec

Solve width: 1.000 sec

Solve width: 1.000 sec

Solve width: 1.000 sec

Solve width: 1.000 sec

Solve width: 1.000 sec

Solve width: 1.000 sec

Solve width: 1.000 sec

Solve width: 1.000 sec

Solve width: 1.000 sec

Solve width: 1.000 sec

Solve width: 1.000 sec

Solve width: 1.000 sec

Solve width: 1.000 sec

Solve width: 1.000 sec

Solve width: 1.000 sec

Solve width: 1.000 sec

Solve width: 1.000 sec

Solve width: 1.000 sec

Solve width: 1.000 sec

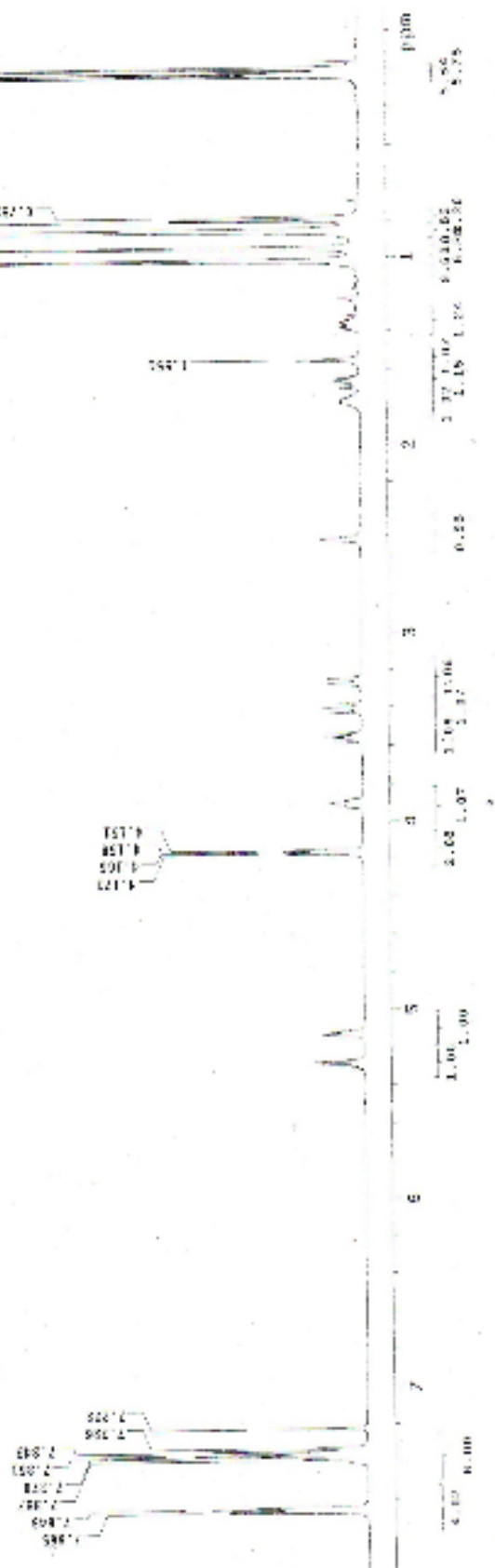
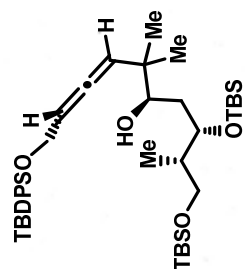
Solve width: 1.000 sec

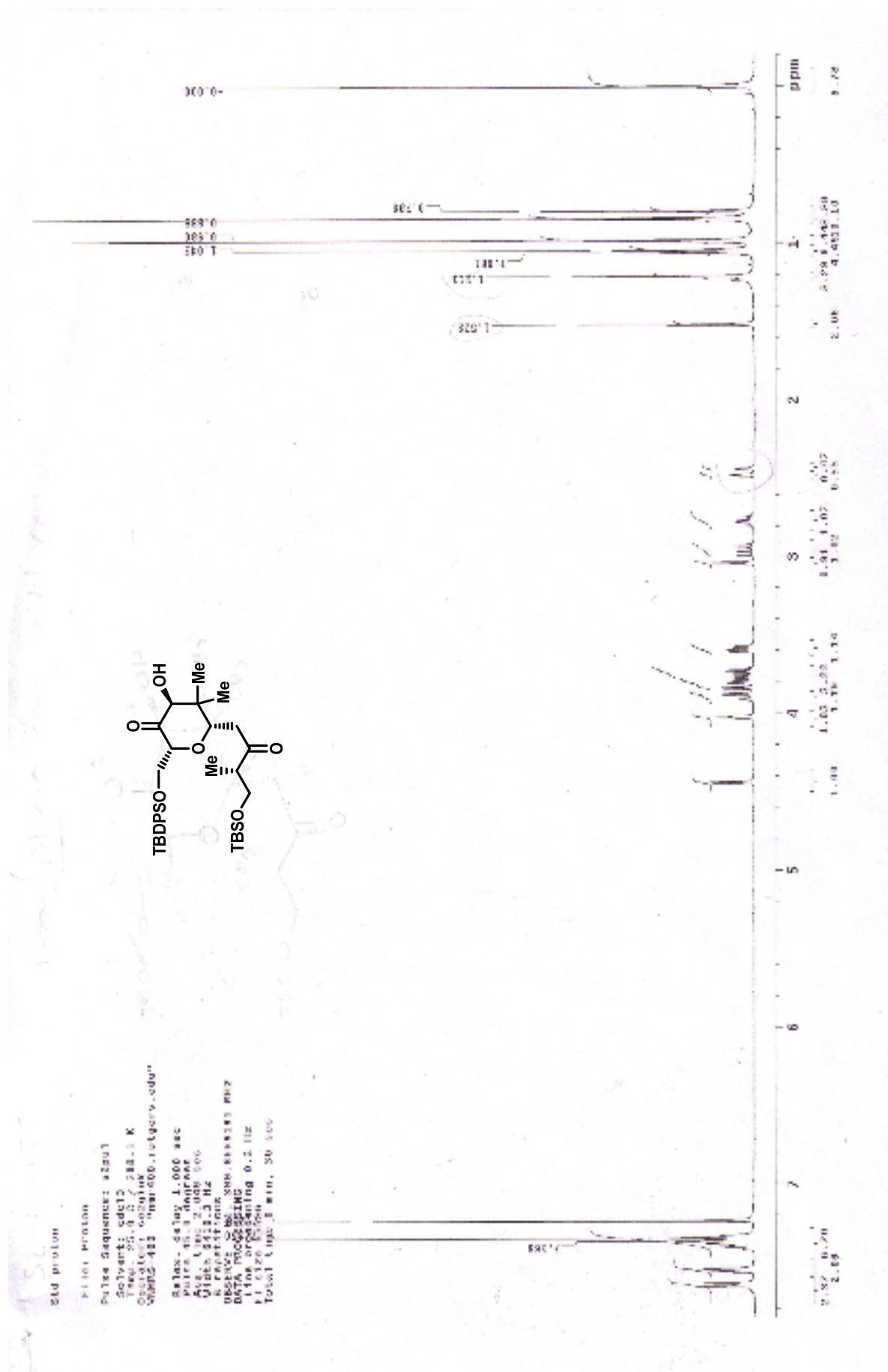
Solve width: 1.000 sec

Solve width: 1.000 sec

Solve width: 1.000 sec

Solve width: 1.000 sec





5th cycle

File: 44000

Pulse Sequence: zgpg30

Solvent: DMSO

Temp: 25.0 C / 232.1 K

Acquisition: 0001000

WBHS-400 400MHz, 4.7mm, 5mm, 5mm

Relax. delay: 3.00 sec

AQ: 0.00000000

AQ: 0.00000000

AQ: 0.00000000

AQ: 0.00000000

AQ: 0.00000000

AQ: 0.00000000

AQ: 0.00000000

AQ: 0.00000000

AQ: 0.00000000

AQ: 0.00000000

AQ: 0.00000000

AQ: 0.00000000

AQ: 0.00000000

AQ: 0.00000000

AQ: 0.00000000

AQ: 0.00000000

AQ: 0.00000000

AQ: 0.00000000

AQ: 0.00000000

AQ: 0.00000000

AQ: 0.00000000

AQ: 0.00000000

AQ: 0.00000000

AQ: 0.00000000

AQ: 0.00000000

AQ: 0.00000000

AQ: 0.00000000

AQ: 0.00000000

AQ: 0.00000000

AQ: 0.00000000

AQ: 0.00000000

AQ: 0.00000000

AQ: 0.00000000

AQ: 0.00000000

AQ: 0.00000000

AQ: 0.00000000

AQ: 0.00000000

AQ: 0.00000000

AQ: 0.00000000

AQ: 0.00000000

AQ: 0.00000000

AQ: 0.00000000

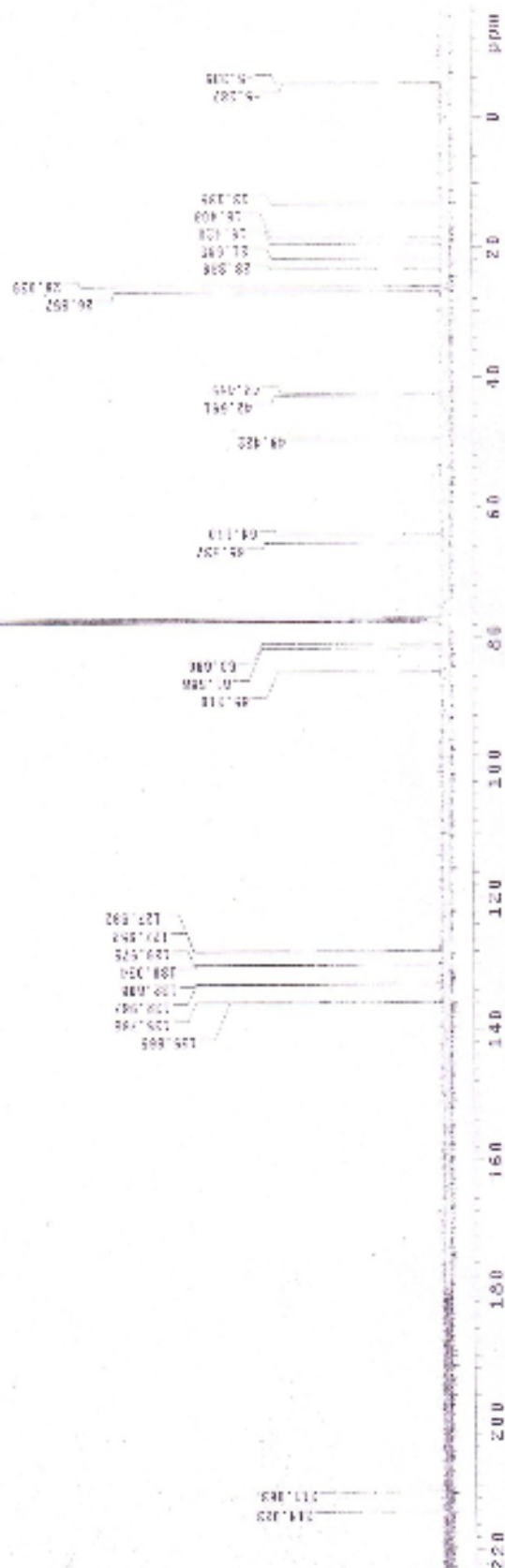
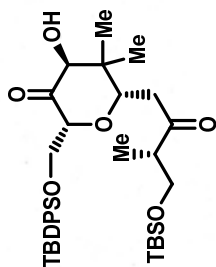
AQ: 0.00000000

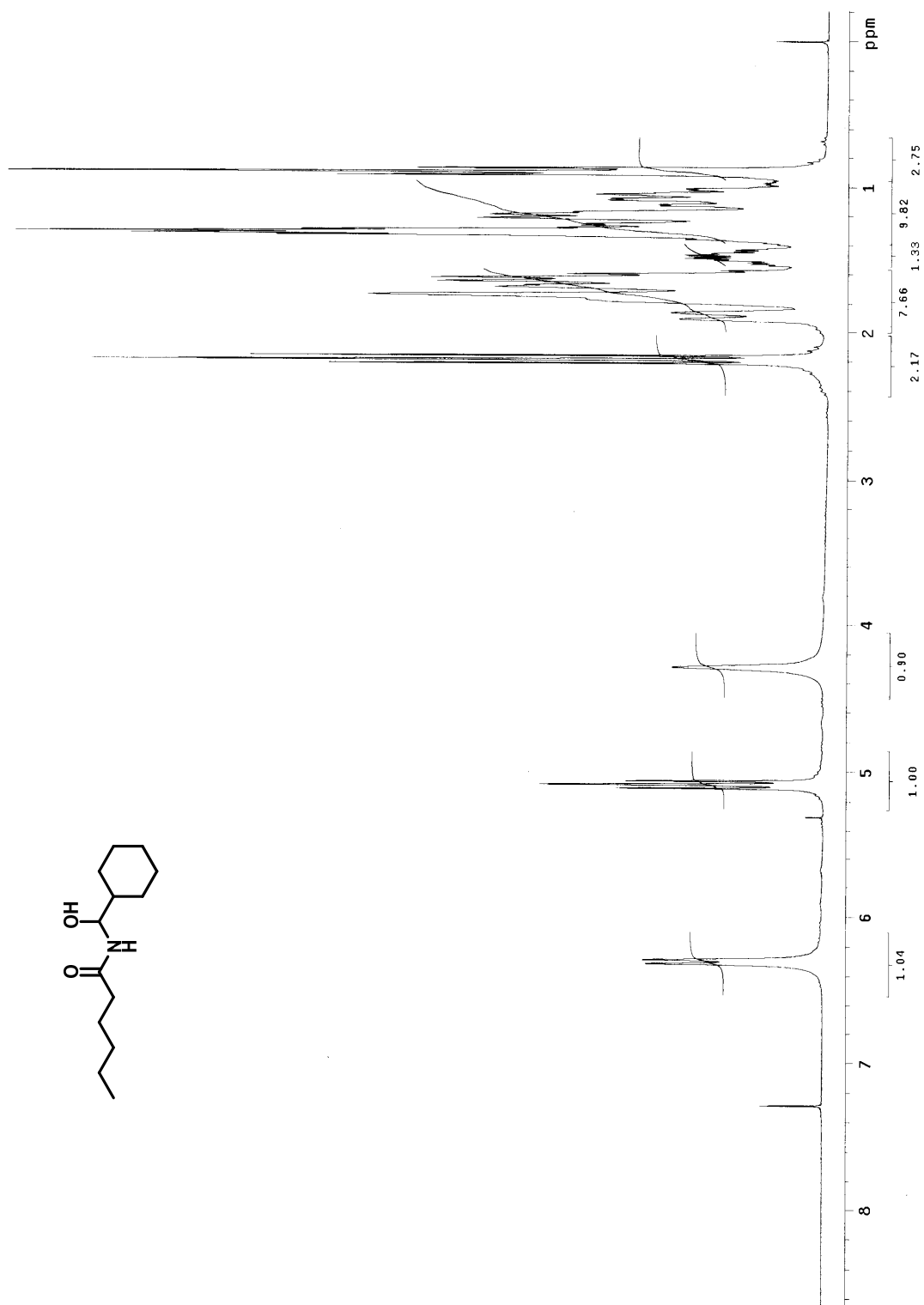
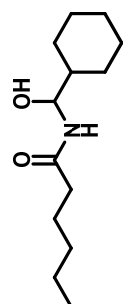
AQ: 0.00000000

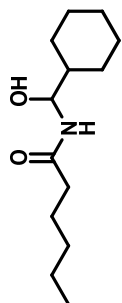
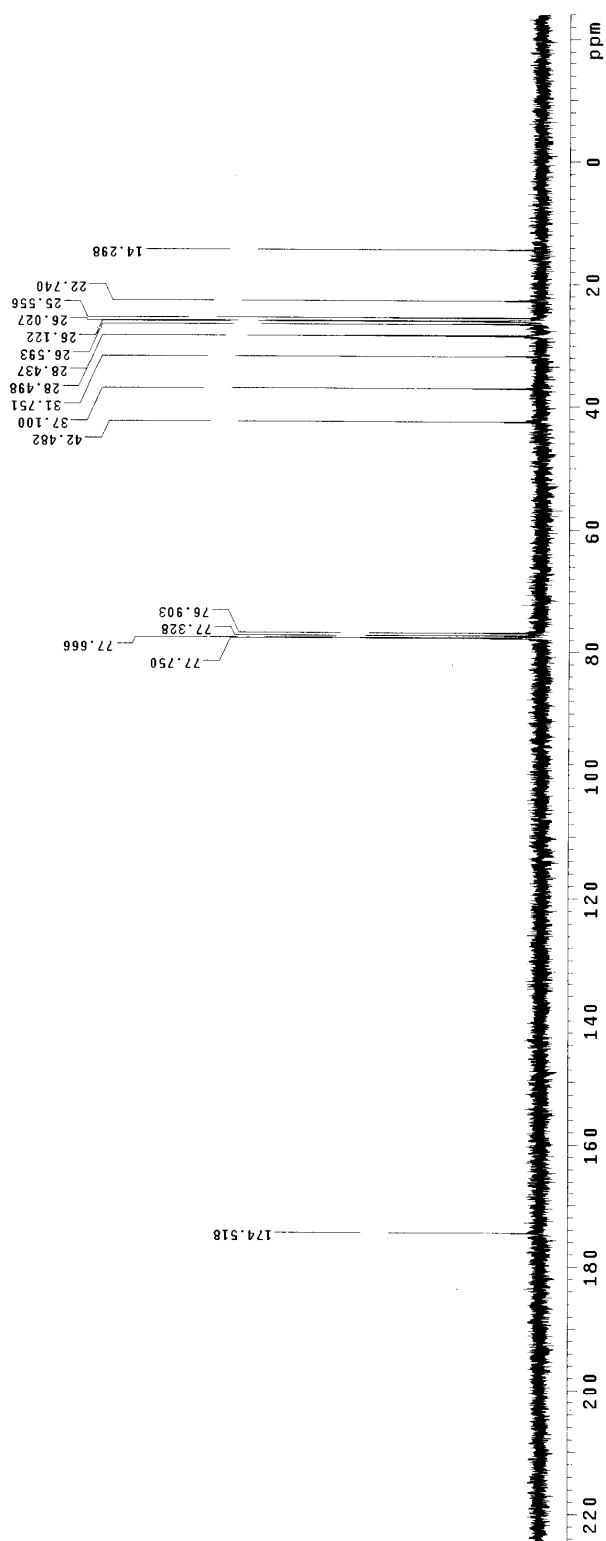
AQ: 0.00000000

AQ: 0.00000000

AQ: 0.00000000







Std proton

File: Proton

Pulse Sequence: zgpg30

Solvent: cdcl3

Temp: 25.3 C / 298.1 K

Decoupler: zgpg30

VHNS-400 400MHz, 100um, 100um, 100um

Relax. delay: 1.000 sec

Pulse 45.8 degrees

Dec. time 0.000 sec

VHNS-400 400MHz

Pulse 45.8 degrees

Dec. time 0.000 sec

VHNS-400 400MHz

Pulse 45.8 degrees

Dec. time 0.000 sec

VHNS-400 400MHz

Pulse 45.8 degrees

Dec. time 0.000 sec

VHNS-400 400MHz

Pulse 45.8 degrees

Dec. time 0.000 sec

VHNS-400 400MHz

Pulse 45.8 degrees

Dec. time 0.000 sec

VHNS-400 400MHz

Pulse 45.8 degrees

Dec. time 0.000 sec

VHNS-400 400MHz

Pulse 45.8 degrees

Dec. time 0.000 sec

VHNS-400 400MHz

Pulse 45.8 degrees

Dec. time 0.000 sec

VHNS-400 400MHz

Pulse 45.8 degrees

Dec. time 0.000 sec

VHNS-400 400MHz

Pulse 45.8 degrees

Dec. time 0.000 sec

VHNS-400 400MHz

Pulse 45.8 degrees

Dec. time 0.000 sec

VHNS-400 400MHz

Pulse 45.8 degrees

Dec. time 0.000 sec

VHNS-400 400MHz

Pulse 45.8 degrees

Dec. time 0.000 sec

VHNS-400 400MHz

Pulse 45.8 degrees

Dec. time 0.000 sec

VHNS-400 400MHz

Pulse 45.8 degrees

Dec. time 0.000 sec

VHNS-400 400MHz

Pulse 45.8 degrees

Dec. time 0.000 sec

VHNS-400 400MHz

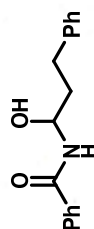
Pulse 45.8 degrees

Dec. time 0.000 sec

VHNS-400 400MHz

Pulse 45.8 degrees

Dec. time 0.000 sec



Std proton

File: Carbon

Pulse Sequence: s2pul

Solvent: cdc13

Temp: 25.0 C / 298.1 K

Operator: szglnk

VNMR-400 "nmr400.rutgers.edu"

Relax. delay 1.000 sec

Puls. prg. 1300

Acq. time 1.300 sec

Width 24509.8 Hz

736 Repetitions

OBSERVE C13, 100.5717377 MHz

DECOUPLE H1, 399.5689190 MHz

Puls. prg. 1300

Continuous on

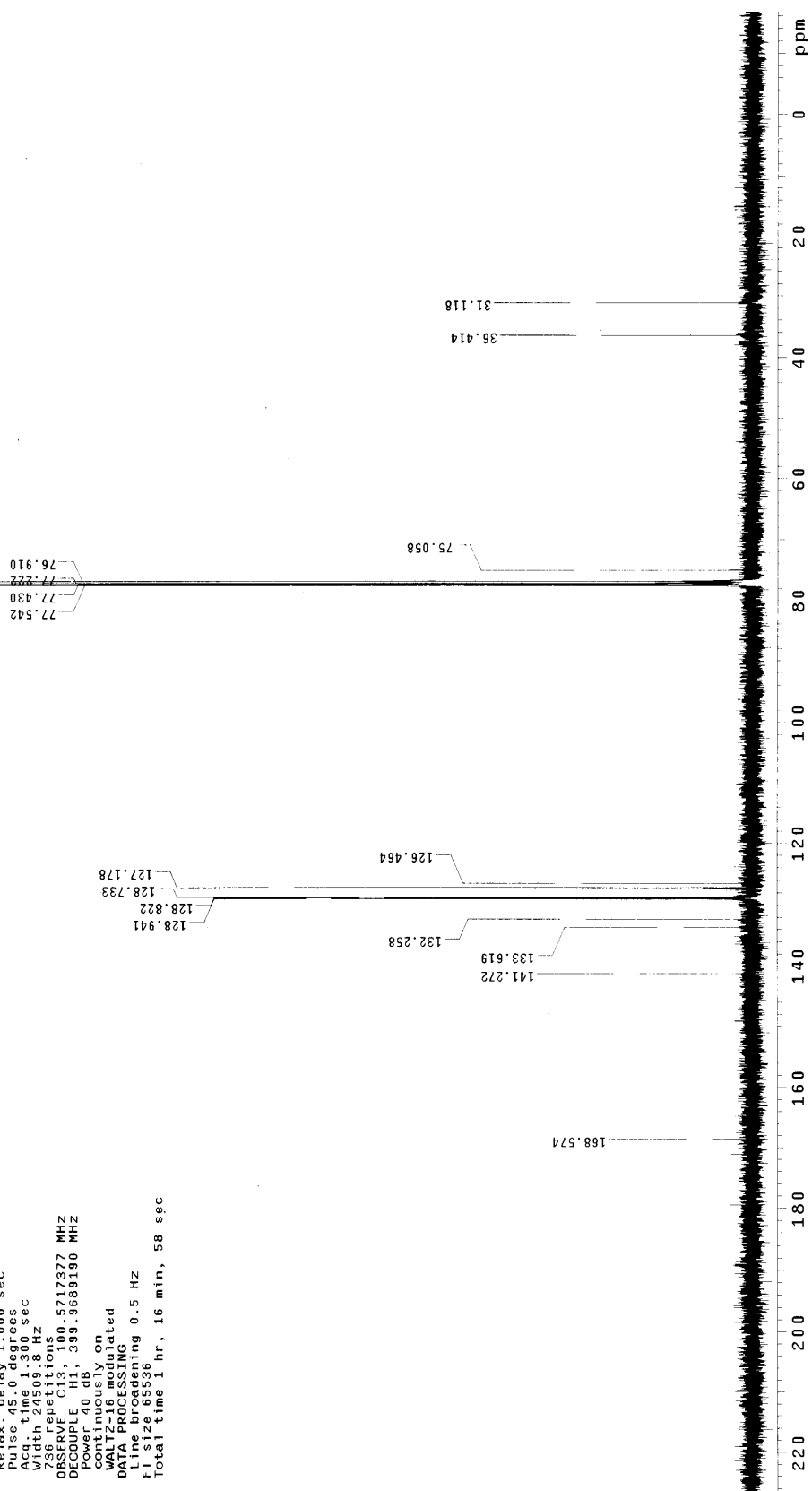
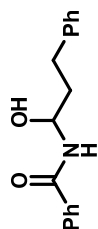
WALTZ-16 modulated

DATA PROCESSING

Line broadening 0.5 Hz

FT size 65536

Total time 1 hr, 16 min, 58 sec

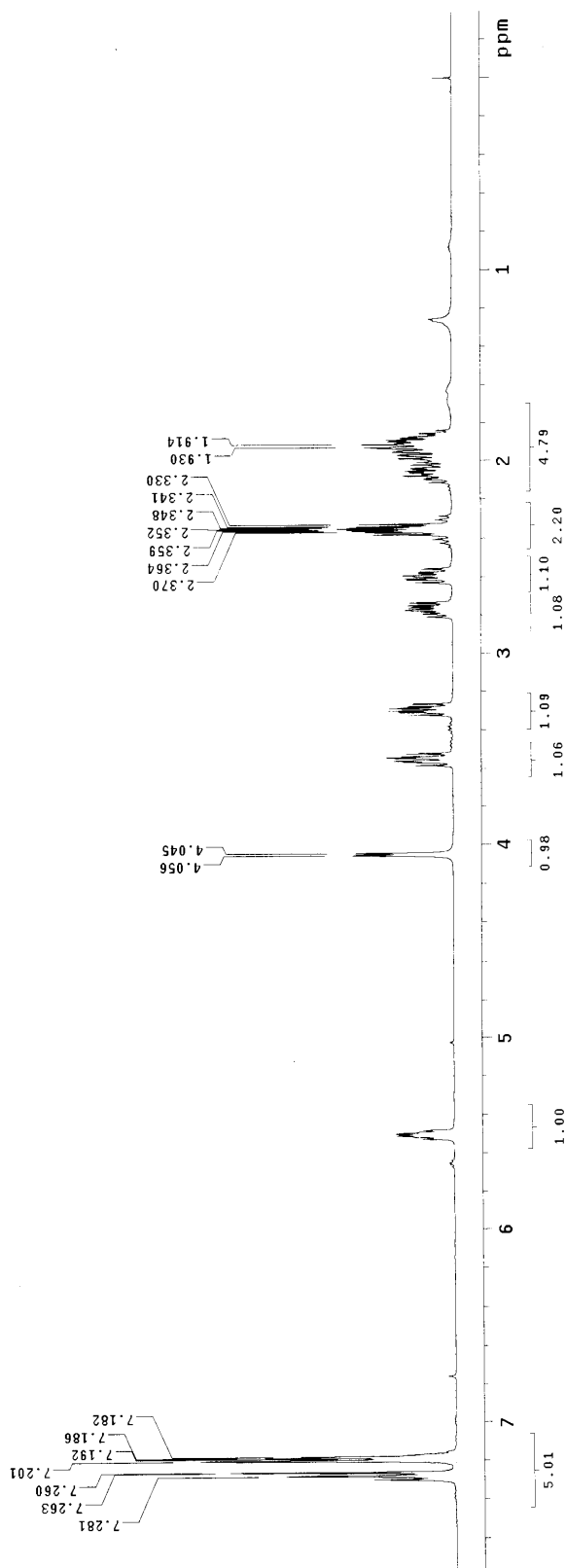
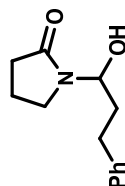


Std proton

File: Proton

Pulse Sequence: s2pul1
 Solvent: cdcl3
 Temp: 25.0 C / 298.1 K
 Operator: sezgink
 VNMR-400 "nmr400.futgers.edu"

Relax. delay 1.000 sec
 Pulse 45.0 degrees
 Acq. time 2.043 sec
 Width 30.30 Hz
 8 repetitions
 OBSERVE H1, 399.9669120 MHz
 DATA PROCESSING
 Line broadening 0.2 Hz
 FT size 65536
 Total time 0 min, 30 sec



Std proton

File: Carbon

Pulse Sequence: s2pul

Solvent: cdcl3

Chemical shift: 200.1 K

Temperature: 300.2 K

P1: 12.00 sec

P2: 12.00 sec

P3: 12.00 sec

P4: 12.00 sec

P5: 12.00 sec

P6: 12.00 sec

P7: 12.00 sec

P8: 12.00 sec

P9: 12.00 sec

P10: 12.00 sec

P11: 12.00 sec

P12: 12.00 sec

P13: 12.00 sec

P14: 12.00 sec

P15: 12.00 sec

P16: 12.00 sec

P17: 12.00 sec

P18: 12.00 sec

P19: 12.00 sec

P20: 12.00 sec

P21: 12.00 sec

P22: 12.00 sec

P23: 12.00 sec

P24: 12.00 sec

P25: 12.00 sec

P26: 12.00 sec

P27: 12.00 sec

P28: 12.00 sec

P29: 12.00 sec

P30: 12.00 sec

P31: 12.00 sec

P32: 12.00 sec

P33: 12.00 sec

P34: 12.00 sec

P35: 12.00 sec

P36: 12.00 sec

P37: 12.00 sec

P38: 12.00 sec

P39: 12.00 sec

P40: 12.00 sec

P41: 12.00 sec

P42: 12.00 sec

P43: 12.00 sec

P44: 12.00 sec

P45: 12.00 sec

P46: 12.00 sec

P47: 12.00 sec

P48: 12.00 sec

P49: 12.00 sec

P50: 12.00 sec

P51: 12.00 sec

P52: 12.00 sec

P53: 12.00 sec

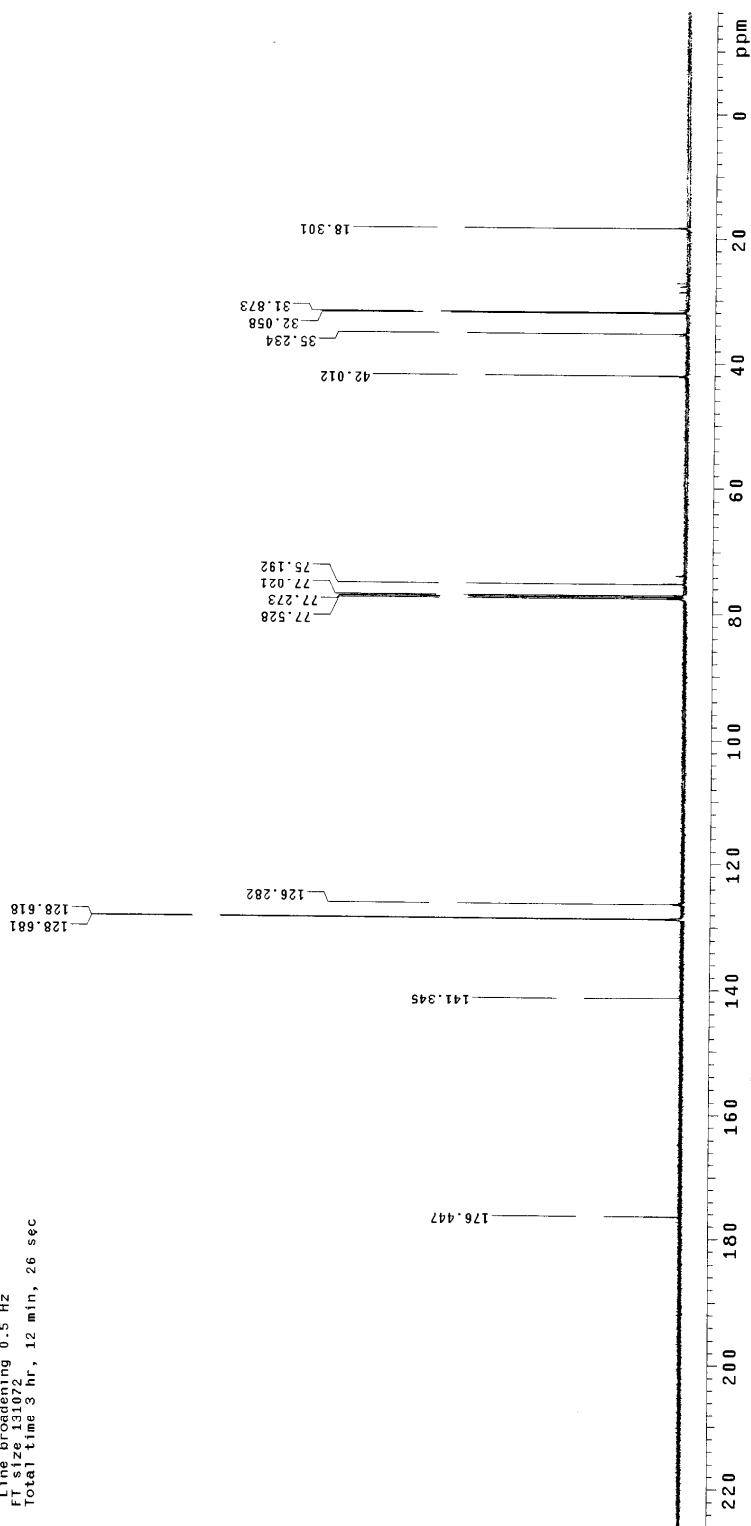
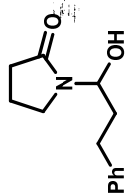
P54: 12.00 sec

P55: 12.00 sec

P56: 12.00 sec

P57: 12.00 sec

P58: 12.00 sec



Std proton

File: Proton

Pulse Sequence: s2pu1

Solvent: cdcl3

Temp: 25.0 C

QNP: 101.25 MHz

VPMR: 500 MHz

Relax. delay: 1.000 sec

Pulse: 45.0 degrees

Acq. time: 2.0195 sec

Width: 8012.8 Hz

8 repetitions

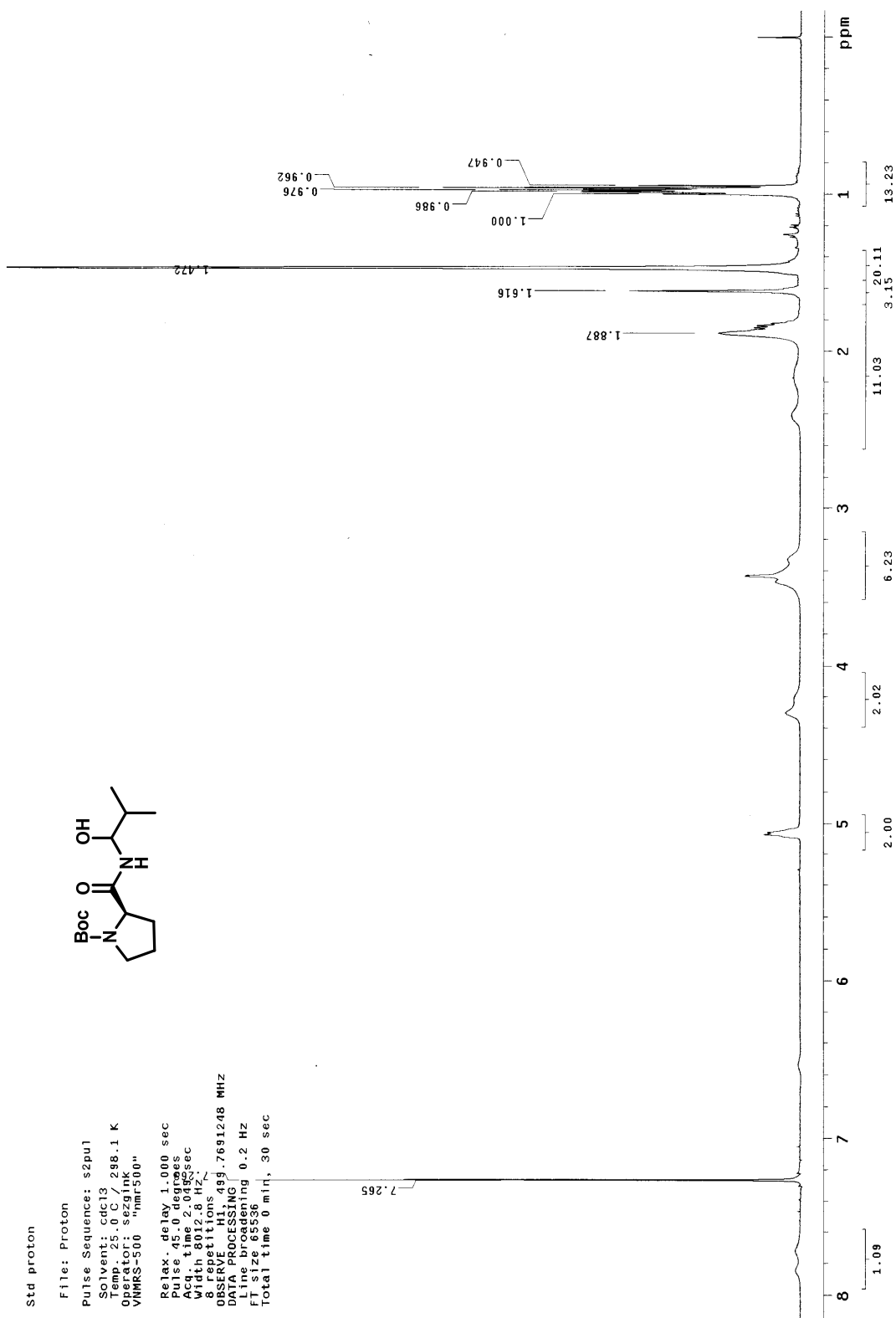
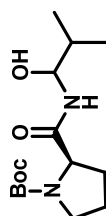
F2: 499.7691248 MHz

DQ: 1.0000000 sec

Line broadening: 0.2 Hz

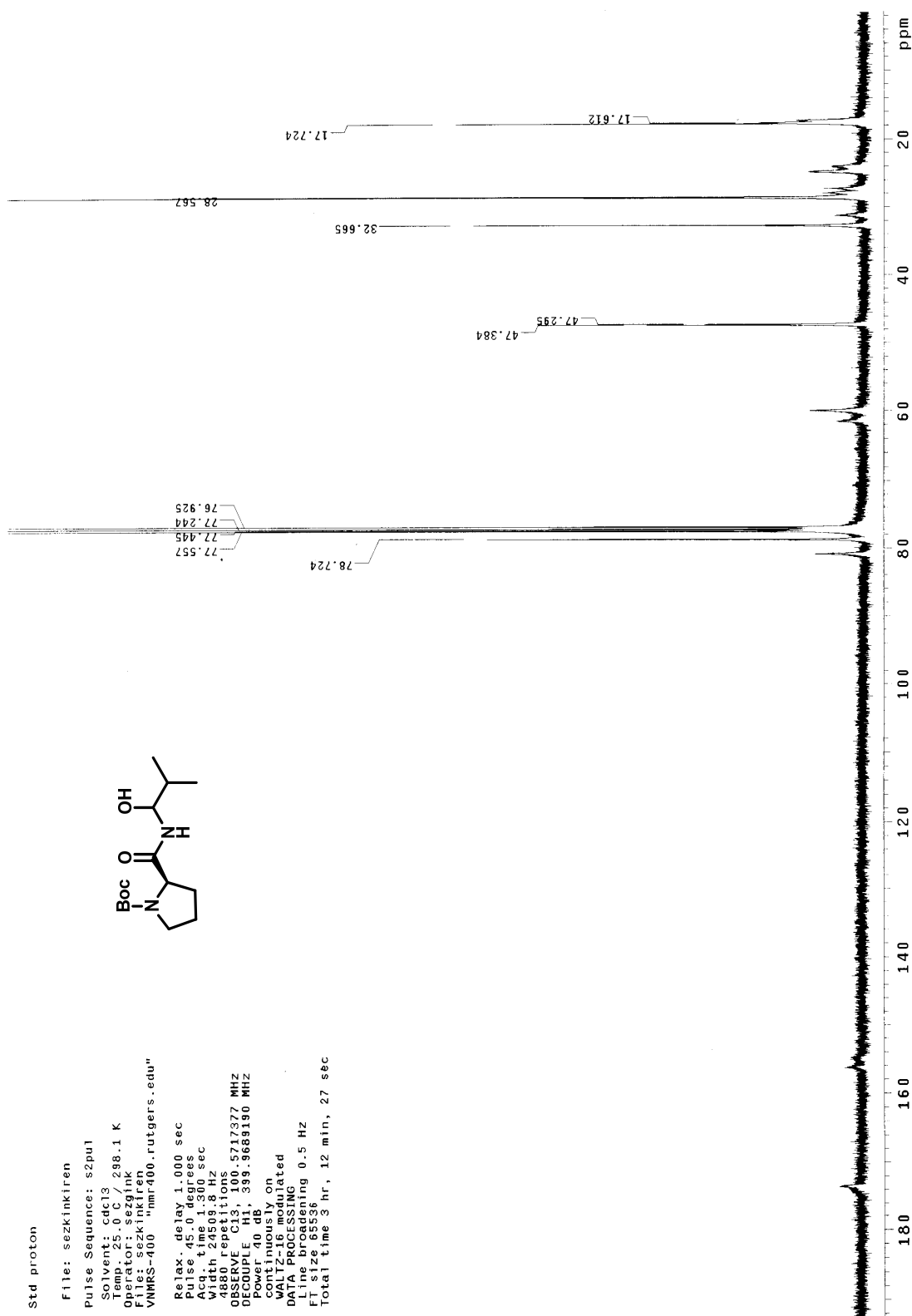
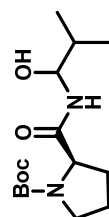
FT size: 65536

Total time: 0 min, 30 sec



Std proton

File: sezinkiren
 Pulse Sequence: s2pu1
 Solvent: cdcl3 298.1 K
 Temp: 298.2 K
 Operator: sezink
 File: sezinkiren
 VNMR-400 "nmr400.rutgers.edu"
 Relax. delay 1.000 sec
 Pulse 45.0 degrees
 Acq. time 1.300 sec
 Width 24509.8 Hz
 ASSEMBLE PC11.000 5717377 MHz
 OBSERVE PC11.000 5717377 MHz
 DECOUPLE CH1.399.3689190 MHz
 Power 40 dB
 Continuously on
 WALTZ-16 modulated
 DATA PROCESSING
 Line 0.5 Hz
 FT size 65536
 Total time 3 hr, 12 min, 27 sec



Std proton

File: Proton

Pulse Sequence: s2pu1

Solvent: cdcl3 298.1 K

Temp: 25.9631K

Op: to 5.6301K

VNMRS-400 "nmr400.rutgers.edu"

Relax. delay 1.000 sec

Pulse 45.0 degrees

Acq. time 2.049 sec

Width 6410.3 Hz

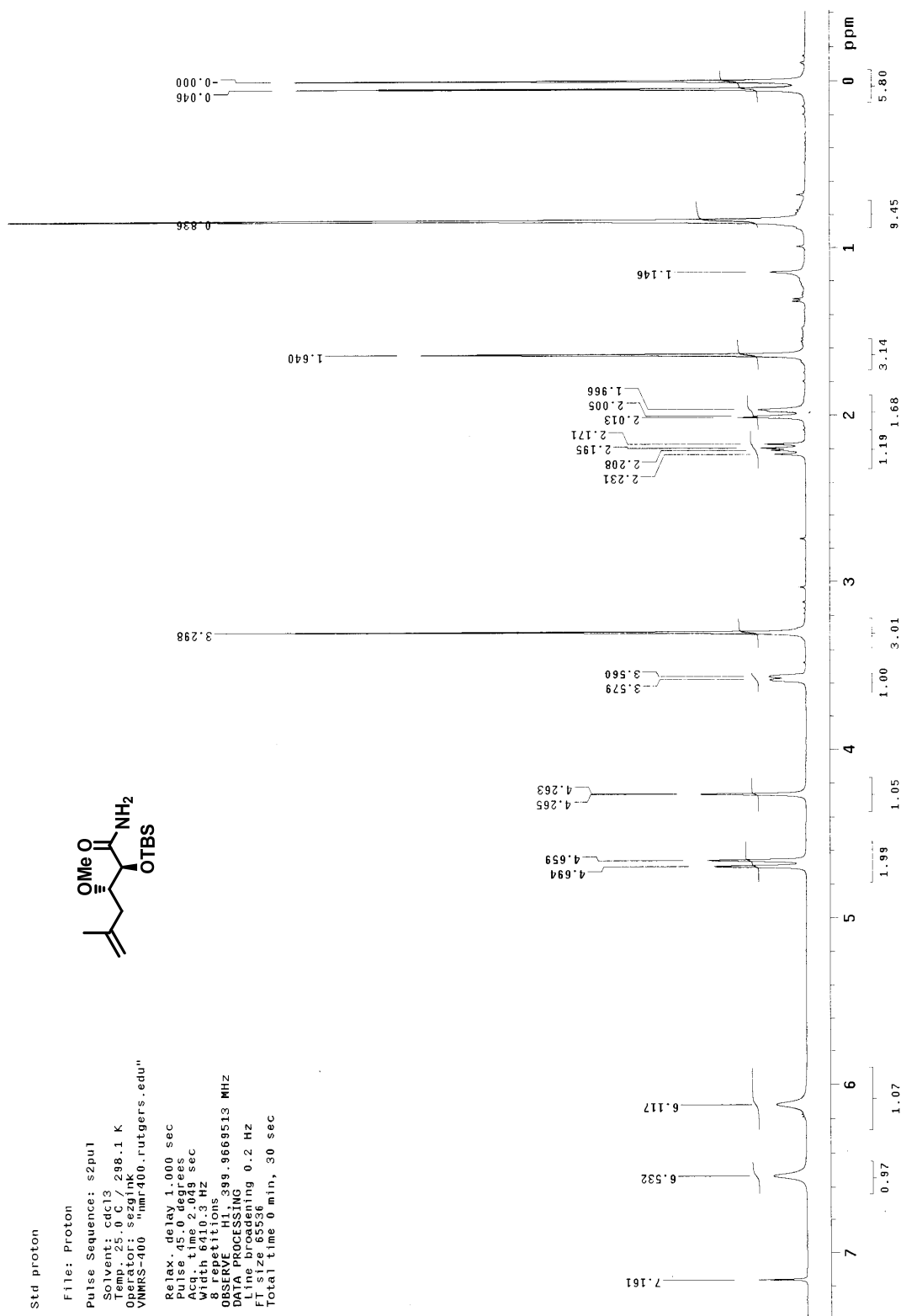
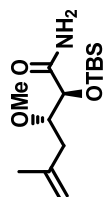
8 repetitions 399.9669513 MHz

DATA PROCESSING

Line broadening 0.2 Hz

FT size 65536

Total time 0 min, 30 sec



Std proton

File: Carbon

Pulse Sequence: s2pul

Solvent: cdcl3

Temp.: 25.0 C / 298.1 K

Observed: 59.96

VMRS-400 "nmr400.ruigers.edu"

Relax. delay 1.000 sec

Pulse: 45.0 degrees

Acq. time 1.300 sec

Width 24509.8 Hz

704 repetitions

OBSERVE C13, 100.571377 MHz

DECOUPLE H1, 399.9669190 MHz

Cont. decoupling

continuously on

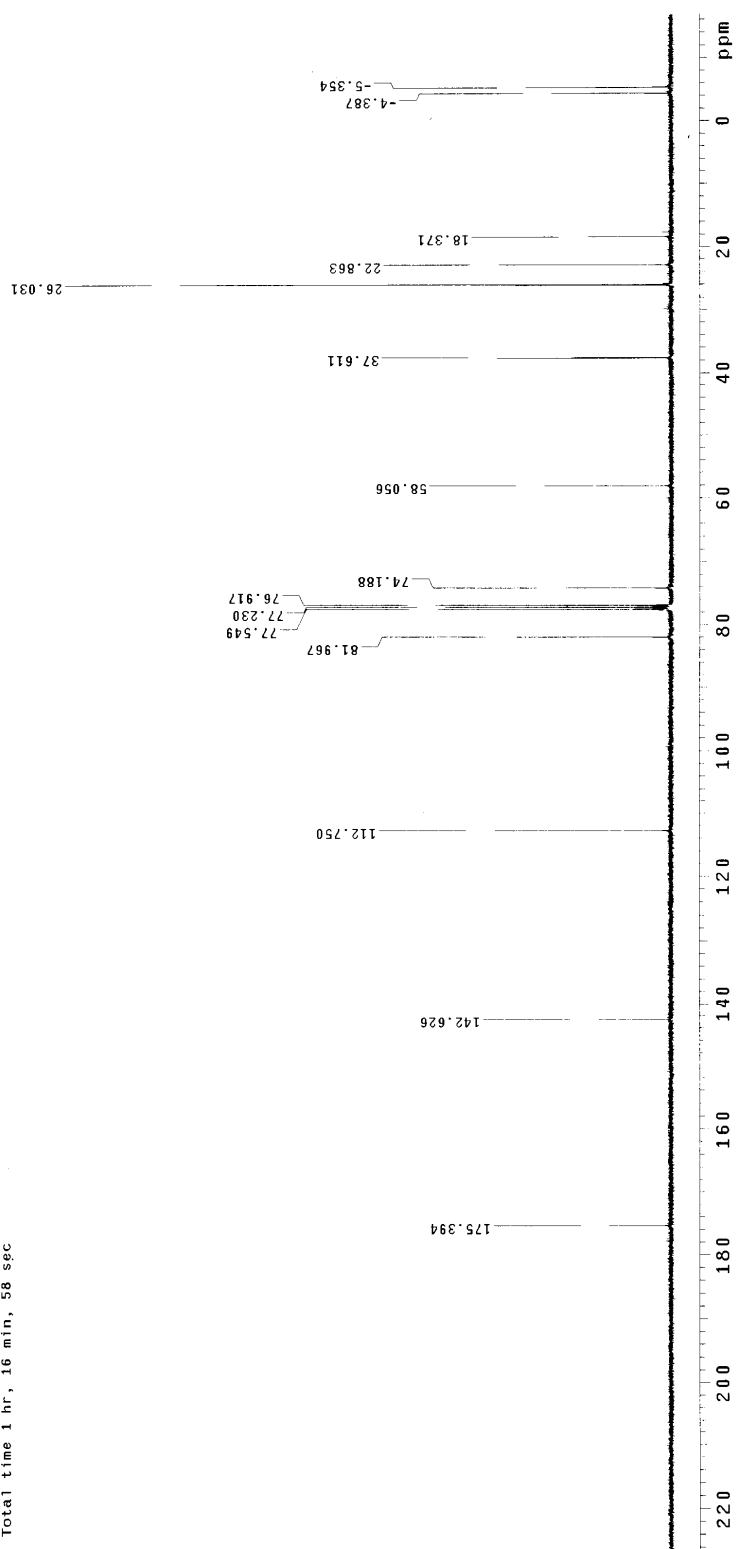
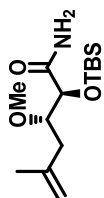
WALTZ-16 modulated

DATA PROCESSING

Line broadening 0.5 Hz

FT size 65536

Total time 1 hr, 16 min, 58 sec



Std proton

File: SK-IV-76

Pulse Sequence: s2pul

Solvent: cdcl3

Temp: 300.2 / 398.1 K

Operator: se2gink

File: SK-IV-76

VNMR-500 "nmr500"

Relax. delay 1.000 sec

Pulse 45.0 degrees

Acq. time 2.049 sec

Width 6012.8 Hz

SFO 499.7691214 MHz

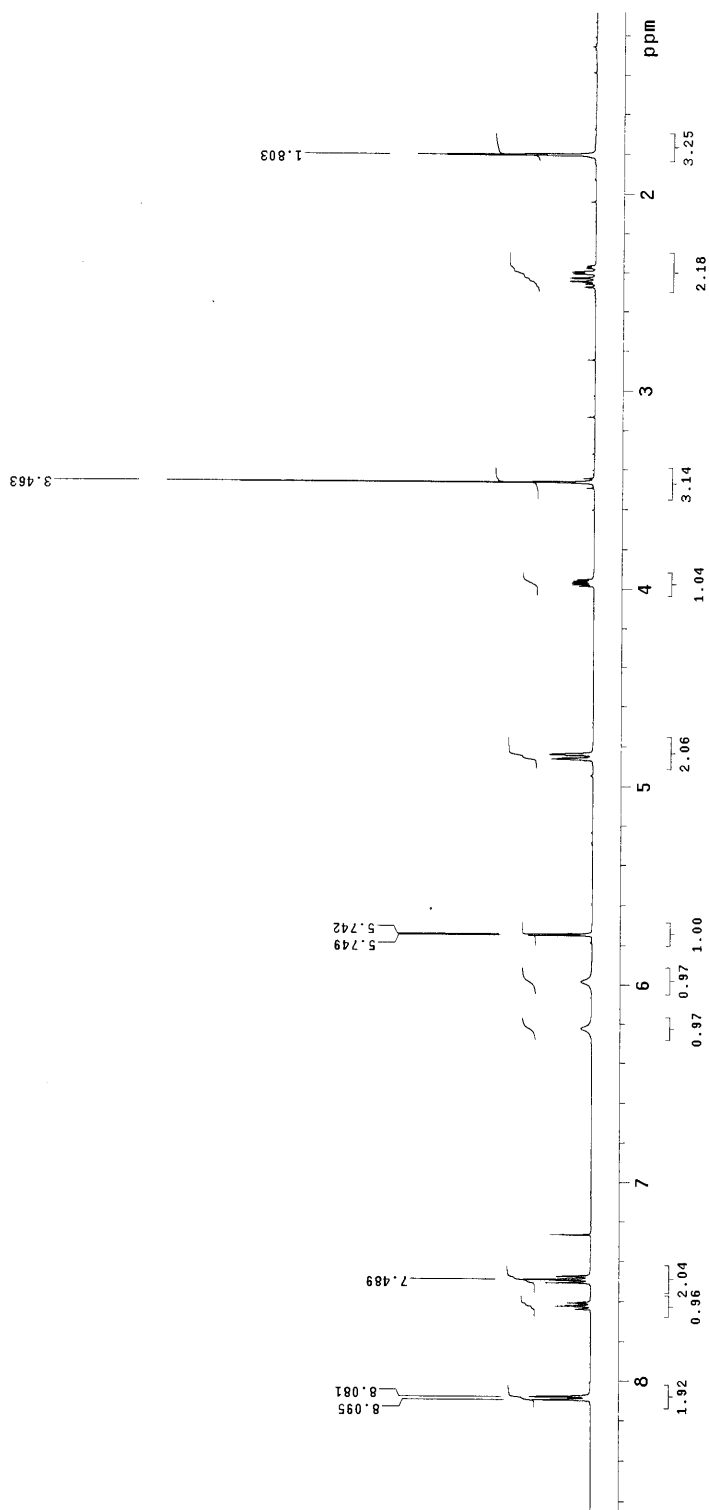
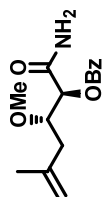
OBSERVE H1

DATA PROCESSING

Line broadening 0.2 Hz

FT size 65536

Total time 0 min, 30 sec



Std proton

File: SK-IV-76c13

Pulse Sequence: s2pul

Solvent: cdcl3 298.1 K

Temp: 25.0 C / 298.1 K

Observed: 1H

File: SK-IV-76c13

VNMR-500 "nmr500"

Relax. delay 1.000 sec

Pulse 45.0 degrees

Acq. time 1.300 sec

Width 30487.8 Hz

Observed: 1H

OBSERVE F105, 6670162 MHz

DECOUPLE C13, 439.7716228 MHz

Power 40 dB

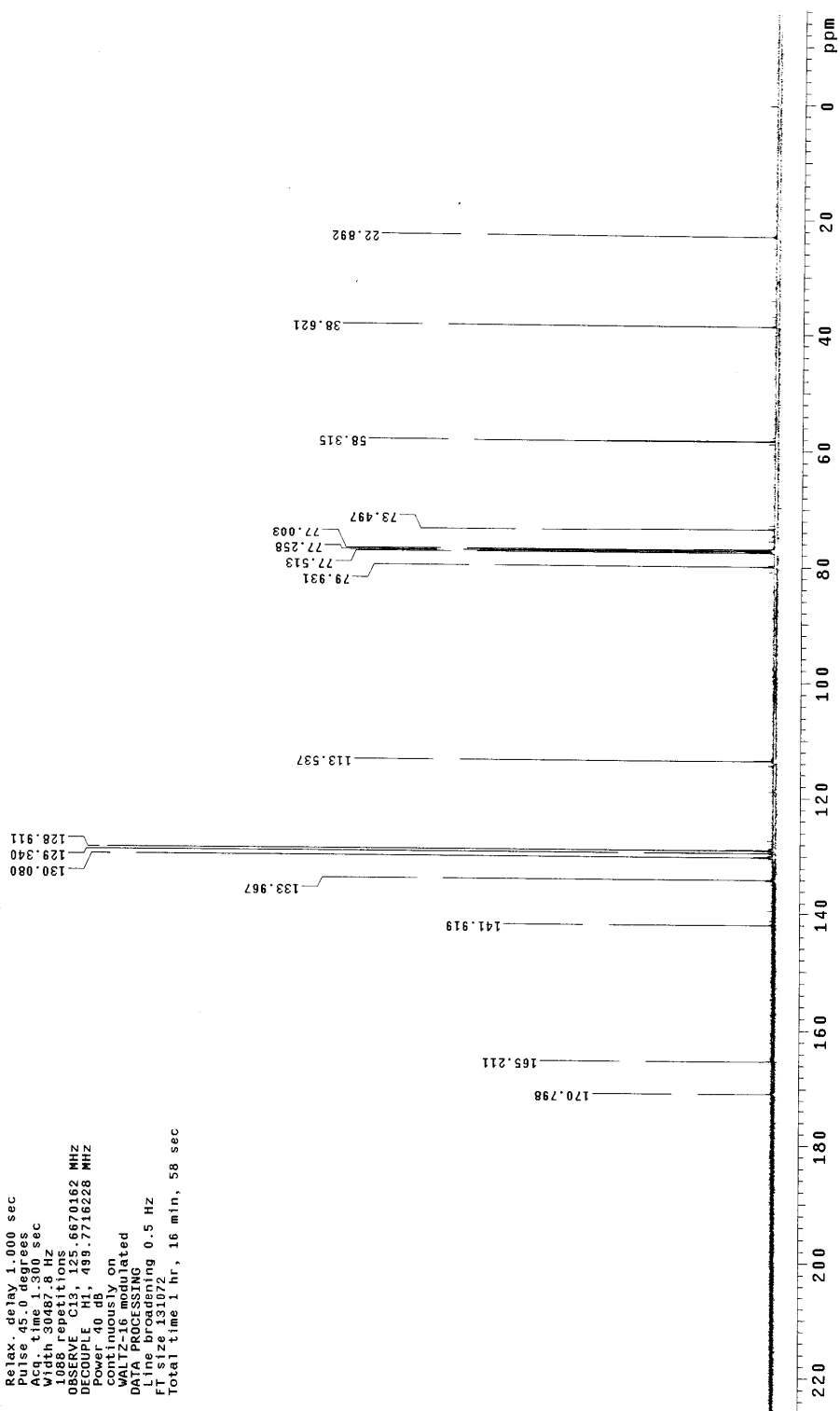
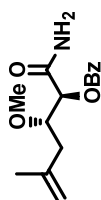
Continuously on

WALTZ-16 modulated

DATA PROCESSING 0.5 Hz

FT size 131072

Total time 1 hr, 16 min, 58 sec



Std proton

File: Proton

Pulse Sequence: s2pul

Solvent: cdcl3 298.1 K

Temp: 23.0 C / 100 K

QNP: 101.25 MHz

VNMRS-500 "nmr500"

Relax. delay 1.000 sec

Pulse 45.0 degrees

Acq. time 2.049 sec

Width 8012.8 Hz

16 repetitions

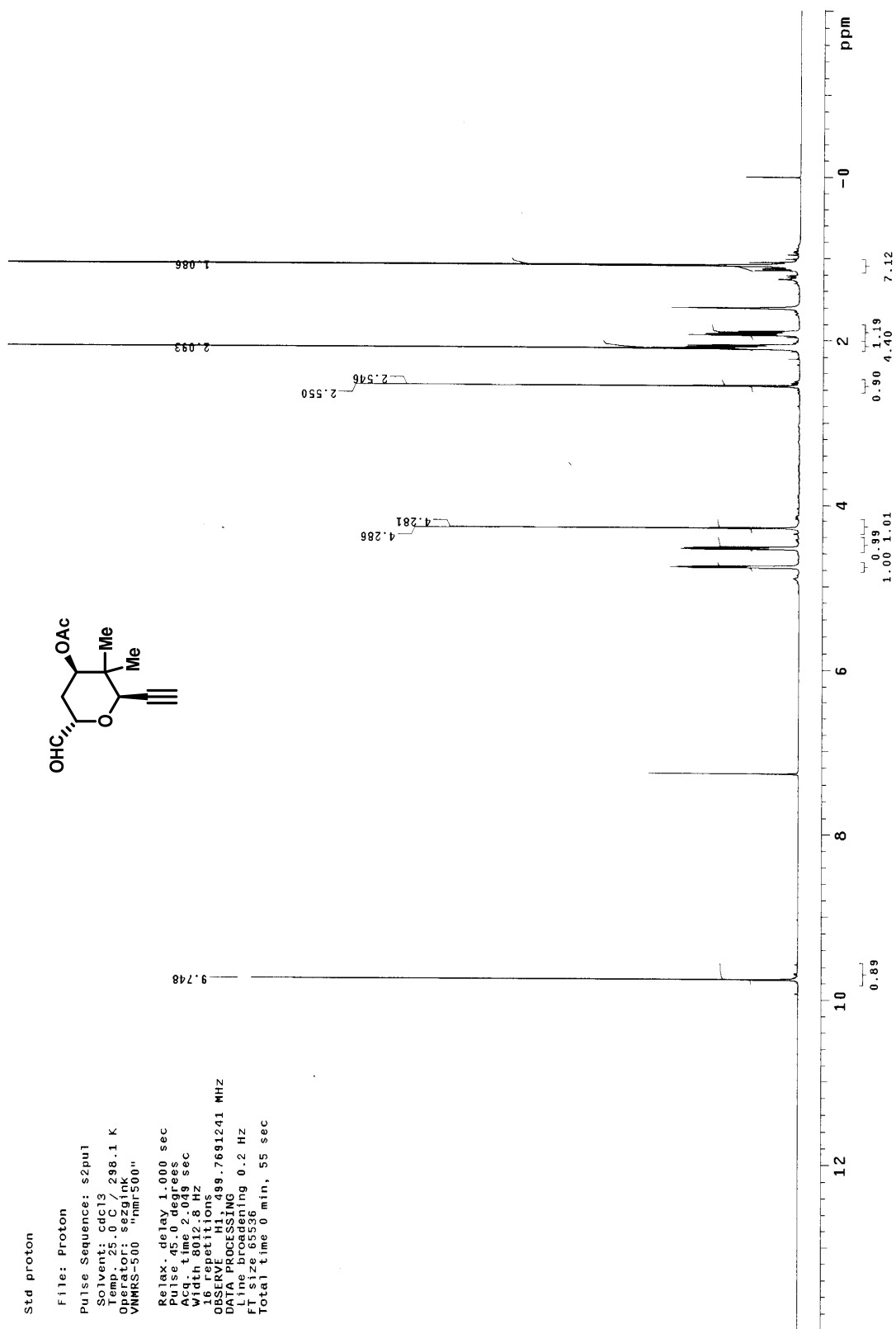
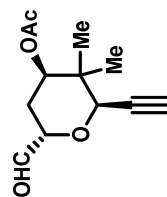
Observed F1 499.7691241 MHz

Data processing

Line broadening 0.2 Hz

FT size 65536

Total time 0 min, 55 sec



Std proton

File: Carbon

Pulse Sequence: s2pu1

Solvent: cdcl3 298.1 K

Operator: sezaink

VNMRS-500 "nmr500"

Relax. delay 1.000 sec

Pulse 45.0 degrees

Acq. time 1.300 sec

Width 30487.8 Hz

Sweep 125.000 MHz

OBSERVE C13, 489.7716226 MHz

DECOUPLE H1, 489.7716226 MHz

Power 40 dB

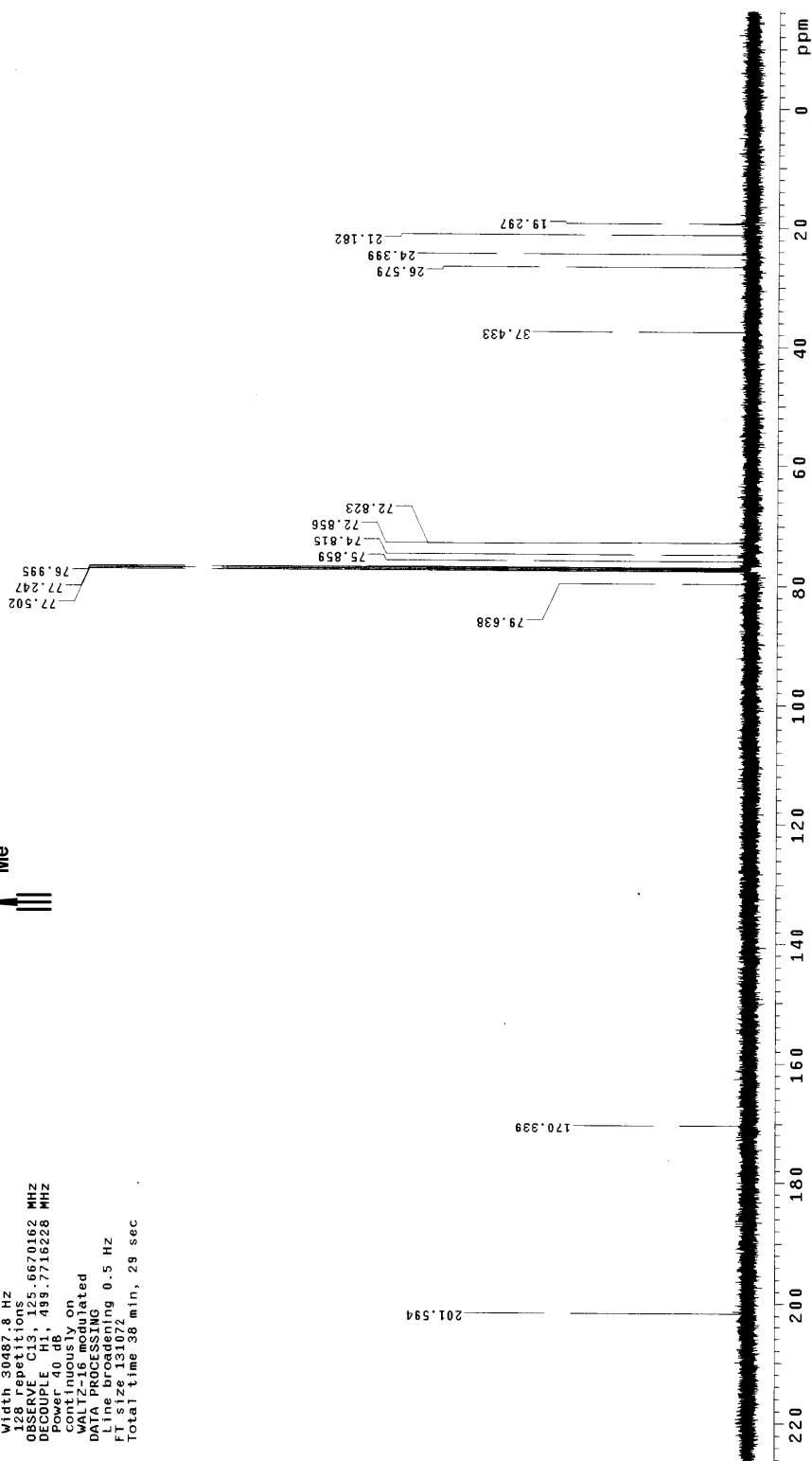
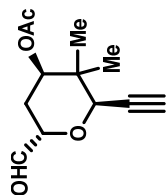
continuously on

WALTZ-16 modulated

DPMACROSSING 0.5 Hz

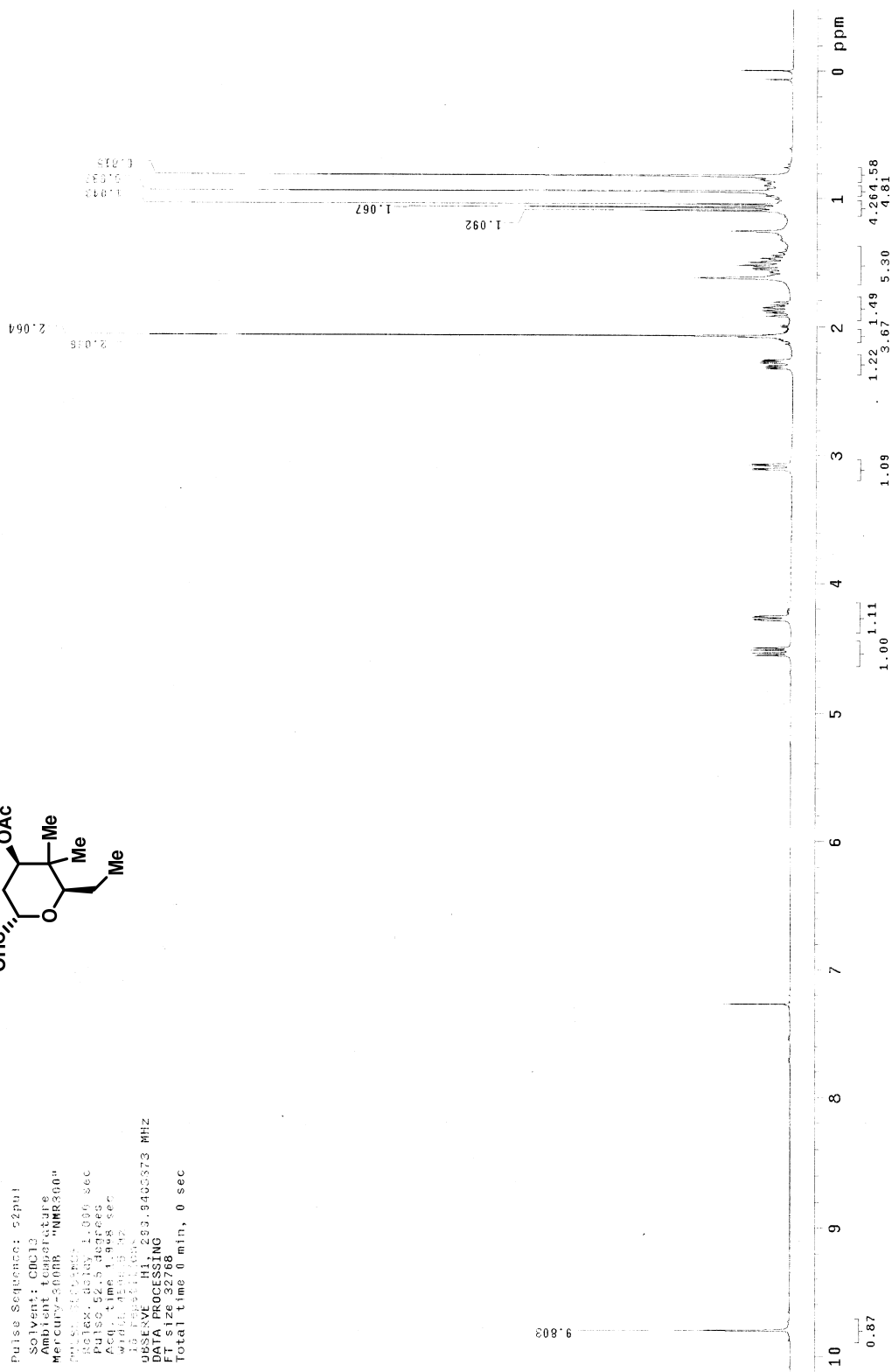
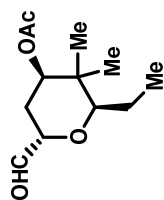
Time 131072

Total time 38 min, 29 sec



STANDARD 1H OBSERVE

Pulse Sequence: zgpg30
 Solvent: CDCl3
 Ambient Temperature
 Mercury-300MR "NMR300"
 Date_01-20-2007
 Relax delay 1.000 sec
 Acq 0.025 sec
 Acq 0.025 sec
 Width 1.000 Hz
 10.000 Hz
 OBSERVE H1, 293.940573 MHz
 DATA PROCESSING
 File size 32786
 Total time 8 min, 0 sec



Std proton

File: Carbon

Pulse Sequence: s2pul

Solvent: cdcl3

Temp: 25.0 C / 298.1 K

OBS: 500 MHz

VMRS-500 "nmr500"

Relax. delay 1.000 sec

Pulse 45.0 degrees

Acq. time 1.300 sec

Width 30487.8 Hz

2016 repetitions

OBSFREQ 500.136299 MHz

DECOUPLE CH1 439.7716228 MHz

Power 40 dB

continuously on

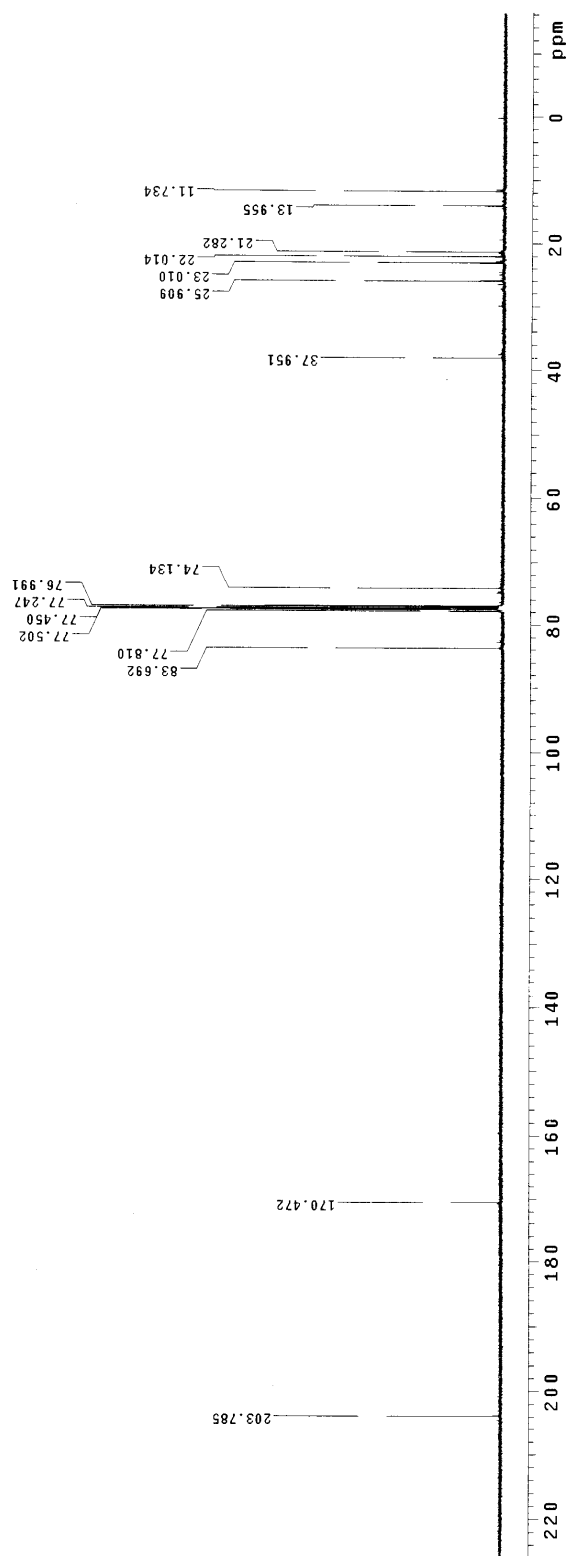
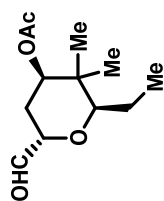
WALTZ-16 modulated

DATA PROCESSING

F1 500.136299 MHz

F2 125.76131072 MHz

Total time 3 hr, 12 min, 26 sec



Std proton

File: Proton

Pulse Sequence: s2pul

Solvent: cdcl3

Temp. 10.0 C / 283.1 K

Operator: sezgink

VNMR5-500 "nmr500"

Relax. delay 1.000 sec

Pulse 45.0 degrees

Acq. time 2.049 sec

Width 8012.8 Hz

Spectrum

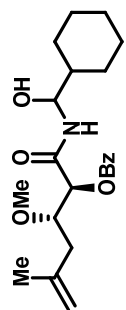
Observed F1 499.7691253 MHz

DATA PROCESSING

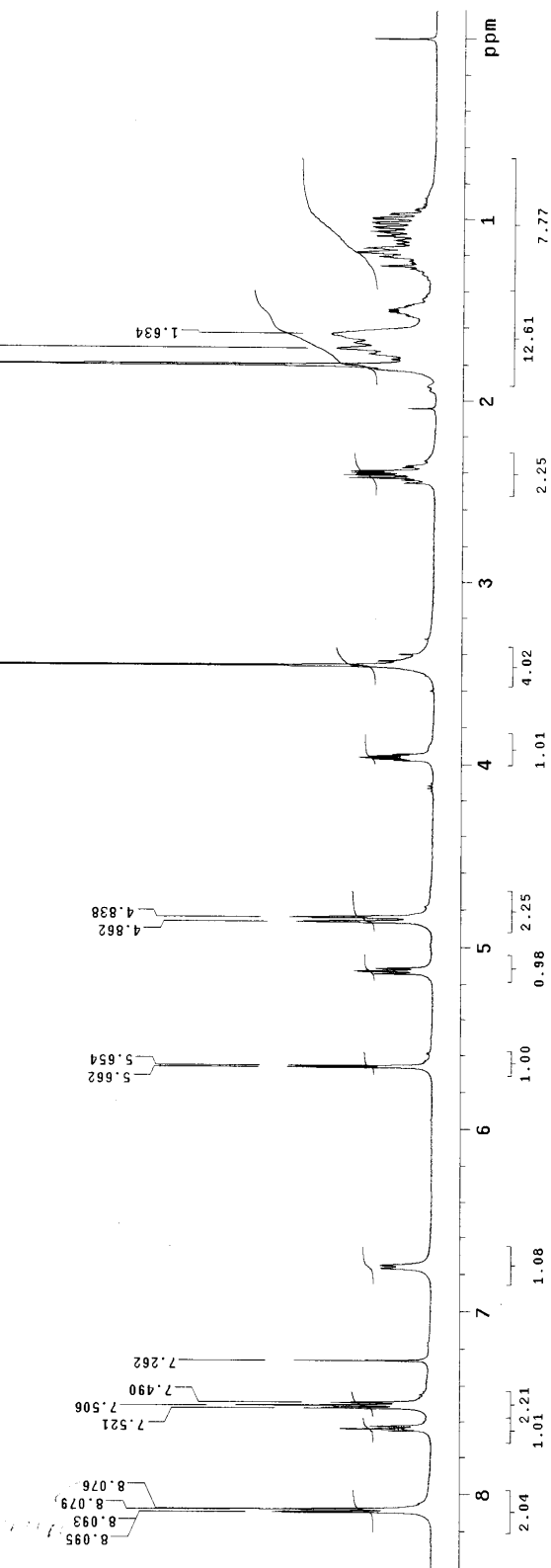
Line broadening 0.2 Hz

FT size 65536

Total time 0 min, 30 sec



Isomer A



Std proton

File: Carbon

Pulse Sequence: s2pul

Solvent: cdcl3

Temp: 10.0 C / 283.1 K

Operator: sezkink

VNMR-500 "nmr500"

Relax. delay 1.000 sec

Pulse 45.0 degrees

Acq. time 1.300 sec

Width 5049.8 Hz

480 cps/Hz

OBSERVE C13 125.6670162 MHz

DECOUPLE H1 489.7716228 MHz

Power 40 dB

continuously on

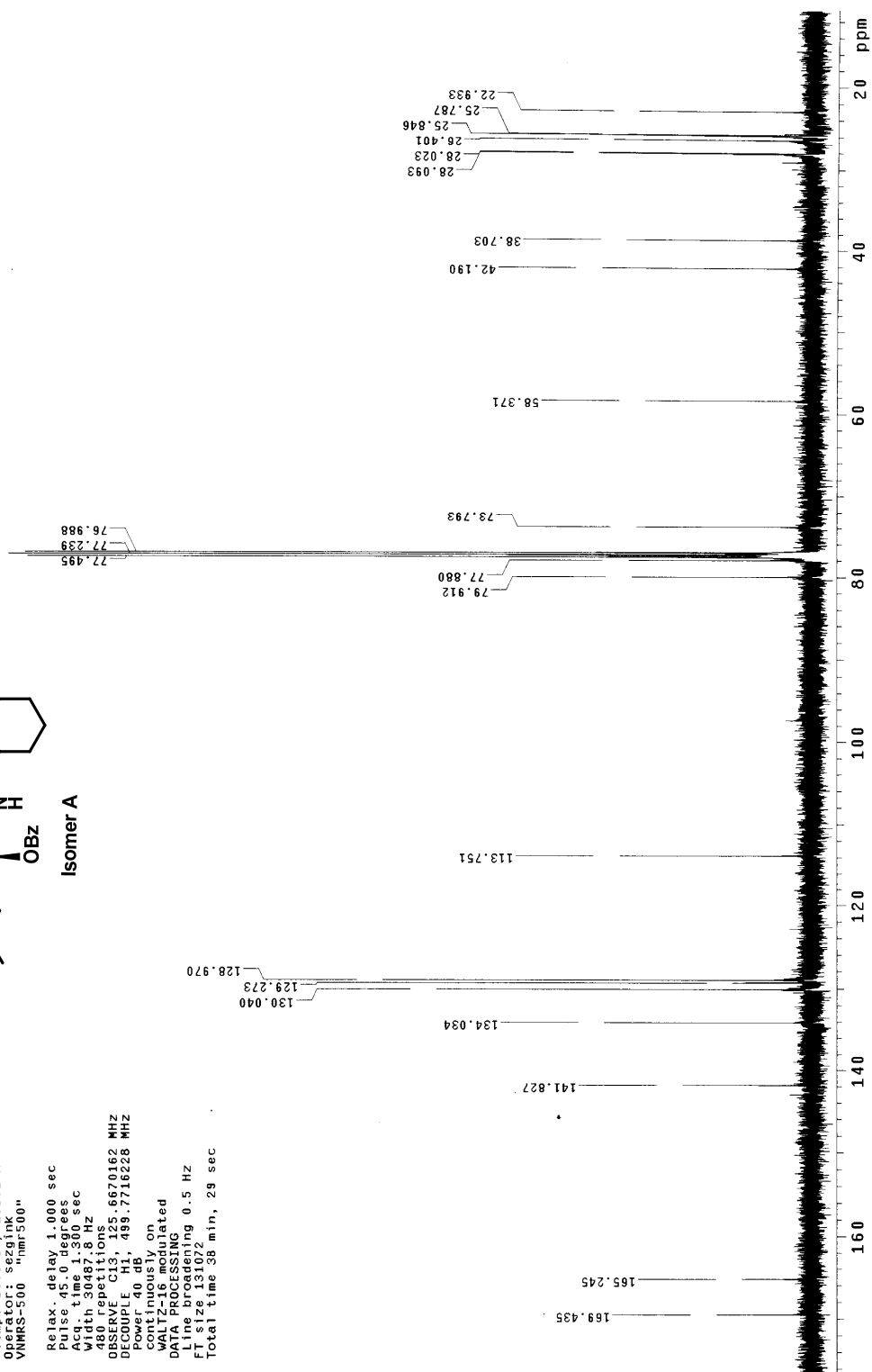
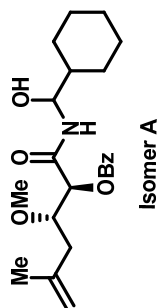
WALTZ-16 modulated

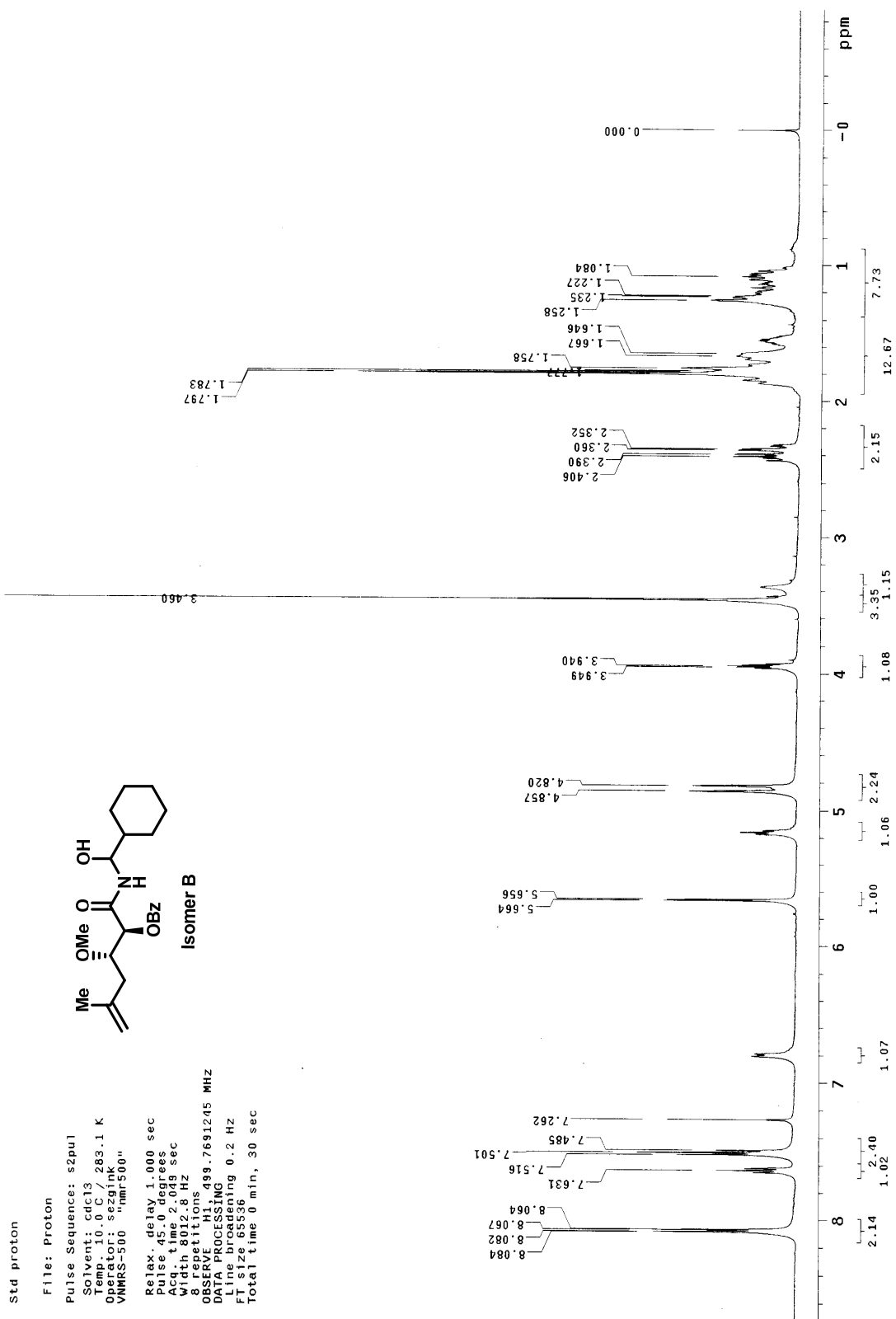
DATA PROCESSING

Sweep rate 0.5 Hz

FT size 131072

Total time 38 min, 29 sec





Std proton

File: Carbon

Pulse Sequence: s2pul

Solvent: cdcl3 283.1 K

Scan rate: 0.5 Hz

Operator: seza/nk

VNMR5-500 "nmr500"

Relax. delay 1.000 sec

Pulse 45.0 degrees

Acq. time 1.300 sec

Width 30487.8 Hz

Observed repetitions

Observed C13, 128.951

Observed C13, 129.347

Observed C13, 130.036

Observed C13, 133.986

Observed C13, 141.827

Observed C13, 165.145

Observed C13, 169.228

Observed C13, 173.072

Observed C13, 177.072

Observed C13, 181.072

Observed C13, 185.072

Observed C13, 189.072

Observed C13, 193.072

Observed C13, 197.072

Observed C13, 201.072

Observed C13, 205.072

Observed C13, 209.072

Observed C13, 213.072

Observed C13, 217.072

Observed C13, 221.072

Observed C13, 225.072

Observed C13, 229.072

Observed C13, 233.072

Observed C13, 237.072

Observed C13, 241.072

Observed C13, 245.072

Observed C13, 249.072

Observed C13, 253.072

Observed C13, 257.072

Observed C13, 261.072

Observed C13, 265.072

Observed C13, 269.072

Observed C13, 273.072

Observed C13, 277.072

Observed C13, 281.072

Observed C13, 285.072

Observed C13, 289.072

Observed C13, 293.072

Observed C13, 297.072

Observed C13, 301.072

Observed C13, 305.072

Observed C13, 309.072

Observed C13, 313.072

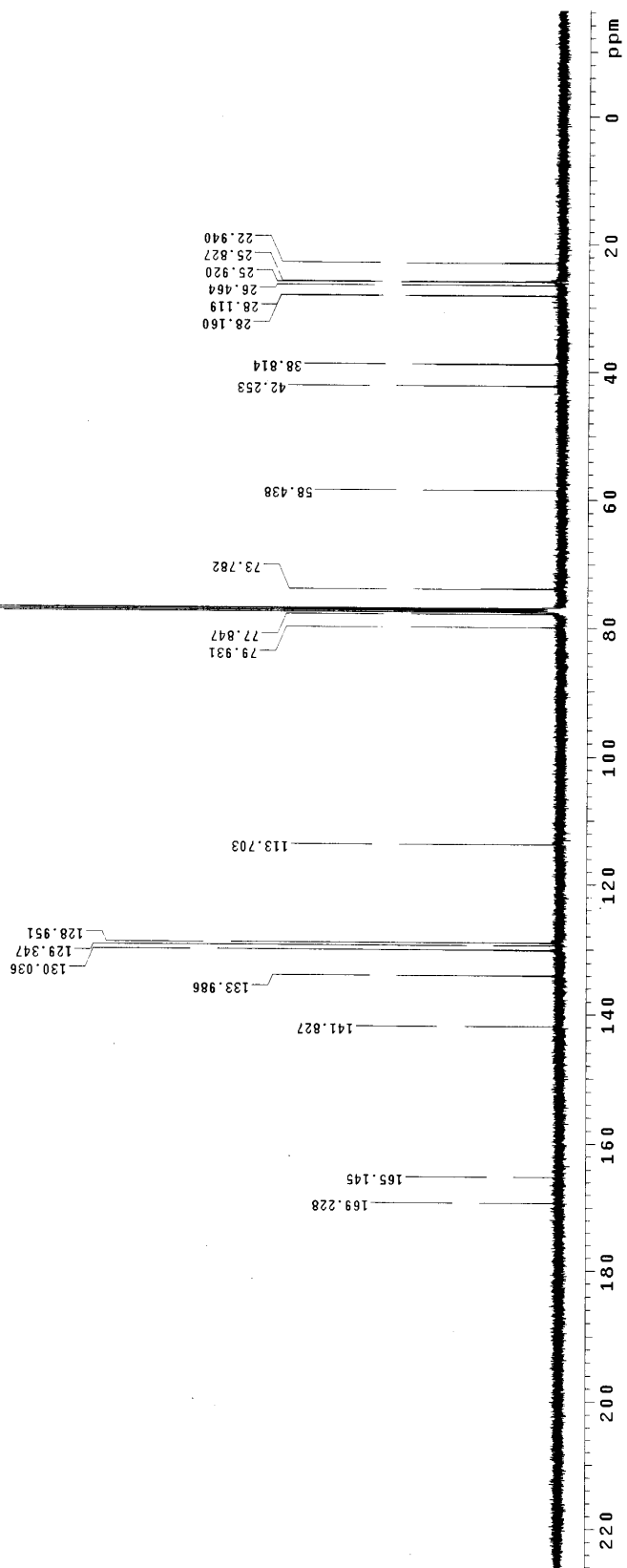
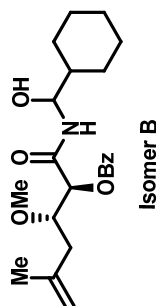
Observed C13, 317.072

Observed C13, 321.072

Observed C13, 325.072

Observed C13, 329.072

Observed C13, 333.072



File: Proton

Pulse Sequence: s2pu1

Solvent: cdc13

Temp. 25.0 C / 298.1 K

```
Operator: sezgink  
VNMR5-500 "nmr500"
```

○
○
○
■
■
■
○
○
○
○
●
●
●
●

Relax. delay 1.000 sec

Pulse 45.0 degrees
Acq. time 2.049 sec

Width 8012.8 Hz

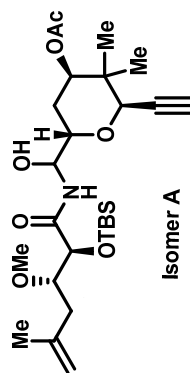
272 repetitions
OBSERVE H1 199 769

OBSERVE HI, 499.7691223 MHZ
DATA PROCESSING

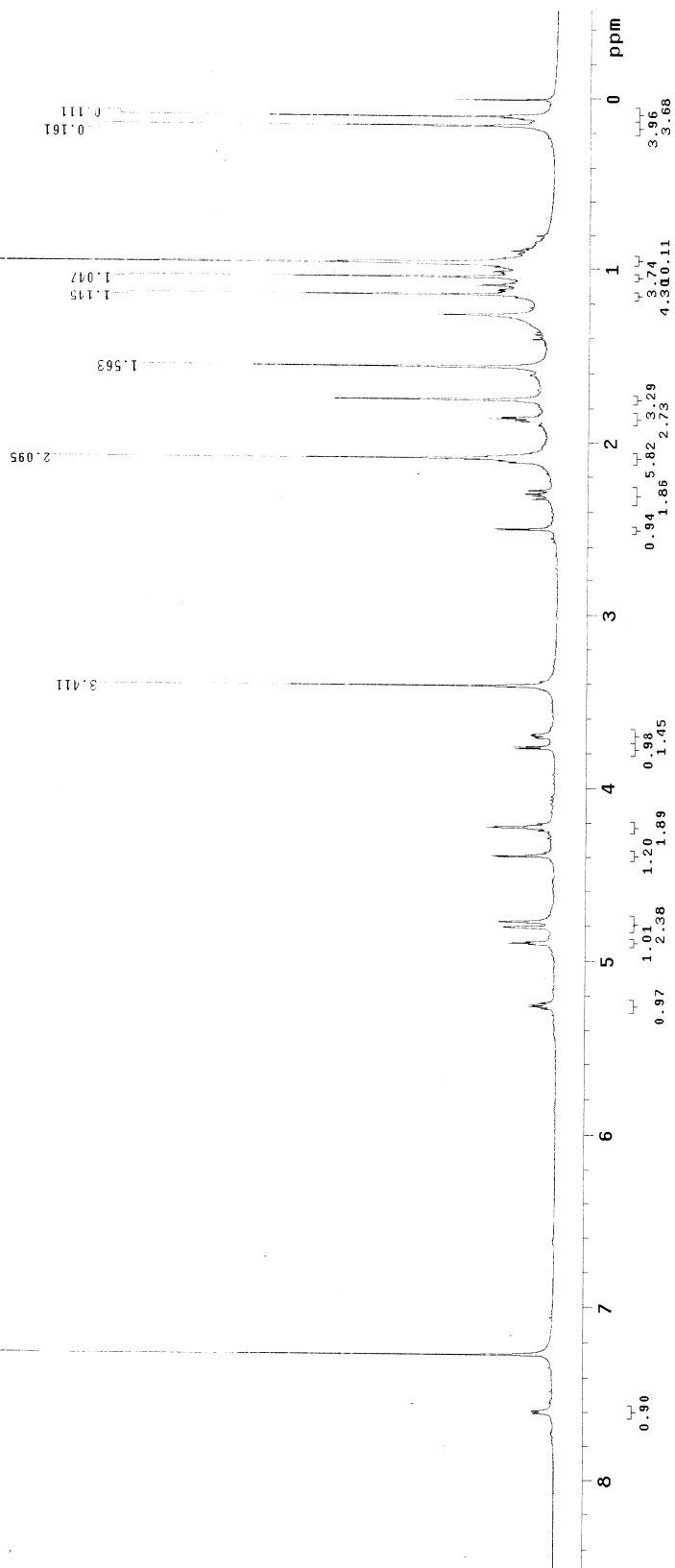
Line broadening 0.2 Hz

File size	65536	
Total time	26 min, 12 sec	

2.2.4



Isomer A



Std proton

File: Proton

Pulse Sequence: s2pu1

Solvent: cdcl3

Temp: 25.0 C / 298.1 K

Operator: sezgink

VMKS-500 "nmr500"

Relax. delay 1.000 sec

Pulse 15.0 degrees

Acq. time 2.200 sec

Width 8012.8 Hz

176 repetitions

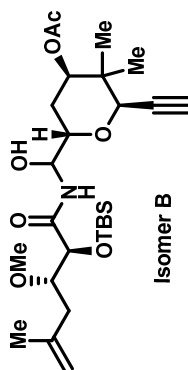
OBSERVE H1, 499.7691223 MHz

DATA PROCESSING

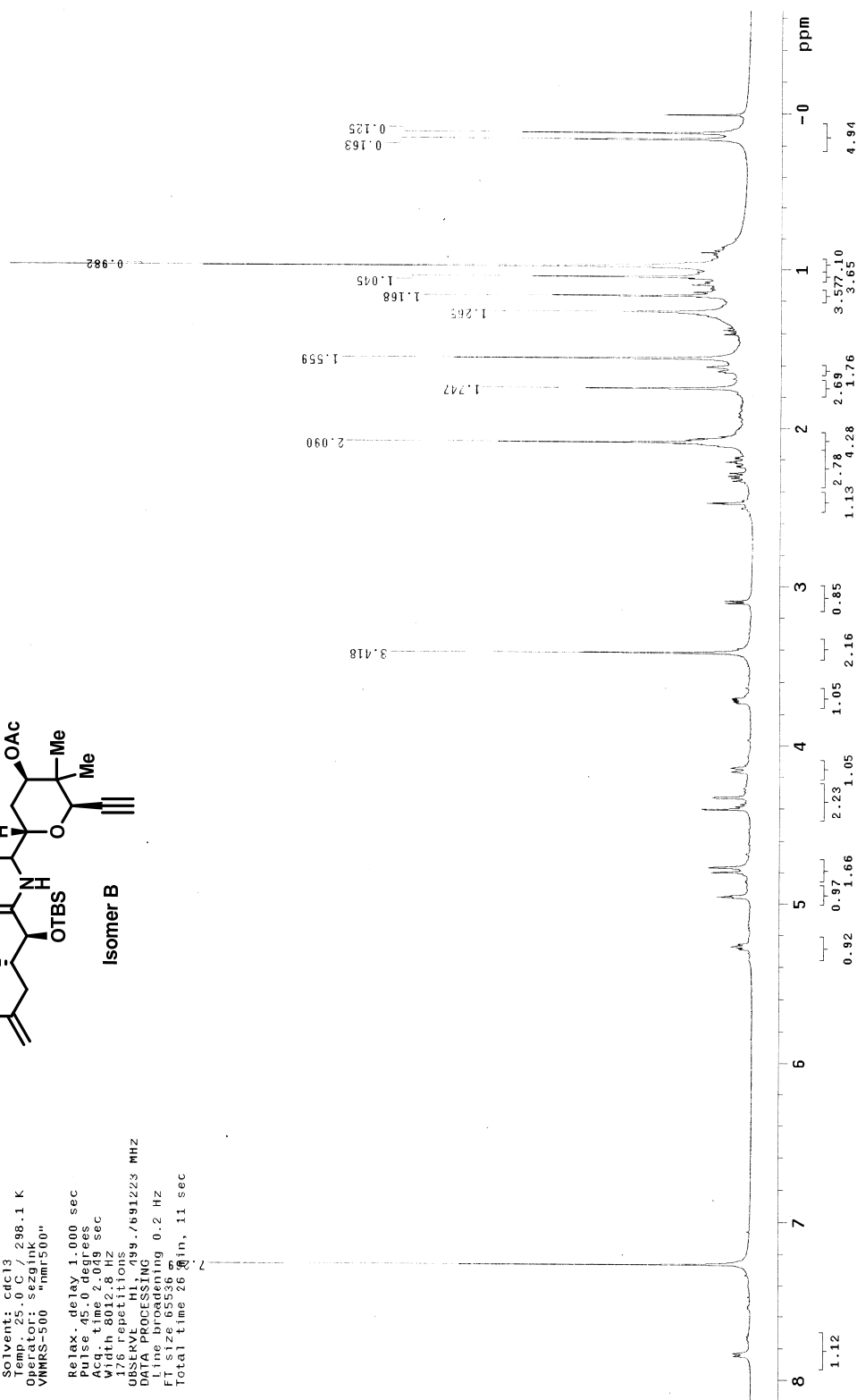
F1, fine broadening 0.2 Hz

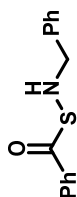
F2, phase 0.000000000000

Total time 26.8 min, 11 sec

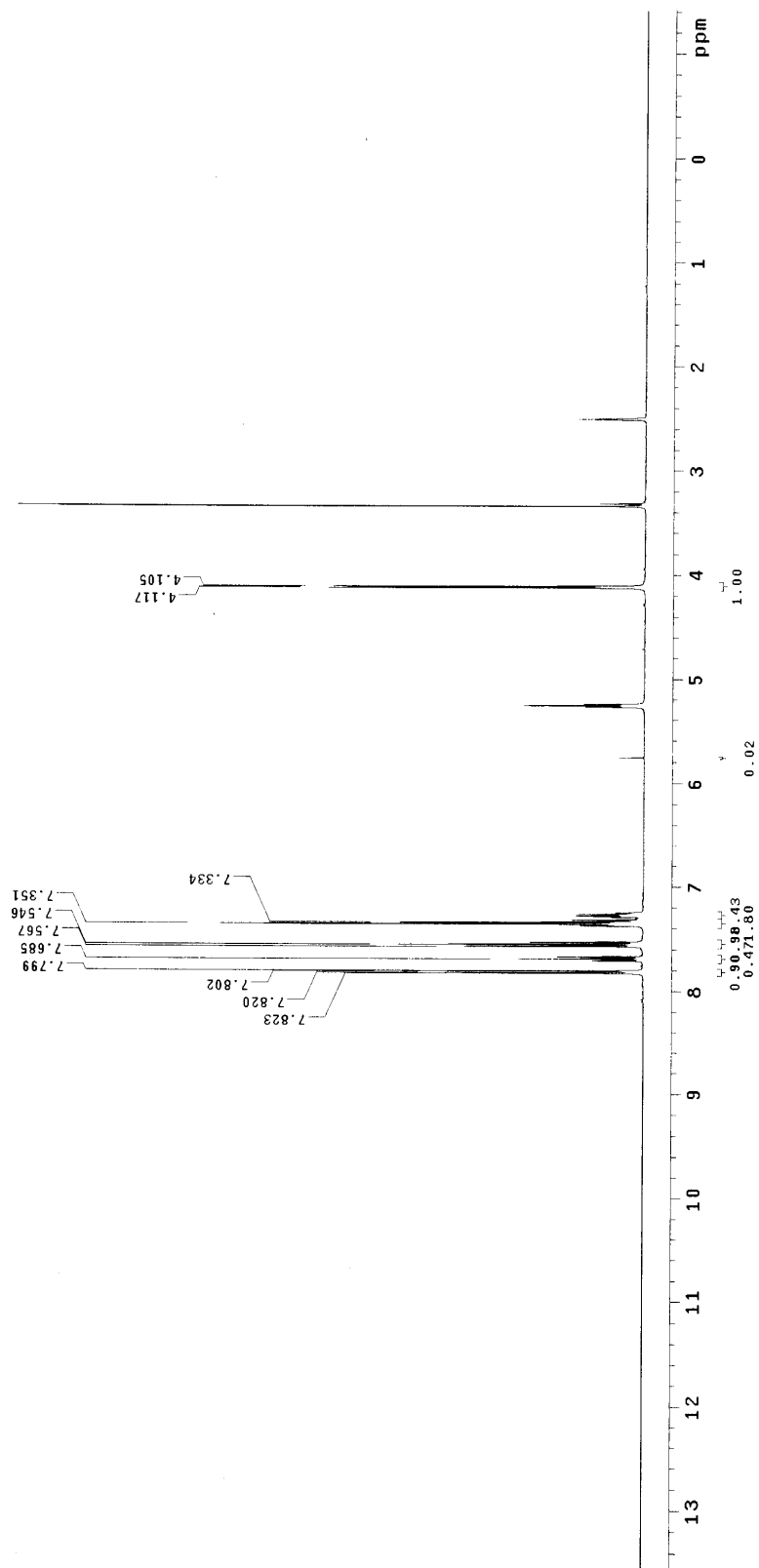


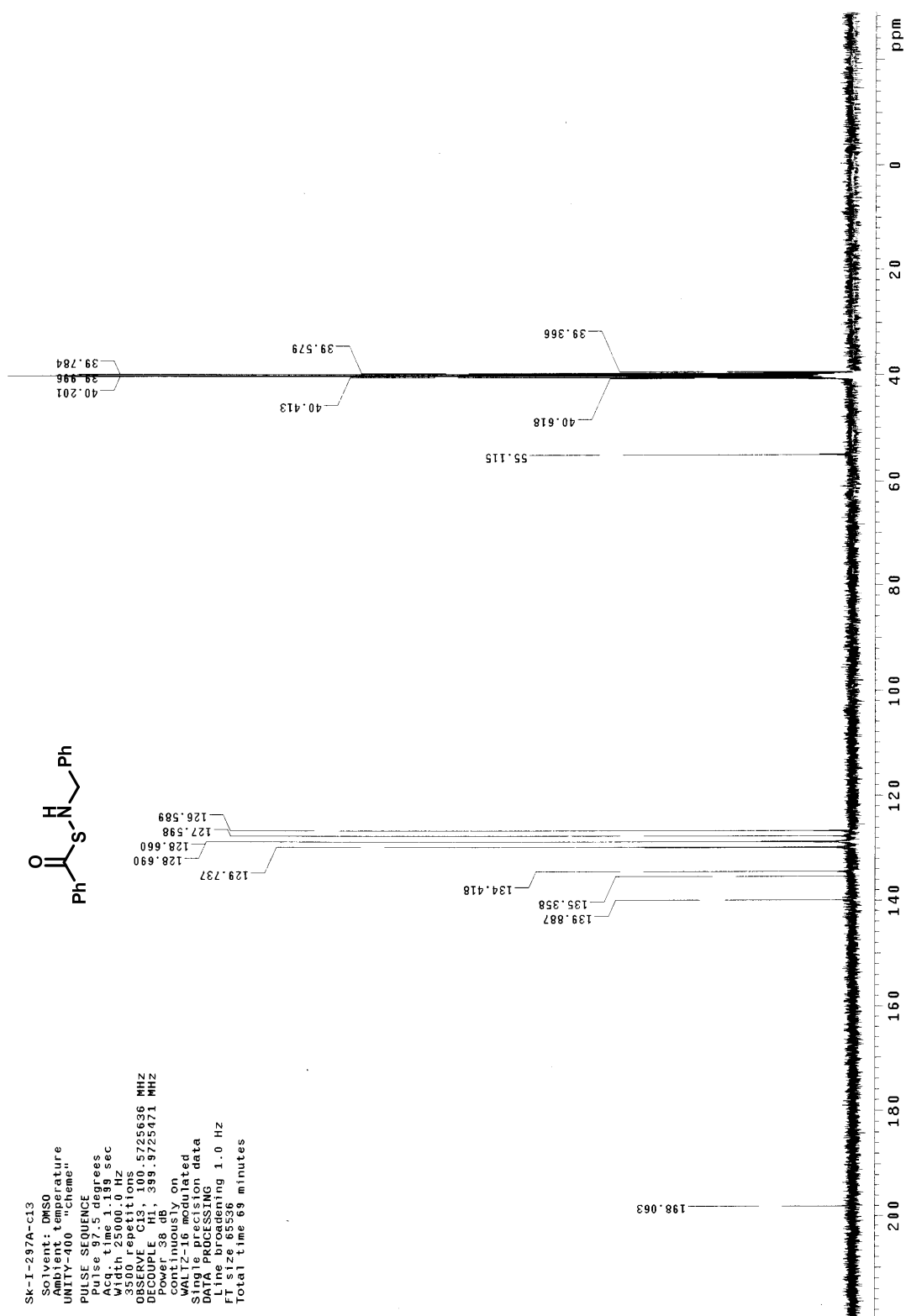
Isomer B

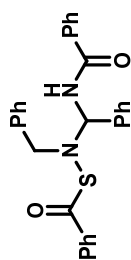




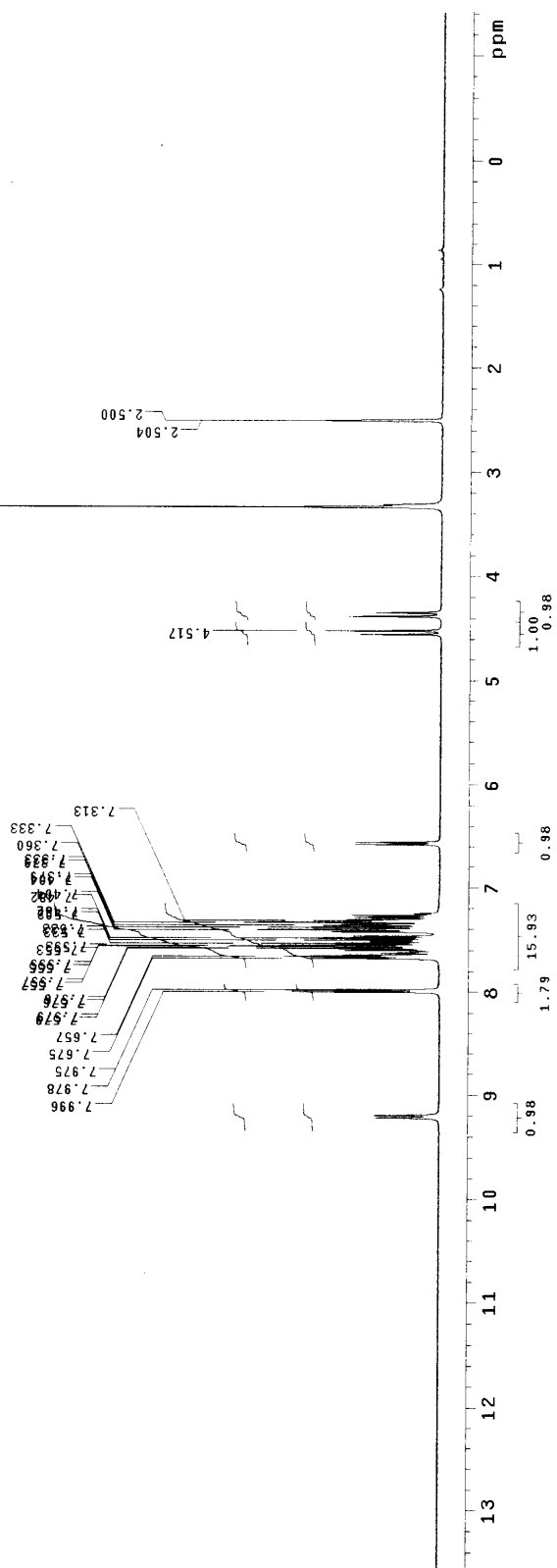
SK-I-297A
 Solvent: DMSO
 Ambient temperature
 UNITY-400 "cheme"
 PULSE SEQUENCE
 Pulse 63.0 degrees
 Acq. time 3.744 sec
 Width 6000.6 Hz
 16 Spectral Lines
 OBSERVE H1: 399.9701139 MHZ
 DATA PROCESSING
 FT size 65536
 Total time 1 minute







SK-I-297Bdmso
 Solvent: DMSO
 Ambient temperature
 UNITY-400 "cheme"
 PULSE SEQUENCE
 Pulse 63.0 degrees
 Acq. time 3.744 sec
 Width 6000.6 Hz
 Frequency 399.9701139 MHz
 OBSERVED
 DATA PROCESSING
 FT size 65536
 Total time 1 minute



Side B

Std proton

File: Carbon

Pulse Sequence: s2pu1

Solvent: cdc13

Temp: 25.0 C / 298.1 K

Operator: sezgink

VNMR3-500 "nmr500"

Relax. delay 1.000 sec

Pulse 15.0 degrees

Acq time 1.000 sec

Width 30487.8 Hz

896 repetitions

OBSERVE C13, 125.6670162 MHz

DECOUPLE H1, 499.7716226 MHz

Power 40 dB

Contaminant ON

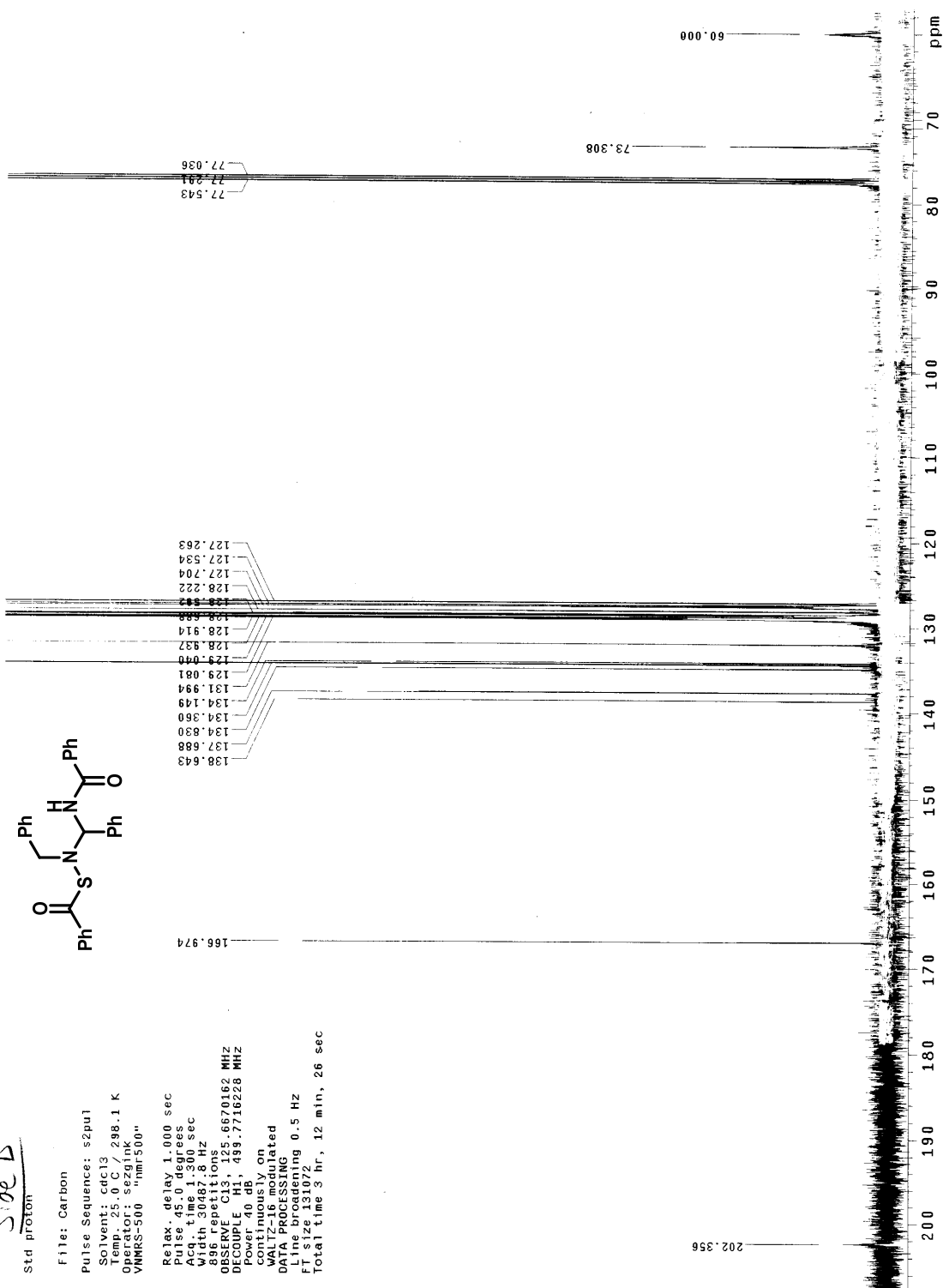
WALTZ-16 modulated

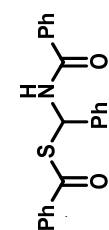
DATA PROCESSING

Line broadening 0.5 Hz

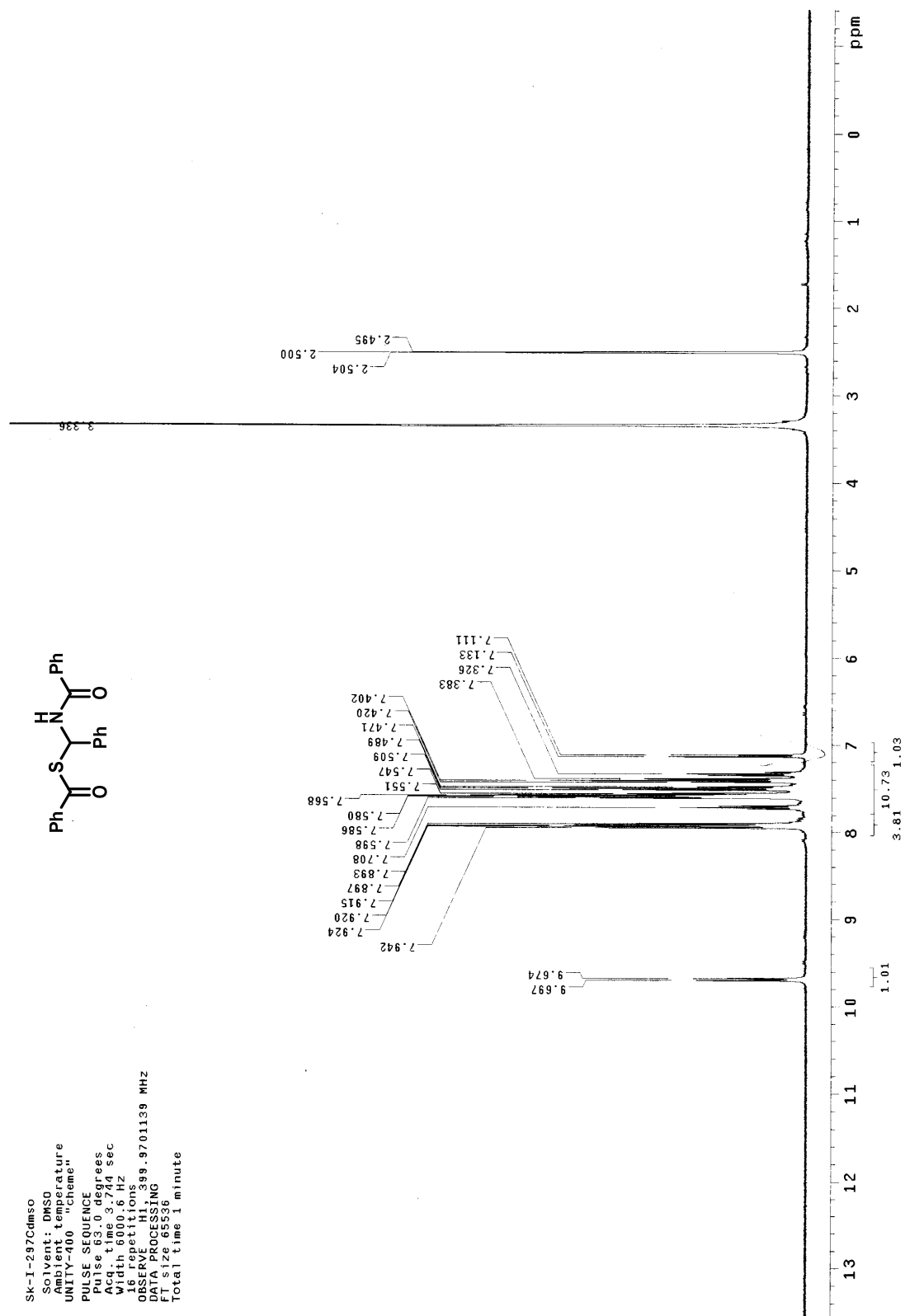
FT size 131072

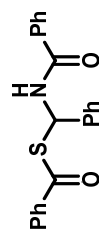
Total time 3 hr, 12 min, 26 sec





SK-I-297Cdmso
 Solvent: DMSO
 Acquisition temperature
 400 MHz
 PULSE SEQUENCE
 zgpg30
 Pulse time 3.00 sec
 Acquisition time 3.04 sec
 Width 6000.6 Hz
 16 repetitions
 OBSERVE H1, 399.970139 MHz
 DATA PROCESSING
 F1 size 65536
 Total time 1 minute





Std proton

File: Carbon

Pulse Sequence: s2pul

Solvent: cdc13

Temp: 25.0 C / 298.1 K

Observed: s2gmg

VMRS-500 "nmr500"

Relax. delay 1.000 sec

Pulse 45.0 degrees

Acq. time 1.300 sec

Width 30487.8 Hz

1072 repetitions

250 MHz 13C NMR

OBSERVED CH, 125.6570162 MHz

DECODED CH, 433.7718228 MHz

Power 40 dB,

continuously on

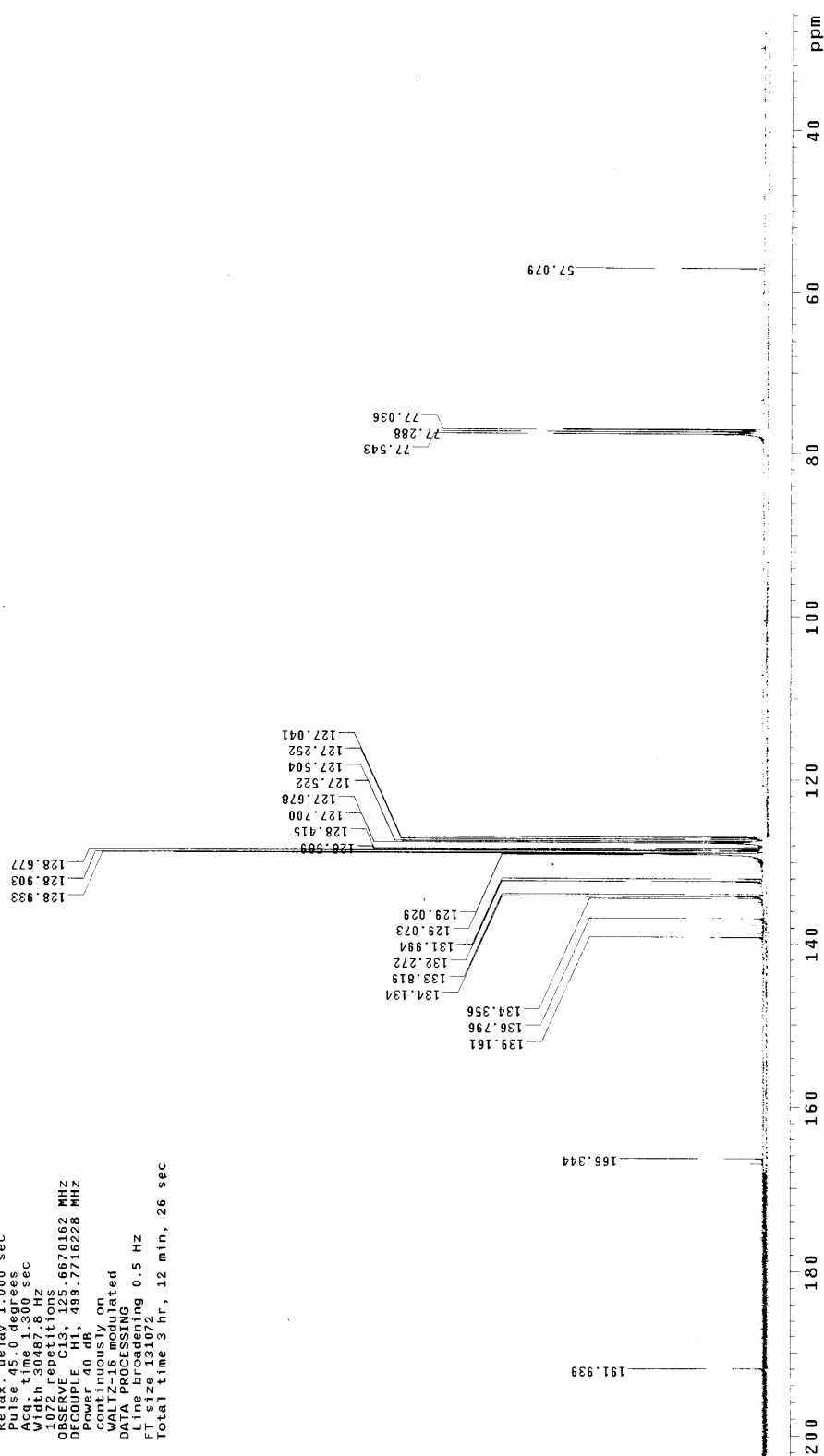
WALTZ-16 modulated

DATA PROCESSING

Line broadening 0.5 Hz

F2 size 32768

Total time 3 hr, 12 min, 26 sec



Vita

SEZGIN KIREN

Education

2007 PhD in Chemistry

Rutgers, The State University of New Jersey, Piscataway, NJ

2005 Ms in Chemistry

Rutgers, The State University of New Jersey, Piscataway, NJ

1999 BS in Chemistry

Marmara University, Istanbul, Turkey

Academic & Teaching Activities

2002-2007 Teaching Assistant, for Organic Chemistry

Rutgers University, Piscataway, NJ

Publications

Journal Papers:

- Kiren, S.; Shangguan, N.; Williams, L. J. Direct Carbinolamide Synthesis. *Tetrahedron Lett.* **2007**, 48, 7456-7459.
- Lotesta, S. D.; Kiren, S.; Sauers, R. R.; Williams, L. J. Spirodiepoxides: Heterocycle Synthesis and Mechanistic insight *Angew. Chem. Int. Ed.* **2007**, 46, 7108-7111.
- Shangguan, N.; Kiren, S.; Williams, L. J. A Formal Synthesis of Psymberin. *Org. Lett.* **2007**, 9, 1093-1096.
- Kiren, S.; Williams, L. J. Configuration of the Psymberin Side Chain. *Org. Lett.* **2005**, 7, 2905-2908.
- Kiren, S.; Wang, Z.; Williams, L. J. Iron (III) Chloride and DMAP promoted Thioacid-azide coupling. (Manuscript in preparation).

Books:

- Concise Organic Chemistry for the Students of Chemistry, Biology and Medicine with Study Guide, Salih Yaslak, Sezgin Kiren, **2001**, Beta Basim Yayim Dagitim A. S. Istanbul/Turkey.